2nd International Conference on Particle Physics
in Memoriam Engin Arık and Her Colleagues
Doğuş University, İstanbul, Turkey
20 - 25 June 2011

PHINPhotoinjector
as the CLIC Drive Beam e- Source

Dr. Öznur**METE**

CERN, European Laboratory for Nuclear Research

On behalf of the PHIN Team

- **Preface,** the original contribution in a deductive view of the CLIC project
    - Compact Linear Collider Project
    - What have we achieved in the third phase of the CLIC test facility?
    - Quest for an adequate electron source for the CLIC drive beam (thermionic or laser-driven)
- **PHIN photoinjector**, objectives of the research
    - What is a photoinjector?
    - Intro to PHIN photoinjector
    - Objectives of the research program
- **Beam instrumentation & characterization,** commissioning highlights of PHIN
    - Properties of the laser, cathode and the charge production studies
    - RF gun for PHIN
    - High intensity electron beam diagnostics at the injector stage (@high charge, low energy)
    - Some of the highlights from the characterization of our system
- **More, more and more (backup)**
- **Conclusions**

- **Preface,** the original contribution in a deductive view of the CLIC project
  - Compact Linear Collider Project
  - What have we achieved in the third phase of the CLIC test facility?
  - Quest for an adequate electron source for the CLIC drive beam (thermionic or laser-driven)

Ken's Talk - ICPP, Thursday

- **PHIN photoinjector**, objectives of the research
  - What is a photoinjector?
  - Intro to PHIN photoinjector
  - Objectives of the research program
- **Beam instrumentation & characterization,** commissioning highlights of PHIN
  - Properties of the laser, cathode and the charge production studies
  - RF gun for PHIN
  - High intensity electron beam diagnostics at the injector stage (@high charge, low energy)
  - Some of the highlights from the characterization of our system
- **More, more and more (backup)**
- **Conclusions**

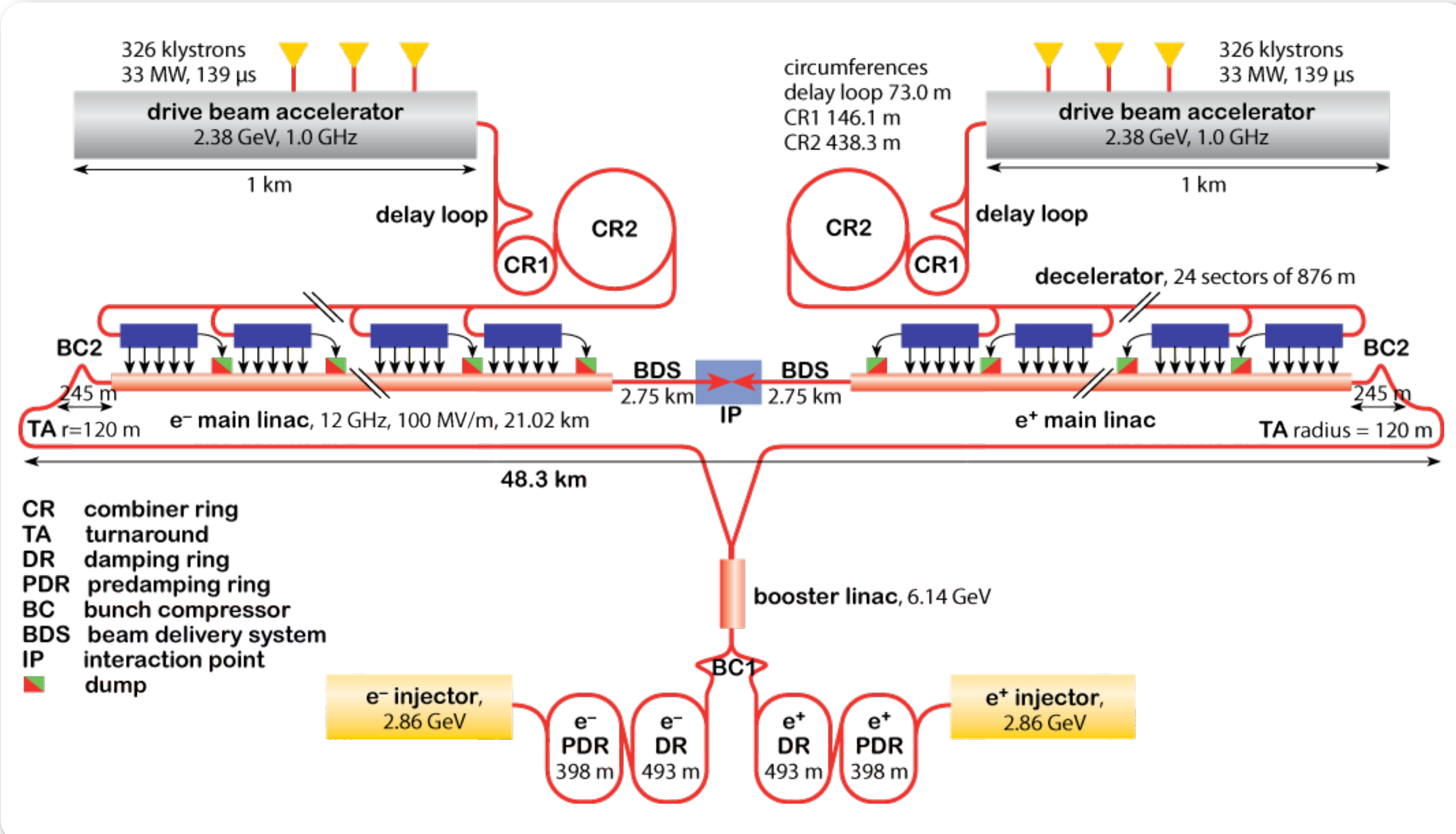
326 klystrons
33 MW, 139 μs
drive beam accelerator
2.38 GeV, 1.0 GHz
1 km
delay loop
CR2
CR1
circumferences
delay loop 73.0 m
CR1 146.1 m
CR2 438.3 m
326 klystrons
33 MW, 139 μs
drive beam accelerator
2.38 GeV, 1.0 GHz
1 km
CR2
CR1
delay loop
decelerator, 24 sectors of 876 m
BC2
BDS
2.75 km
BDS
2.75 km
BC2
245 m
IP
245 m
TA r=120 m
e⁻ main linac, 12 GHz, 100 MV/m, 21.02 km
e⁺ main linac
TA radius = 120 m
48.3 km
CR combiner ring
TA turnaround
DR damping ring
PDR predamping ring
BC bunch compressor
BDS beam delivery system
IP interaction point
dump
booster linac, 6.14 GeV
BC1
e⁻ injector,
2.86 GeV
e⁻
PDR
398 m
e⁻
DR
493 m
e⁺
DR
493 m
e⁺
PDR
398 m
e⁺ injector,
2.86 GeV

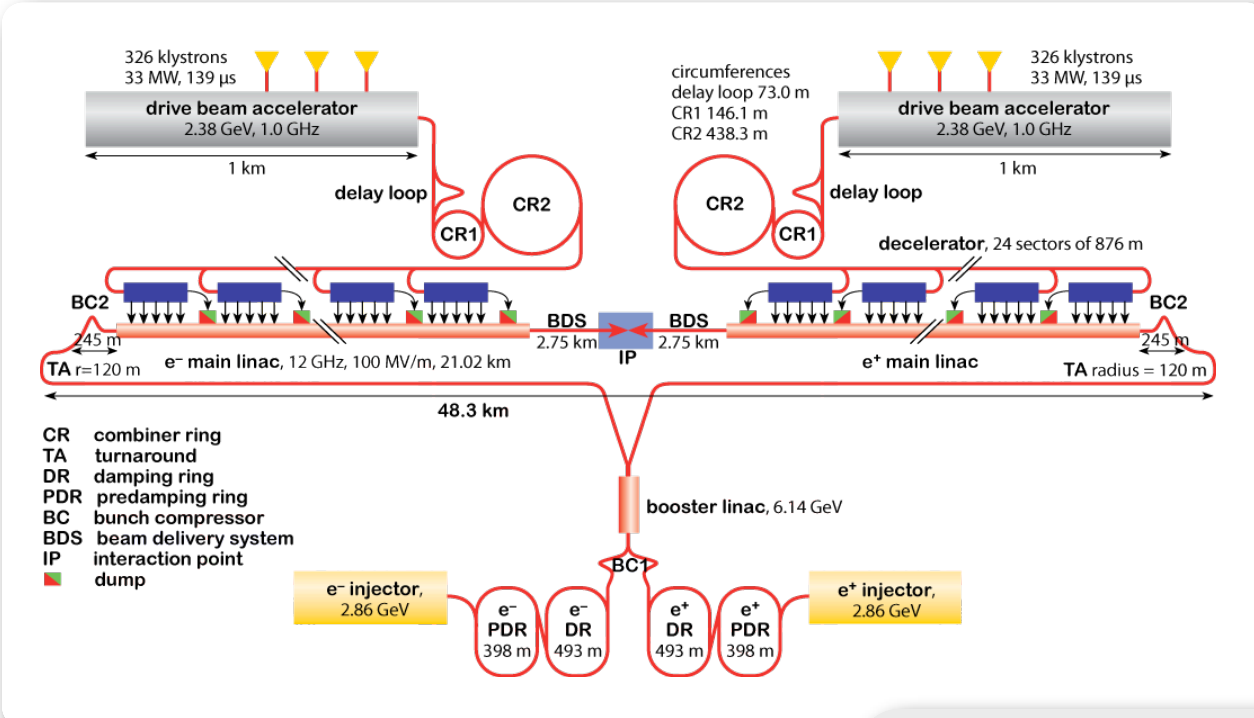
326 klystrons
33 MW, 139 μs
drive beam accelerator
2.38 GeV, 1.0 GHz
1 km
delay loop
CR1
CR2
circumferences
delay loop 73.0 m
CR1 146.1 m
CR2 438.3 m
326 klystrons
33 MW, 139 μs
drive beam accelerator
2.38 GeV, 1.0 GHz
1 km
delay loop
CR2
CR1
decelerator, 24 sectors of 876 m
BC2
245 m
TA r=120 m
e⁻ main linac, 12 GHz, 100 MV/m, 21.02 km
BDS
2.75 km
IP
BDS
2.75 km
e⁺ main linac
BC2
245 m
TA radius = 120 m
48.3 km
CR combiner ring
TA turnaround
DR damping ring
PDR predamping ring
BC bunch compressor
BDS beam delivery system
IP interaction point
dump
booster linac, 6.14 GeV
BC1
e⁻ injector, 2.86 GeV
e⁻ PDR 398 m
e⁻ DR 493 m
e⁺ DR 493 m
e⁺ PDR 398 m
e⁺ injector, 2.86 GeV

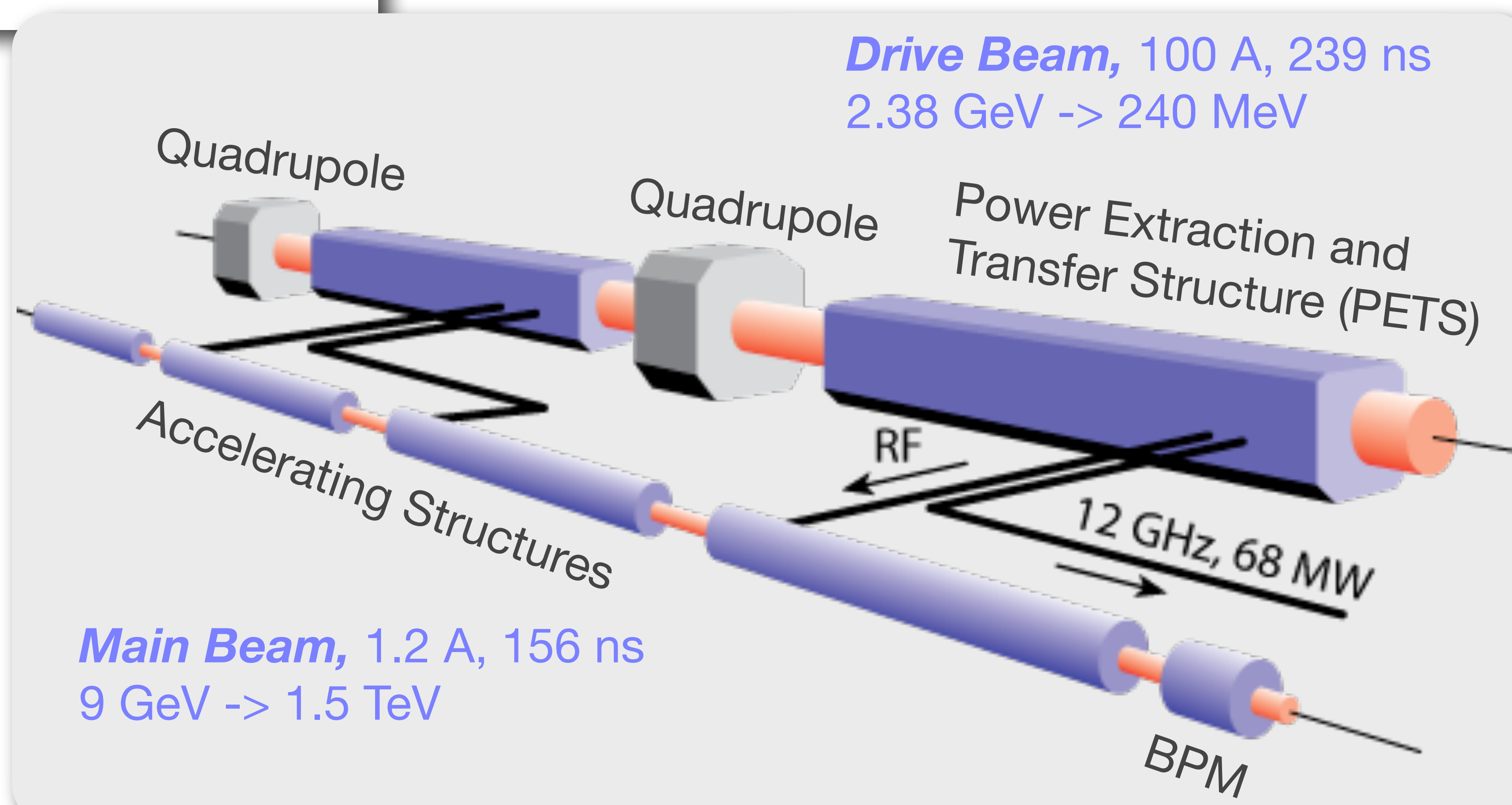
Drive Beam, 100 A, 239 ns
2.38 GeV -> 240 MeV
Quadrupole
Quadrupole
Power Extraction and Transfer Structure (PETS)
RF
Accelerating Structures
12 GHz, 68 MW
Main Beam, 1.2 A, 156 ns
9 GeV -> 1.5 TeV
BPM

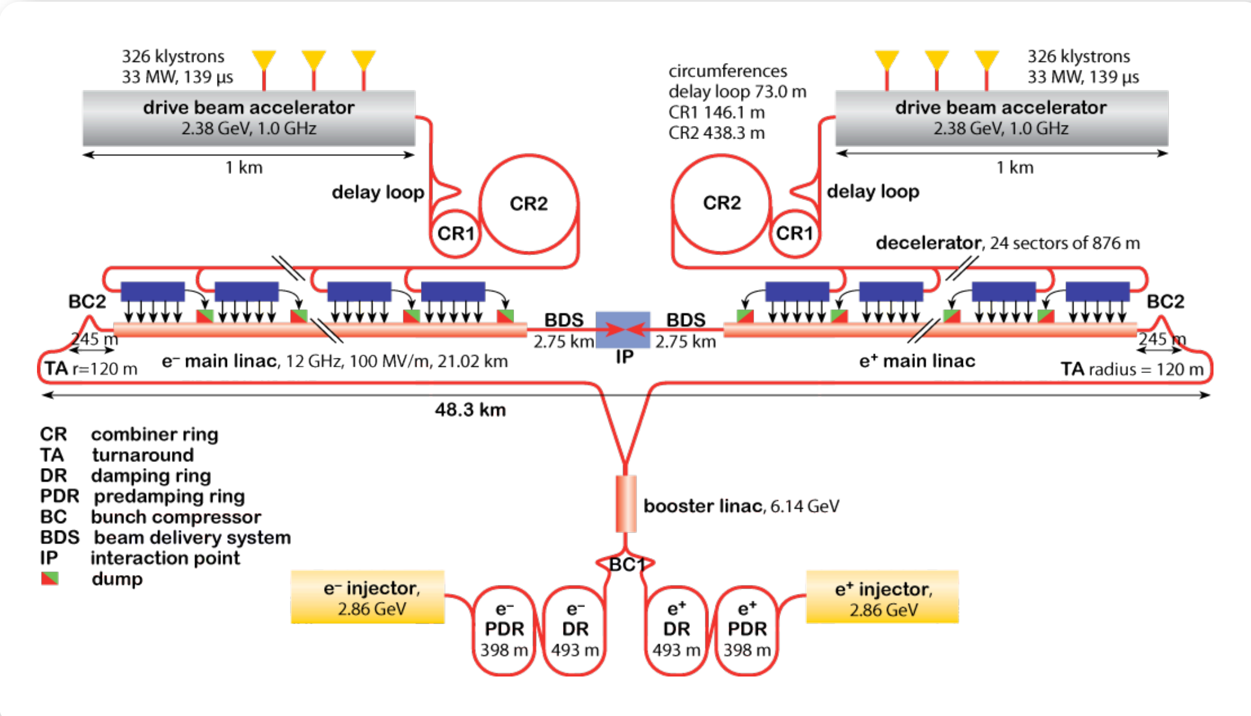
326 klystrons
33 MW, 139 µs
drive beam accelerator
2.38 GeV, 1.0 GHz
1 km
delay loop
CR2
CR1
circumferences
delay loop 73.0 m
CR1 146.1 m
CR2 438.3 m
326 klystrons
33 MW, 139 µs
drive beam accelerator
2.38 GeV, 1.0 GHz
1 km
delay loop
CR2
CR1
decelerator, 24 sectors of 876 m
BC2
245 m
TA r=120 m
e⁻ main linac, 12 GHz, 100 MV/m, 21.02 km
BDS
2.75 km
IP
BDS
2.75 km
e⁺ main linac
BC2
245 m
TA radius = 120 m
48.3 km
CR combiner ring
TA turnaround
DR damping ring
PDR predamping ring
BC bunch compressor
BDS beam delivery system
IP interaction point
dump
booster linac, 6.14 GeV
BC1
e⁻ injector, 2.86 GeV
e⁻ PDR 398 m
e⁻ DR 493 m
e⁺ DR 493 m
e⁺ PDR 398 m
e⁺ injector, 2.86 GeV

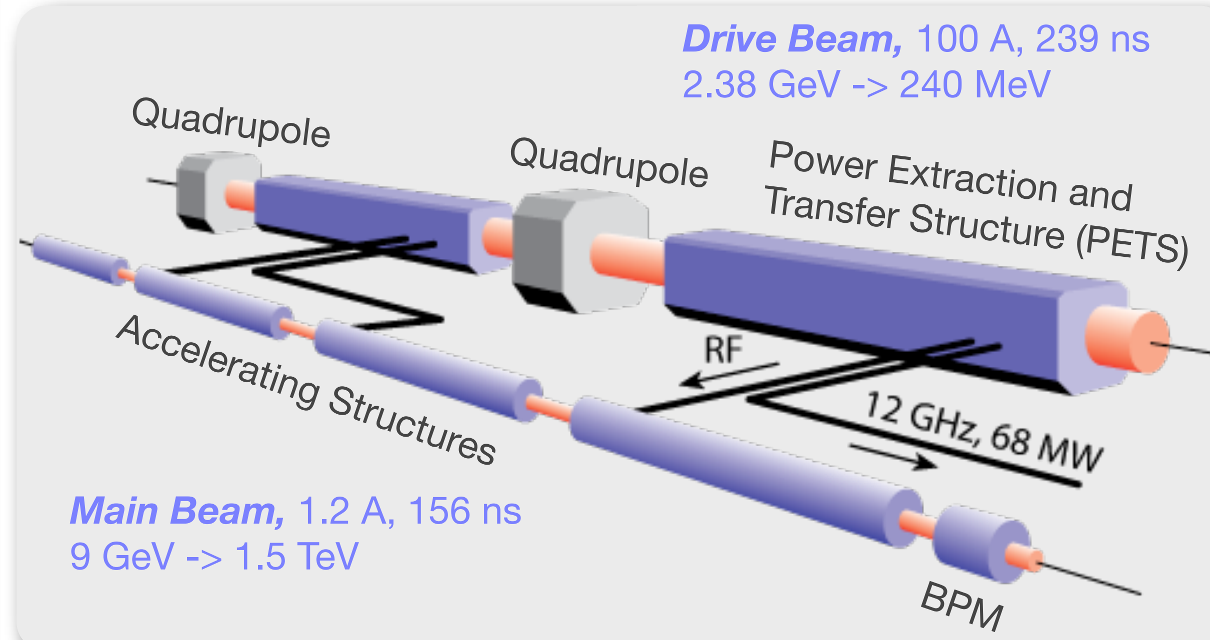
Drive Beam, 100 A, 239 ns
2.38 GeV -> 240 MeV
Quadrupole
Quadrupole
Power Extraction and Transfer Structure (PETS)
Accelerating Structures
RF
12 GHz, 68 MW
Main Beam, 1.2 A, 156 ns
9 GeV -> 1.5 TeV
BPM

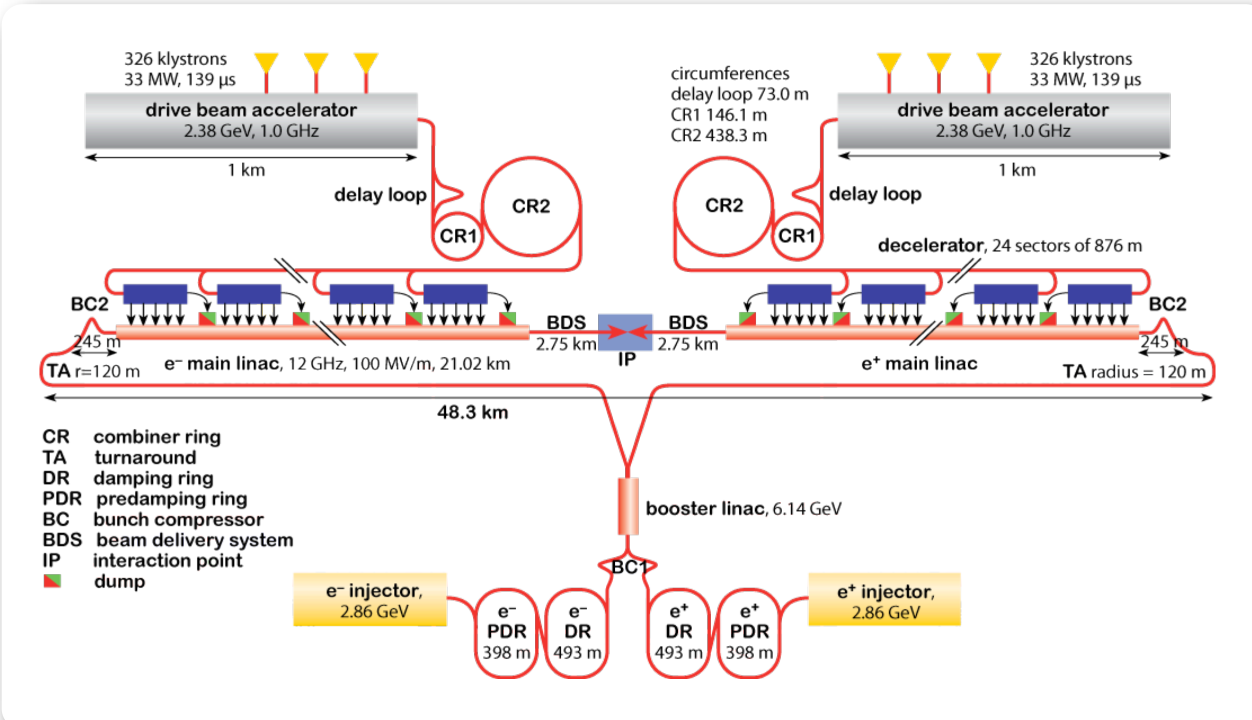

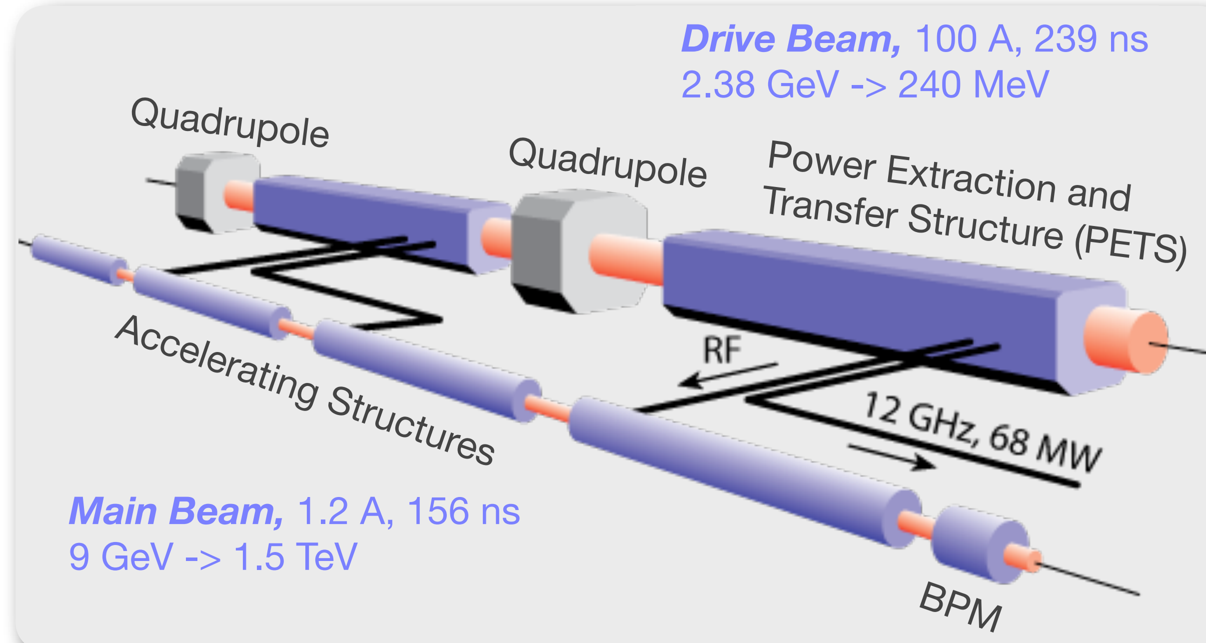

A number of challenges to be mastered for CLIC

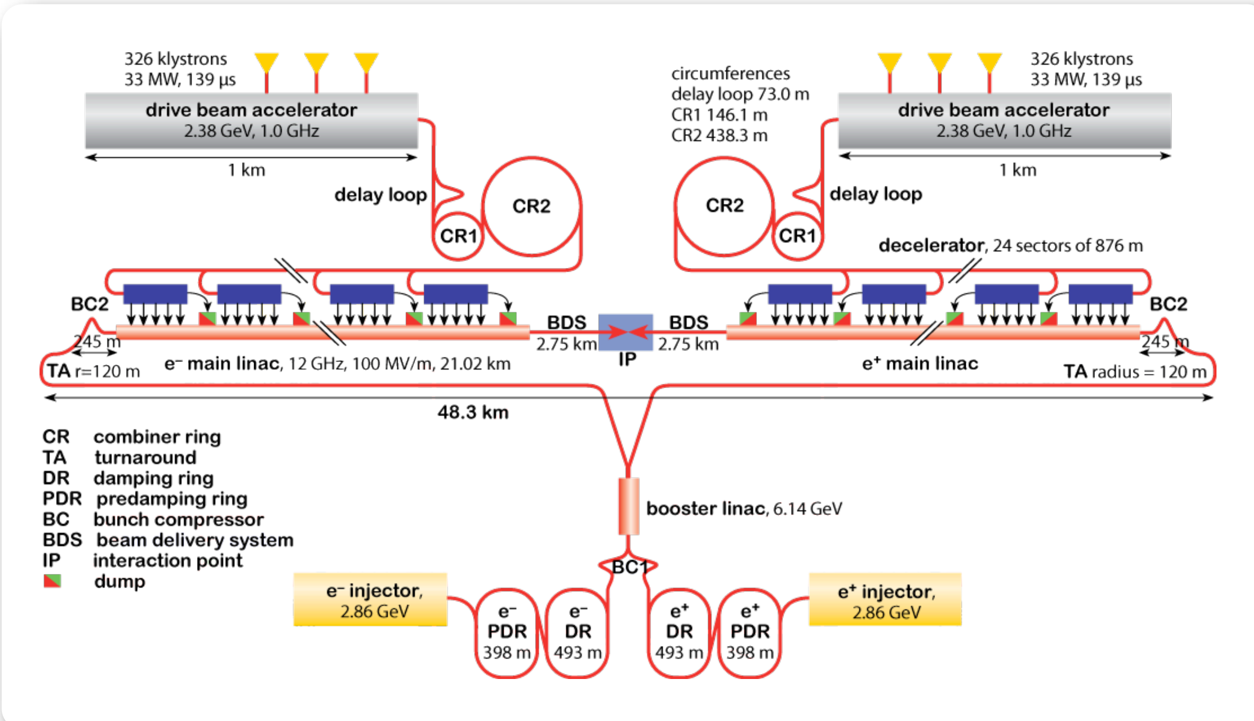

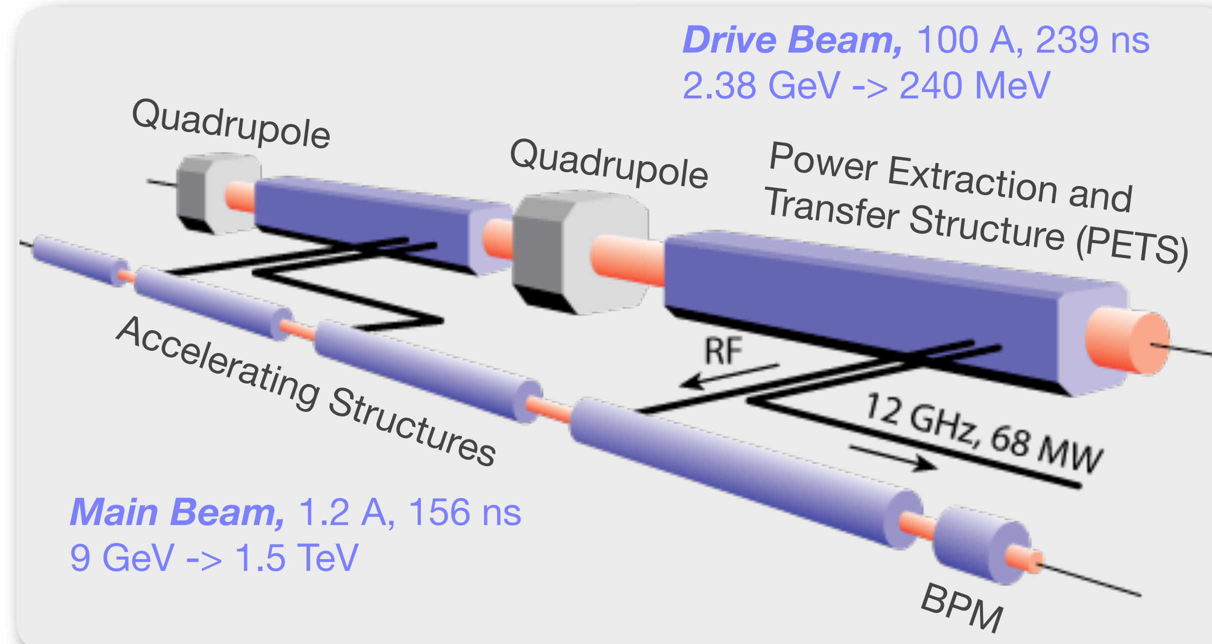

A number of challenges to be mastered for CLIC

- Generation of high-intensity drive beam

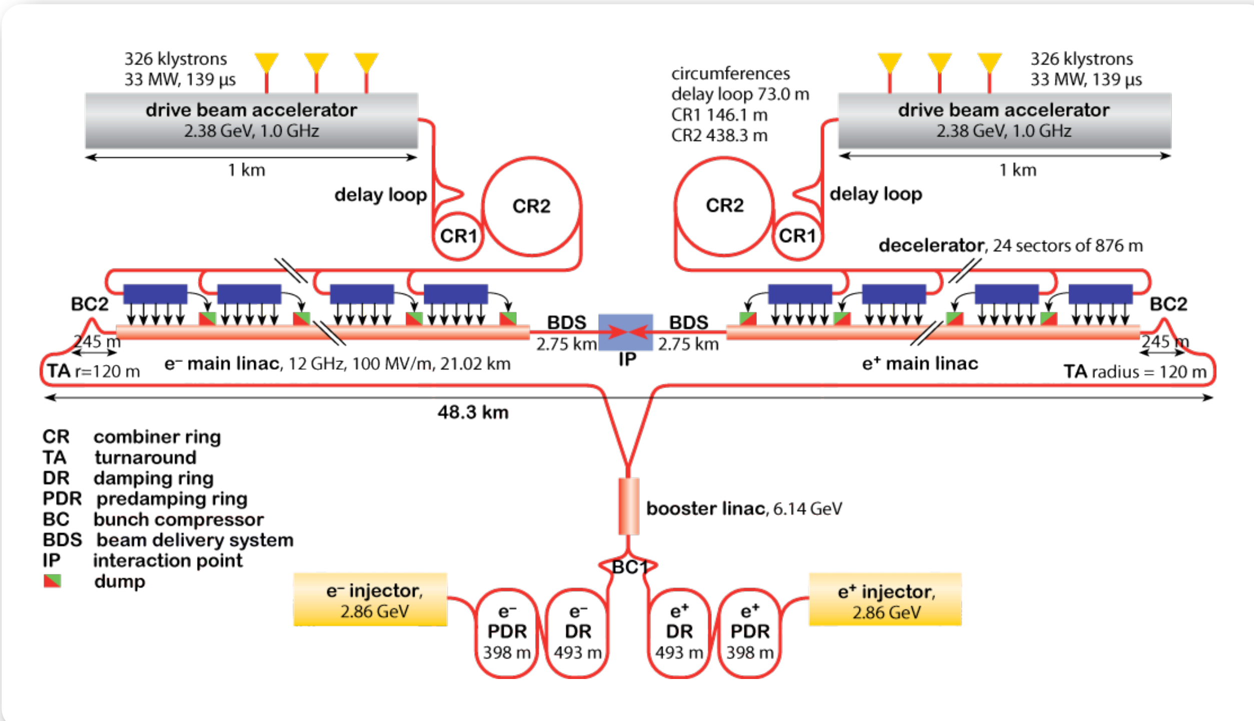

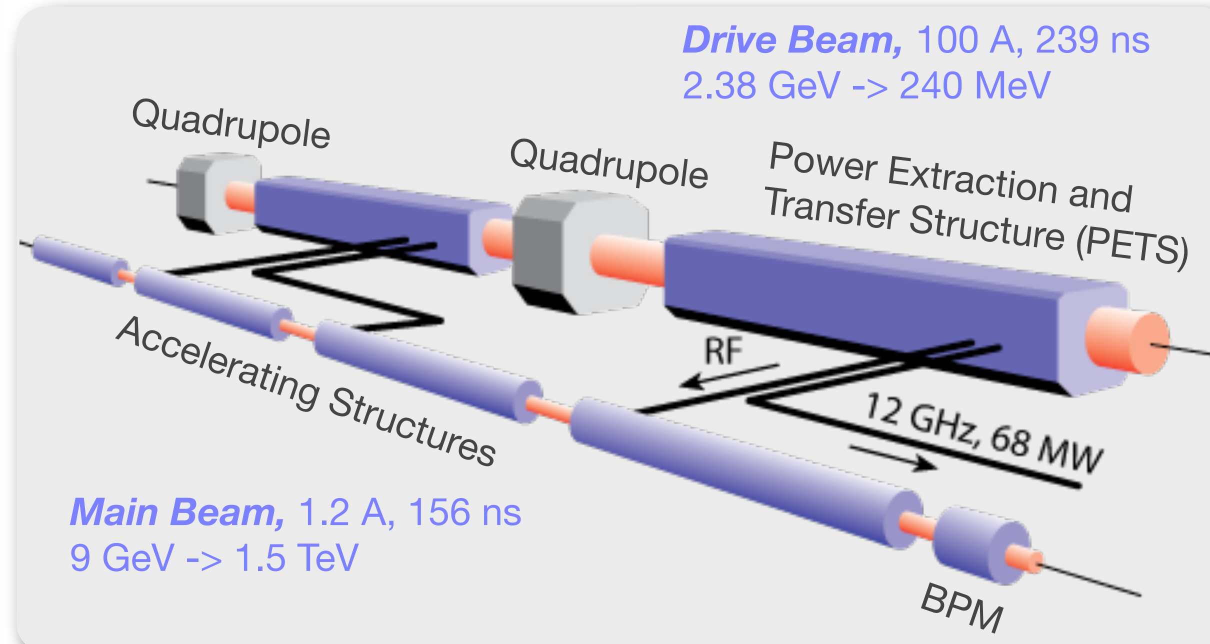

A number of challenges to be mastered for CLIC

- Generation of high-intensity drive beam
- Generation of the required power by PETS

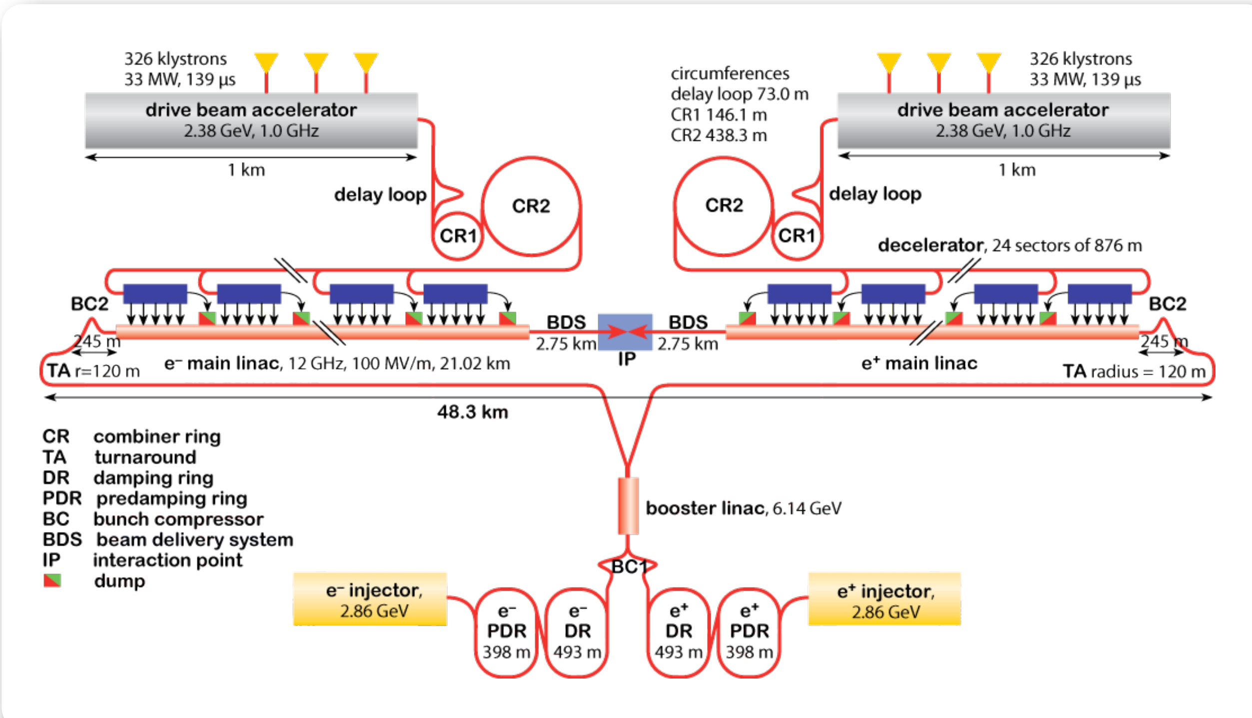

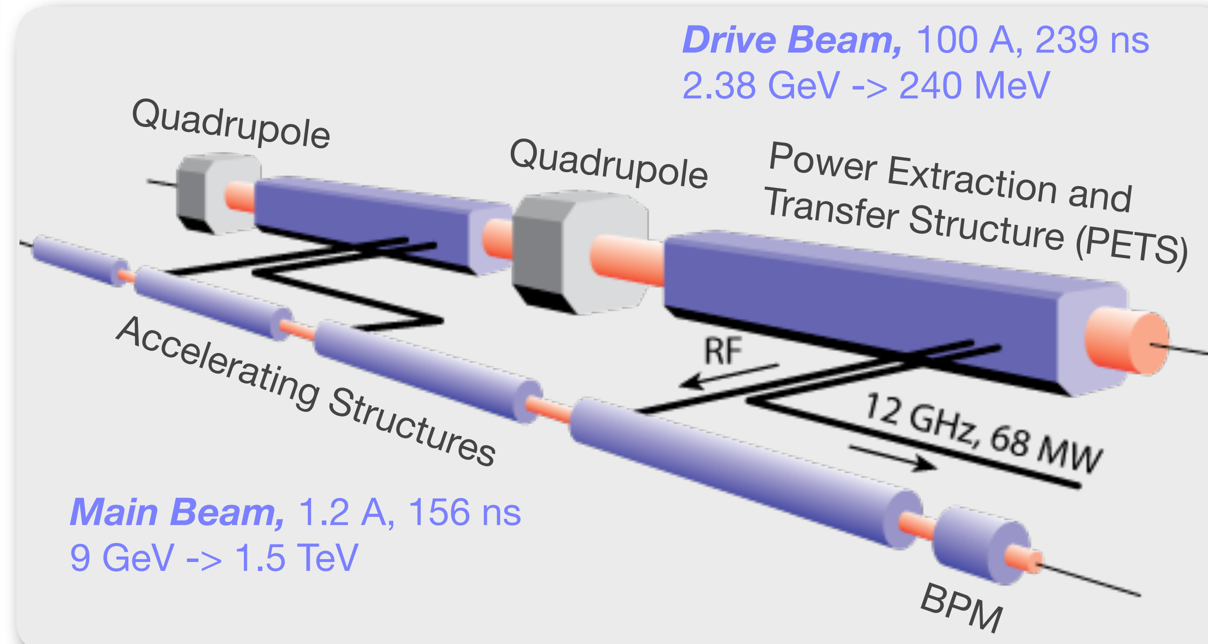

A number of challenges to be mastered for CLIC

- Generation of high-intensity drive beam
- Generation of the required power by PETS
- Focusing of the beam size down to nanometer scale

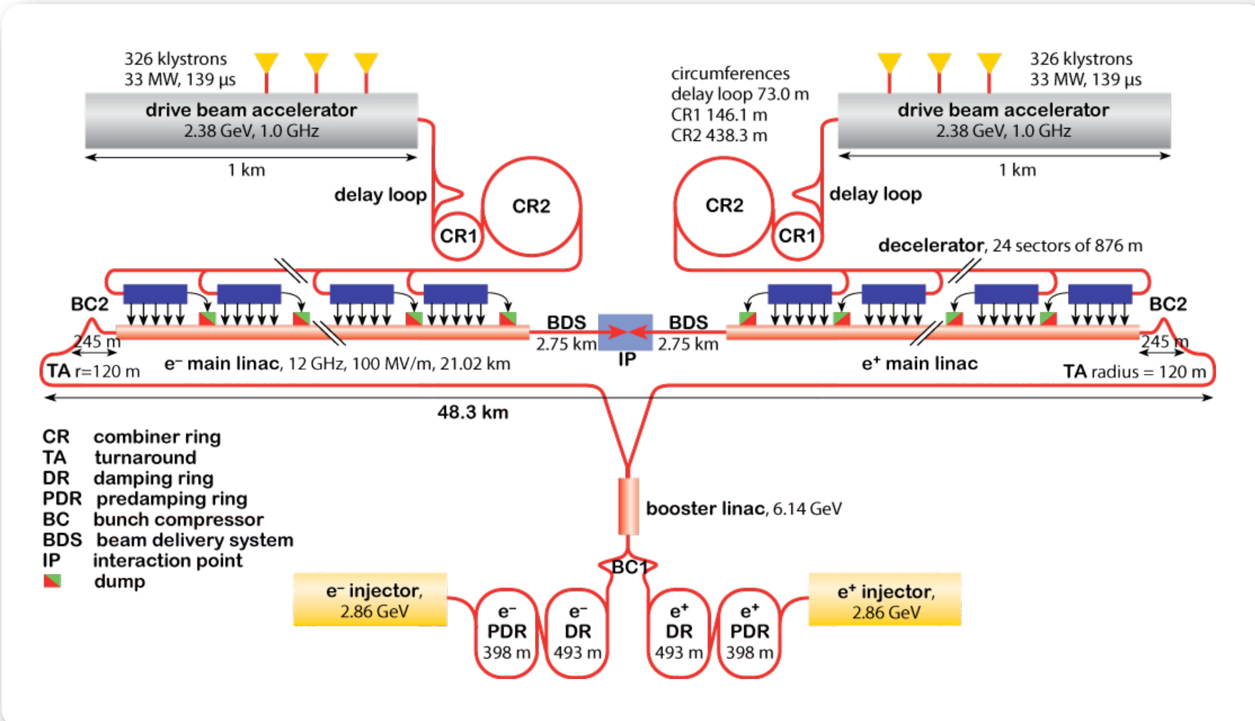

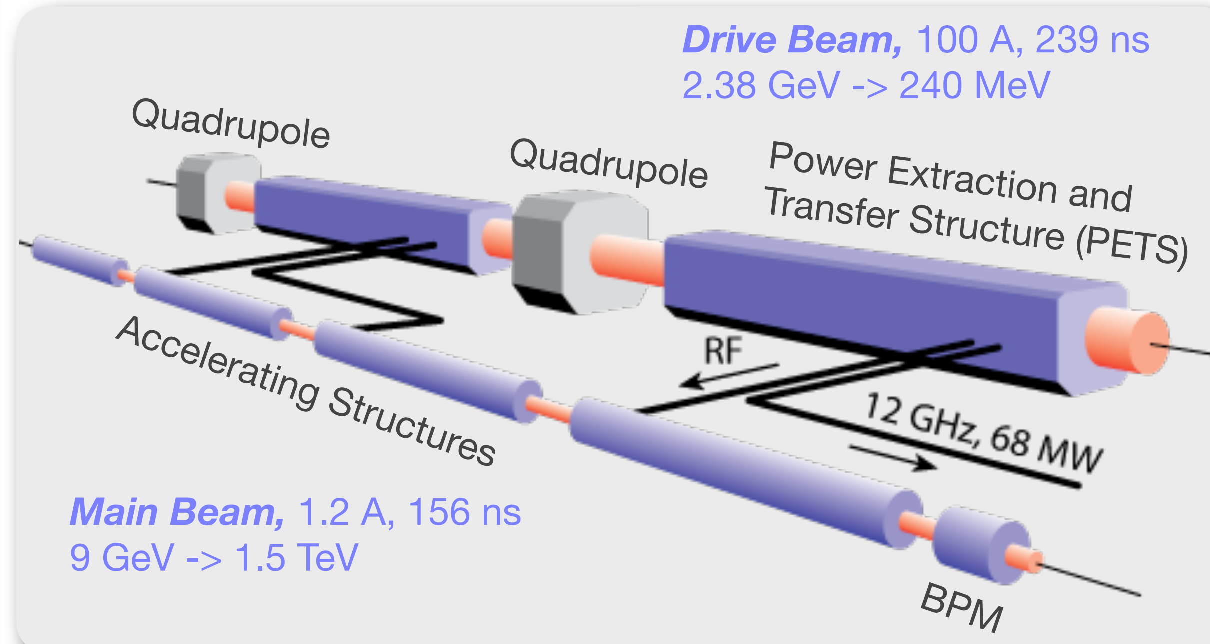

A number of challenges to be mastered for CLIC

- Generation of high-intensity drive beam
- Generation of the required power by PETS
- Focusing of the beam size down to nanometer scale
- Precise alignment of different components

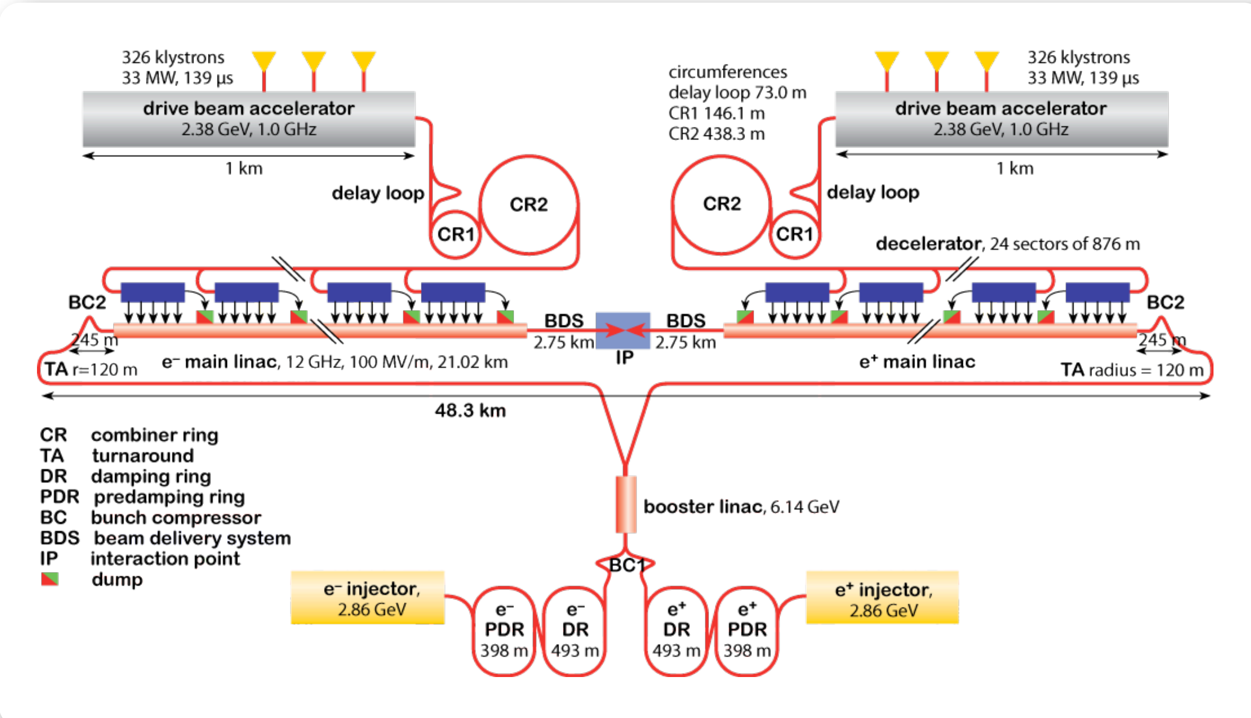

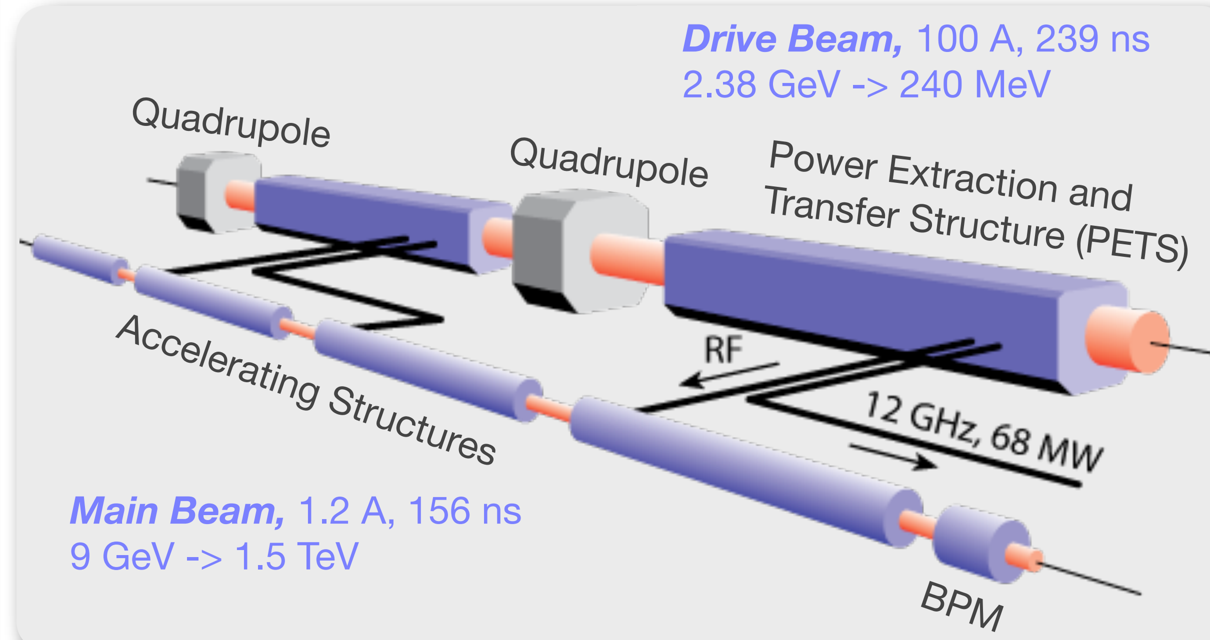

A number of challenges to be mastered for CLIC

- Generation of high-intensity drive beam
- Generation of the required power by PETS
- Focusing of the beam size down to nanometer scale
- Precise alignment of different components

FACT The quality of the main beam acceleration depends on the quality of the drive beam.

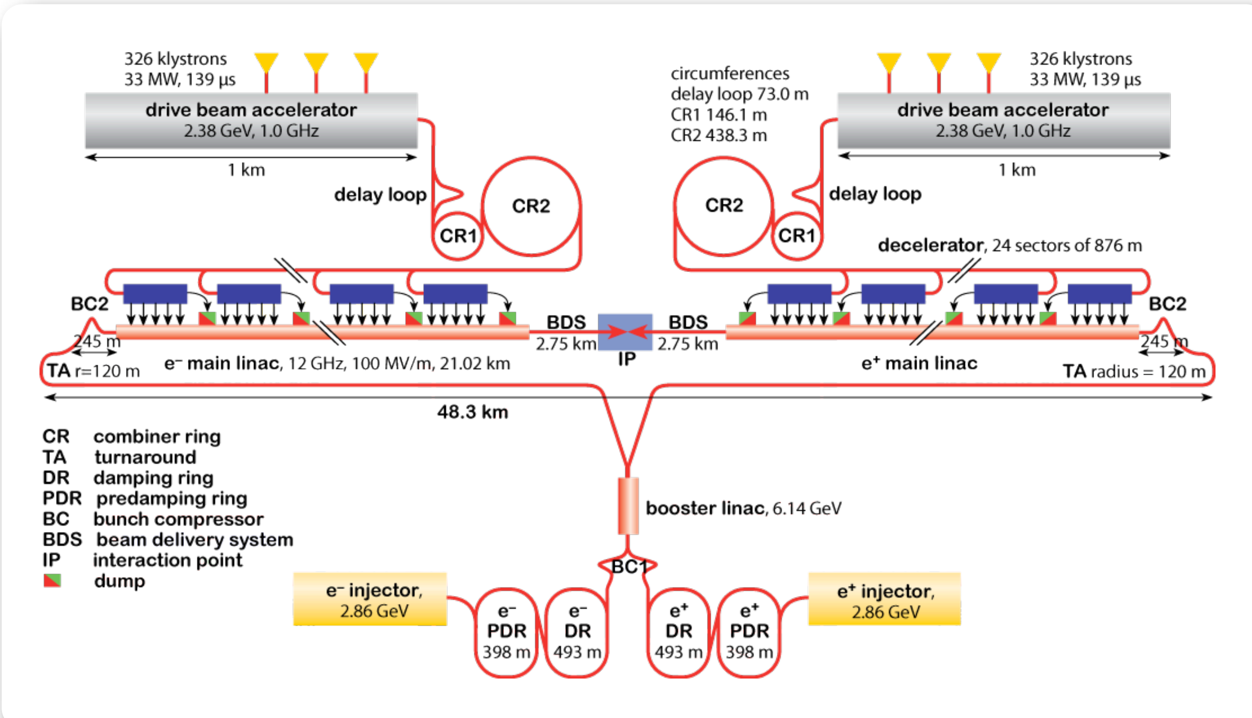

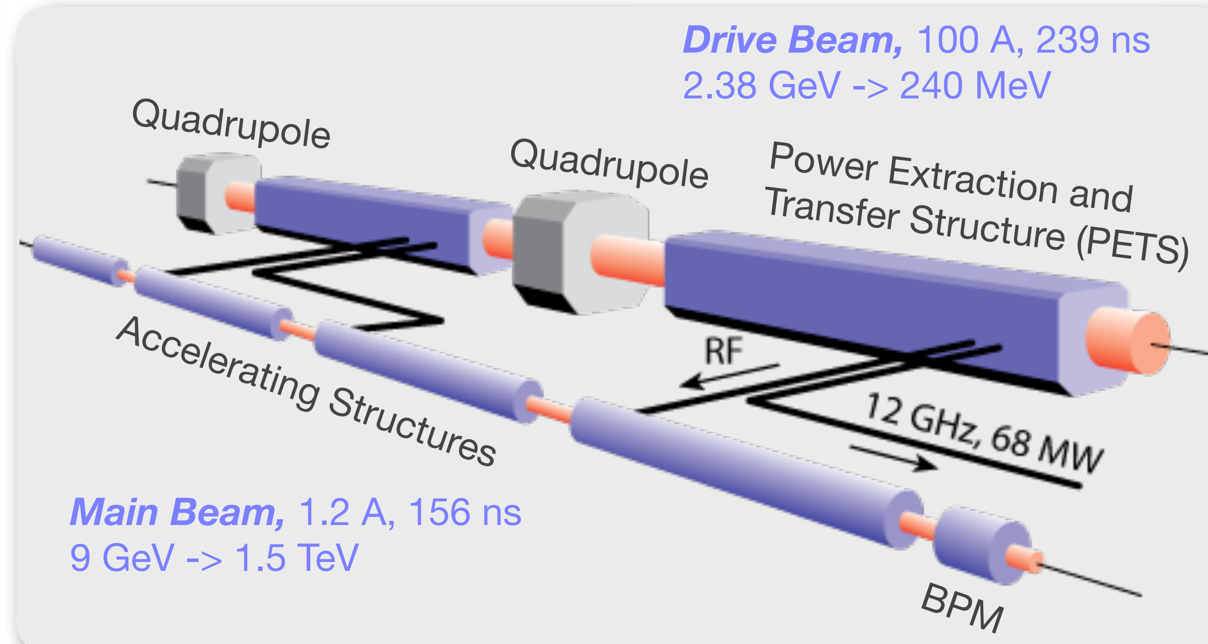

A number of challenges to be mastered for CLIC

- Generation of high-intensity drive beam
- Generation of the required power by PETS
- Focusing of the beam size down to nanometer scale
- Precise alignment of different components

FACT The quality of the main beam acceleration depends on the quality of the drive beam.

MISSION The choice and optimization of the drive beam injector...

The existing thermionic gun for the CLIC Test Facility 3

The existing thermionic gun for the CLIC Test Facility 3

A former step towards the CLIC-DB

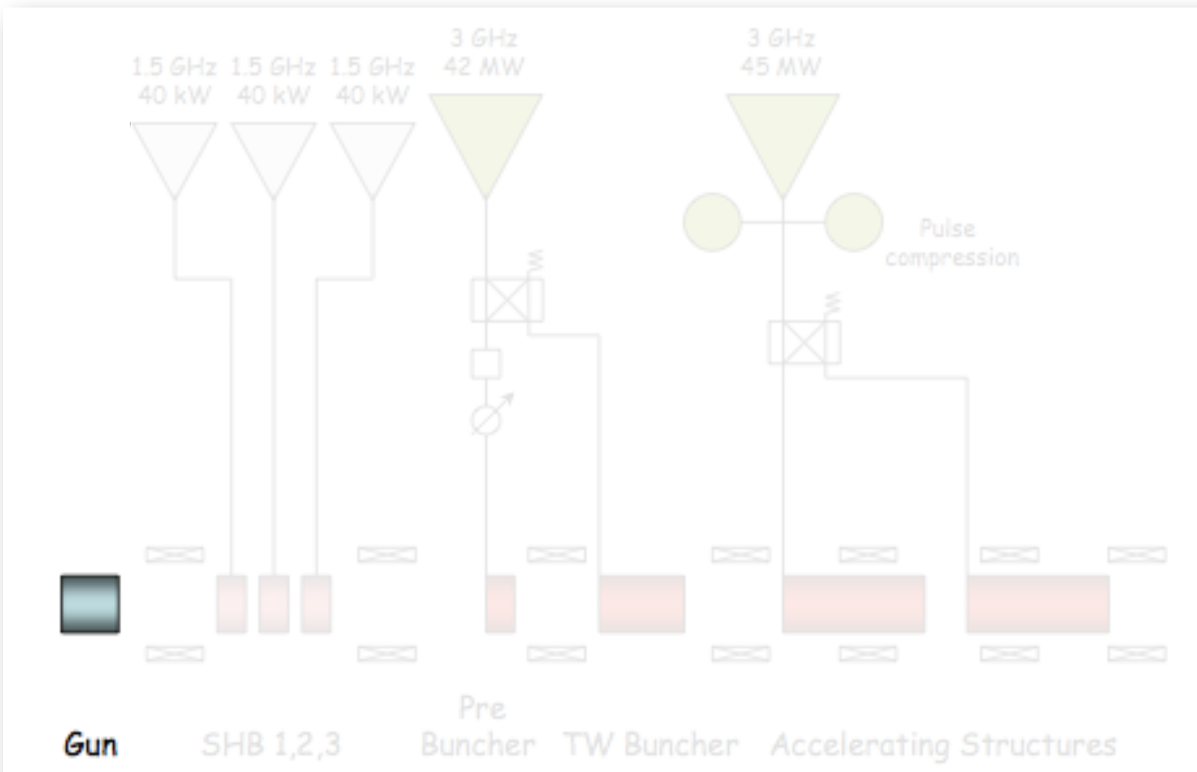

- The continuous 1.6 μs long drive beam pulse is generated by a thermionic gun,

The existing thermionic gun for the CLIC Test Facility 3

A former step towards the CLIC-DB

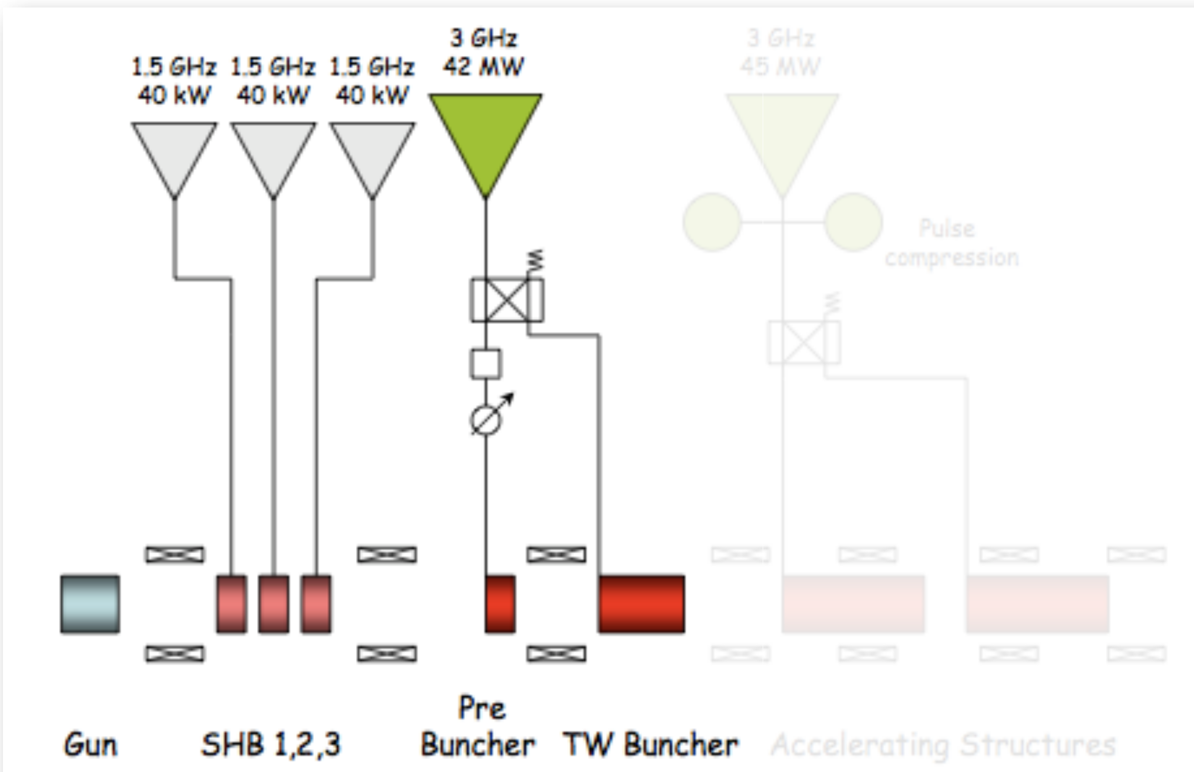

- The continuous 1.6 μs long drive beam pulse is generated by a thermionic gun,
- then, time structure is produced by
  - three 1.5 GHz sub-harmonic bunchers
  - a S-band pre-buncher
  - a traveling wave buncher

The existing thermionic gun for the CLIC Test Facility 3

A former step towards the CLIC-DB

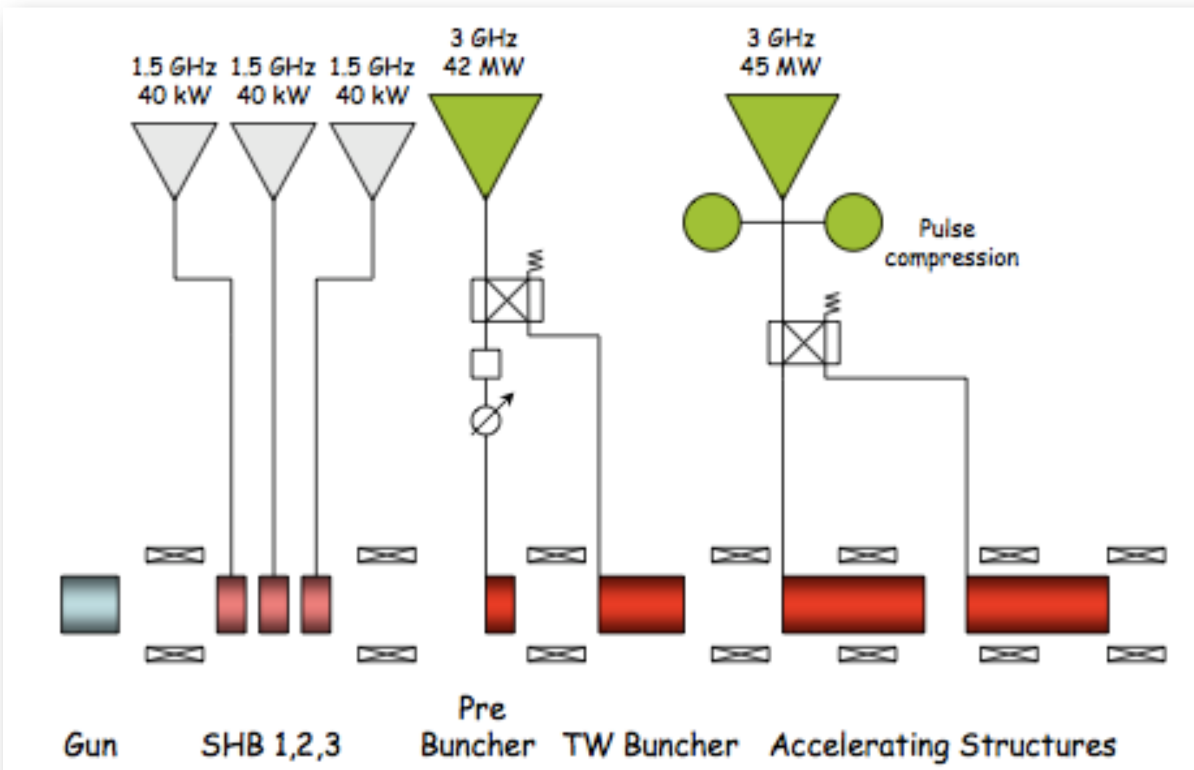

- The continuous 1.6 μs long drive beam pulse is generated by a thermionic gun,
- then, time structure is produced by
  - three 1.5 GHz sub-harmonic bunchers
  - a S-band pre-buncher
  - a traveling wave buncher
- beam proceeds to two accelerating sections.

The existing thermionic gun for the CLIC Test Facility 3

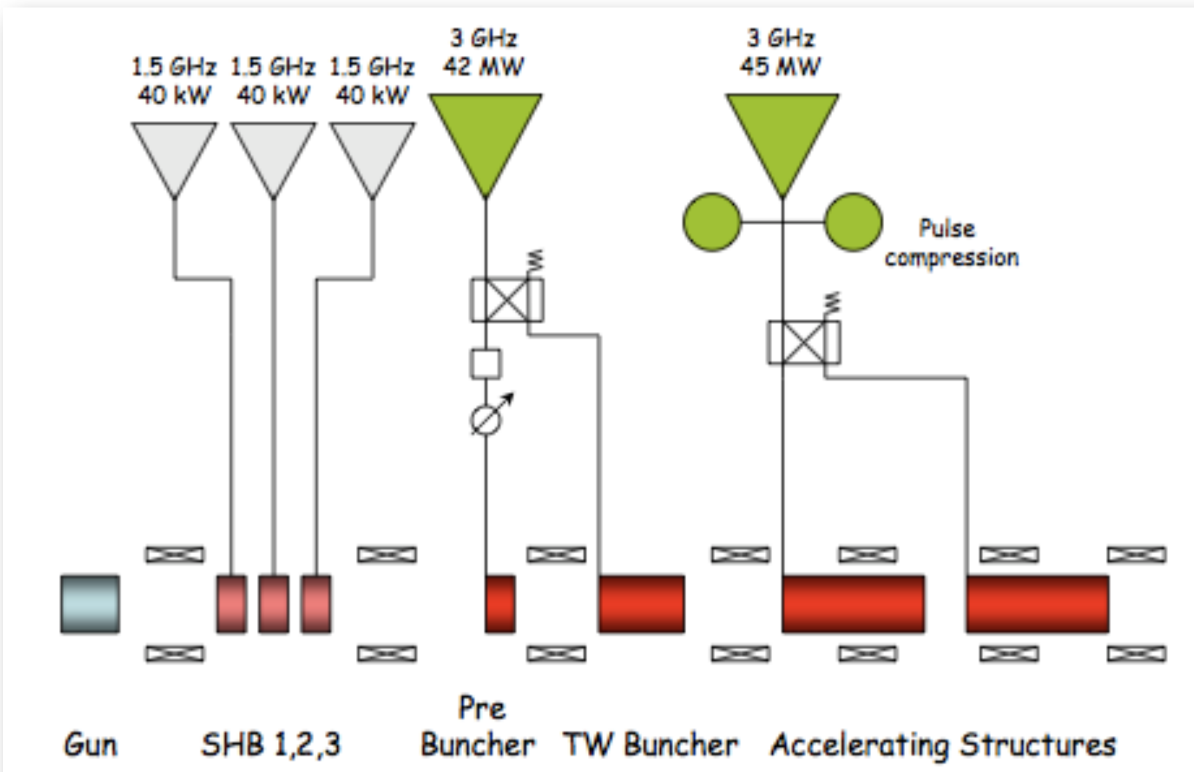

- The 1.6 μs long drive beam pulse is generated by a 140 kV, 9 A thermionic triode gun,
- then, time structure is produced by
    - 1.5 GHz sub-harmonic bunchers
    - S-band pre-buncher
    - travelling wave buncher
- beam proceeds to two accelerating sections.

The existing thermionic gun for the CLIC Test Facility 3

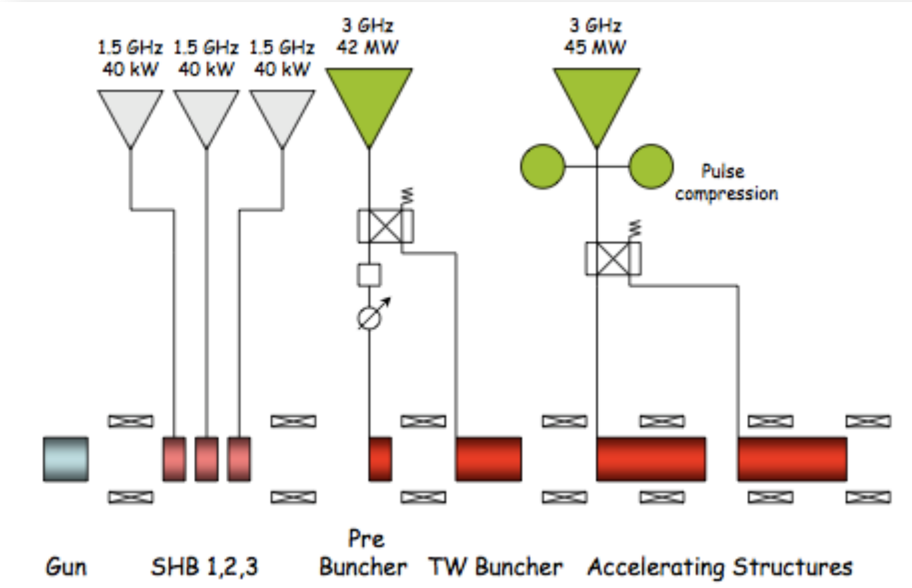

- The 1.6 μs long drive beam pulse is generated by a 140 kV, 9 A thermionic triode gun,
- then, time structure is produced by
  - 1.5 GHz sub-harmonic bunchers
  - S-band pre-buncher
  - travelling wave buncher
- beam proceeds to two accelerating sections.

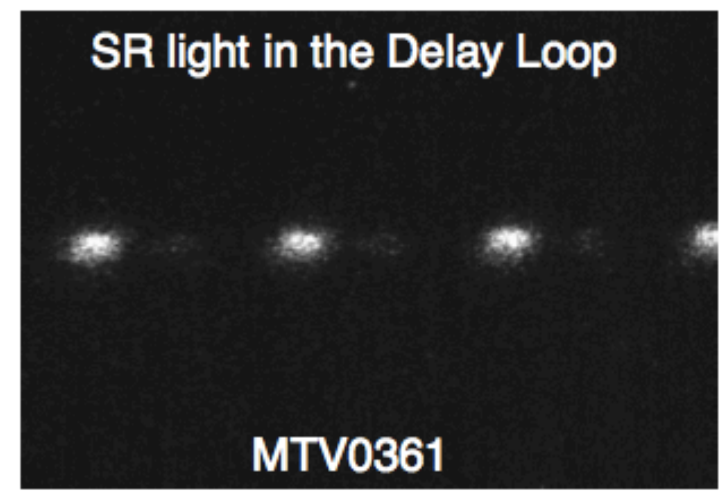

Problem, Parasitic Charge (Satellite Bunches)

Streak camera measurements can reveal the parasitic charge.

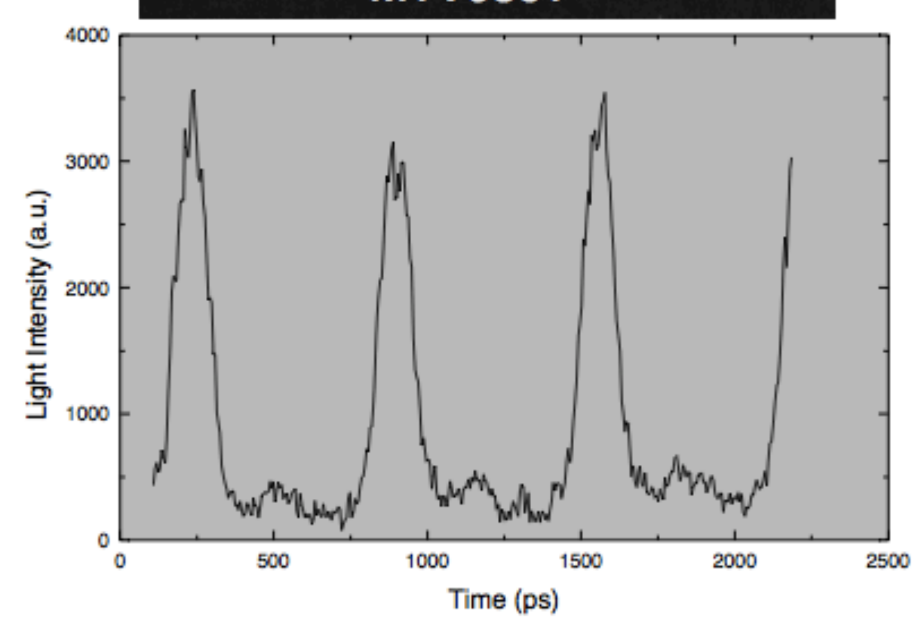

The existing thermionic gun for the CLIC Test Facility 3

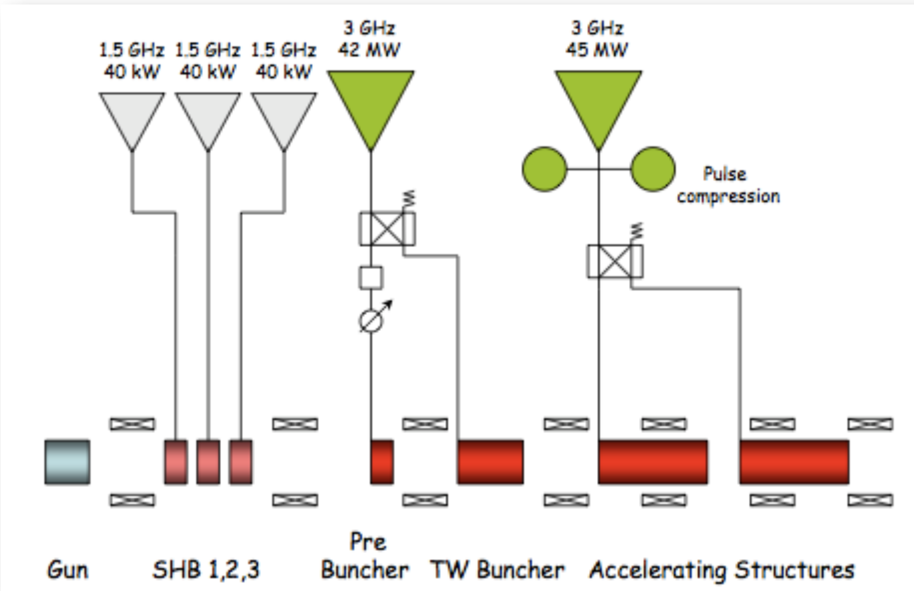

- The 1.6 μs long drive beam pulse is generated by a 140 kV, 9 A thermionic triode gun,
- then, time structure is produced by
  - 1.5 GHz sub-harmonic bunchers
  - S-band pre-buncher
  - travelling wave buncher
- beam proceeds to two accelerating sections.

Problem, Parasitic Charge (Satellite Bunches)

Streak camera measurements can reveal the parasitic charge.

- 7-8% parasitic charge (satellite bunches) due to the sub-harmonic bunchers.

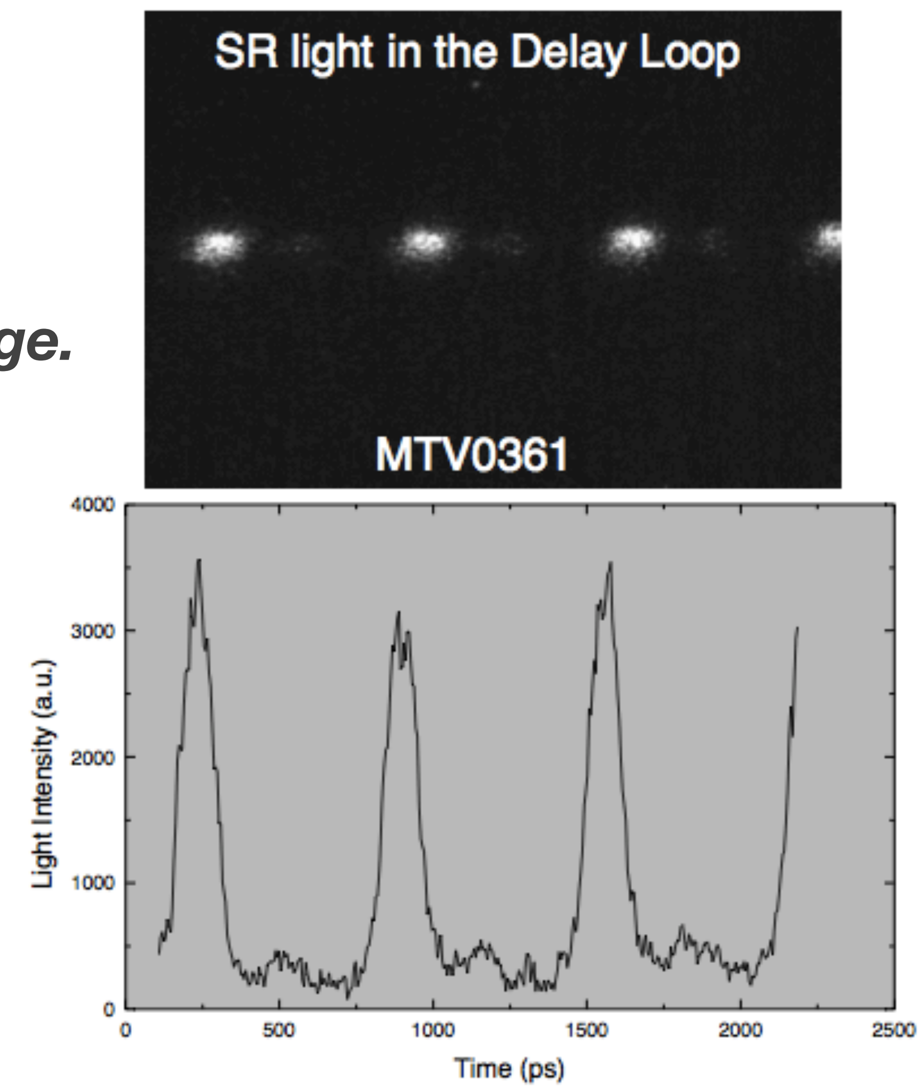

The existing thermionic gun for the CLIC Test Facility 3

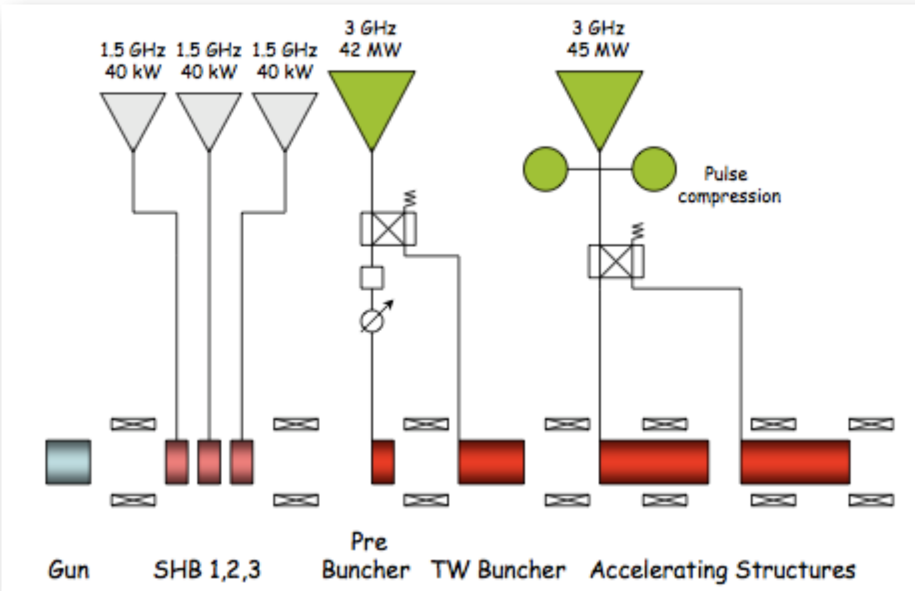

- The 1.6 μs long drive beam pulse is generated by a 140 kV, 9 A thermionic triode gun,
- then, time structure is produced by
  - 1.5 GHz sub-harmonic bunchers
  - S-band pre-buncher
  - travelling wave buncher
- beam proceeds to two accelerating sections.

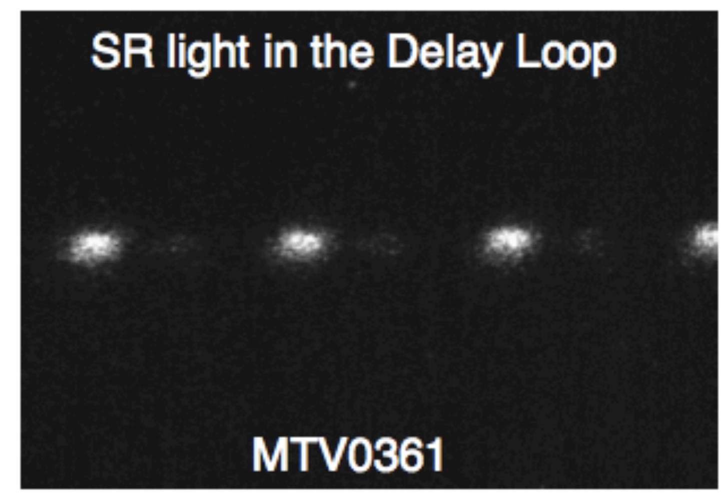

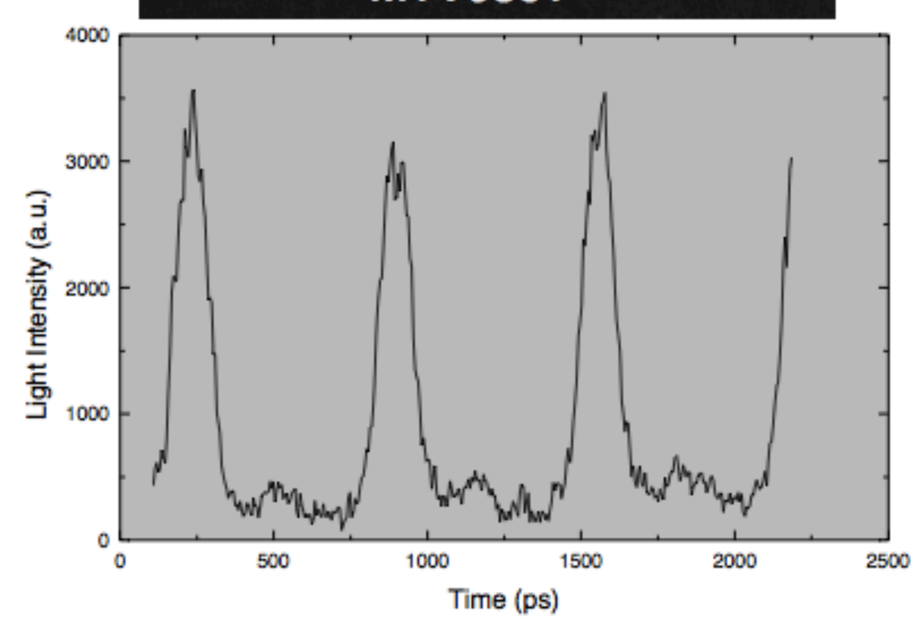

Problem, Parasitic Charge (Satellite Bunches)

Streak camera measurements can reveal the parasitic charge.

- 7-8% parasitic charge (satellite bunches) due to the sub-harmonic bunchers.
- The charge inside the satellite bunches is unusable for the rest of the operation,

The existing thermionic gun for the CLIC Test Facility 3

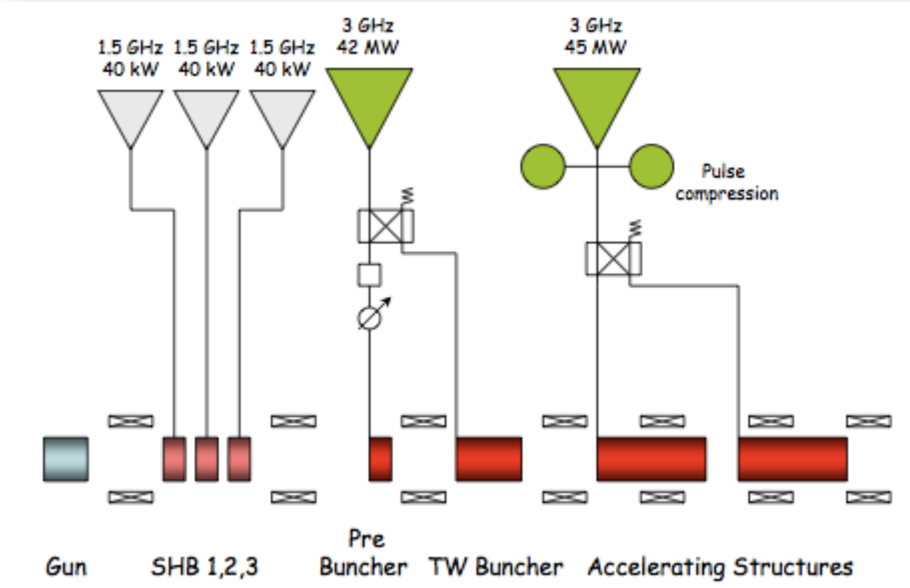

- The 1.6 μs long drive beam pulse is generated by a 140 kV, 9 A thermionic triode gun,
- then, time structure is produced by
  - 1.5 GHz sub-harmonic bunchers
  - S-band pre-buncher
  - travelling wave buncher
- beam proceeds to two accelerating sections.

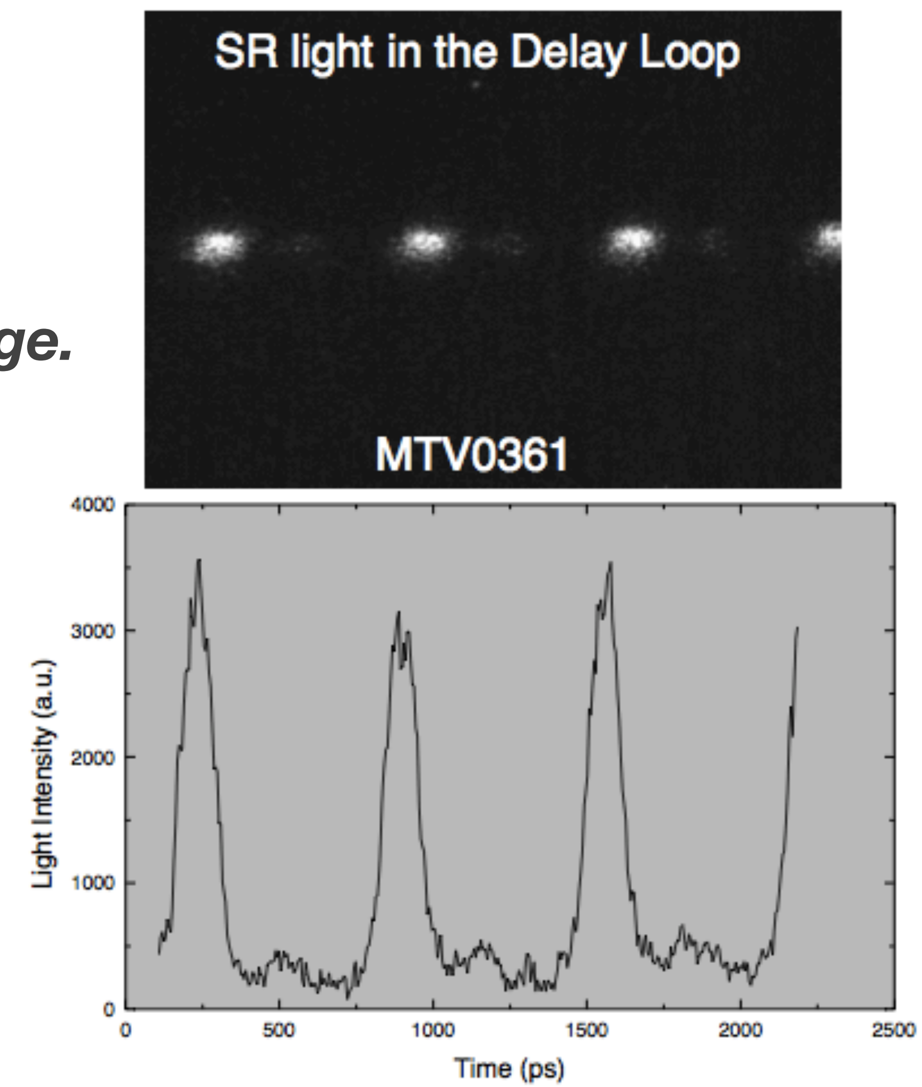

Problem, Parasitic Charge (Satellite Bunches)

Streak camera measurements can reveal the parasitic charge.

- 7-8% parasitic charge (satellite bunches) due to the sub-harmonic bunchers.
- The charge inside the satellite bunches is unusable for the rest of the operation,
- Disturbs the acceleration of the main beam.

The existing thermionic gun for the CLIC Test Facility 3

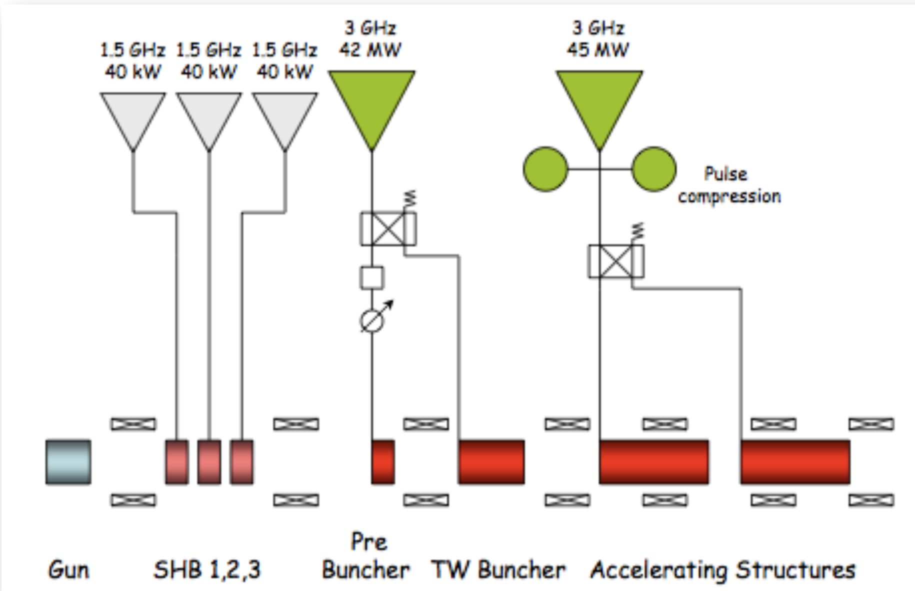

- The 1.6 μs long drive beam pulse is generated by a 140 kV, 9 A thermionic triode gun,
- then, time structure is produced by
  - 1.5 GHz sub-harmonic bunchers
  - S-band pre-buncher
  - travelling wave buncher
- beam proceeds to two accelerating sections.

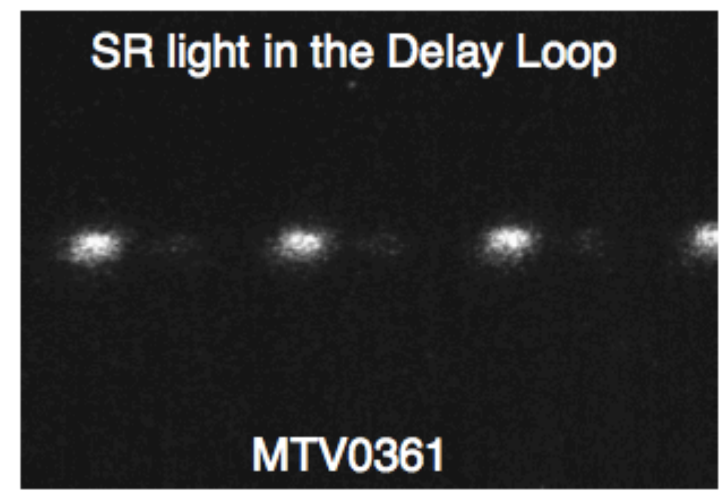

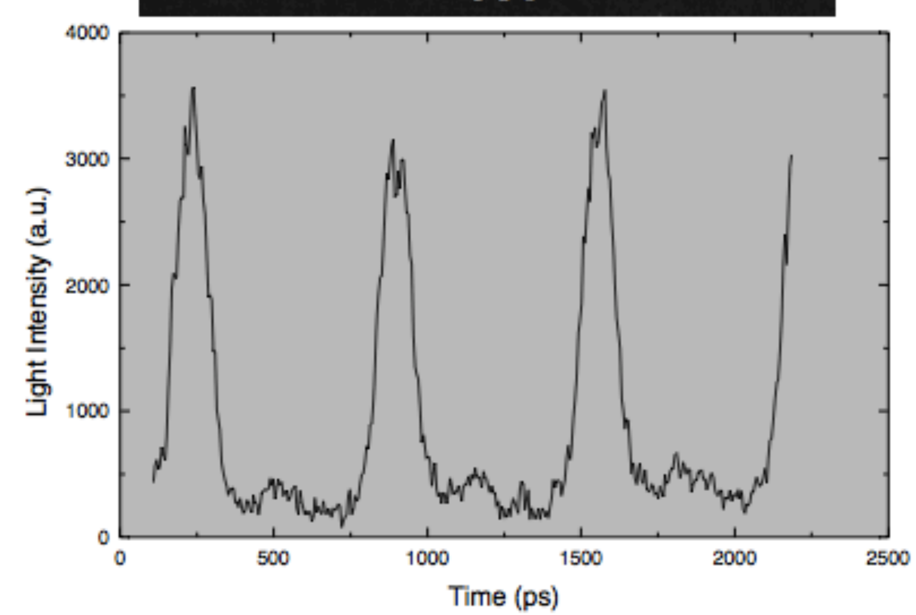

Problem, Parasitic Charge (Satellite Bunches)

Streak camera measurements can reveal the parasitic charge.

- 7-8% parasitic charge (satellite bunches) due to the sub-harmonic bunchers.
- The charge inside the satellite bunches is unusable for the rest of the operation,
- Disturbs the acceleration of the main beam.
- Compactness, flexibility, stability?

- **Preface,** the original contribution in a deductive view of CLIC project
- **PHIN photoinjector**, objectives of the research
- **Beam instrumentation & characterization,** commissioning highlights of PHIN
- **Conclusions**

What is a photoinjector?

What is a photoinjector?

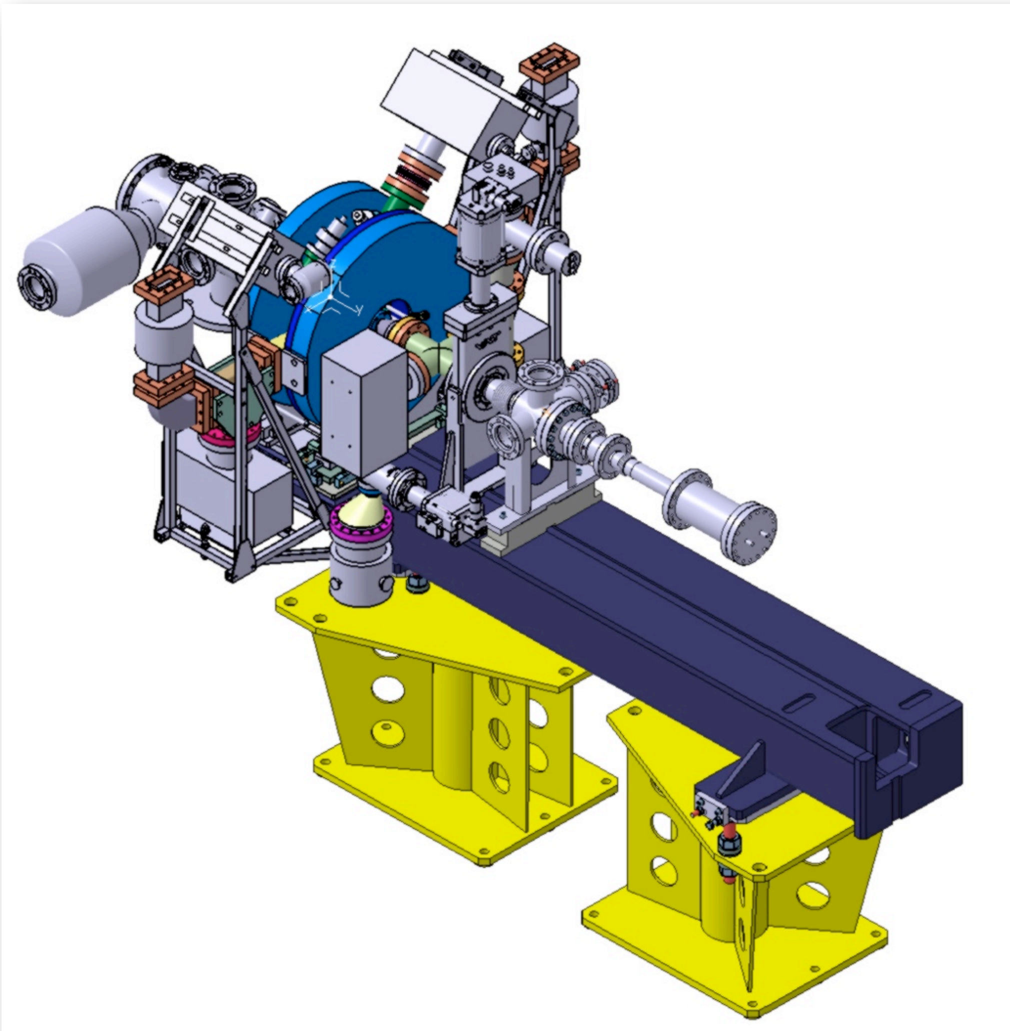

What is a photoinjector?

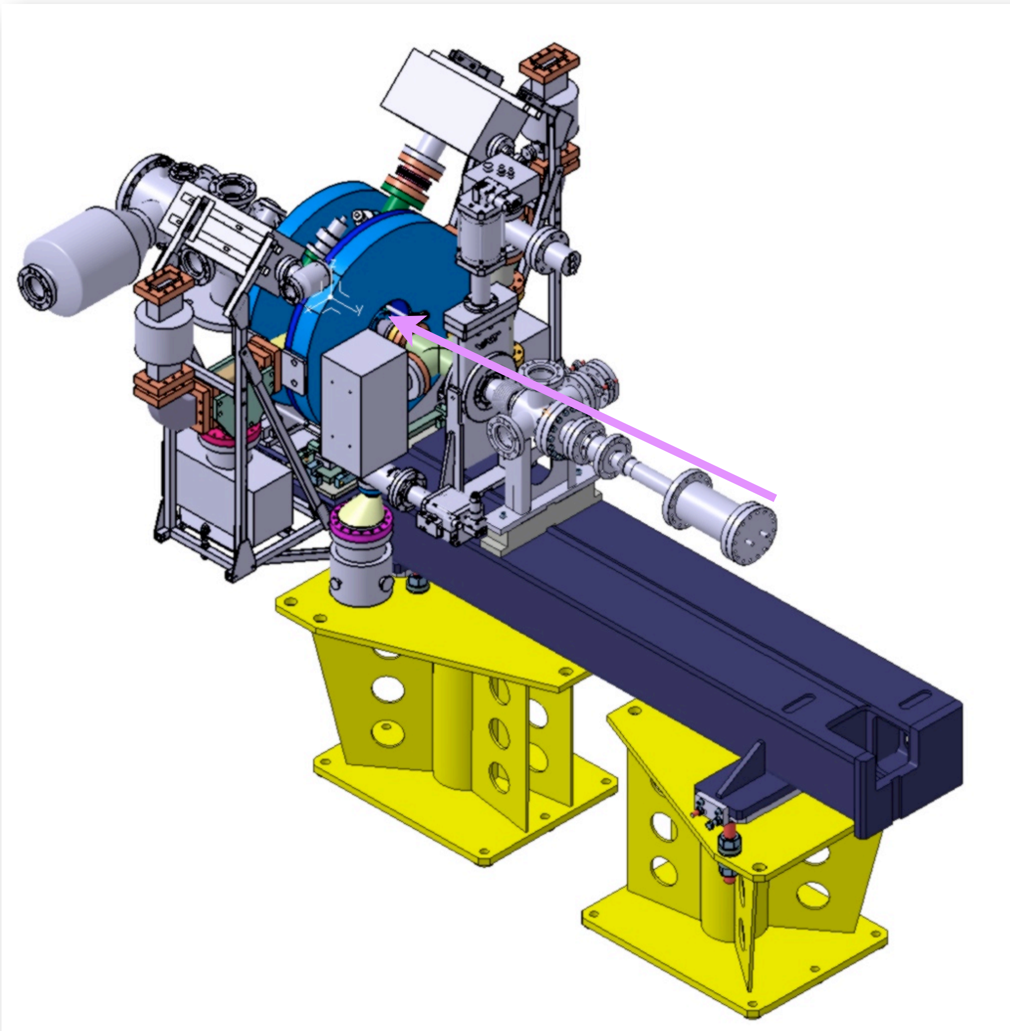

- A photoinjector is an electron source that uses **laser** pulses in order to extract electrons from the surface of a metallic or semiconductor **cathode** by using the **photoemission** process.

What is a photoinjector?

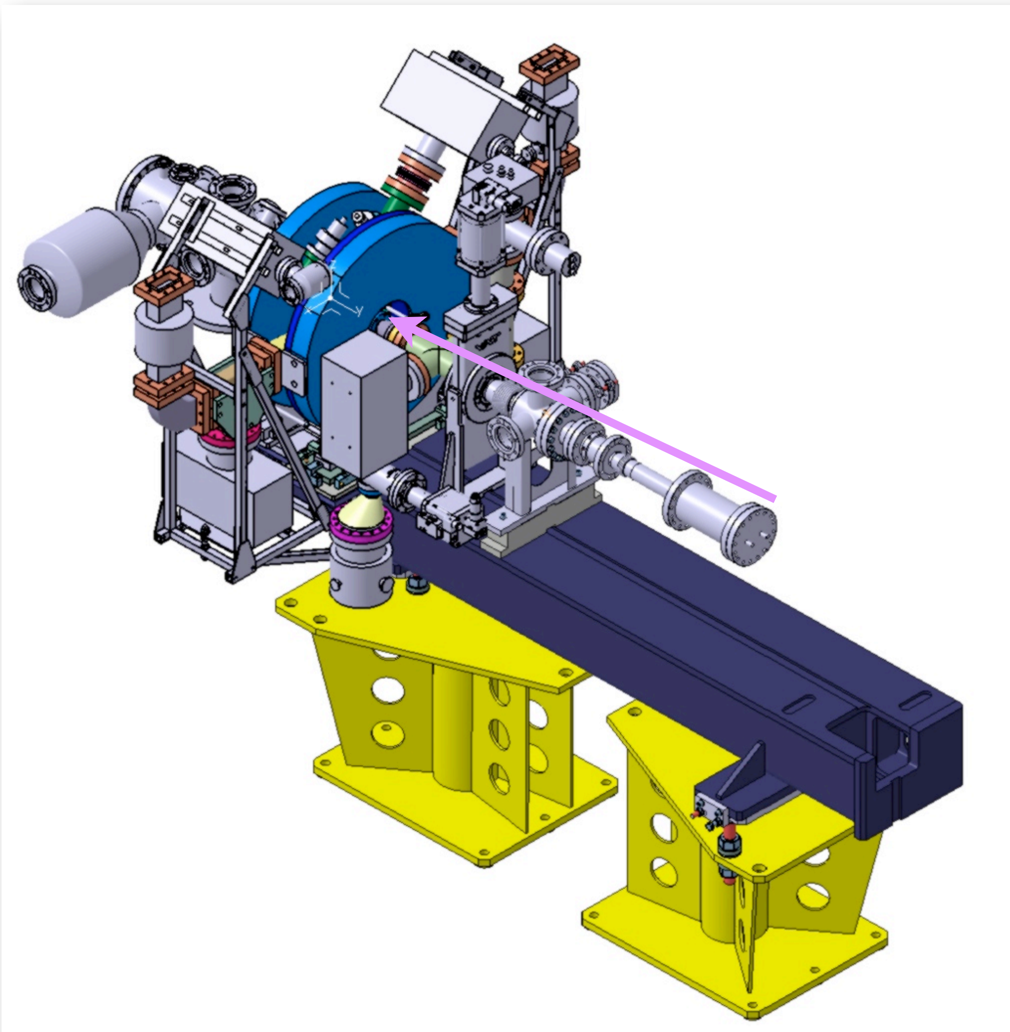

- A photoinjector is an electron source that uses **laser** pulses in order to extract electrons from the surface of a metallic or semiconductor **cathode** by using the **photoemission** process.
- The electron beam resembles the temporal structure of the laser beam therefore it is **a compact system** without need for an additional bunching system.

What is a photoinjector?

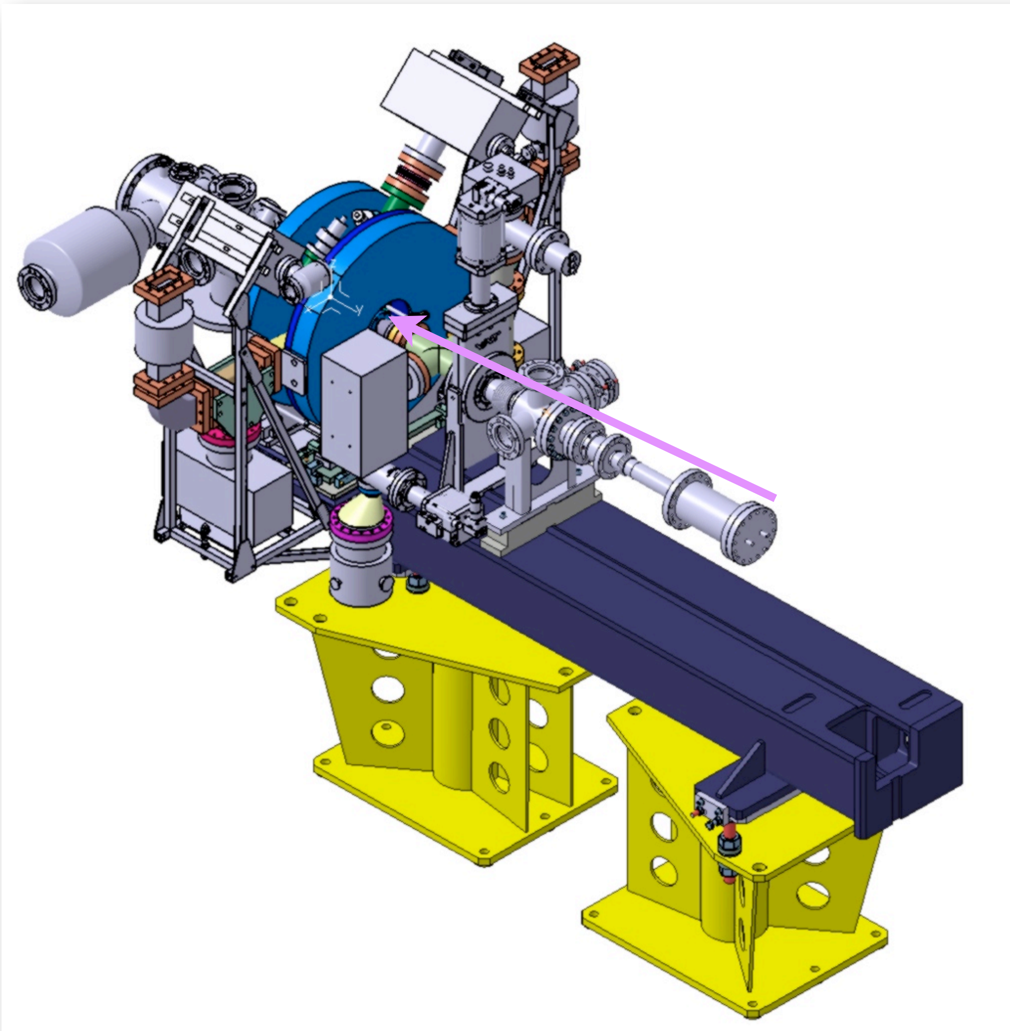

- A photoinjector is an electron source that uses **laser** pulses in order to extract electrons from the surface of a metallic or semiconductor **cathode** by using the **photoemission** process.
- The electron beam resembles the temporal structure of the laser beam therefore it is **a compact system** without need for an additional bunching system.
- An **RF cavity** is used for rapid acceleration of the electrons after the emission.

What is a photoinjector?

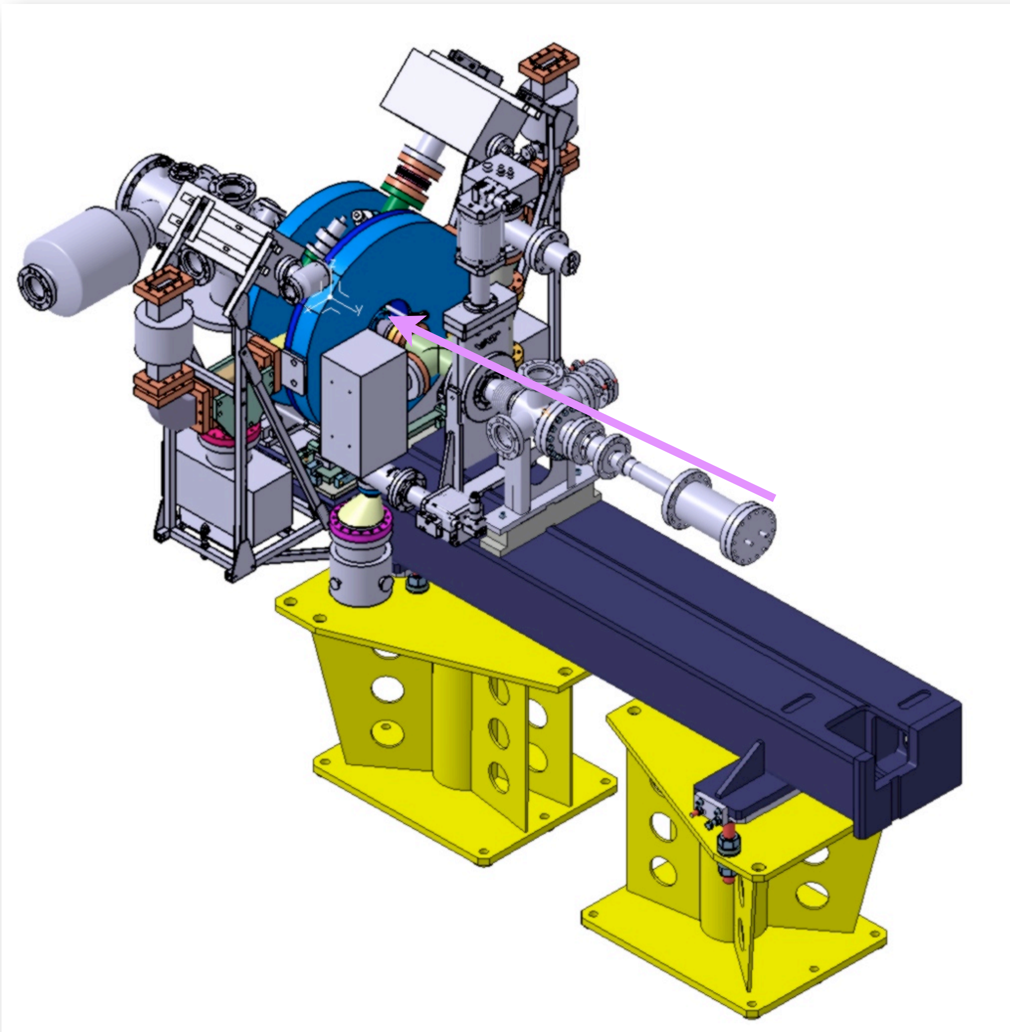

- A photoinjector is an electron source that uses **laser** pulses in order to extract electrons from the surface of a metallic or semiconductor **cathode** by using the **photoemission** process.
- The electron beam resembles the temporal structure of the laser beam therefore it is **a compact system** without need for an additional bunching system.
- An **RF cavity** is used for rapid acceleration of the electrons after the emission.
- Solenoid magnets are placed in order to focus the space charge dominated beam and achieve the **emittance compensation**.

A Photoinjector project for CTF3 and for future CLIC-DB source.

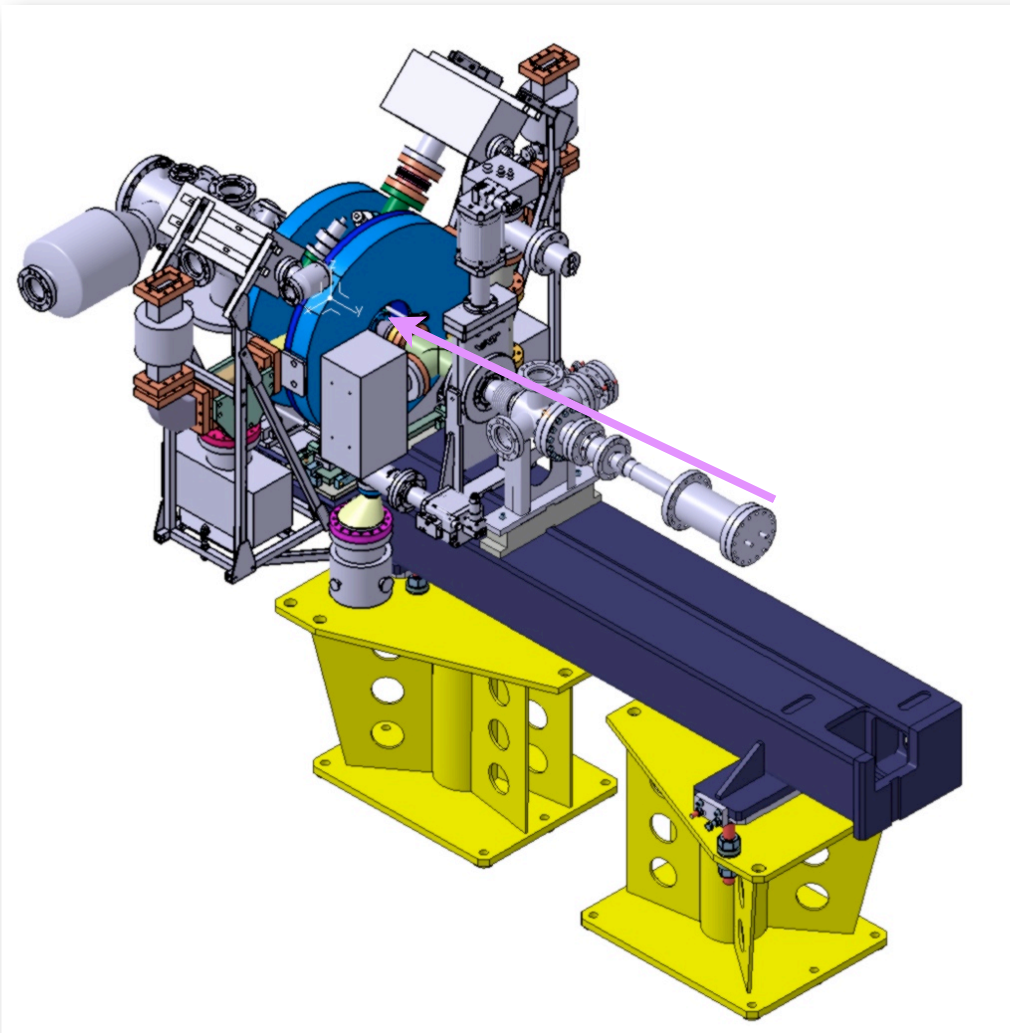

A Photoinjector project for CTF3 ***and for future CLIC-DB source.***

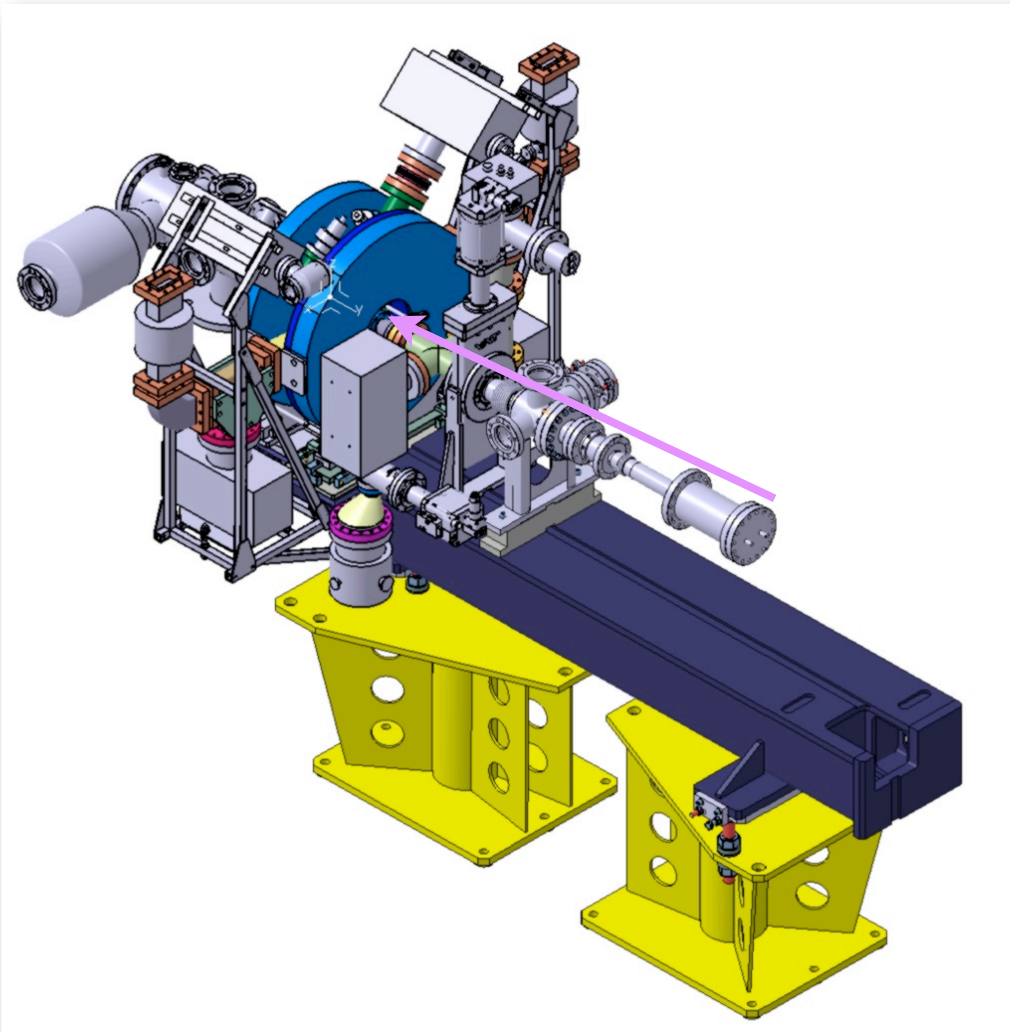

- A photoinjector with the specifications of CTF3 thermionic gun.
- The project is in the framework of the "Coordinated Accelerator Research in Europe (CARE)" program.
- A collaboration...

"Laboratoire de l'Accélérateur Linéaire (LAL)"

RF gun

"Rutherford Appleton Laboratory (RAL)"

Laser

"European Organization for Nuclear Research (CERN)"

Photocathode production,

Overall coordination

Commissioning

A Photoinjector project for CTF3 ***and for future CLIC-DB source.***

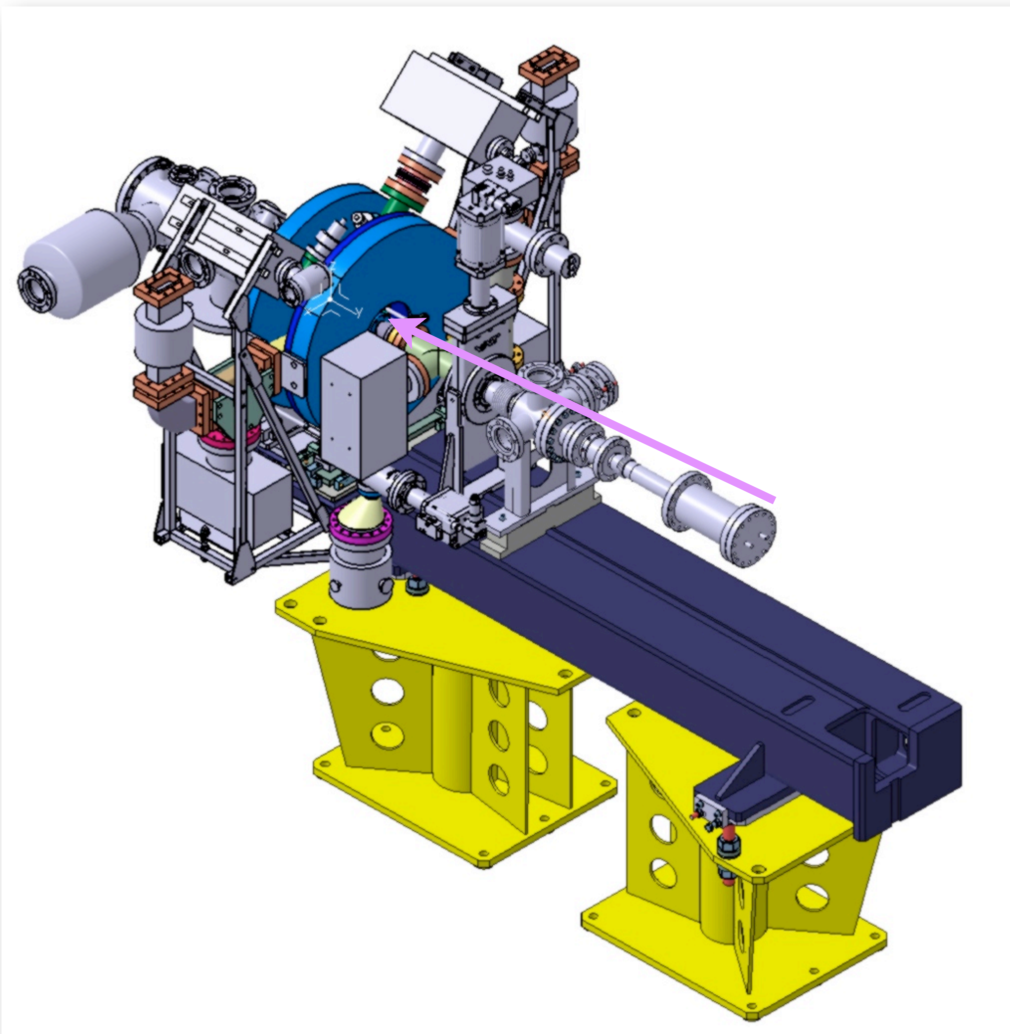

A Photoinjector project for CTF3 *and for future CLIC-DB source.*

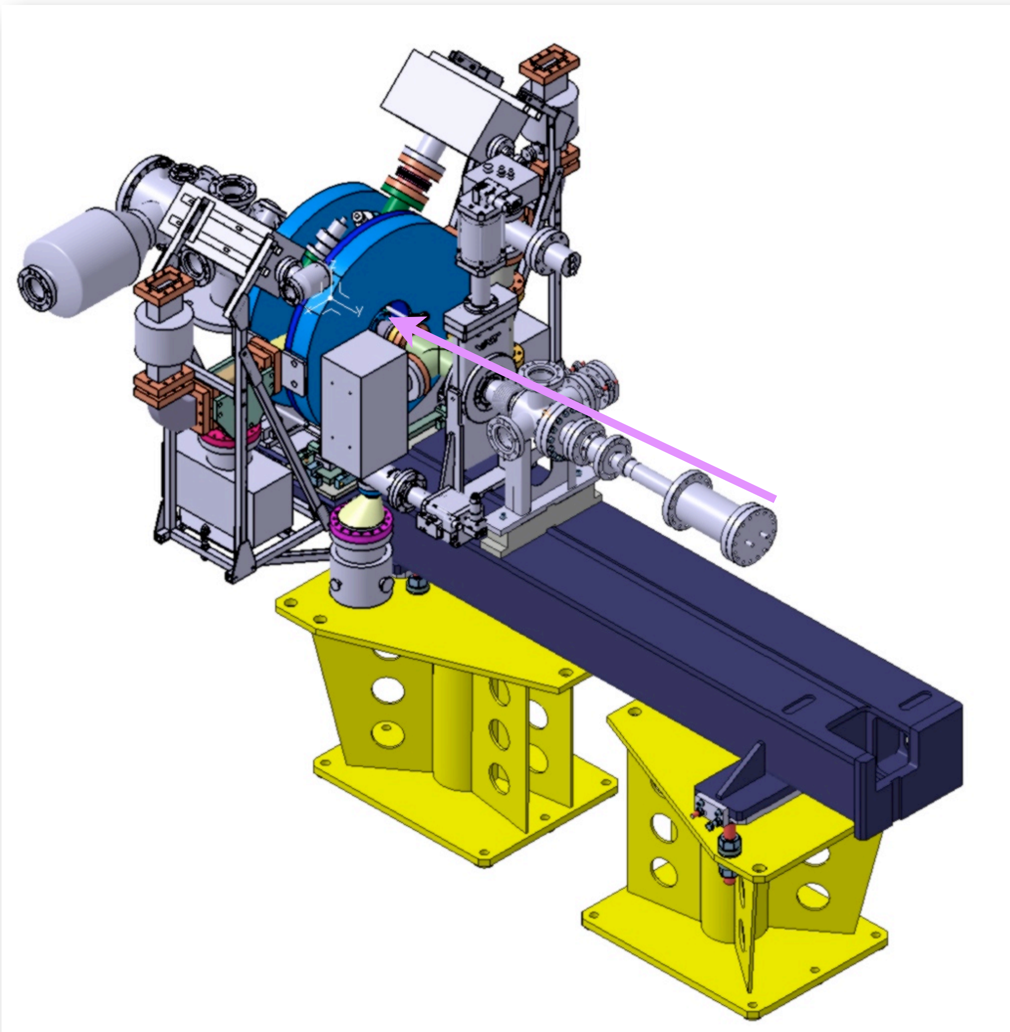

- The basic concepts and the implementation of the photoinjector date back to 1980s. But, ***the PHIN photoinjector is novel due to the following reasons:***

***A Photoinjector project for CTF3** and for future CLIC-DB source.*

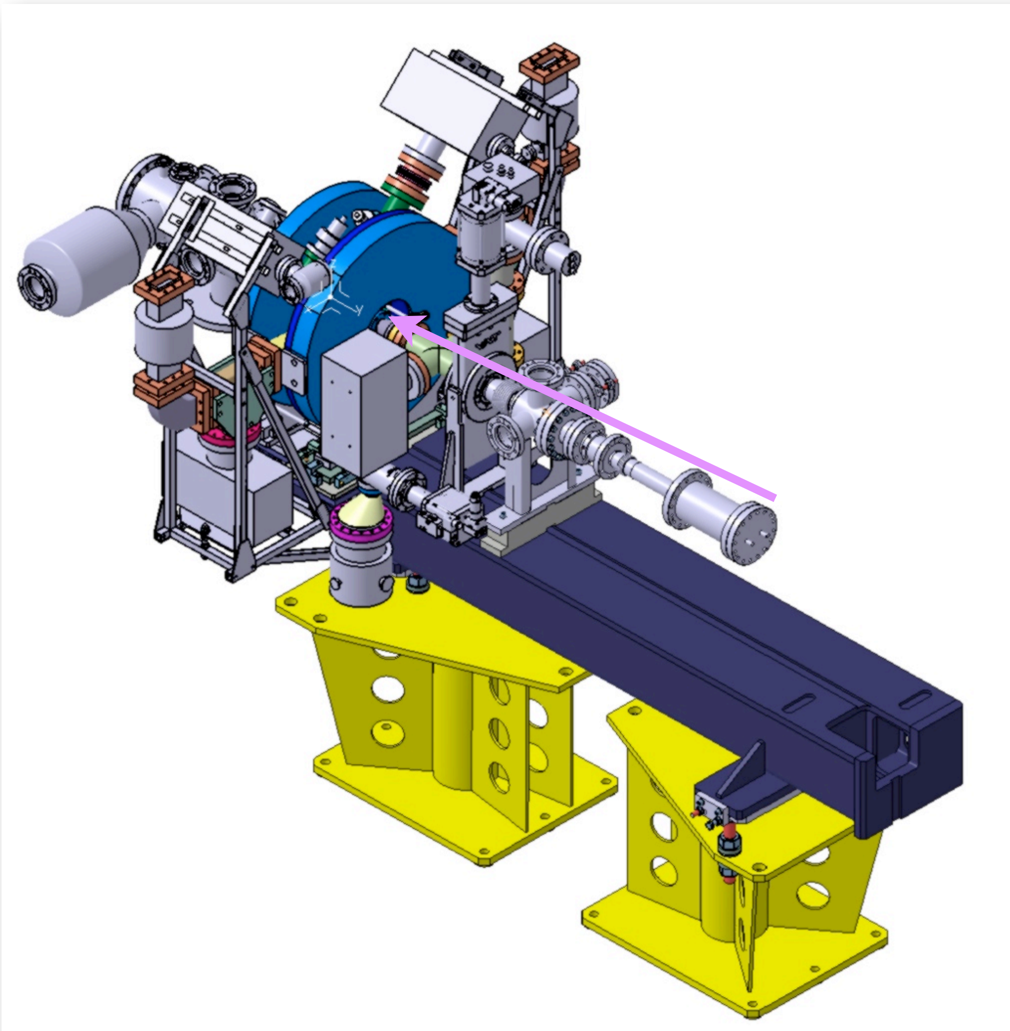

- The basic concepts and the implementation of the photoinjector date back to 1980s. But, ***the PHIN photoinjector is novel due to the following reasons:***
- high charge specification of 2.33 nC

A Photoinjector project for CTF3 ***and for future CLIC-DB source.***

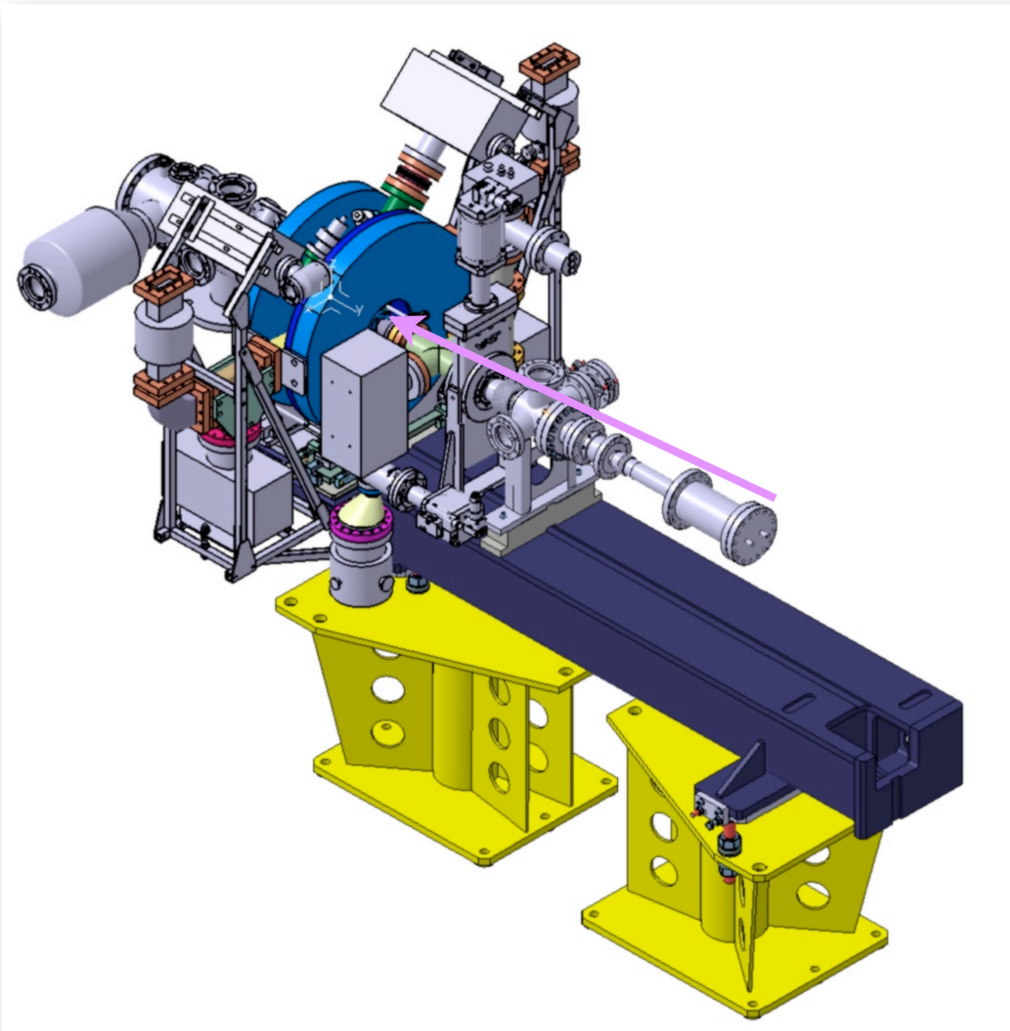

- The basic concepts and the implementation of the photoinjector date back to 1980s. But, ***the PHIN photoinjector is novel due to the following reasons:***
- high charge specification of 2.33 nC
- 1.2 μs long pulse train generation with 1908 bunches,

***A Photoinjector project for CTF3** and for future CLIC-DB source.*

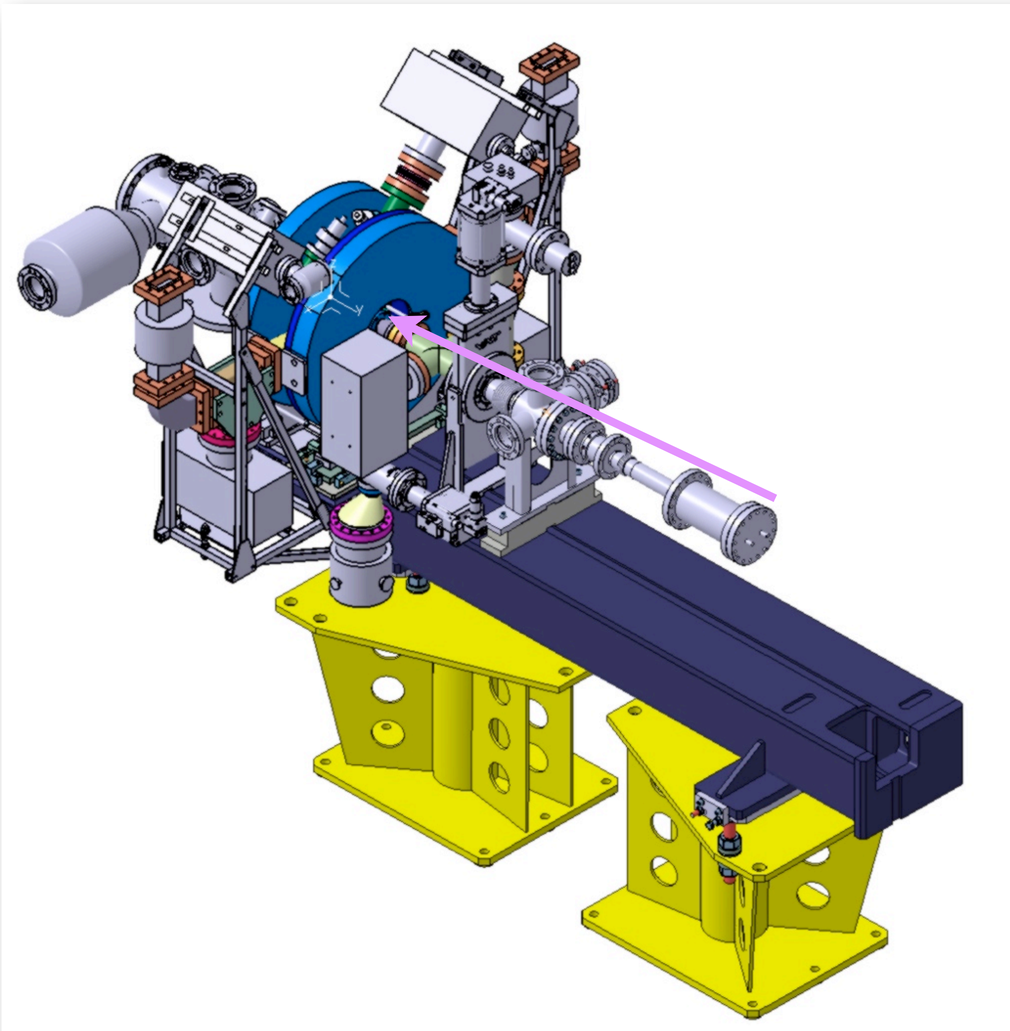

- The basic concepts and the implementation of the photoinjector date back to 1980s. But, ***the PHIN photoinjector is novel due to the following reasons:***
- high charge specification of 2.33 nC
- 1.2 μs long pulse train generation with 1908 bunches,
- challenging stability requirements: amplitude (charge) stability requirement of 0.25%,

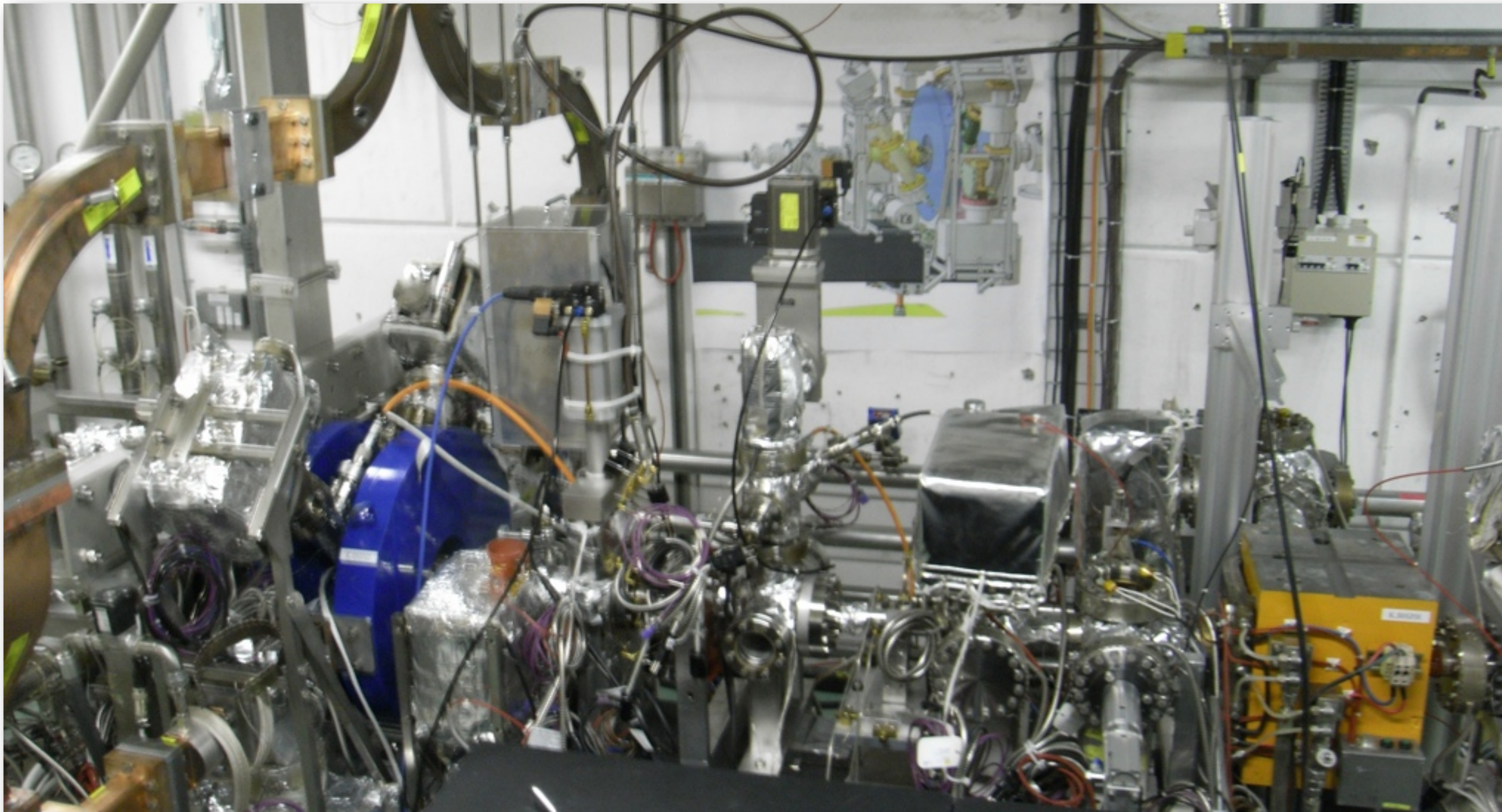

A photoinjector in a nutshell

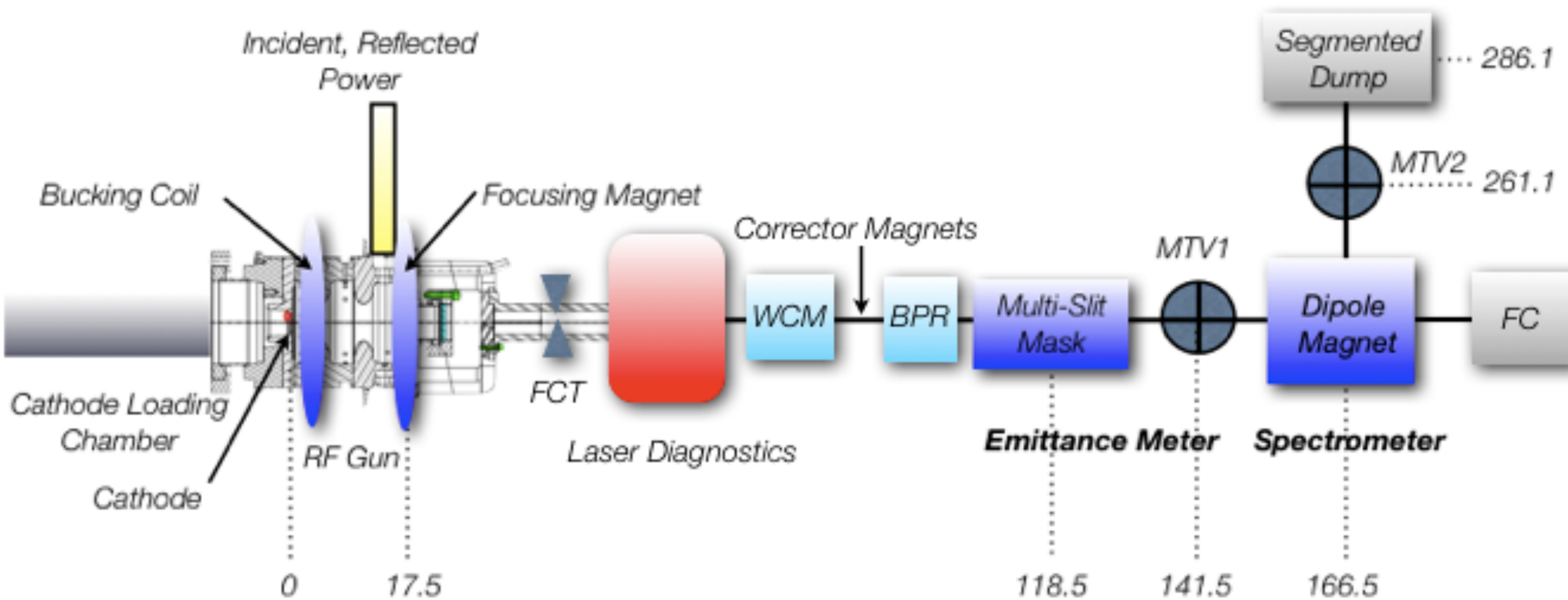

The objectives of the research program

The objectives of the research program

- Comprehensive **simulations** for the PHIN photoinjector beam dynamics,

The objectives of the research program

- Comprehensive **simulations** for the PHIN photoinjector beam dynamics,
- Optimization of the **working point** providing the specifications,

The objectives of the research program

- Comprehensive **simulations** for the PHIN photoinjector beam dynamics,
- Optimization of the **working point** providing the specifications,
- Full **experimental characterization** of the PHIN beam for short and long pulse trains,

The objectives of the research program

- Comprehensive **simulations** for the PHIN photoinjector beam dynamics,
- Optimization of the **working point** providing the specifications,
- Full **experimental characterization** of the PHIN beam for short and long pulse trains,
- Development of a **single shot emittance measurement system** for space charge dominated beams,

The objectives of the research program

- Comprehensive **simulations** for the PHIN photoinjector beam dynamics,
- Optimization of the **working point** providing the specifications,
- Full **experimental characterization** of the PHIN beam for short and long pulse trains,
- Development of a **single shot emittance measurement system** for space charge dominated beams,
- To measure the beam properties and their **stability along the bunch train** (time-resolved measurements),

The objectives of the research program

- Comprehensive **simulations** for the PHIN photoinjector beam dynamics,
- Optimization of the **working point** providing the specifications,
- Full **experimental characterization** of the PHIN beam for short and long pulse trains,
- Development of a **single shot emittance measurement system** for space charge dominated beams,
- To measure the beam properties and their **stability along the bunch train** (time-resolved measurements),
- To compare the measurement results with the simulations,

The objectives of the research program

- Comprehensive **simulations** for the PHIN photoinjector beam dynamics,
- Optimization of the **working point** providing the specifications,
- Full **experimental characterization** of the PHIN beam for short and long pulse trains,
- Development of a **single shot emittance measurement system** for space charge dominated beams,
- To measure the beam properties and their **stability along the bunch train** (time-resolved measurements),
- To compare the measurement results with the simulations,
- Eventually, to study the consequences of the findings to constitute a **preliminary RF gun design for CLIC-DB injector**.

- **Preface,** the original contribution in a deductive view of CLIC project
- **PHIN photoinjector**, objectives of the research
- **Beam instrumentation & characterization,** commissioning highlights of PHIN
- **Conclusions**

Beam Instrumentation & Characterization

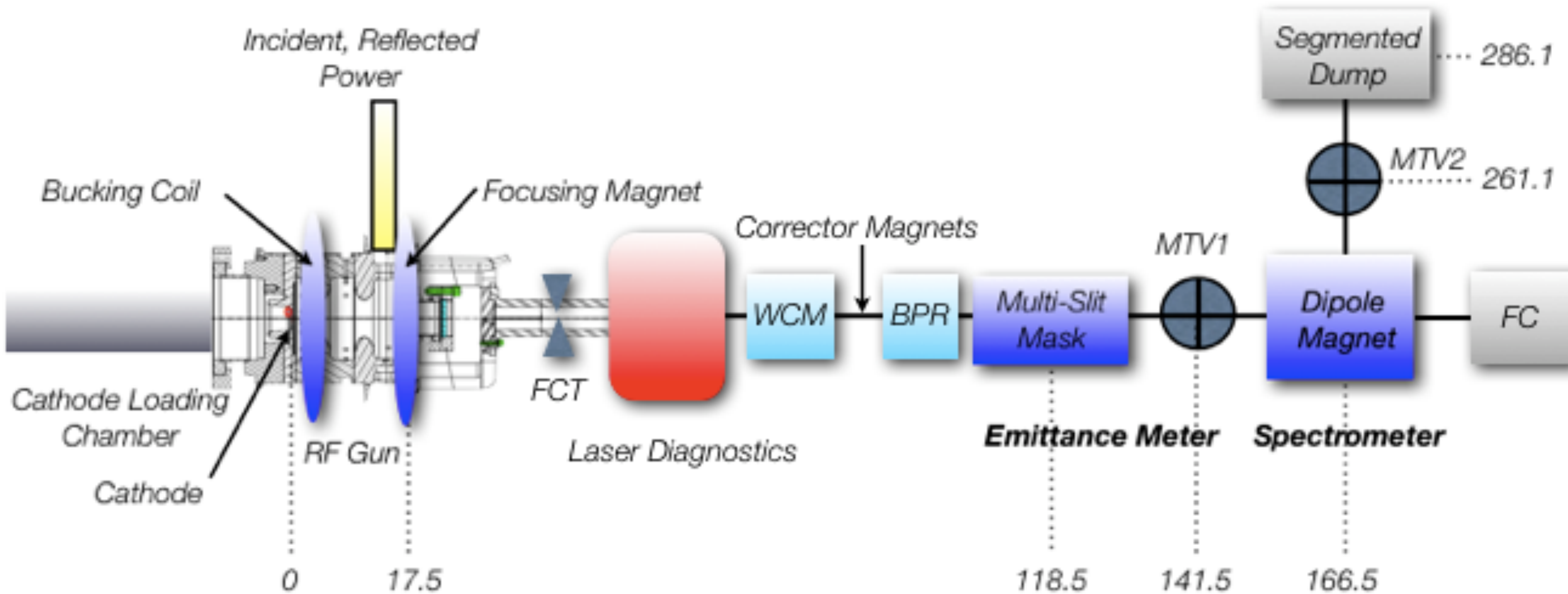

Beam Instrumentation & Characterization

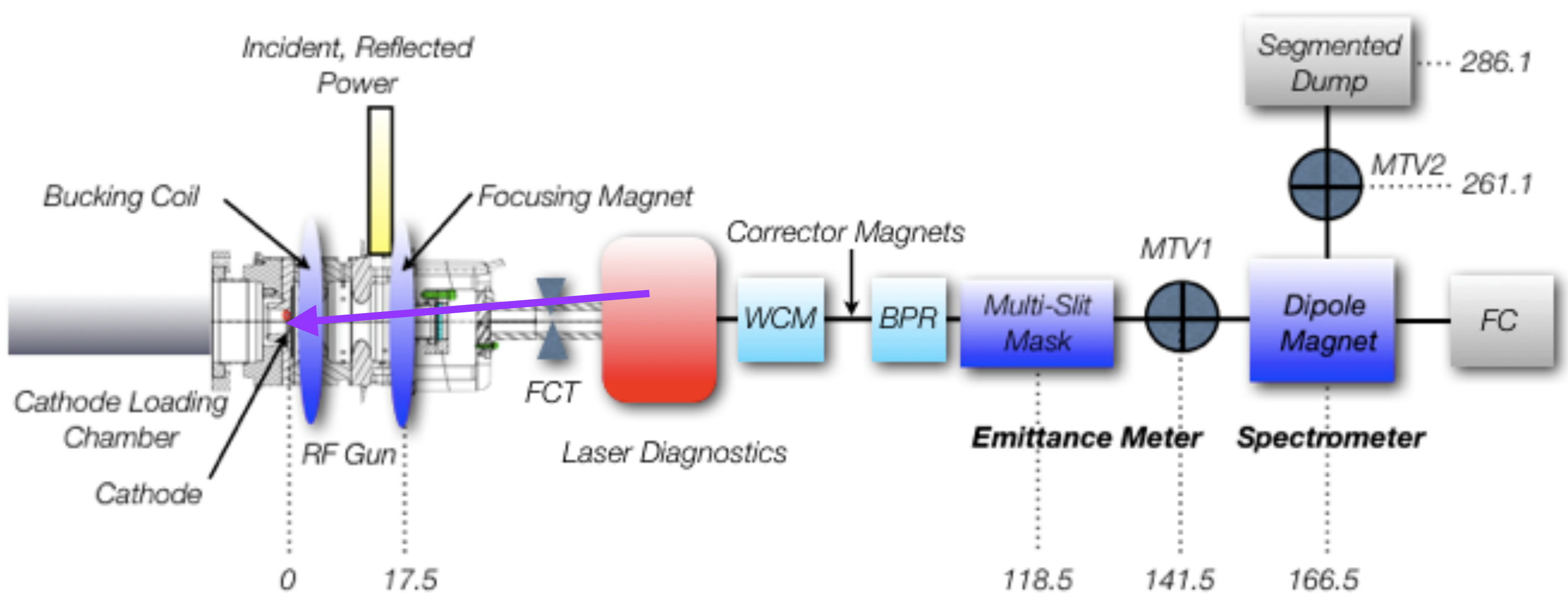

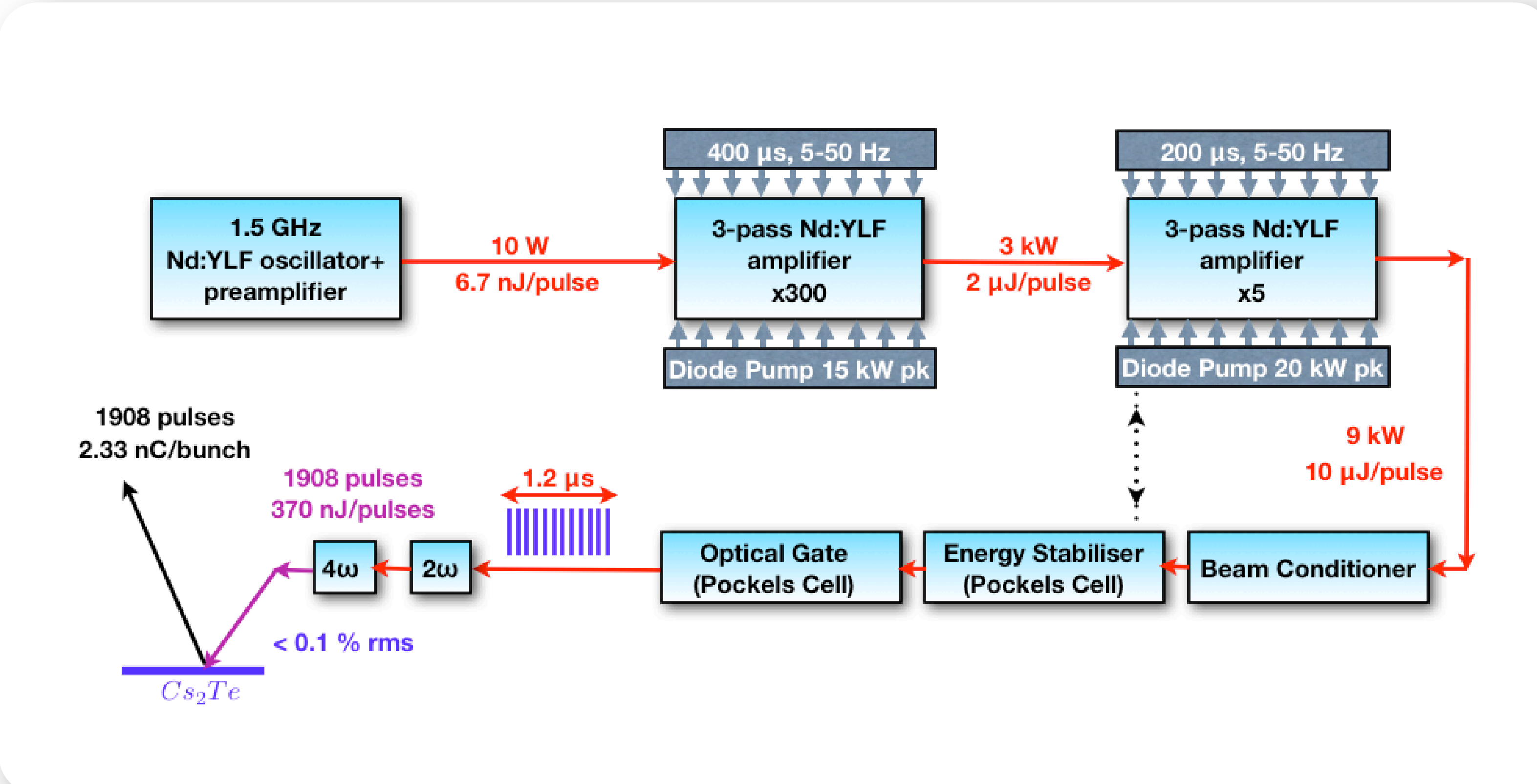
400 μs, 5-50 Hz
200 μs, 5-50 Hz
1.5 GHz Nd:YLF oscillator+ preamplifier
10 W
6.7 nJ/pulse
3-pass Nd:YLF amplifier x300
3 kW
2 μJ/pulse
3-pass Nd:YLF amplifier x5
Diode Pump 15 kW pk
Diode Pump 20 kW pk
1908 pulses
2.33 nC/bunch
1908 pulses
370 nJ/pulses
1.2 μs
9 kW
10 μJ/pulse
4ω
2ω
Optical Gate (Pockels Cell)
Energy Stabiliser (Pockels Cell)
Beam Conditioner
< 0.1 % rms
Cs_2Te

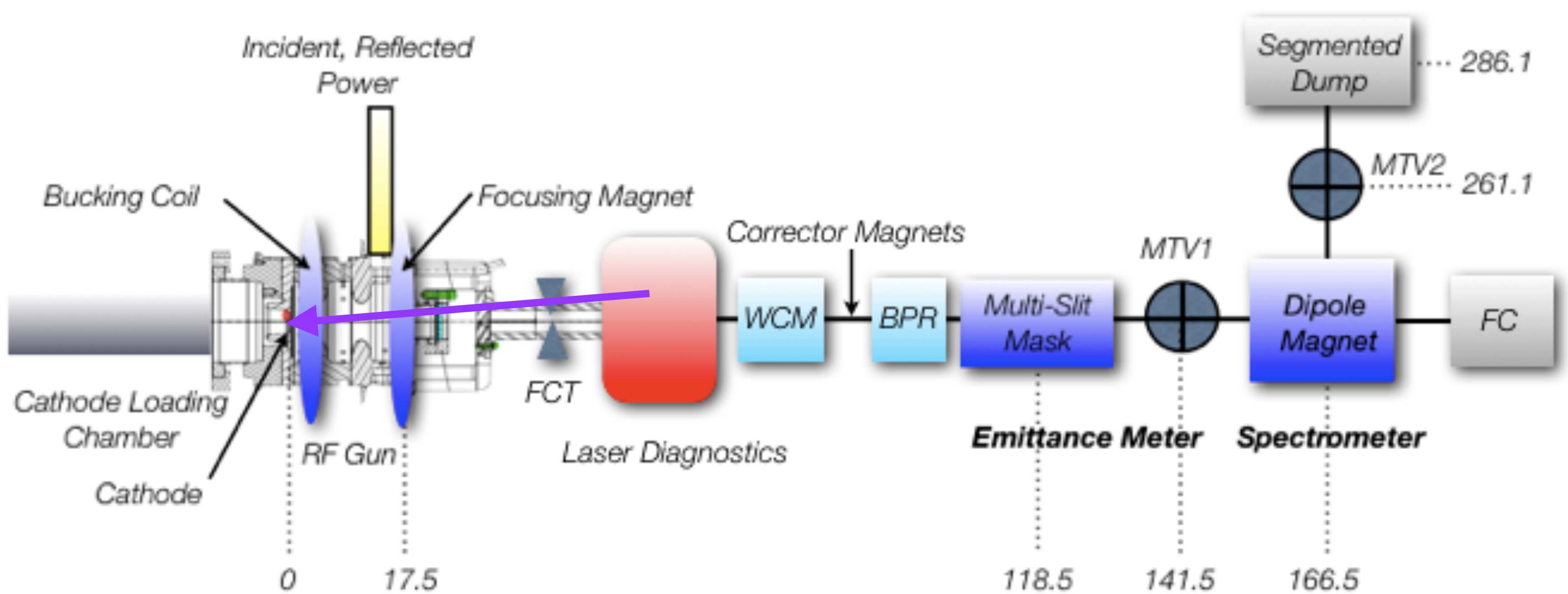
Incident, Reflected Power
Segmented Dump
286.1
MTV2
261.1
Bucking Coil
Focusing Magnet
Corrector Magnets
MTV1
WCM
BPR
Multi-Slit Mask
Dipole Magnet
FC
FCT
Cathode Loading Chamber
RF Gun
Laser Diagnostics
Emittance Meter
Spectrometer
Cathode
0
17.5
118.5
141.5
166.5

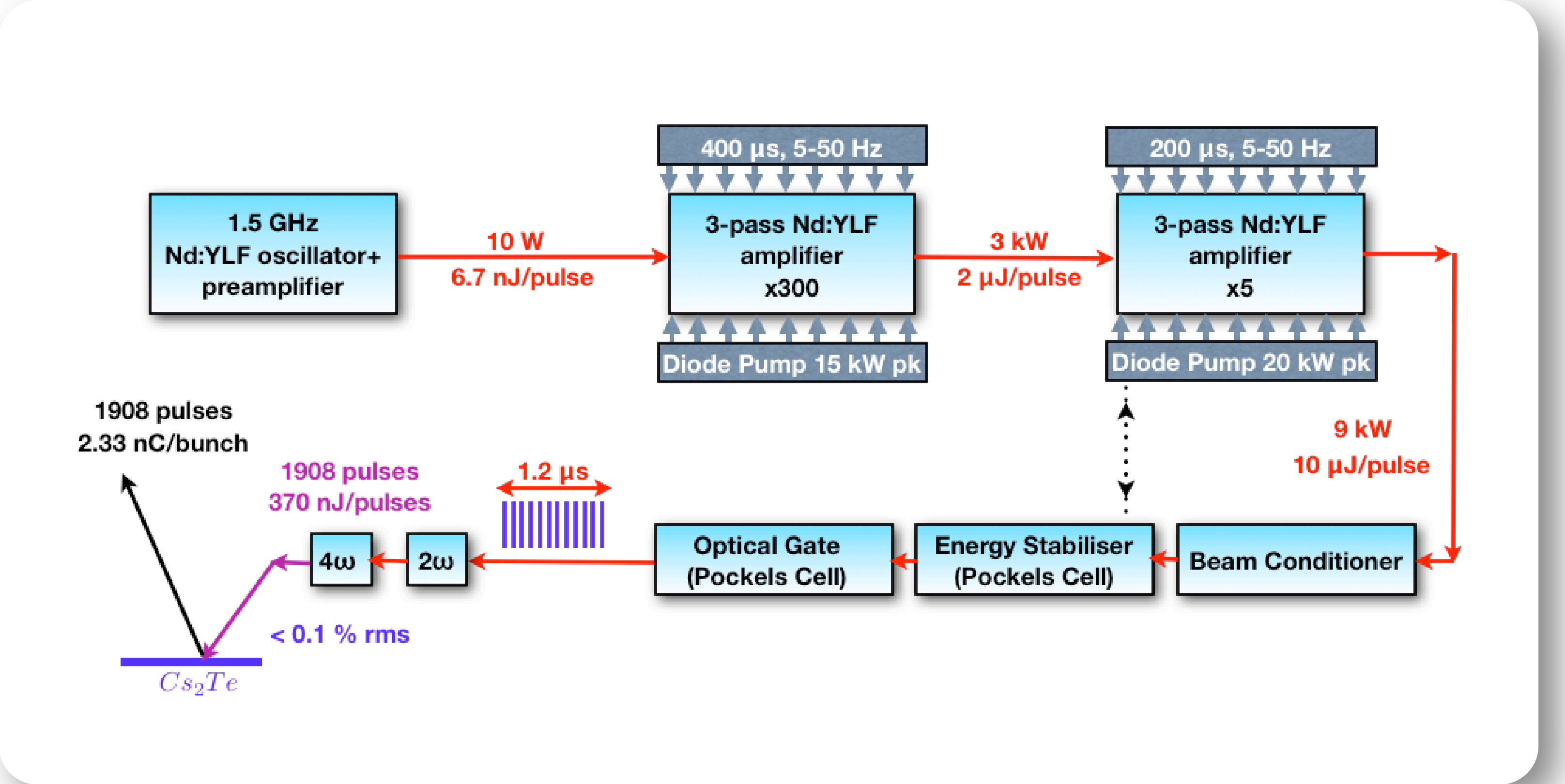

- Continuous pulses from Nd:YLF oscillator @ 1.5 GHz,

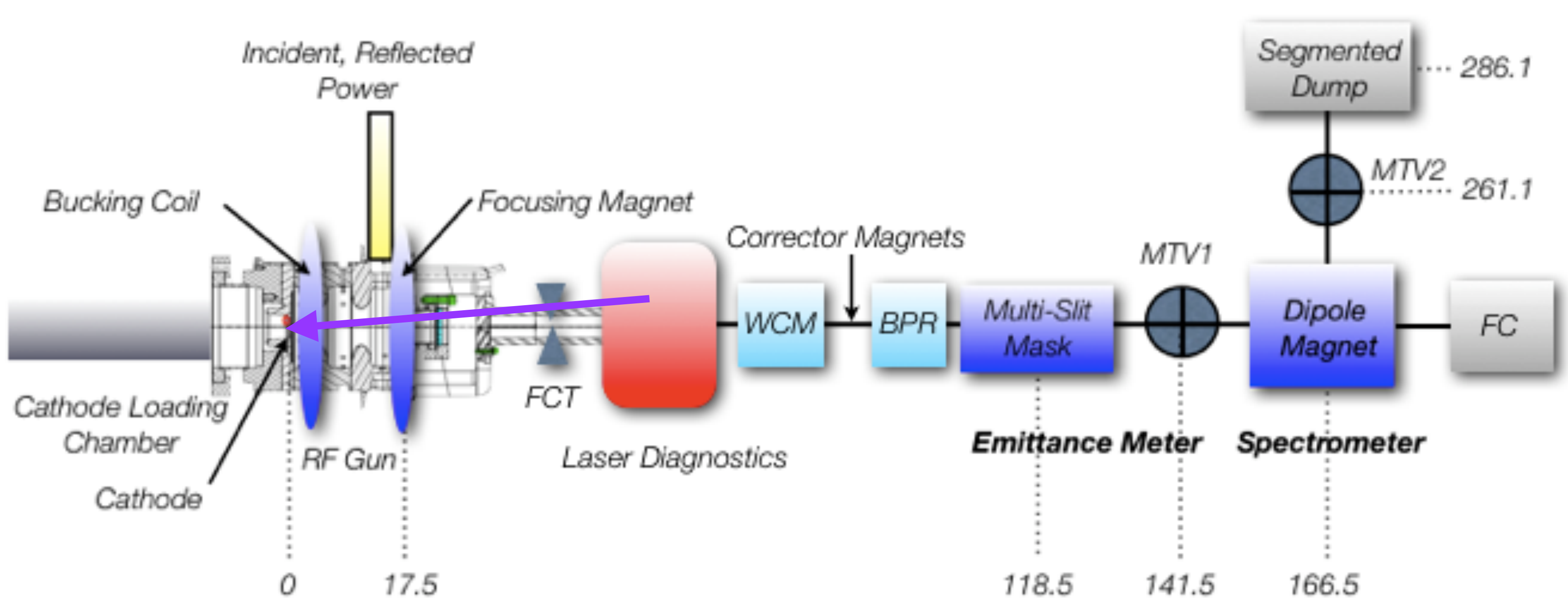

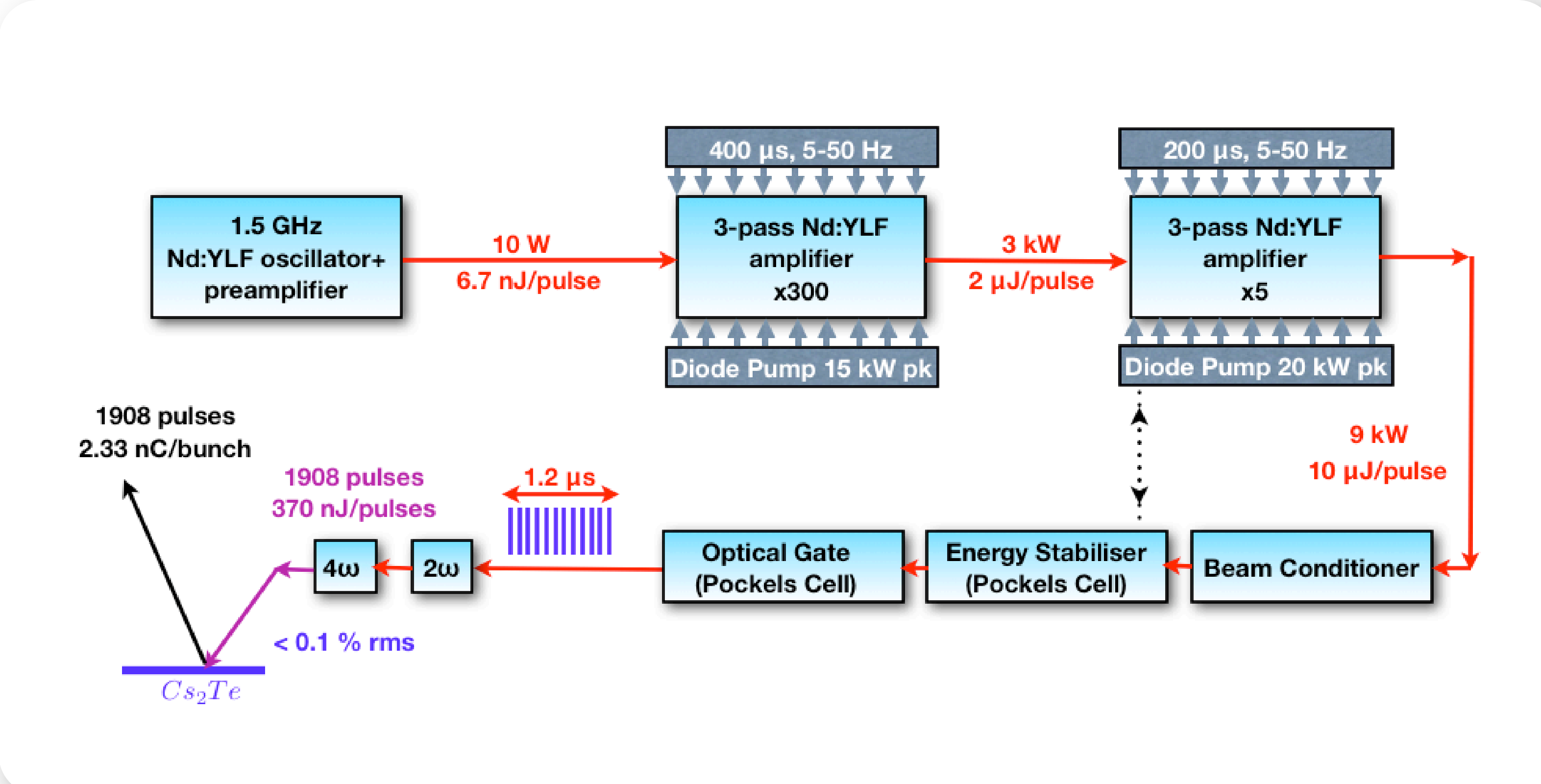

- Continuous pulses from Nd:YLF oscillator @ 1.5 GHz,
- Several amplification stages from 6.7 nJ to 370 nJ (after UV conversion) per pulse,

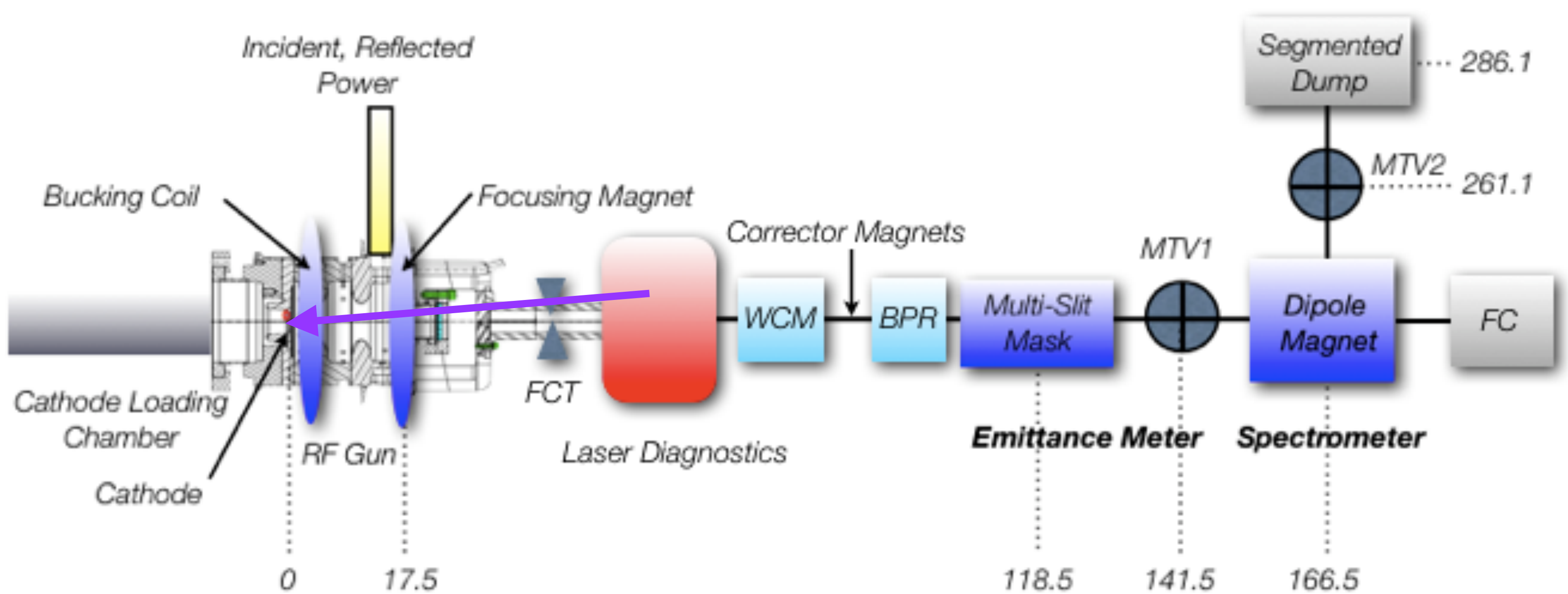

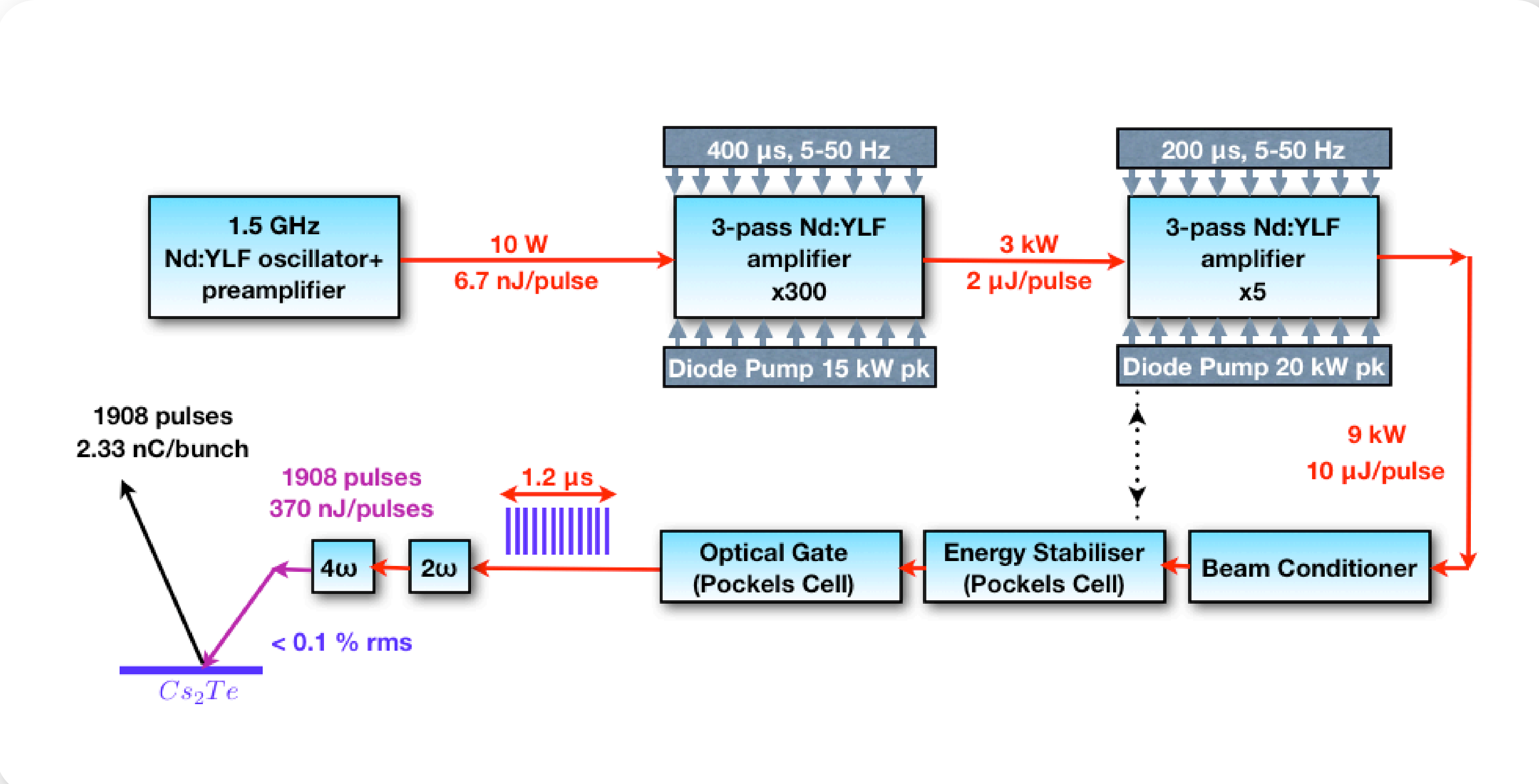

- Continuous pulses from Nd:YLF oscillator @ 1.5 GHz,
- Several amplification stages from 6.7 nJ to 370 nJ (after UV conversion) per pulse,
- Pulse train length adjustment to 1.2 μs by using Pockels cells

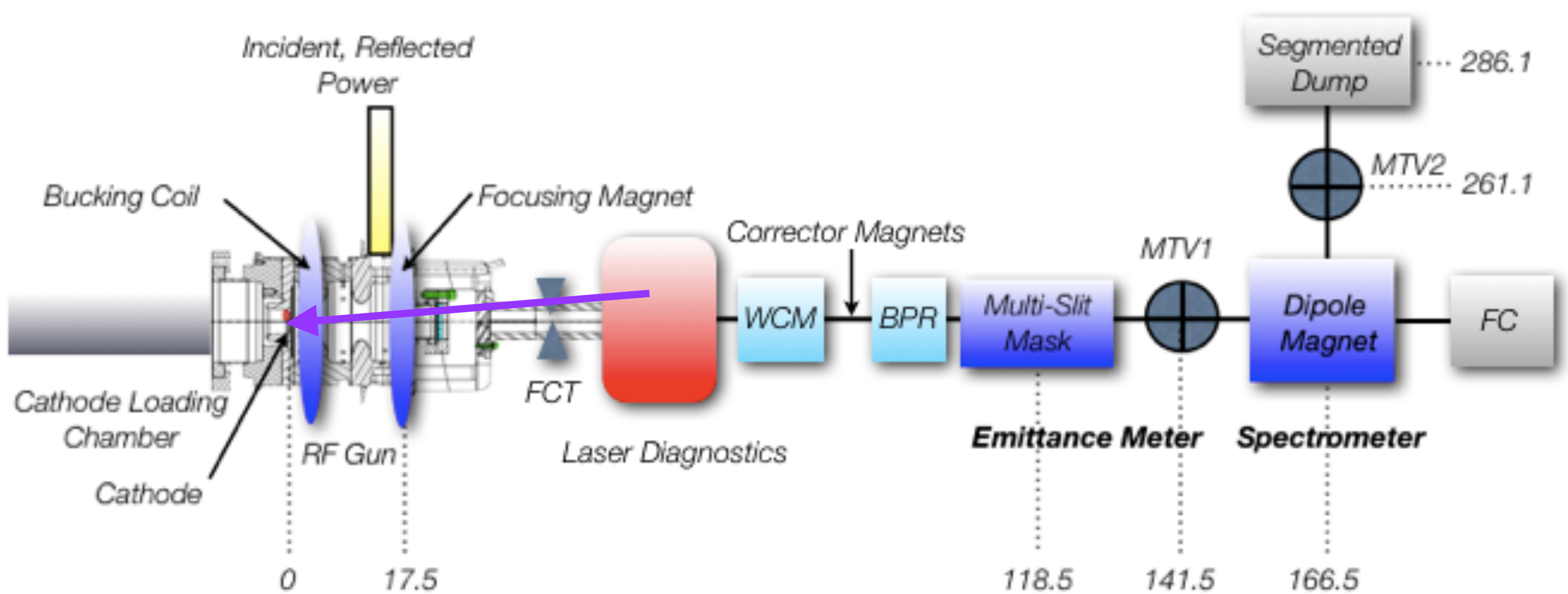

Beam Instrumentation & Characterization

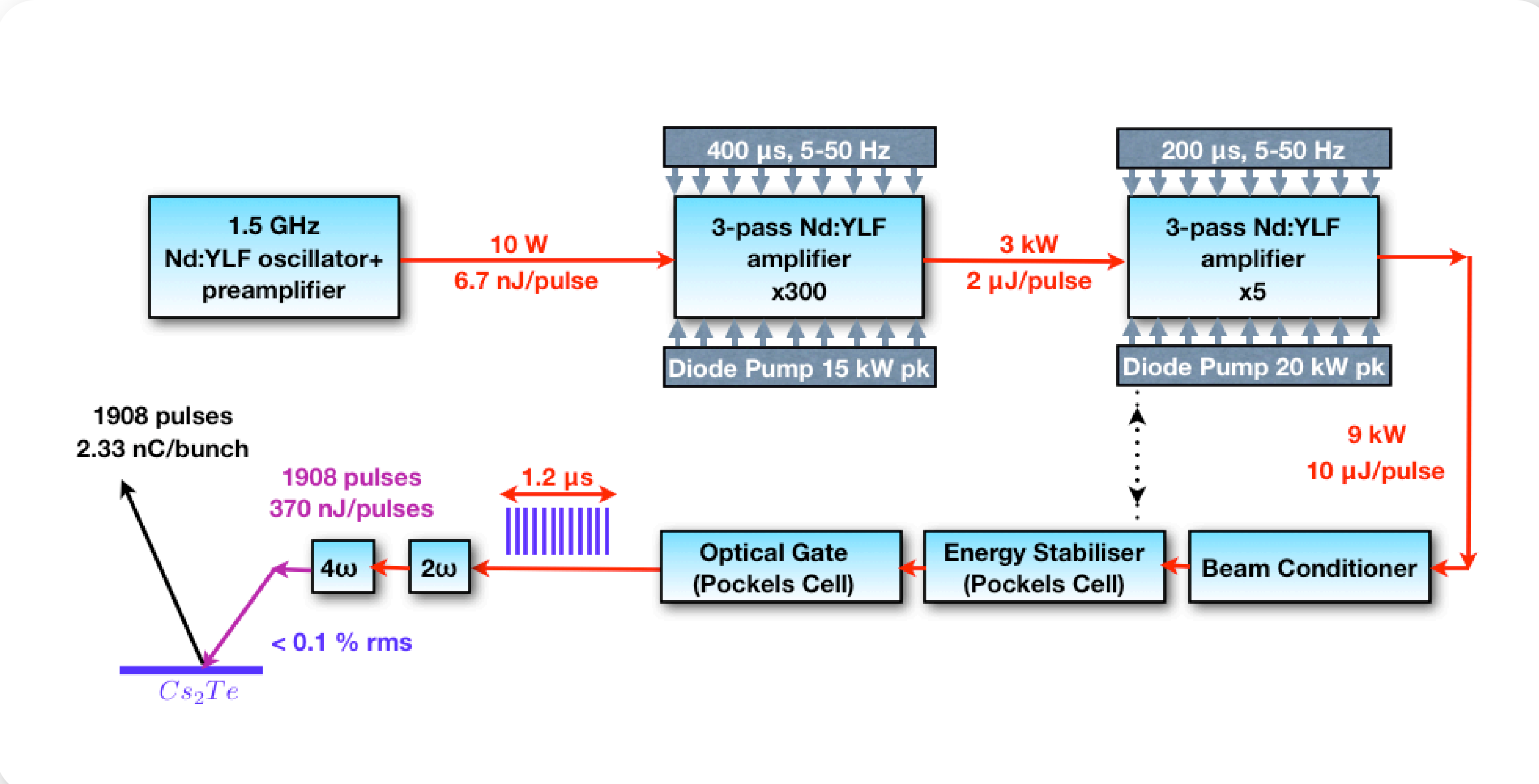

- Continuous pulses from Nd:YLF oscillator @ 1.5 GHz,
- Several amplification stages from 6.7 nJ to 370 nJ (after UV conversion) per pulse,
- Pulse train length adjustment to 1.2 µs by using Pockels cells
- Illuminates a Cs_2Te cathode

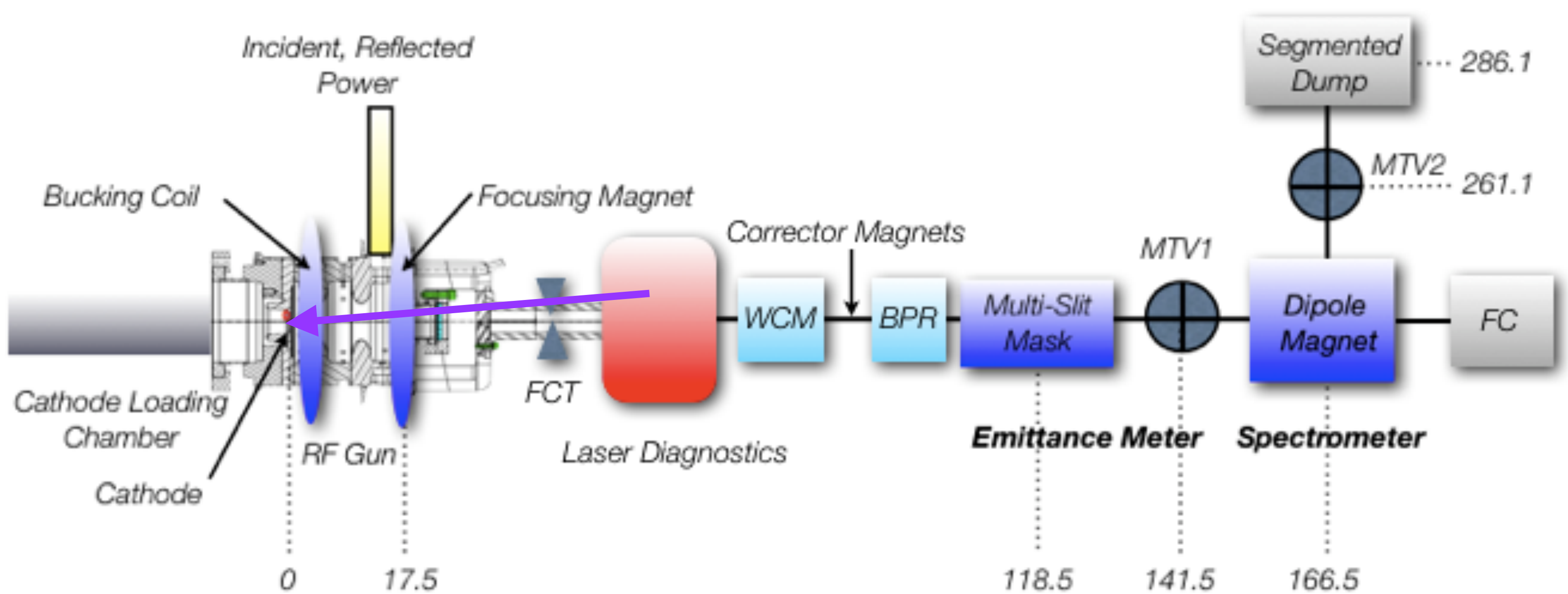

Charge Production

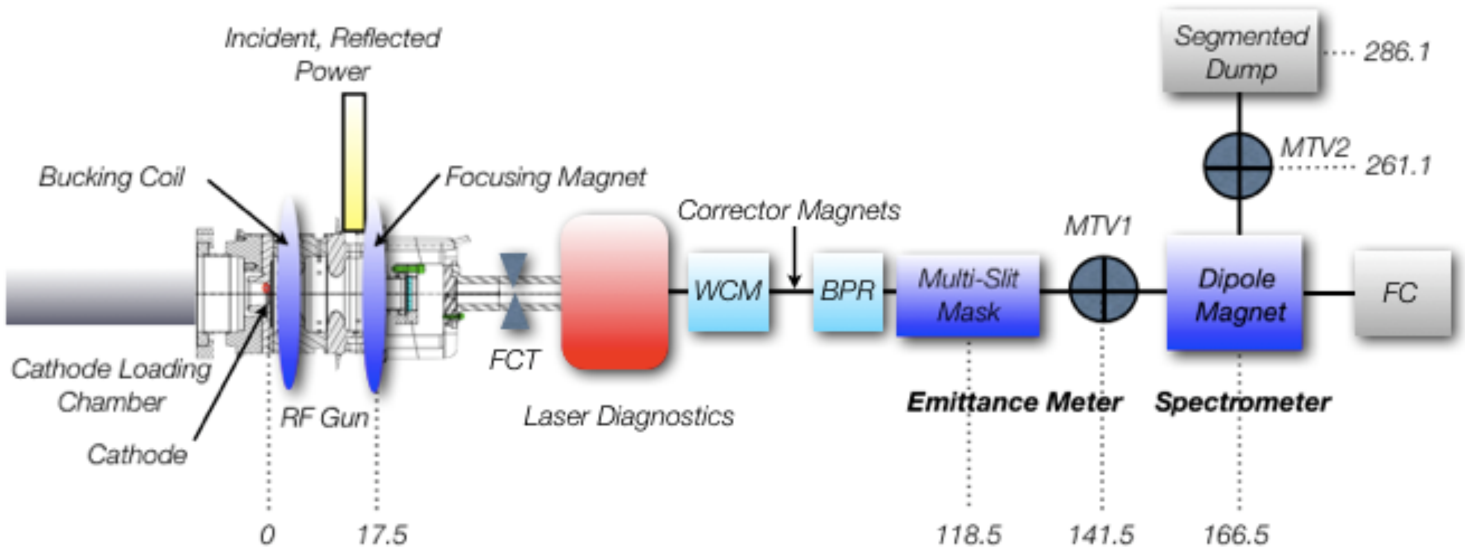

Charge Production

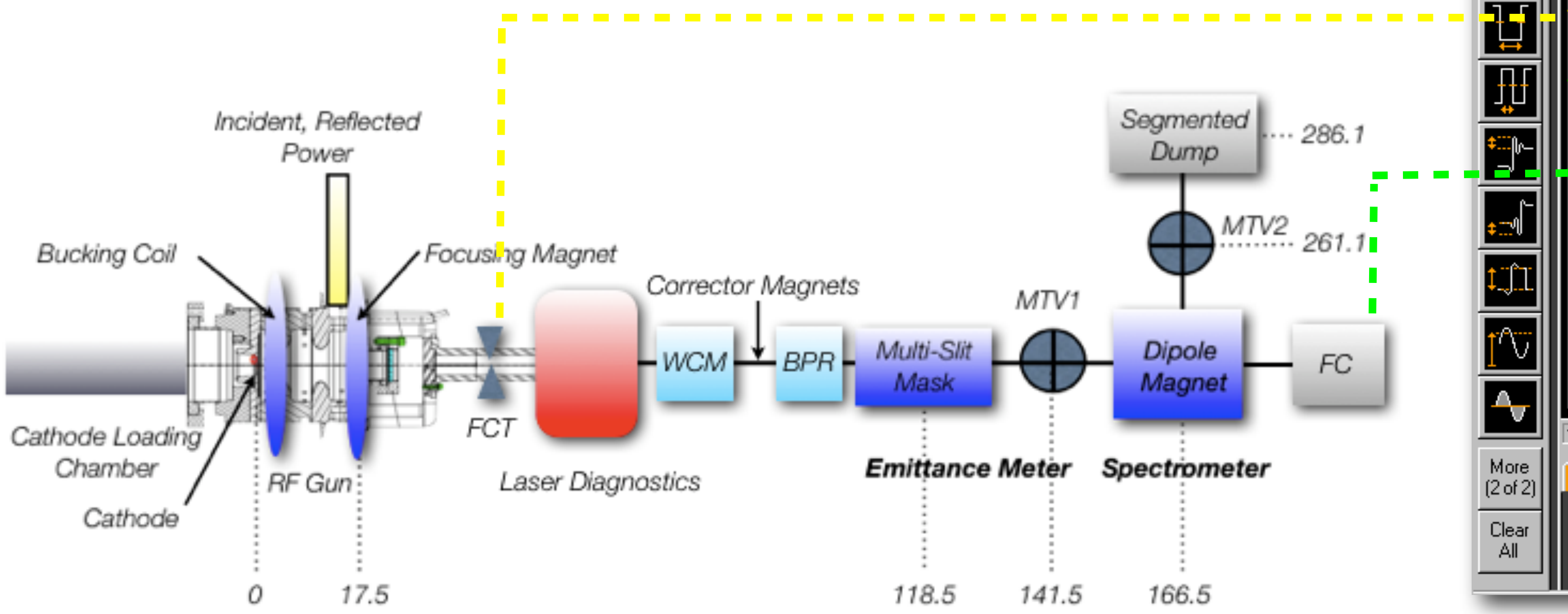

- In the most of the charge measurements, the FCT has been preferred due to its location after the RF gun.

Charge Production

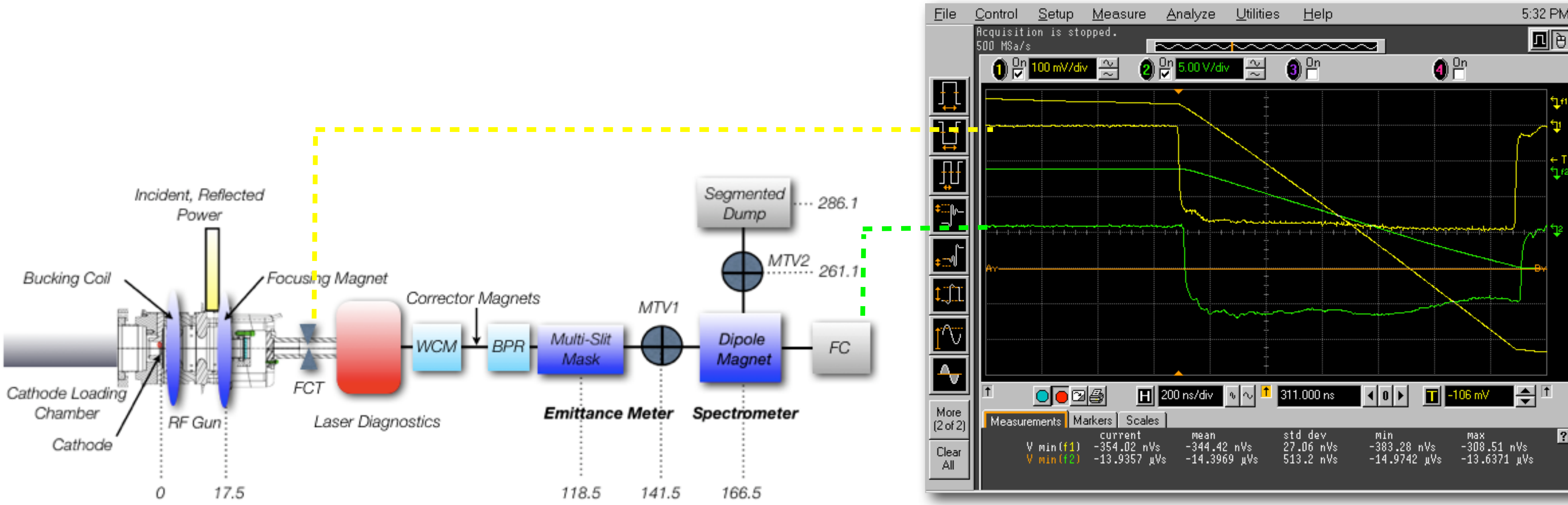

- In the most of the charge measurements, the FCT has been preferred due to its location after the RF gun.

- Nevertheless, the FC is the most useful in order to study the charge transmission along the downstream of the beamline.

Charge Production

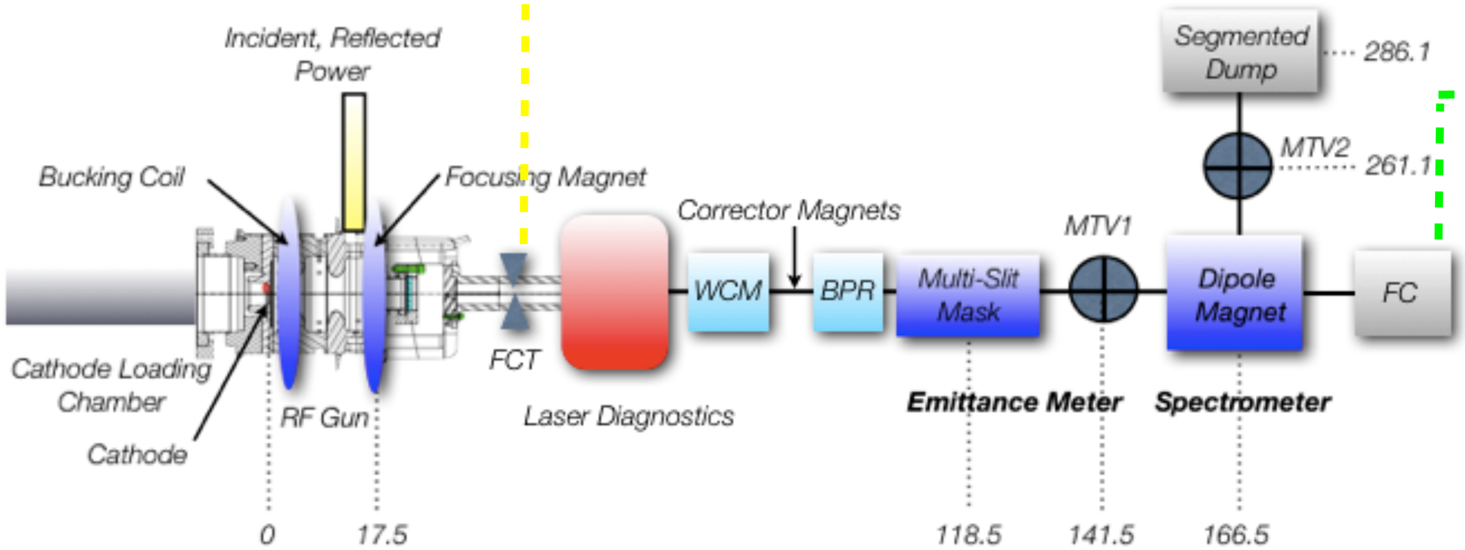

- In the most of the charge measurements, the FCT has been preferred due to its location after the RF gun.
- Nevertheless, the FC is the most useful in order to study the charge transmission along the downstream of the beamline.
- In principle, the charge production saturates with the increasing laser energy per pulse.

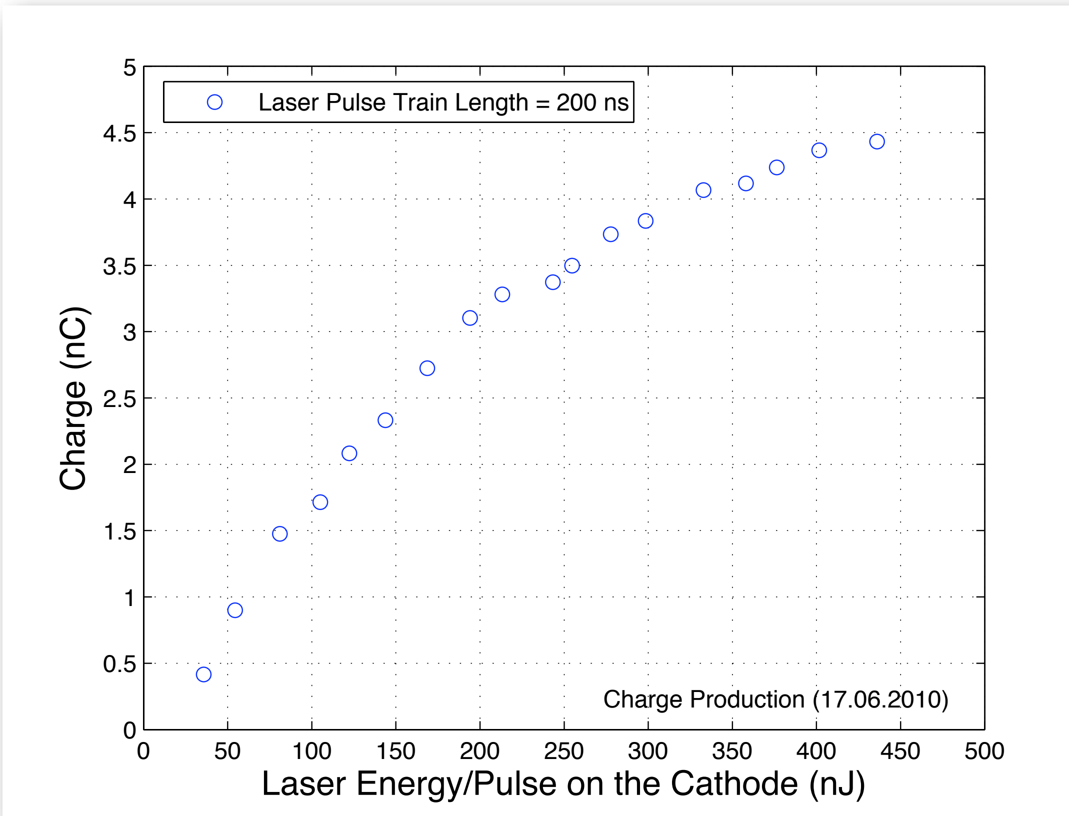

Charge Production

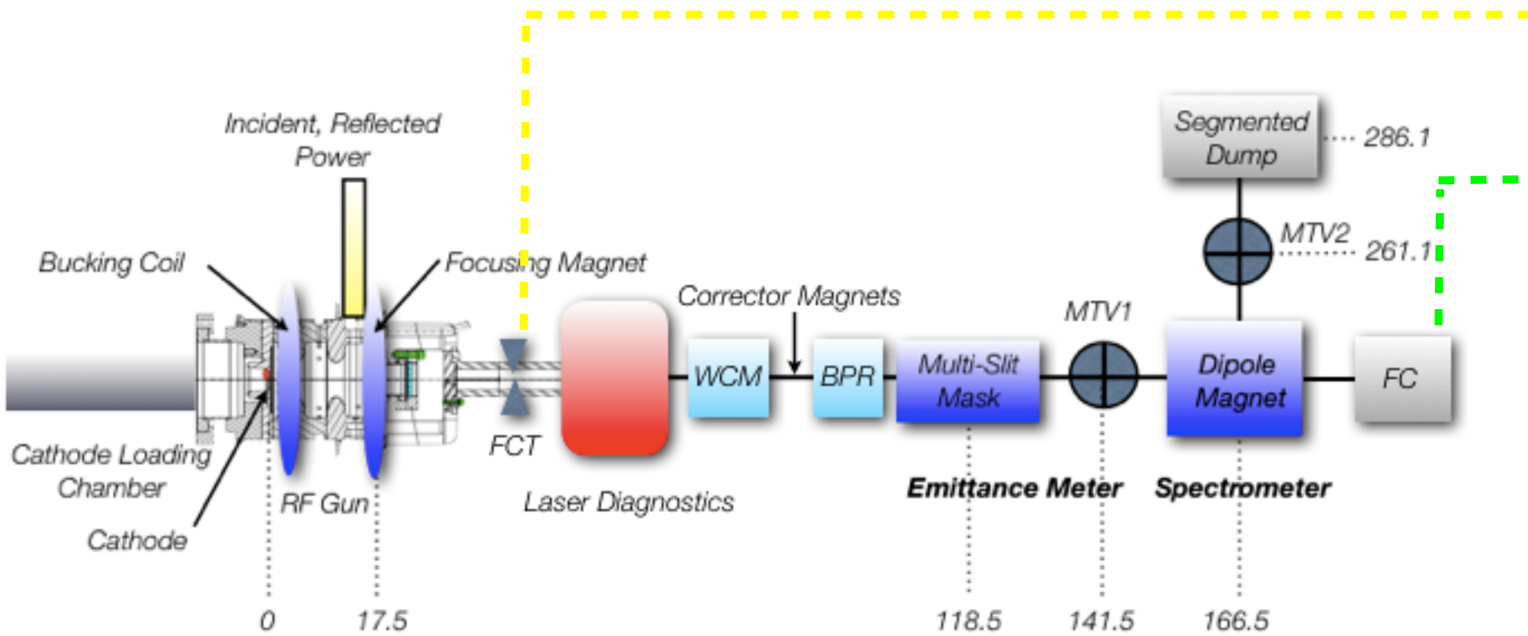

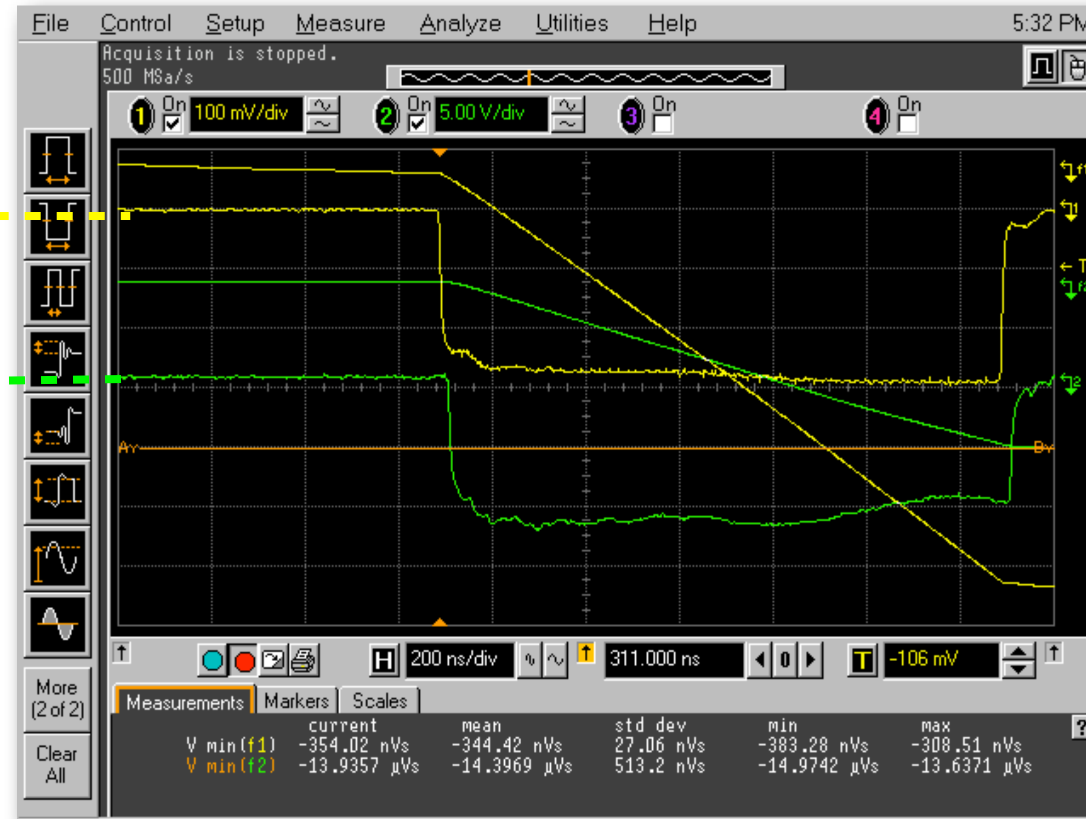

- In the most of the charge measurements, the FCT has been preferred due to its location after the RF gun.
- Nevertheless, the FC is the most useful in order to study the charge transmission along the downstream of the beamline.
- In principle, the charge production saturates with the increasing laser energy per pulse.
- **The maximum achievable charge has been measured as 4.4 nC during the commissioning which even exceeds the specification.**

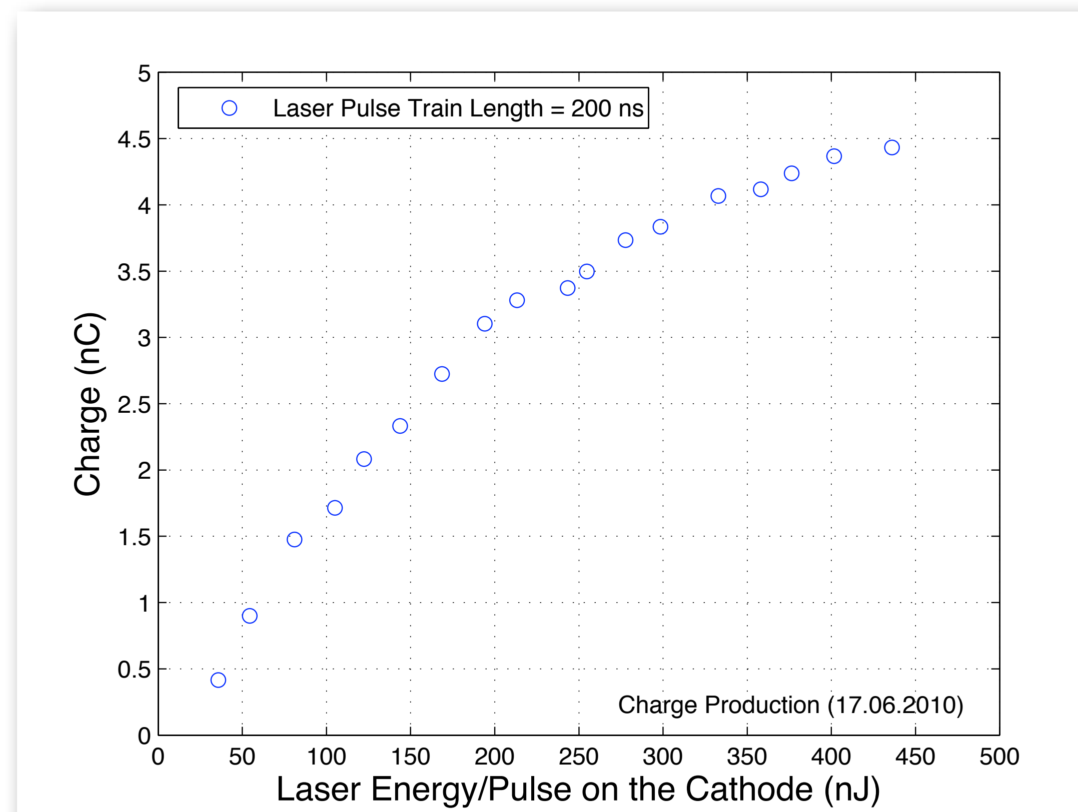

Charge Production

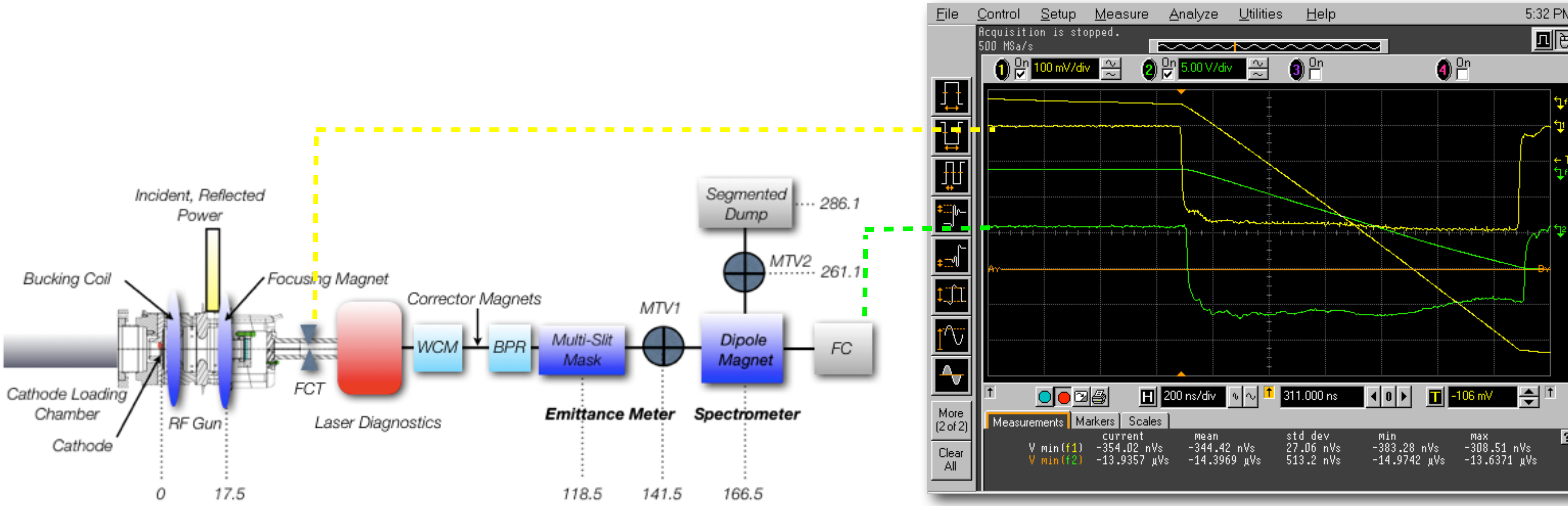

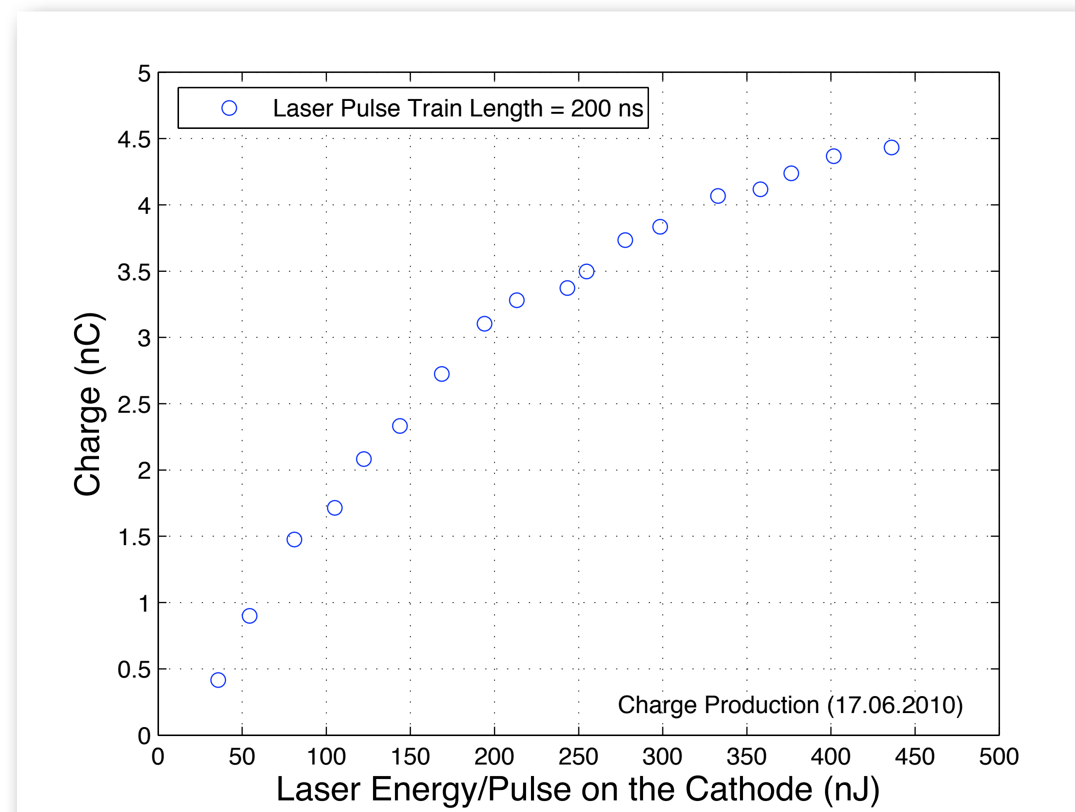

- **The maximum achievable charge has been measured as 4.4 nC during the commissioning which even exceeds the specification.**

Charge Production

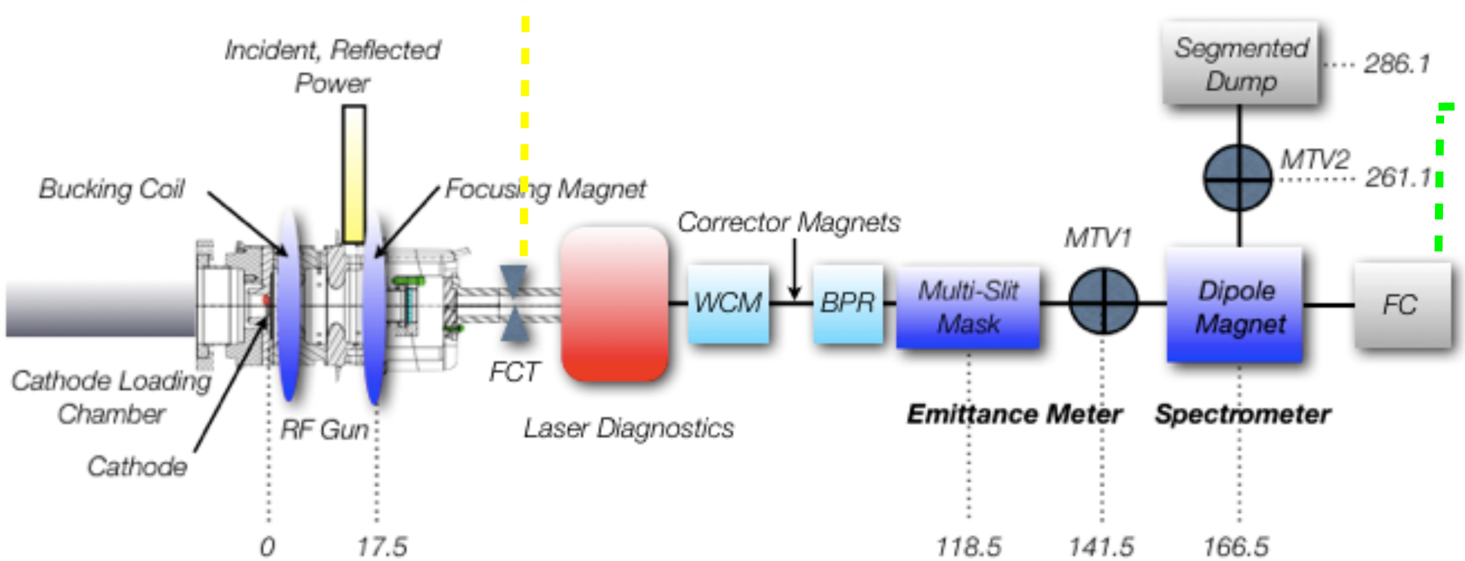

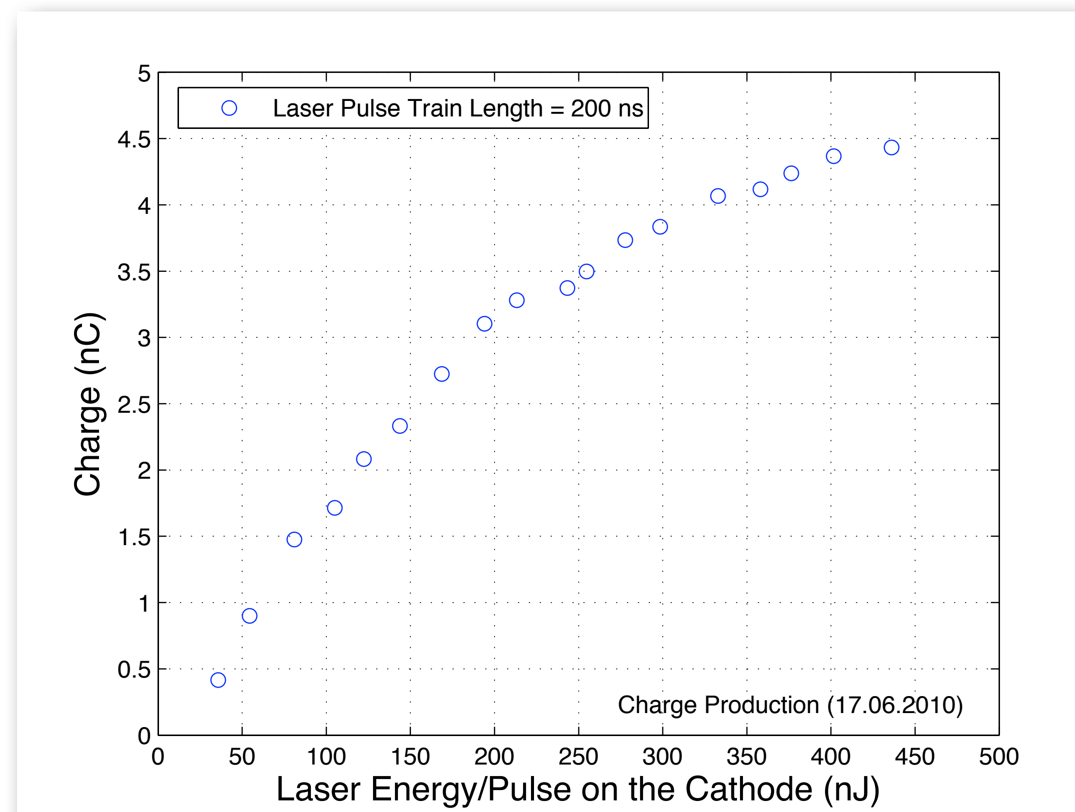

- **The maximum achievable charge has been measured as 4.4 nC during the commissioning which even exceeds the specification.**

Charge Production

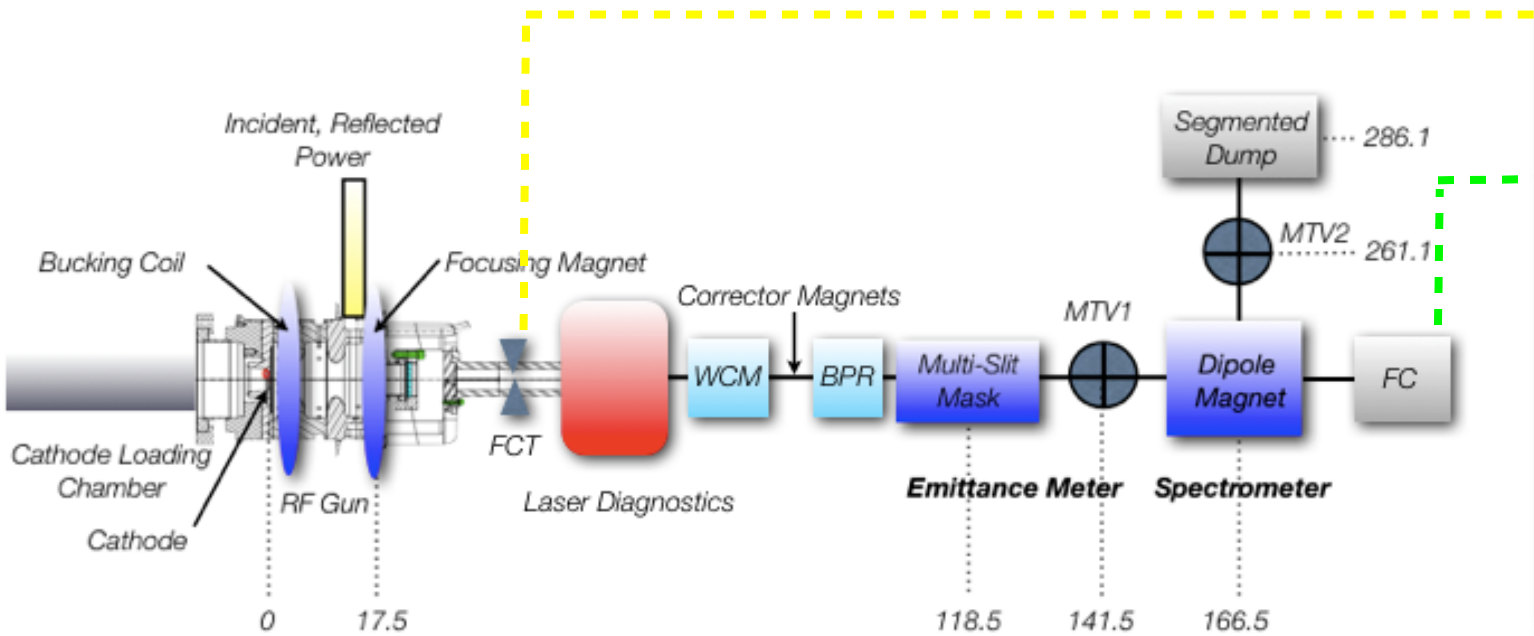

- **The maximum achievable charge has been measured as 4.4 nC during the commissioning which even exceeds the specification.**

$$Q_{max}[nC] = \frac{E_{acc}[MV/m]\sigma_x^2}{18}$$

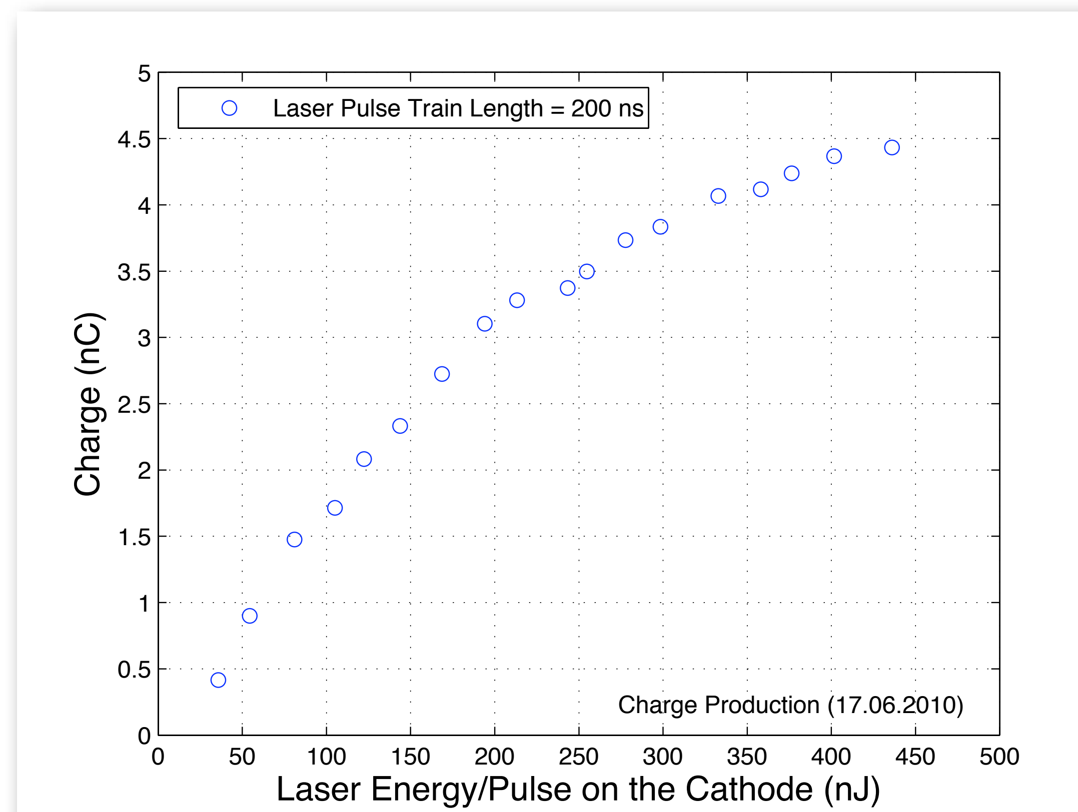

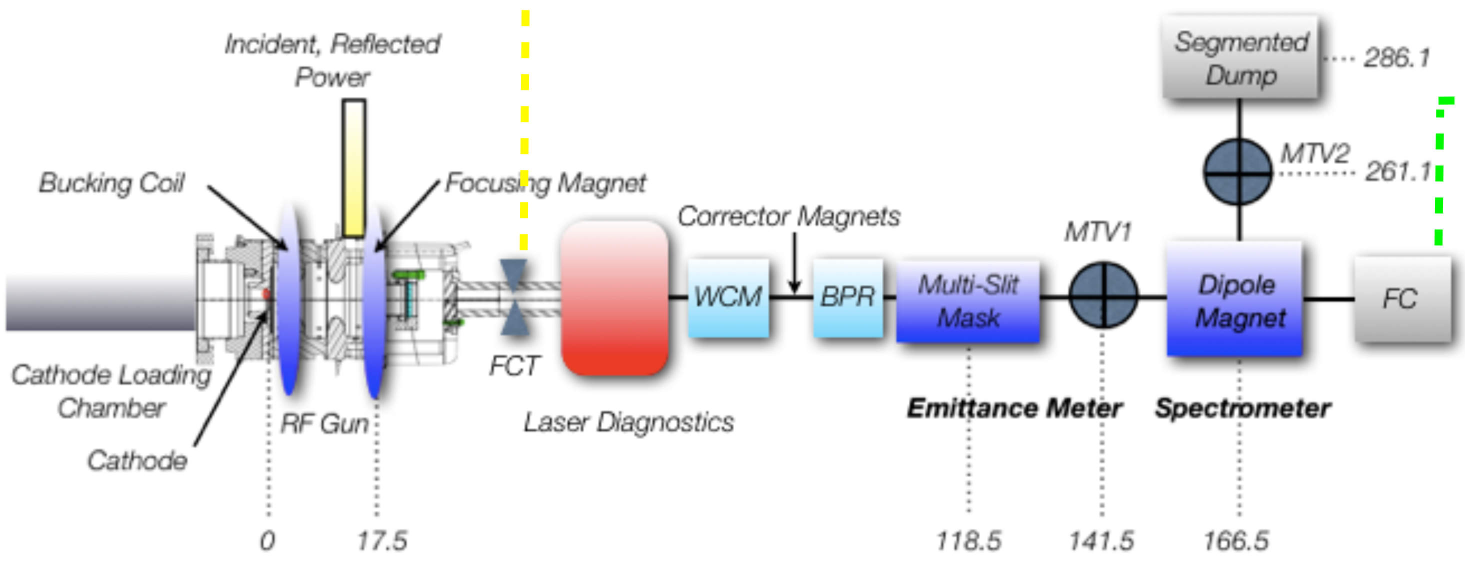

- **The maximum achievable charge has been measured as 4.4 nC during the commissioning which even exceeds the specification.**

$$Q_{max}[nC] = \frac{E_{acc}[MV/m]\sigma_x^2}{18} = \frac{85[MV/m](1[mm])^2}{18} = 4.7nC$$

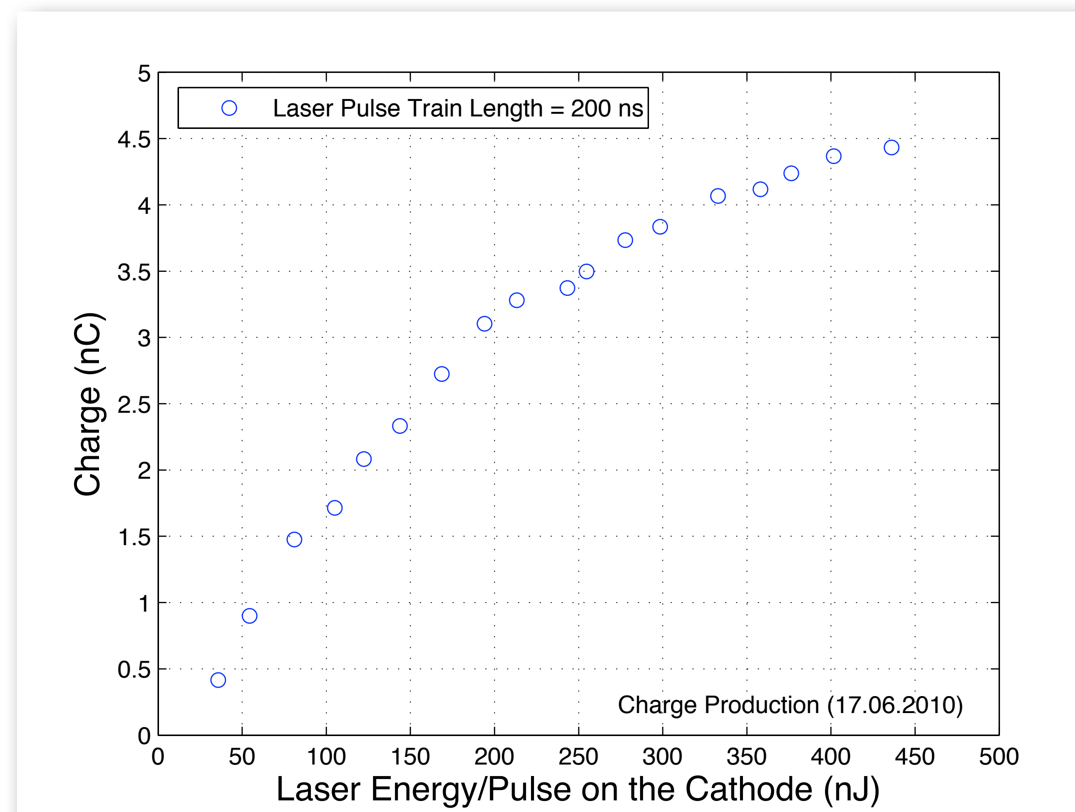

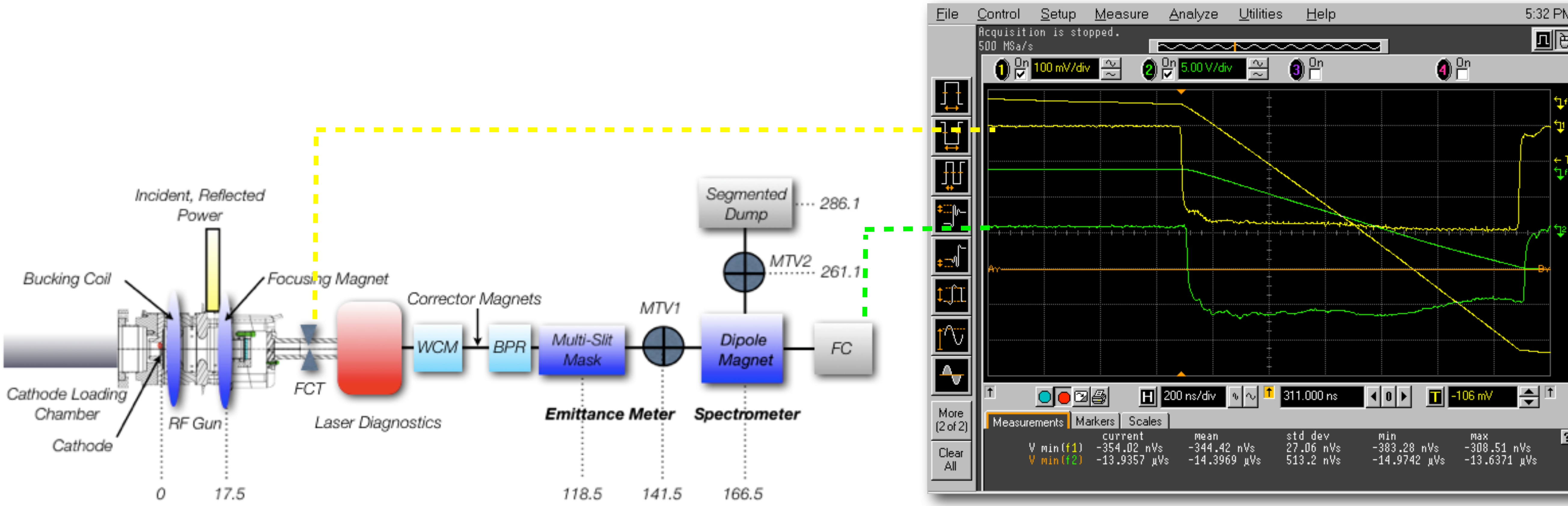

- **The maximum achievable charge has been measured as 4.4 nC during the commissioning which even exceeds the specification.**

$$Q_{max}[nC] = \frac{E_{acc}[MV/m]\sigma_x^2}{18} = \frac{85[MV/m](1[mm])^2}{18} = 4.7nC$$

Consistency with theoretical prediction.

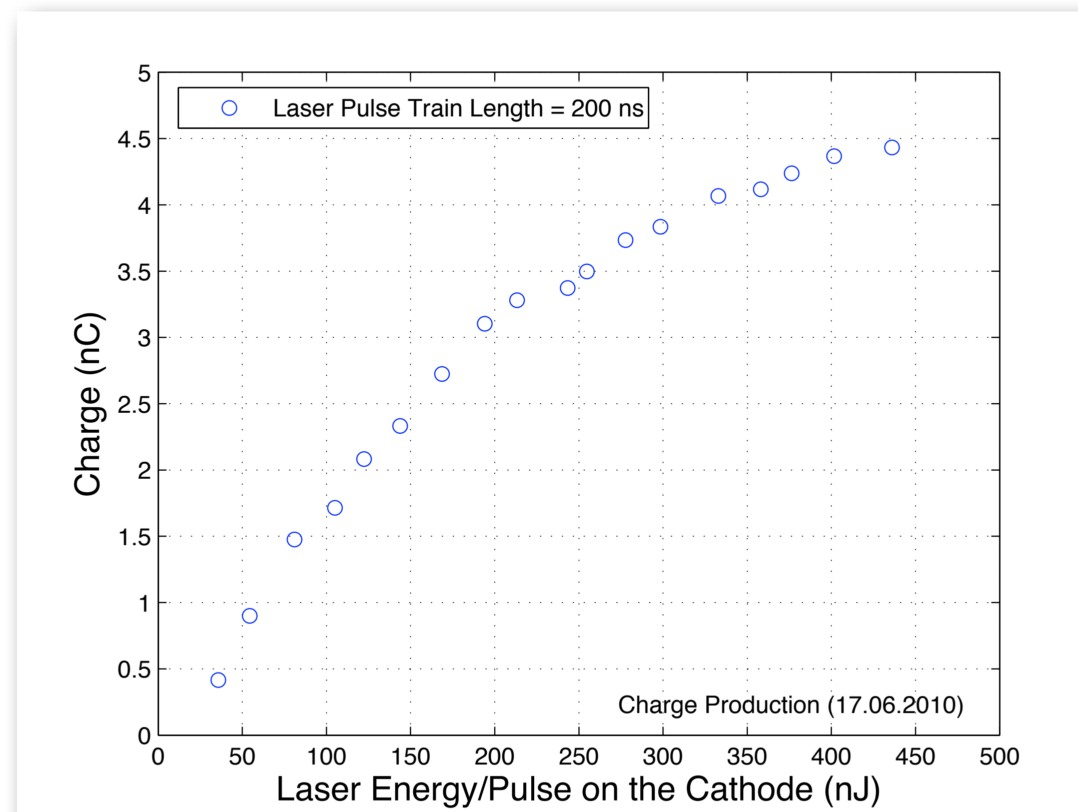

Beam Instrumentation & Characterization

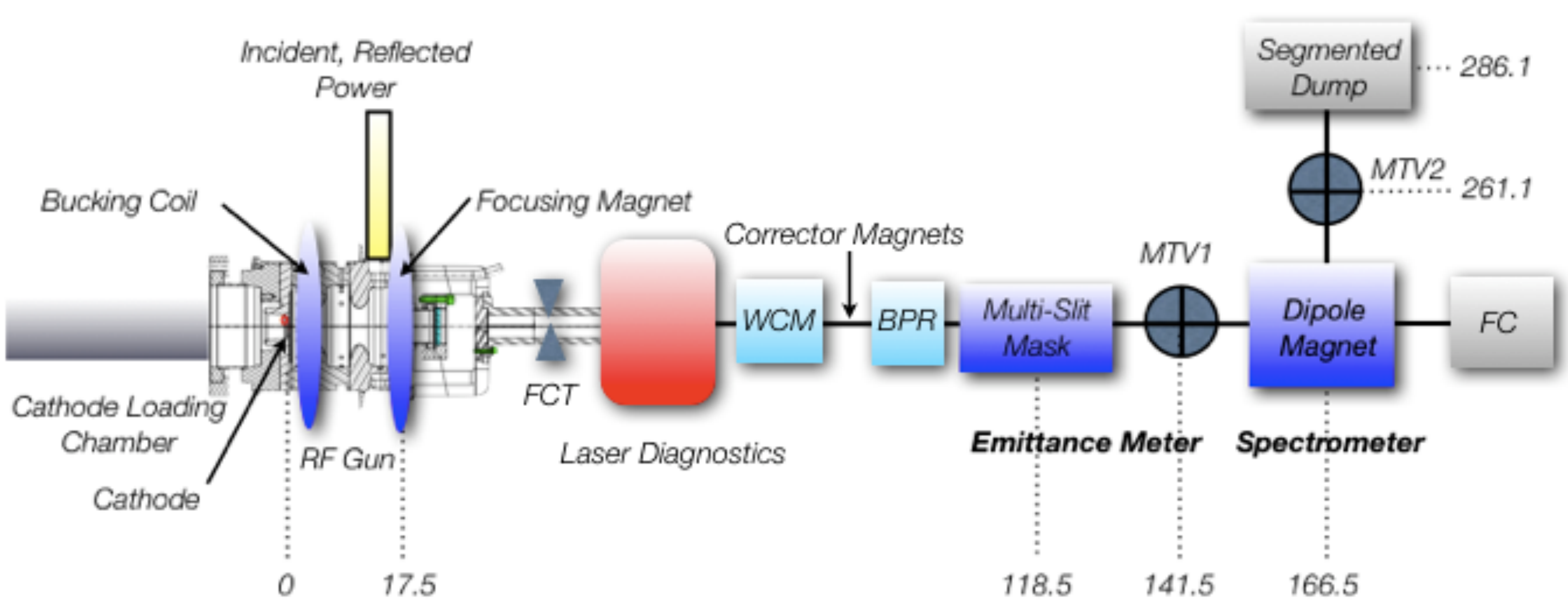

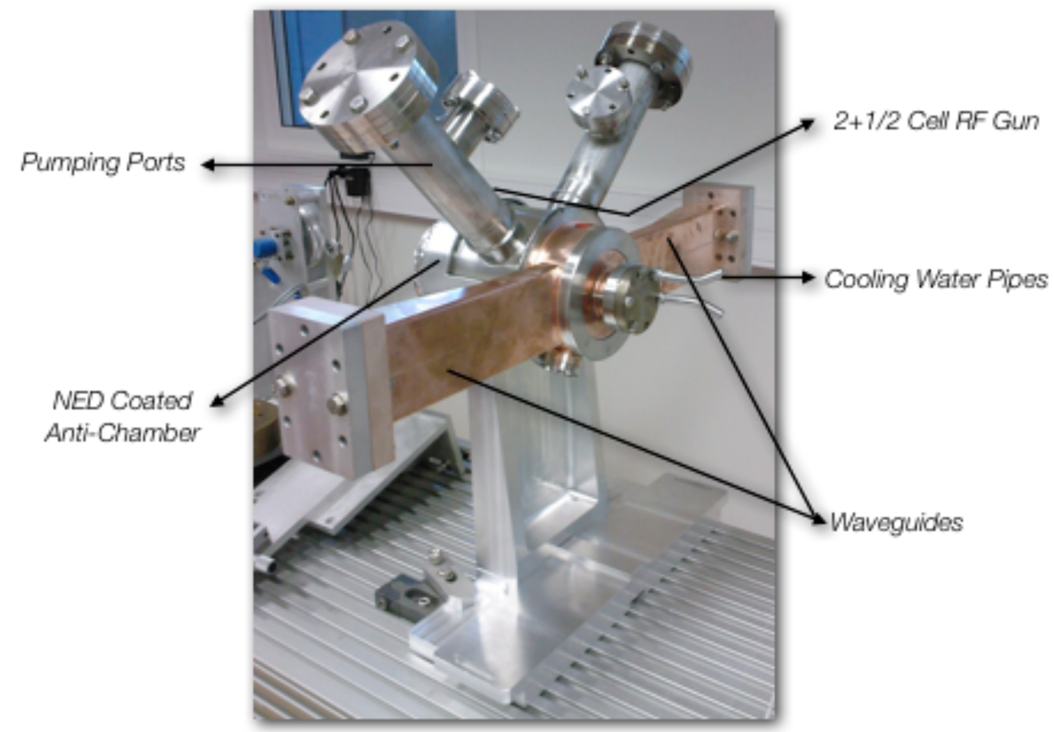
Pumping Ports
2+1/2 Cell RF Gun
Cooling Water Pipes
NED Coated
Anti-Chamber
Waveguides

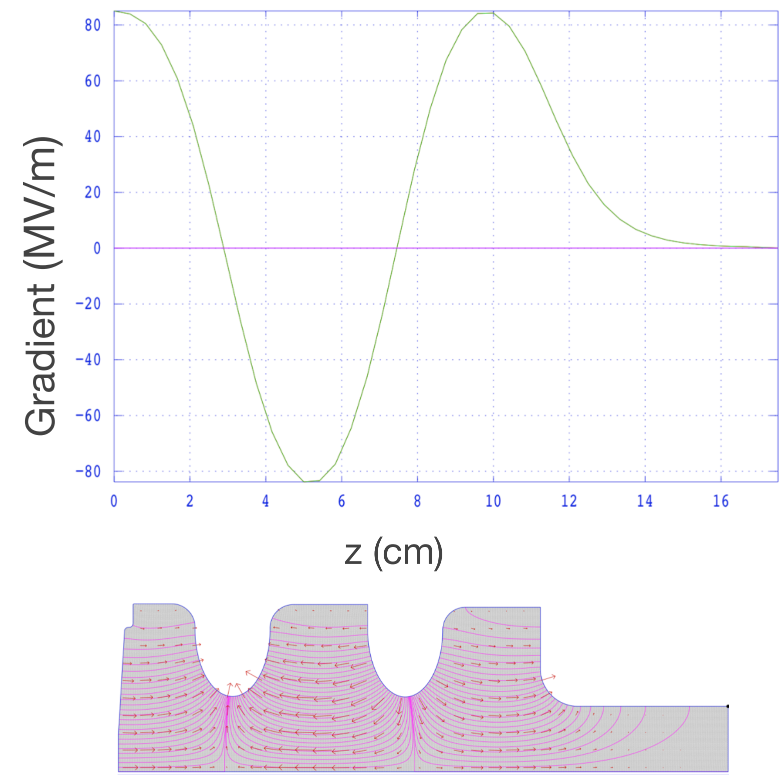
Gradient (MV/m)
z (cm)
80
60
40
20
0
-20
-40
-60
-80
0
2
4
6
8
10
12
14
16

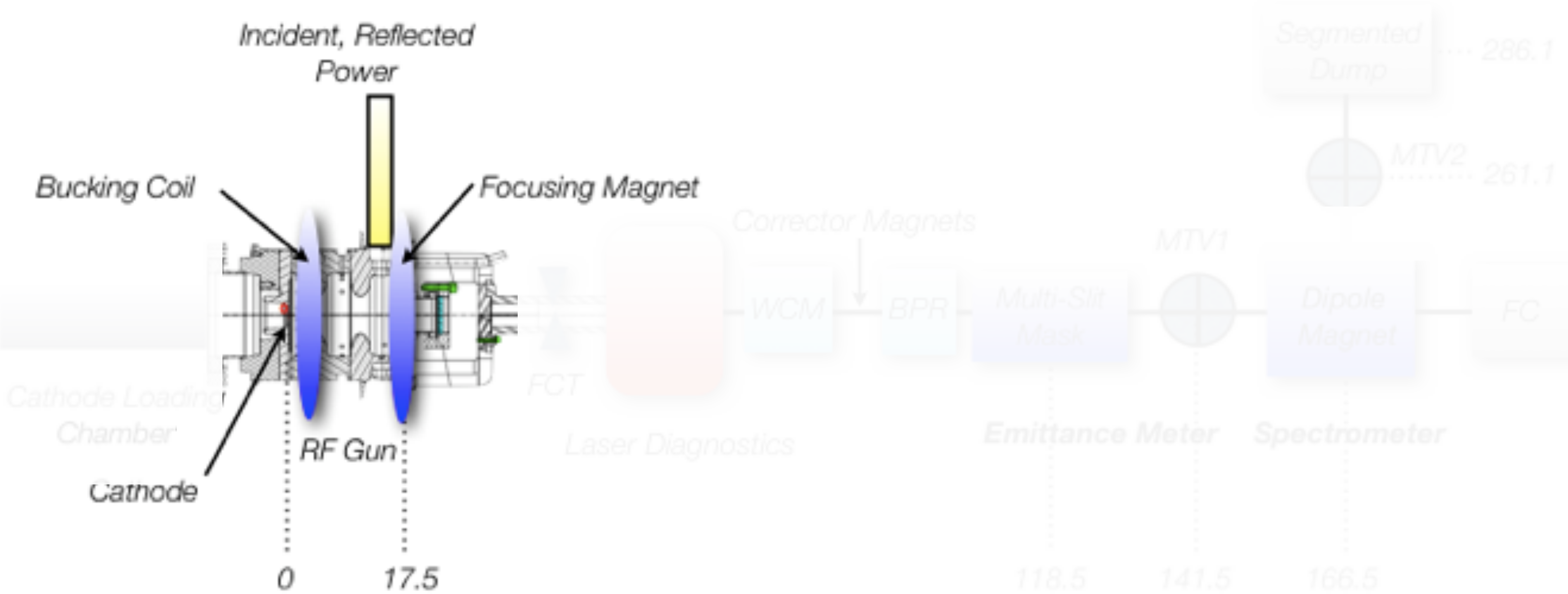
Incident, Reflected
Power
Bucking Coil
Focusing Magnet
RF Gun
Cathode
0
17.5
Cathode Loading
Chamber
FCT
Laser Diagnostics
Corrector Magnets
WCM
BPR
Multi-Slit
Mask
MTV1
Dipole
Magnet
FC
Segmented
Dump
286.1
MTV2
261.1
Emittance Meter
Spectrometer
118.5
141.5
166.5

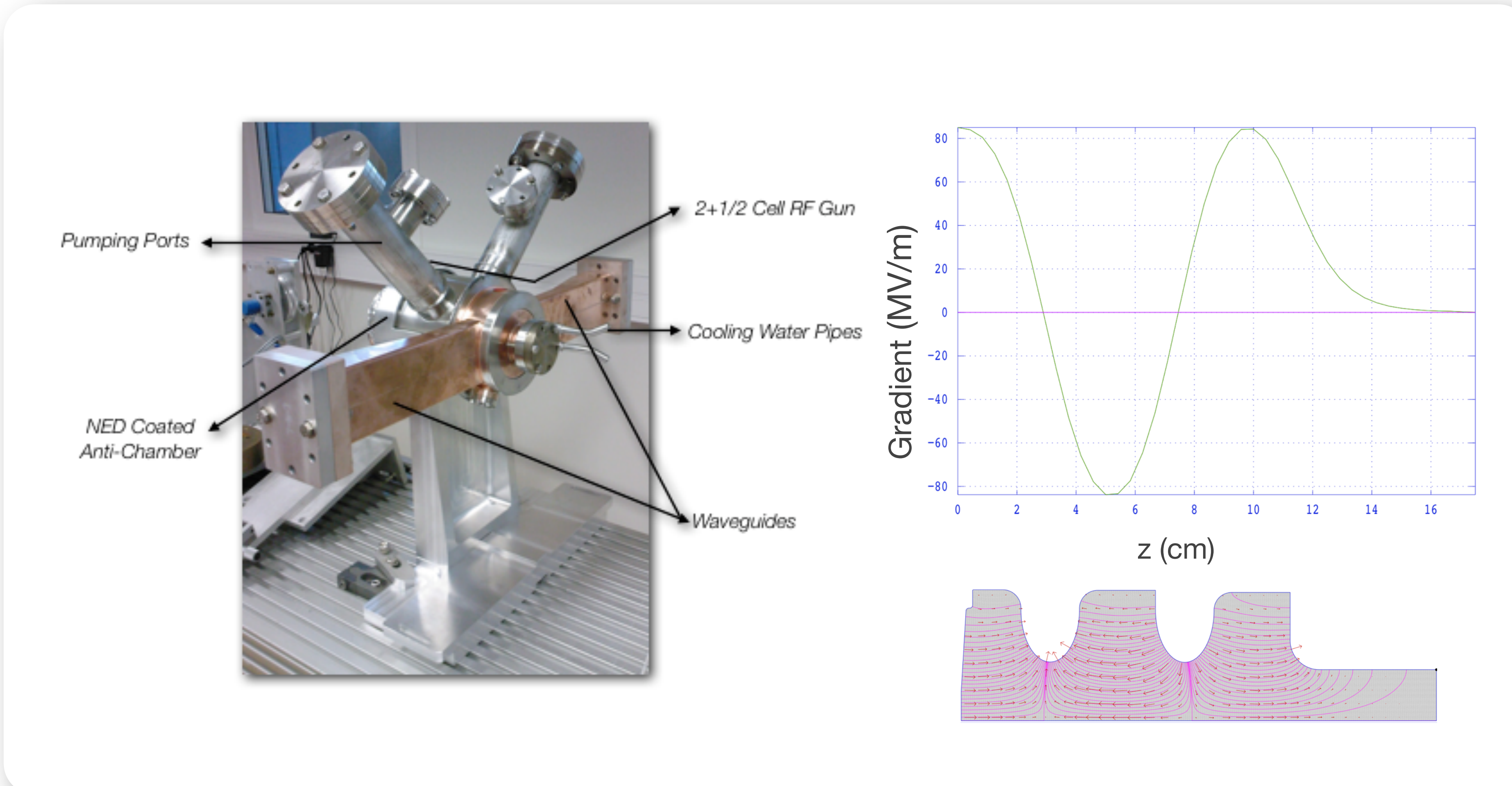

- Normal conducting 2+1/2 cell RF cavity

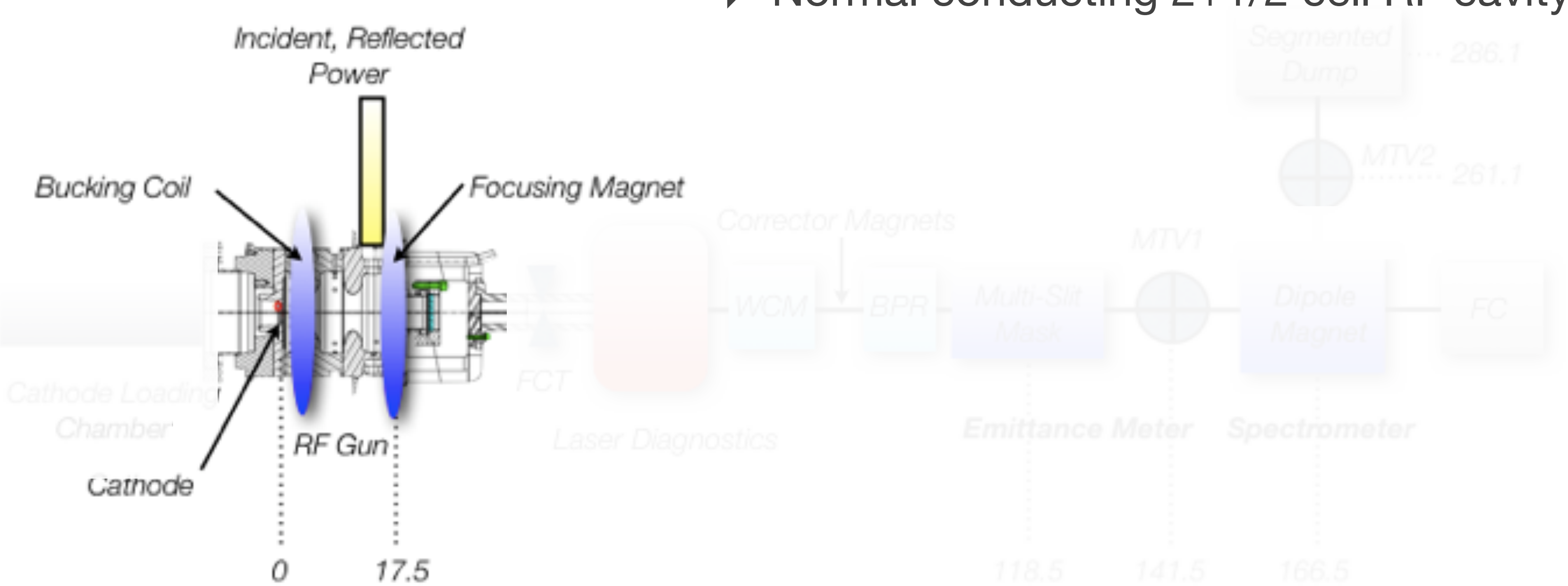

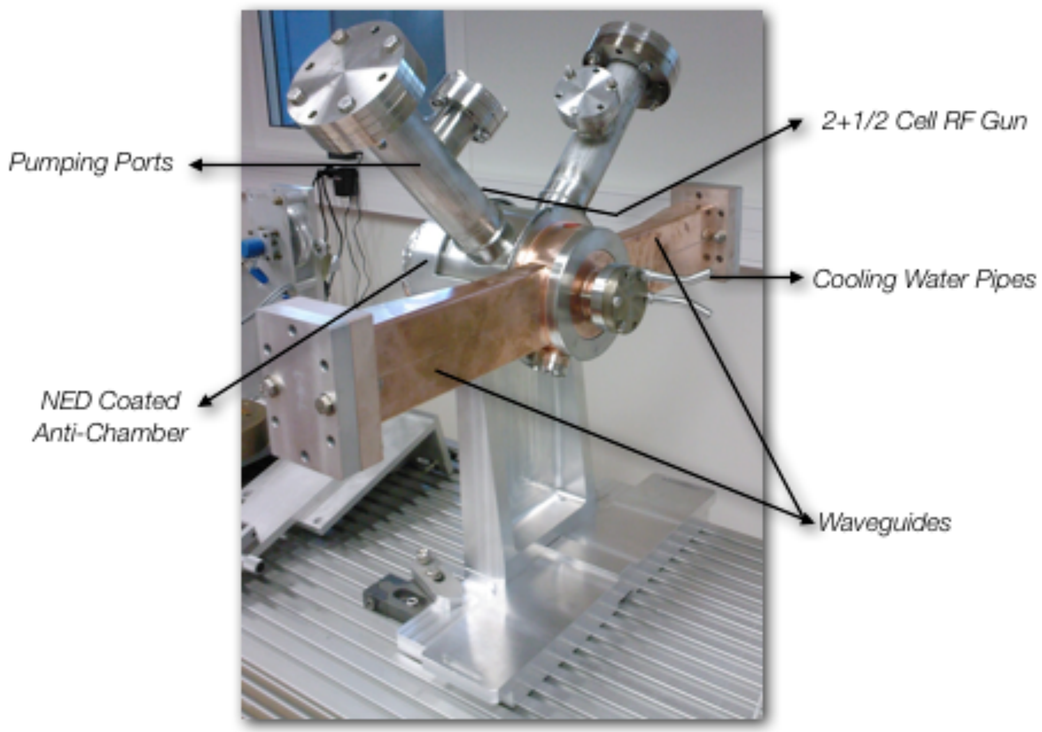

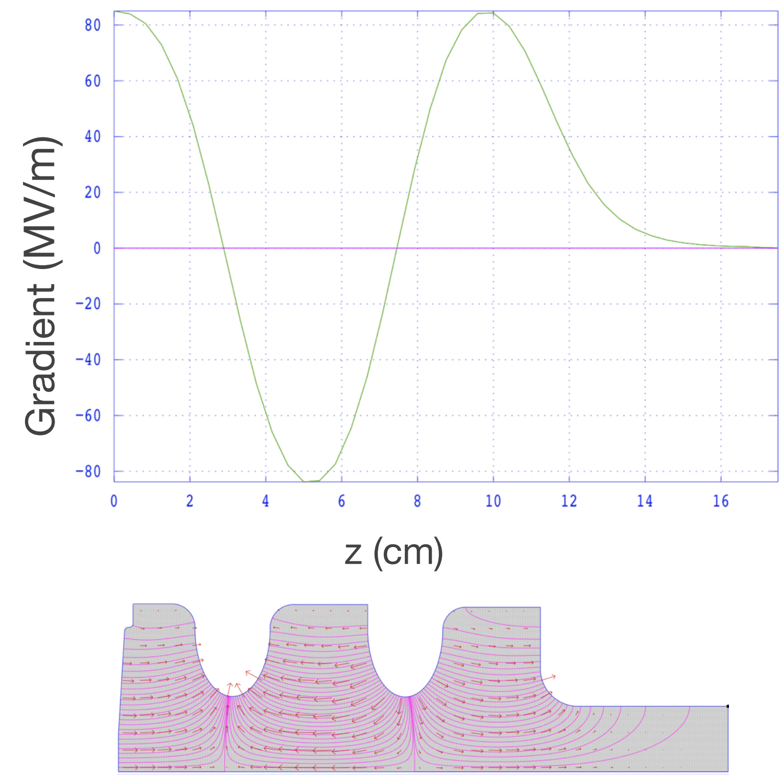

- Normal conducting 2+1/2 cell RF cavity
- Tuned to S-band (3GHz) in π-mode

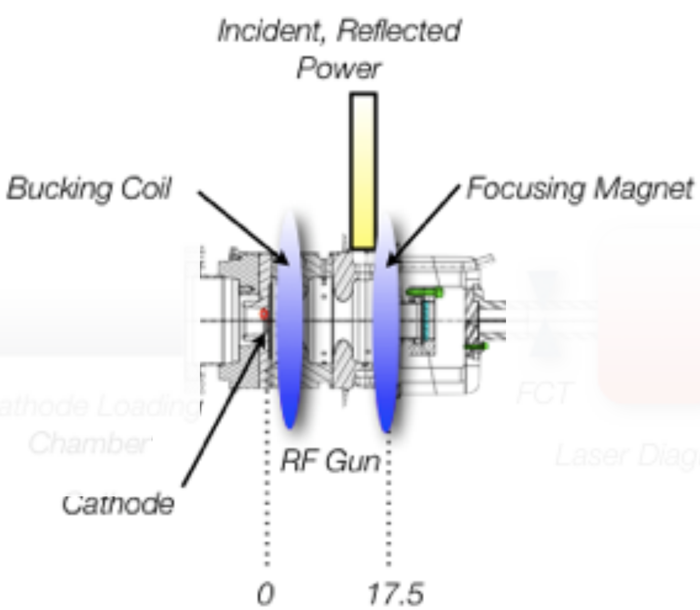

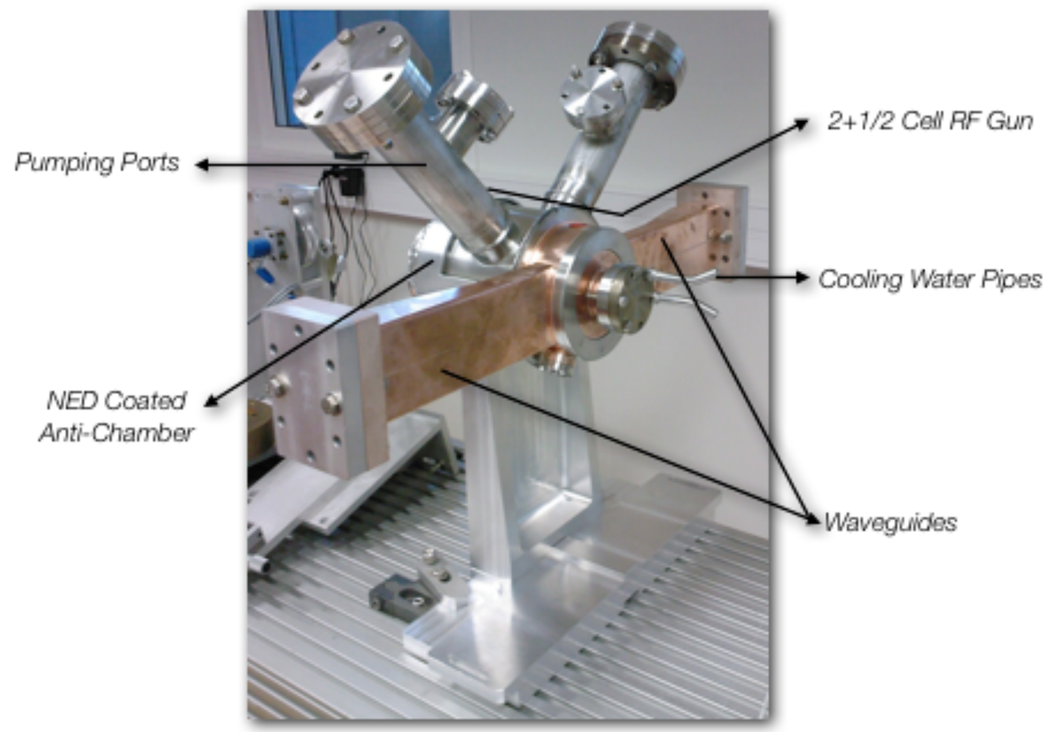

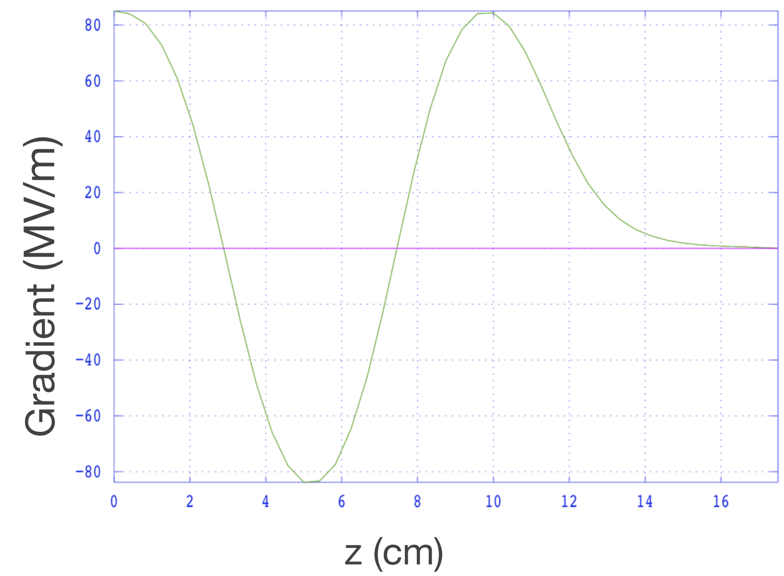

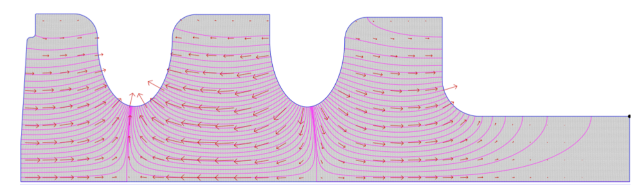

- Normal conducting 2+1/2 cell RF cavity
- Tuned to S-band (3GHz) in π-mode
- Acceleration under the gradient of 85 MV/m

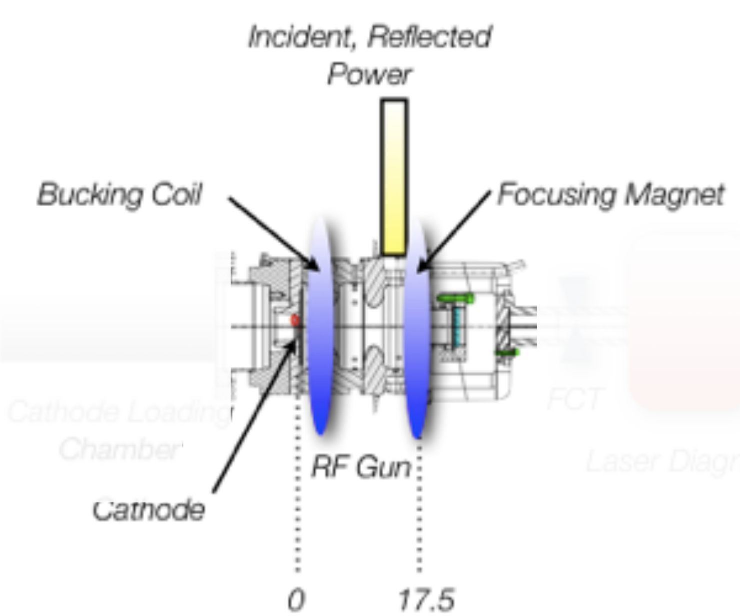

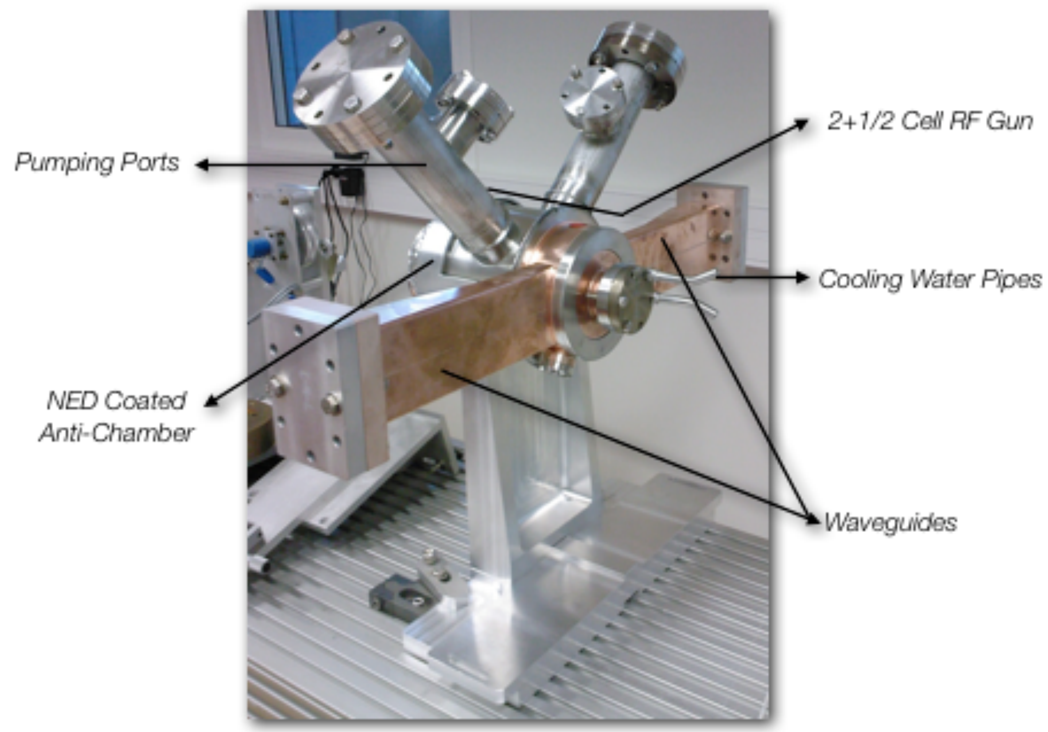

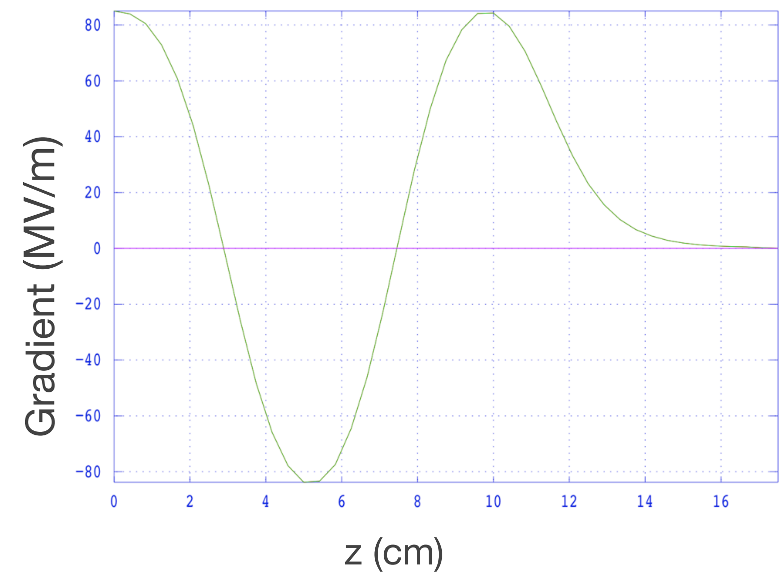

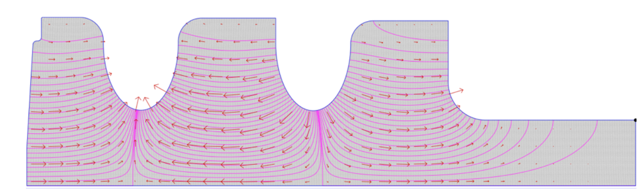

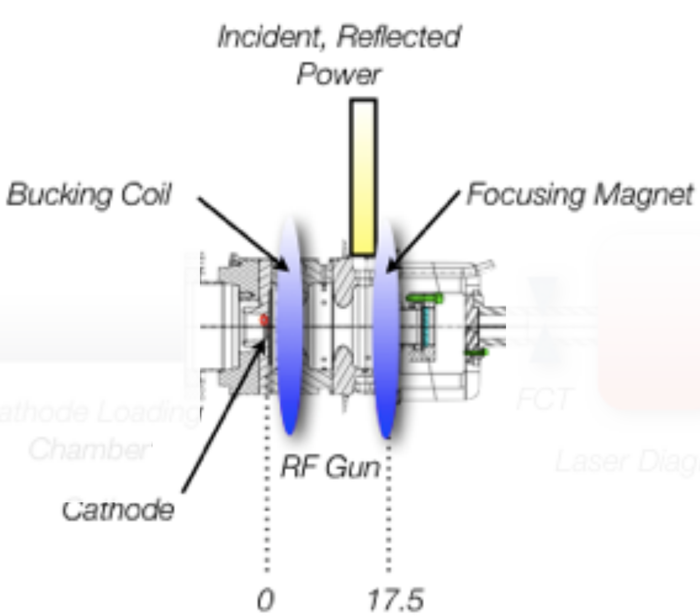

- Normal conducting 2+1/2 cell RF cavity
- Tuned to S-band (3GHz) in π-mode
- Acceleration under the gradient of 85 MV/m
- Simulations by using SUPERFISH

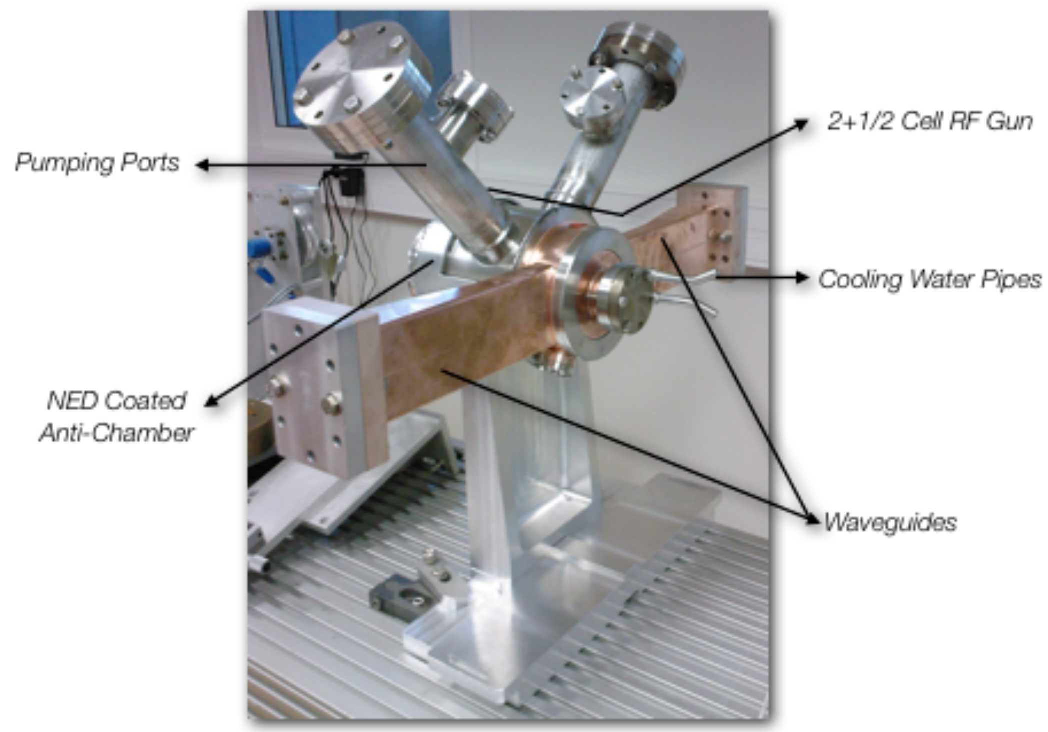

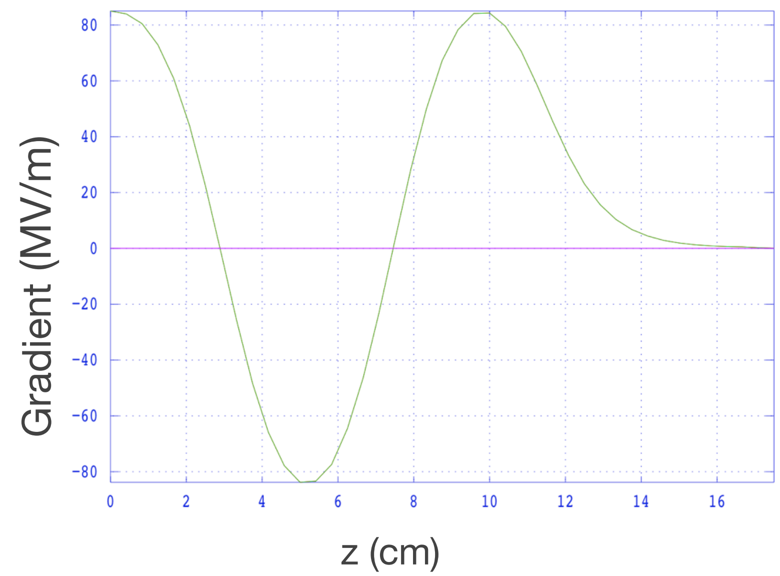

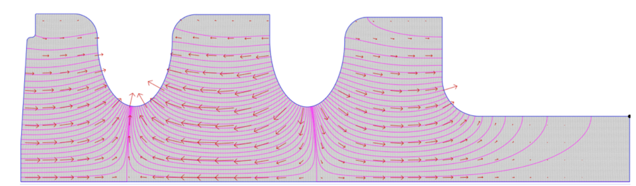

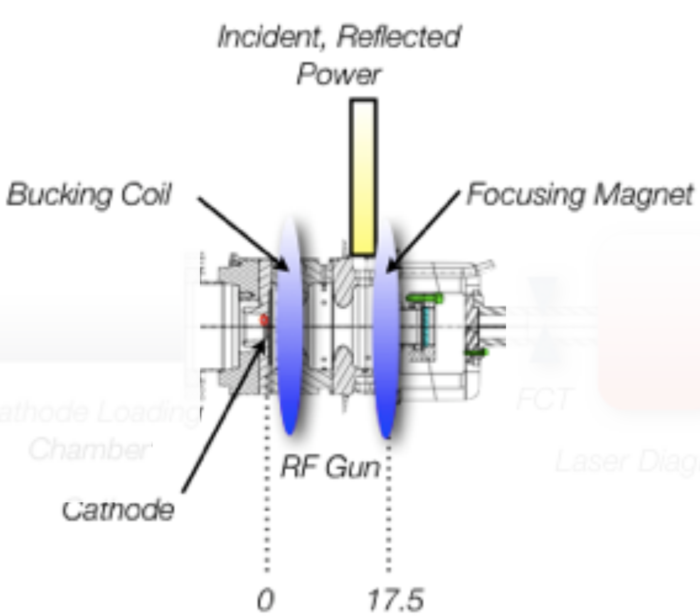

- Normal conducting 2+1/2 cell RF cavity
- Tuned to S-band (3GHz) in π-mode
- Acceleration under the gradient of 85 MV/m
- Simulations by using SUPERFISH
- The field map has been used for the beam dynamics simulations with PARMELA

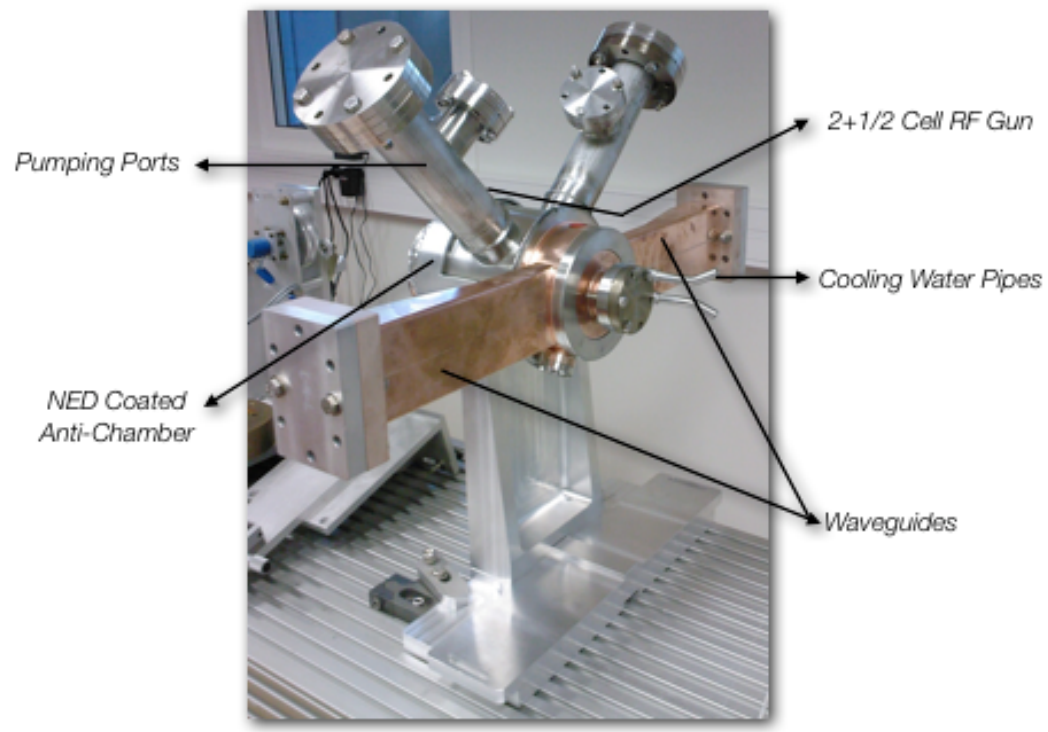

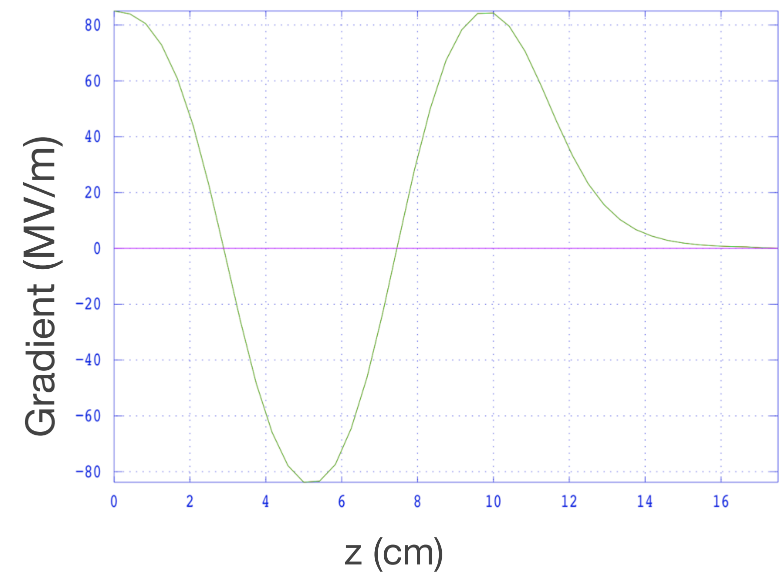

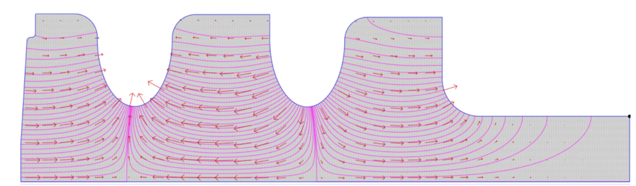

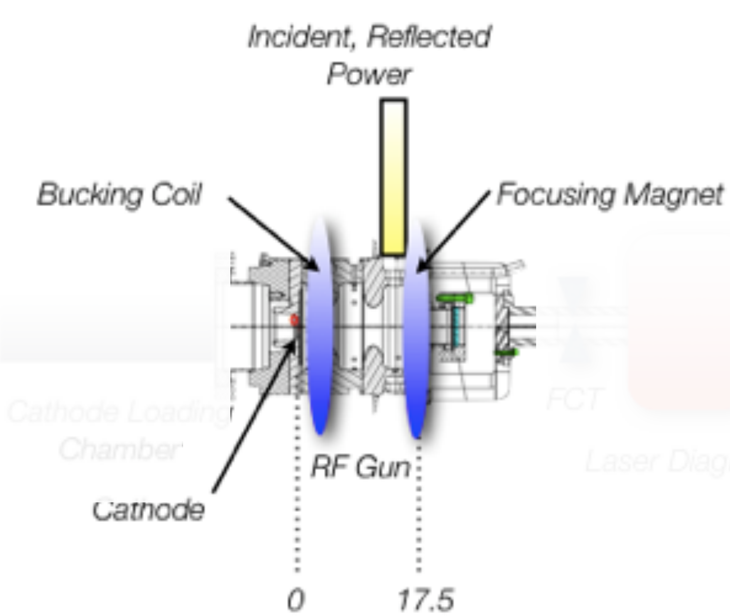

- Normal conducting 2+1/2 cell RF cavity
- Tuned to S-band (3GHz) in π-mode
- Acceleration under the gradient of 85 MV/m
- Simulations by using SUPERFISH
- The field map has been used for the beam dynamics simulations with PARMELA
- Optimized for high charge, low electrical breakdown and dark current (half cell wall angle, elliptical irises)

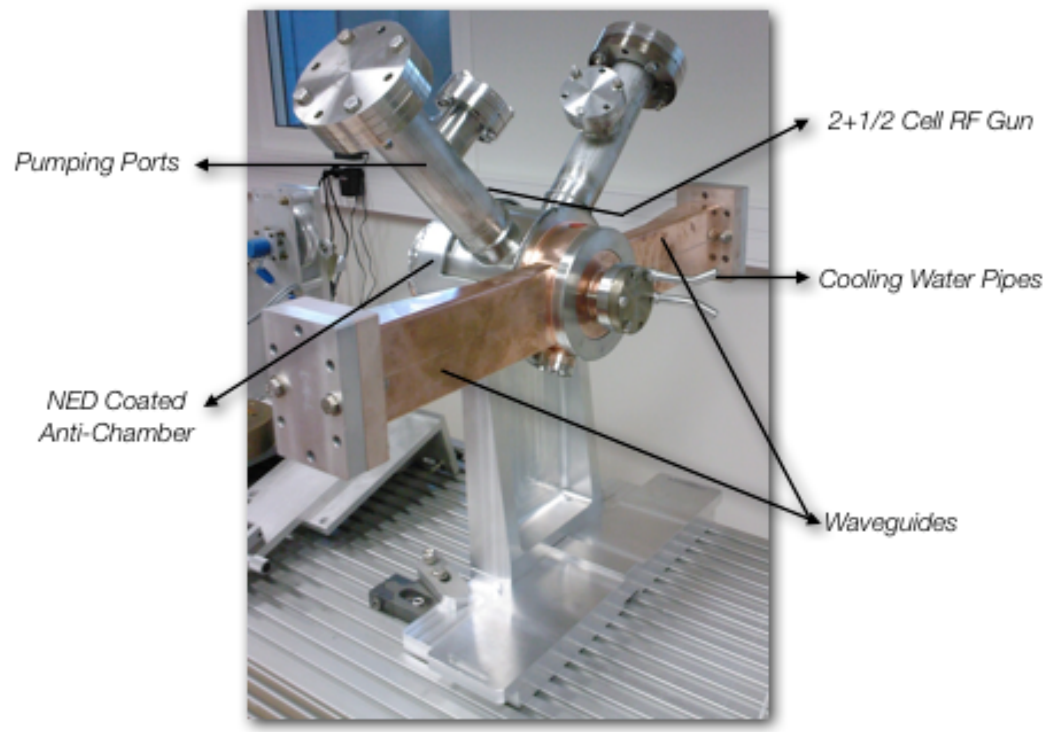

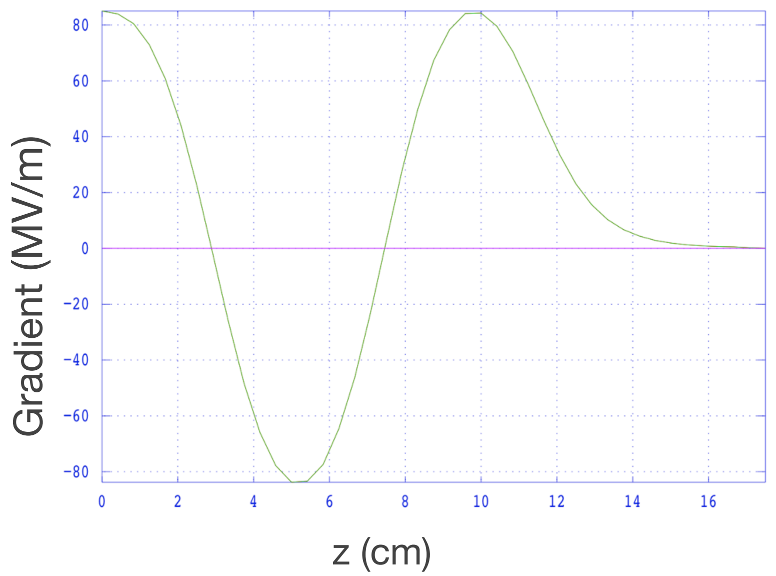

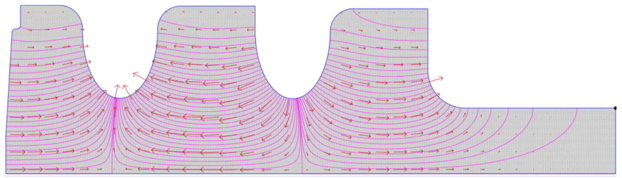

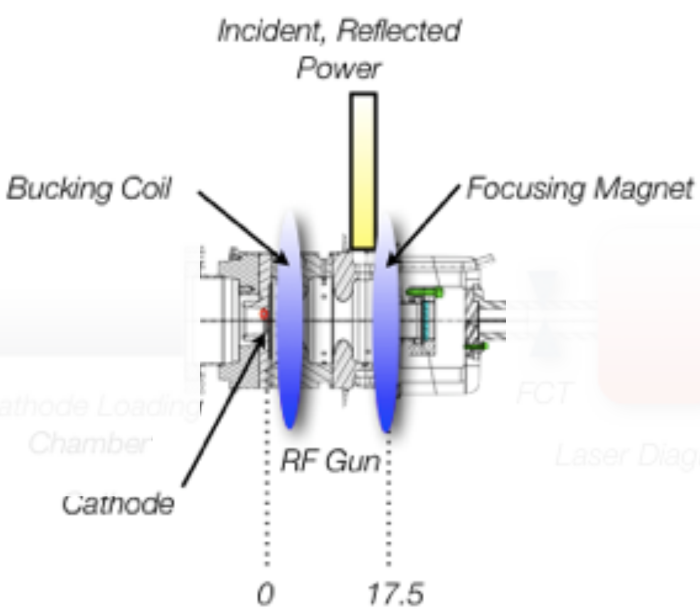

- Normal conducting 2+1/2 cell RF cavity
- Tuned to S-band (3GHz) in π-mode
- Acceleration under the gradient of 85 MV/m
- Simulations by using SUPERFISH
- The field map has been used for the beam dynamics simulations with PARMELA
- Optimized for high charge, low electrical breakdown and dark current (half cell wall angle, elliptical irises)
- Optimized for good dynamic vacuum as a necessity for high charge production (Non-Evaporable Getter, NEG, coating of anti-chamber)

OTR Profiling

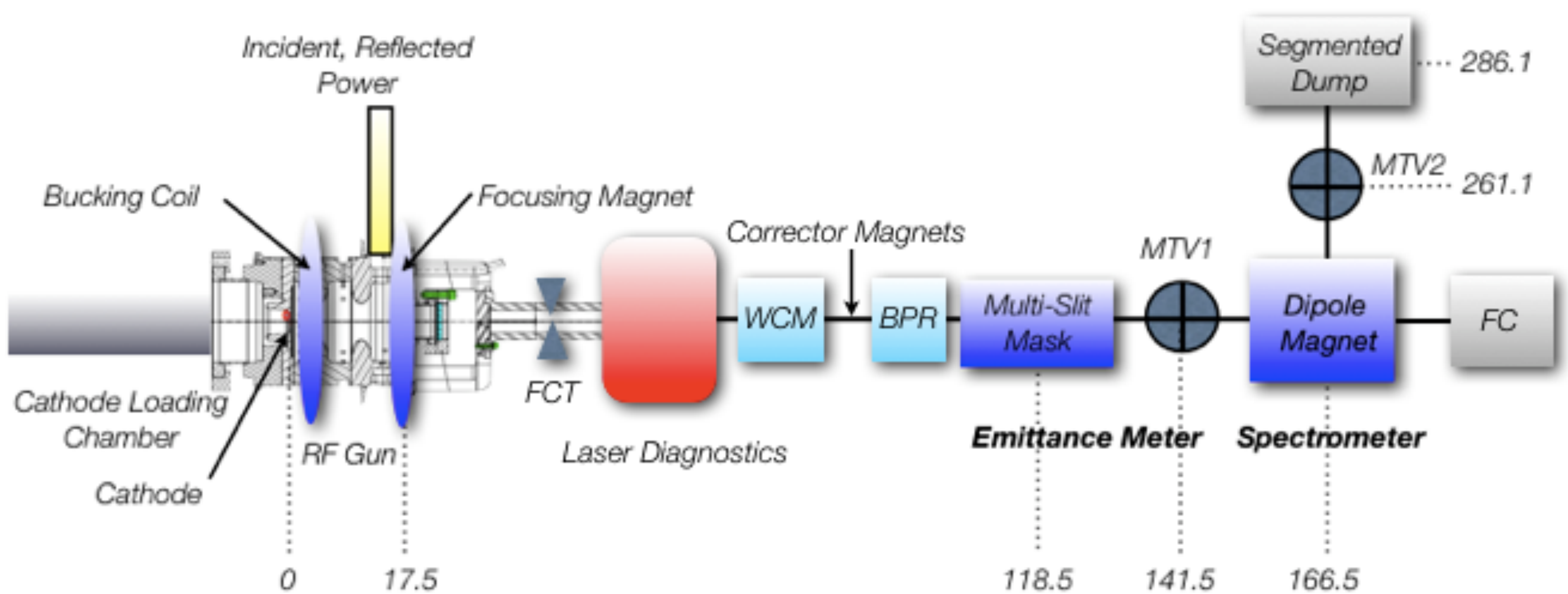

OTR Profiling

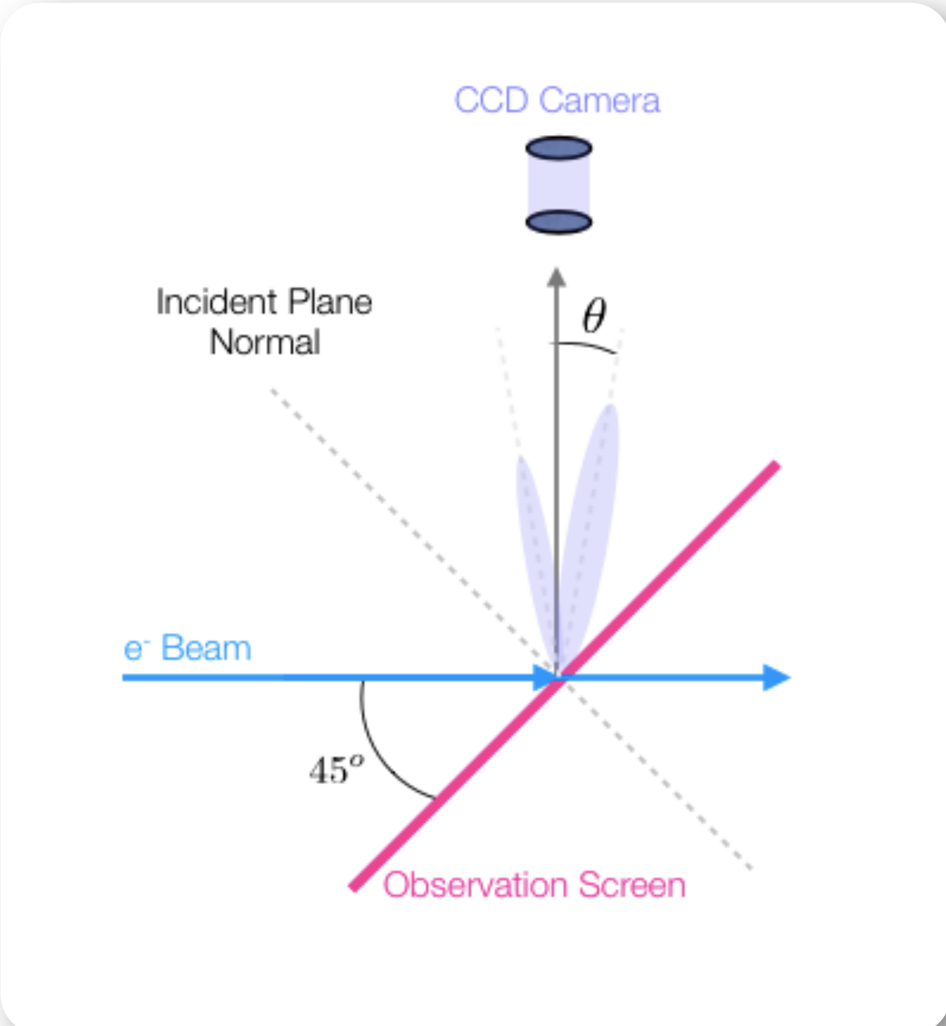

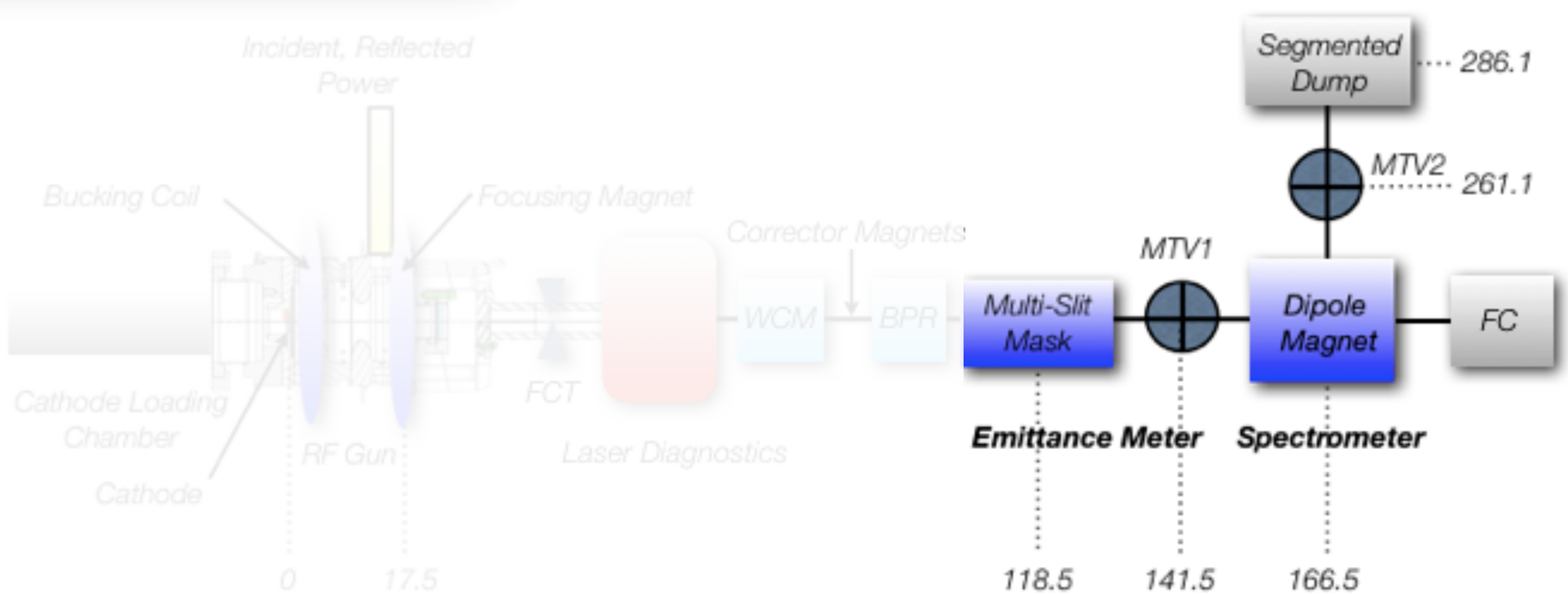

OTR Profiling

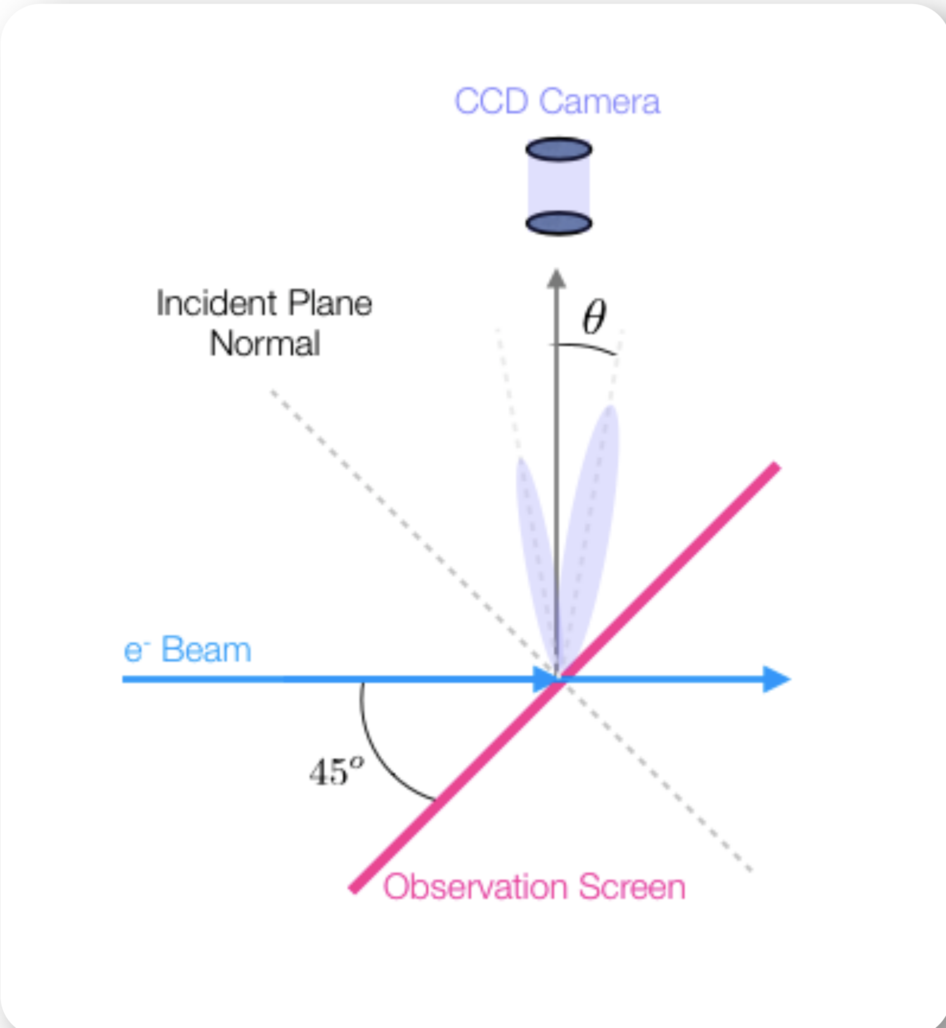

- Charged particles emit **Optical Transition Radiation** (OTR) while crossing a boundary with different dielectric properties.

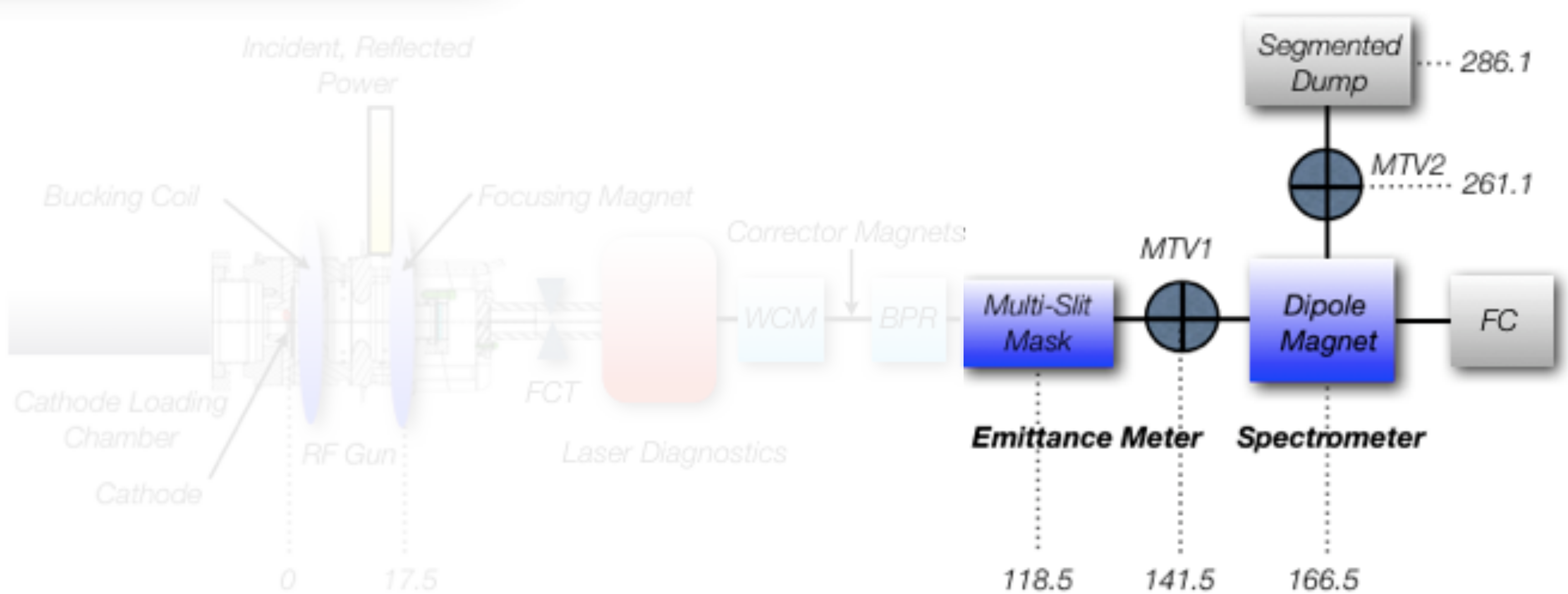

OTR Profiling

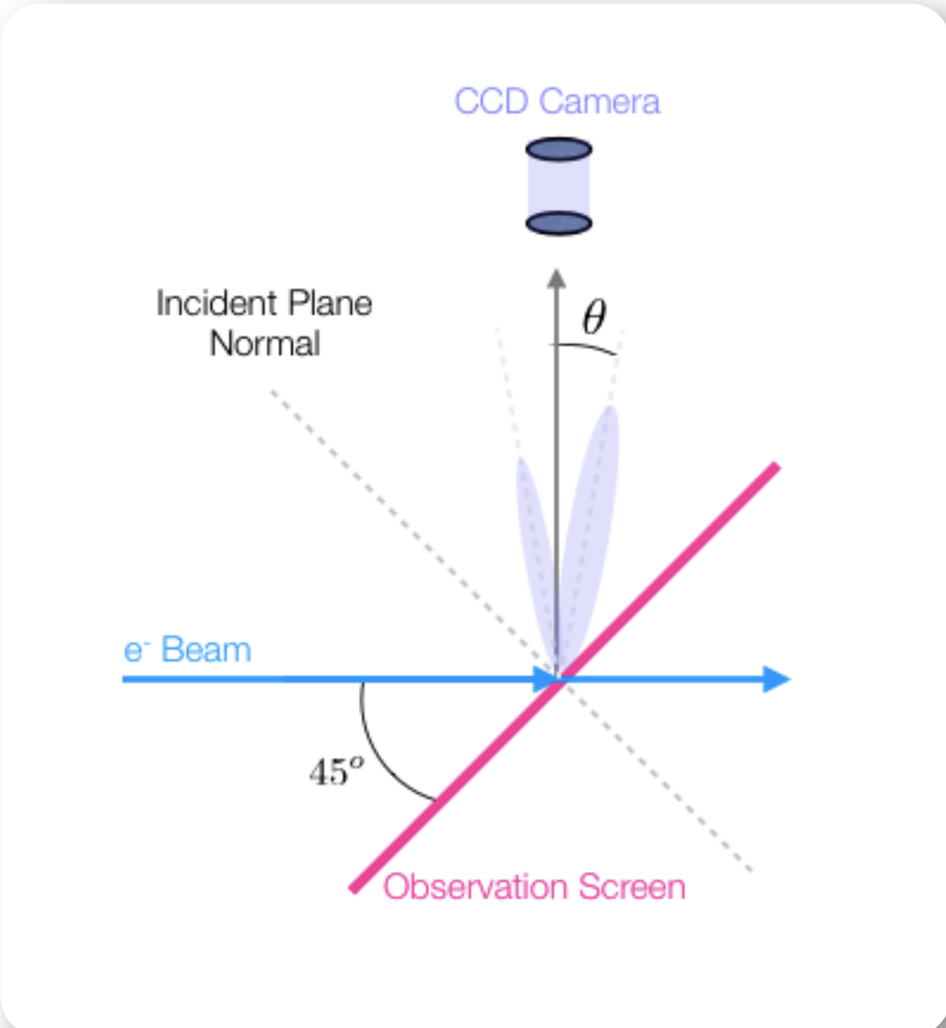

- Charged particles emit **Optical Transition Radiation** (OTR) while crossing a boundary with different dielectric properties.
- **OTR** is used to measure the beam profile as a **diagnostics tool**.

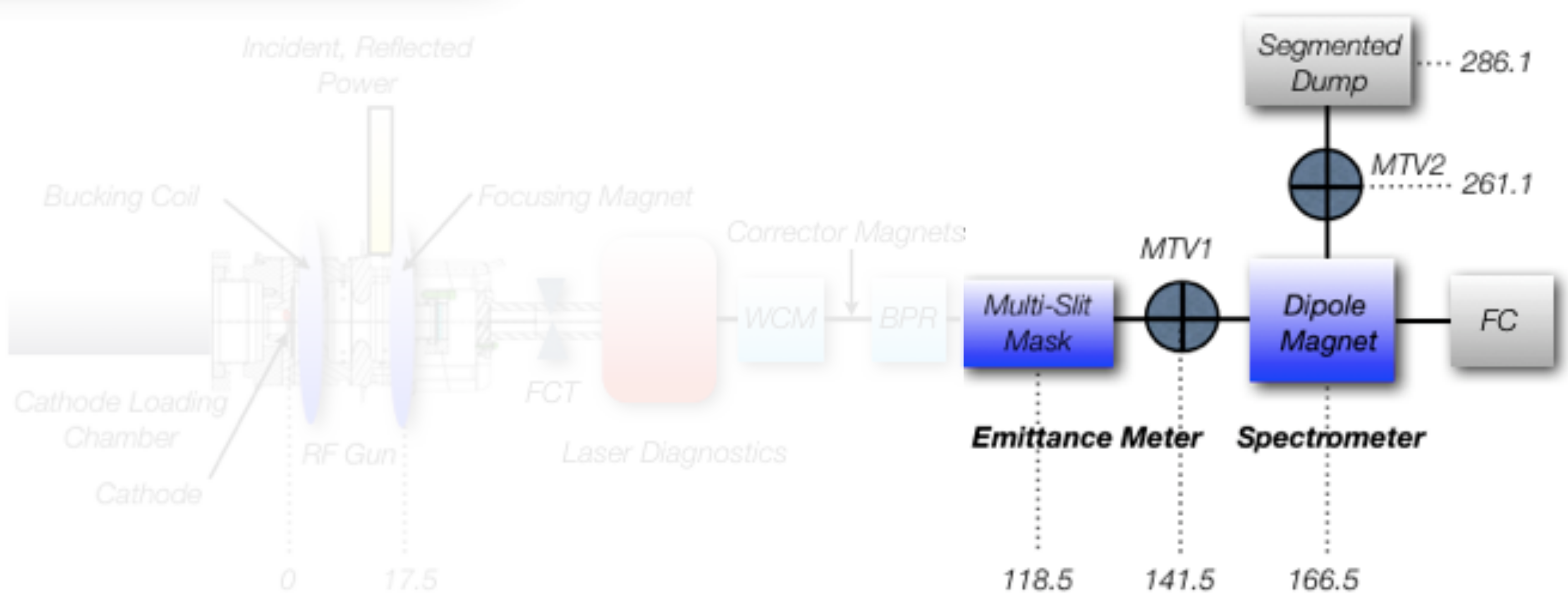

OTR Profiling

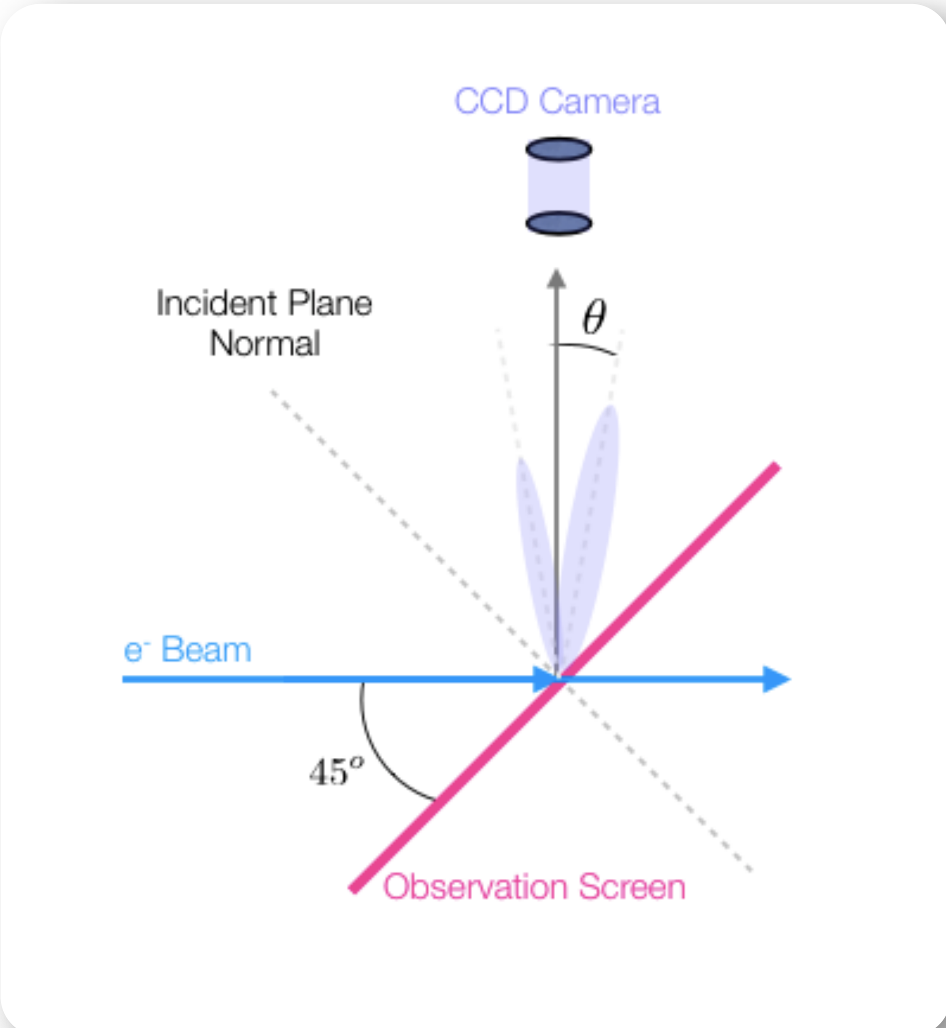

- Charged particles emit **Optical Transition Radiation** (OTR) while crossing a boundary with different dielectric properties.
- **OTR** is used to measure the beam profile as a **diagnostics tool**.
- In PHIN, two OTR monitors for emittance-meter (MTV1) and spectrometer (MTV2).

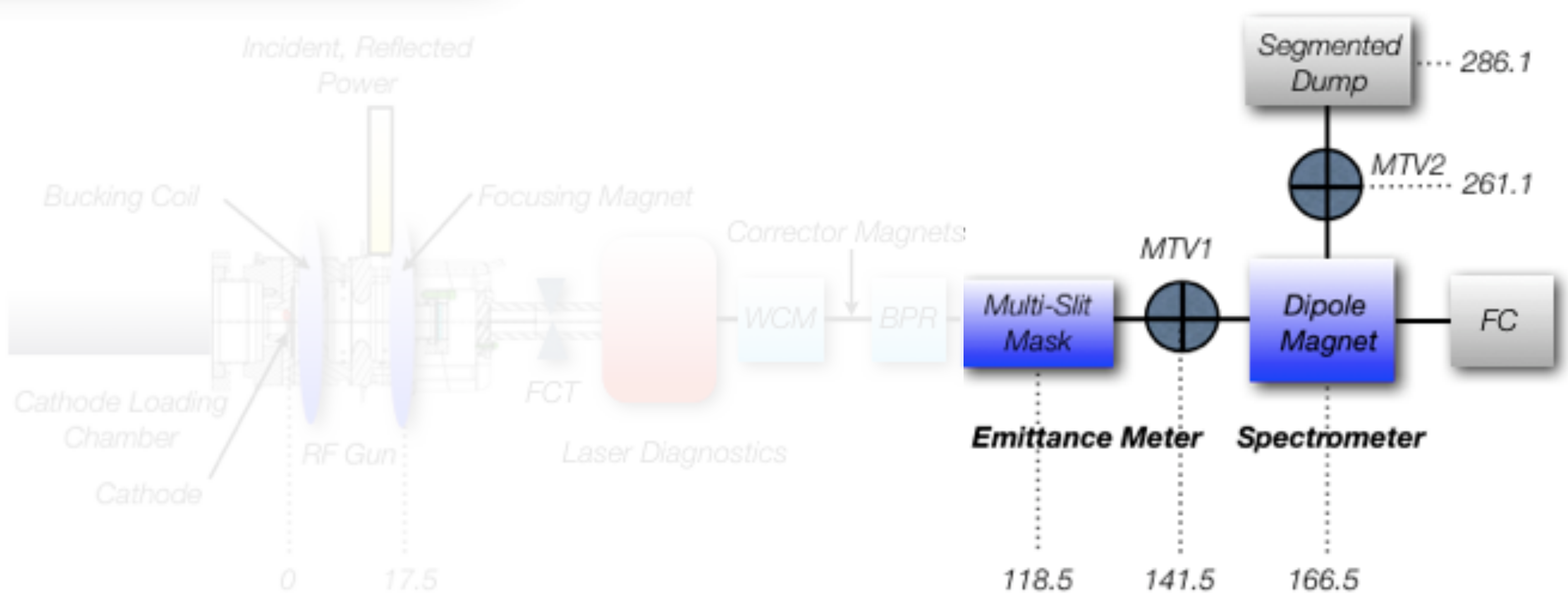

OTR Profiling

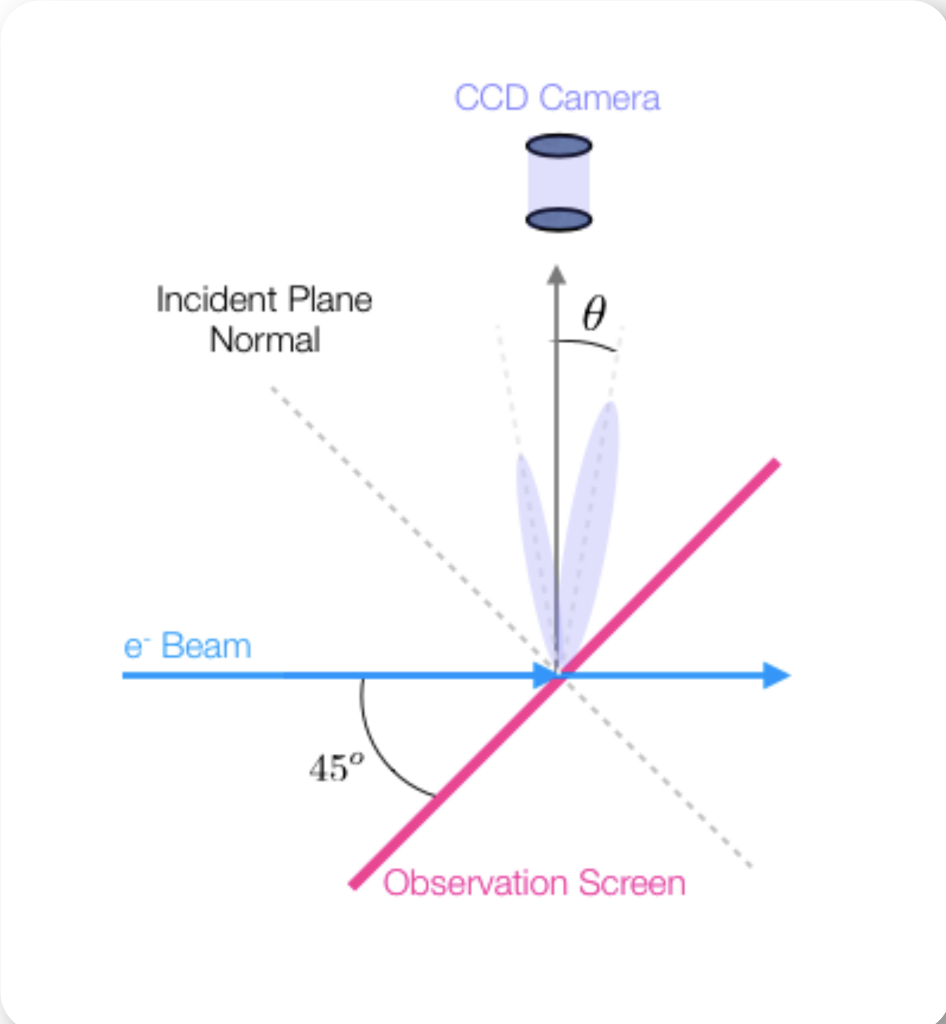

- Charged particles emit **Optical Transition Radiation** (OTR) while crossing a boundary with different dielectric properties.
- **OTR** is used to measure the beam profile as a **diagnostics tool**.
- In PHIN, two OTR monitors for emittance-meter (MTV1) and spectrometer (MTV2).
- OTR can be detected by a **ICCD** (Intensified Charge Coupled Device) camera,
- **Gateability** of ICCD is used for the **time-resolved** measurements.

Time-Resolved OTR Profiling

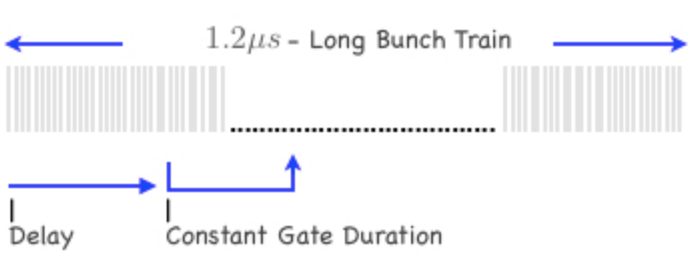

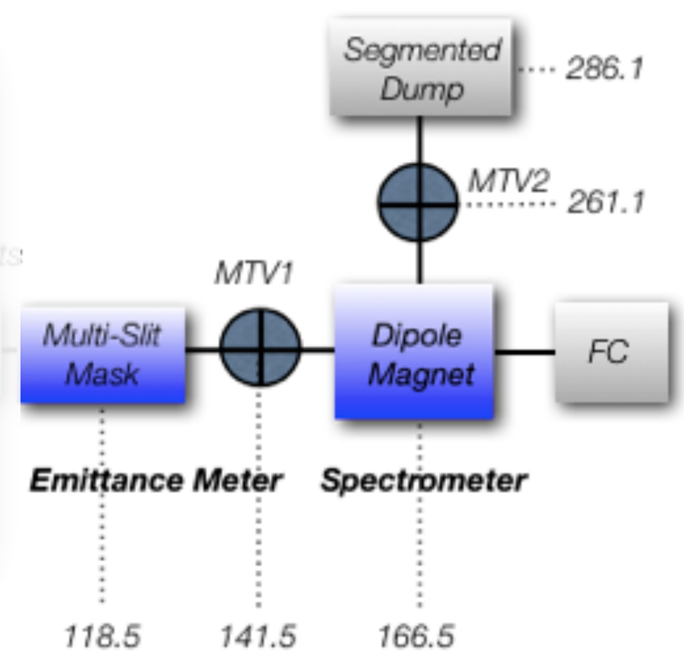

Transverse Phase Space

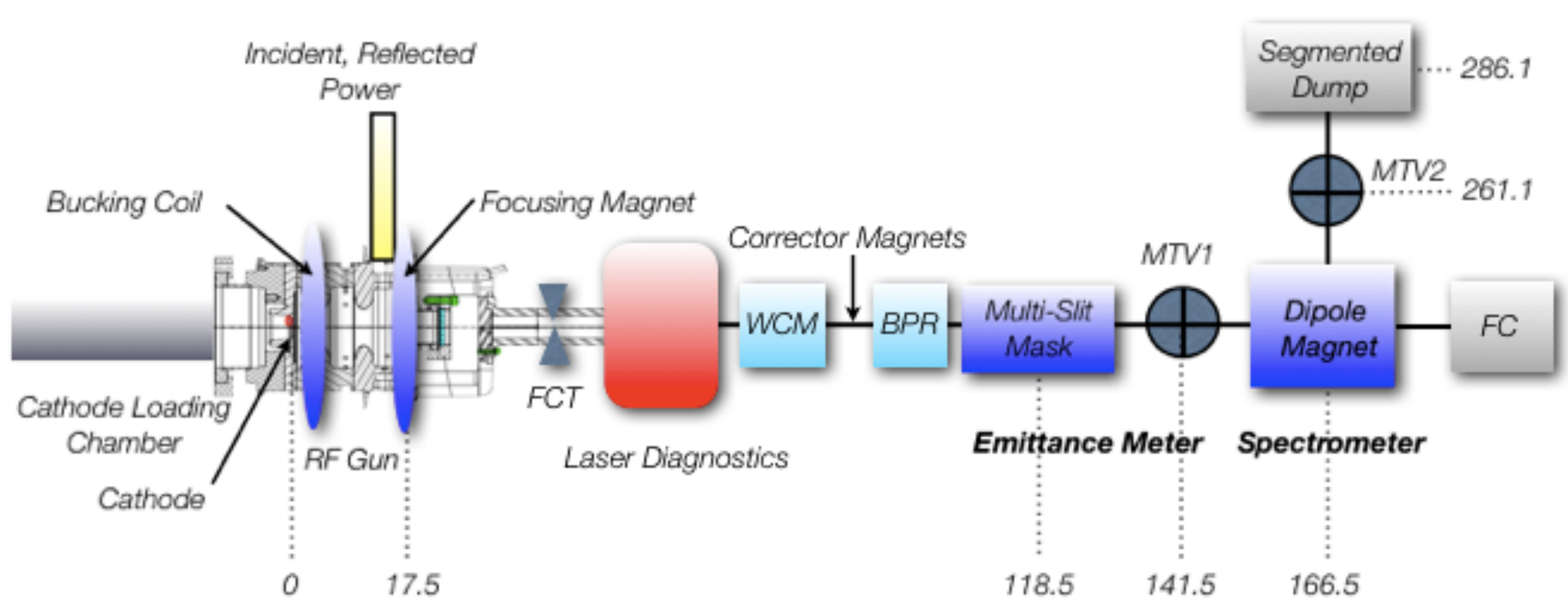

Monitoring the OTR Image of the Beam

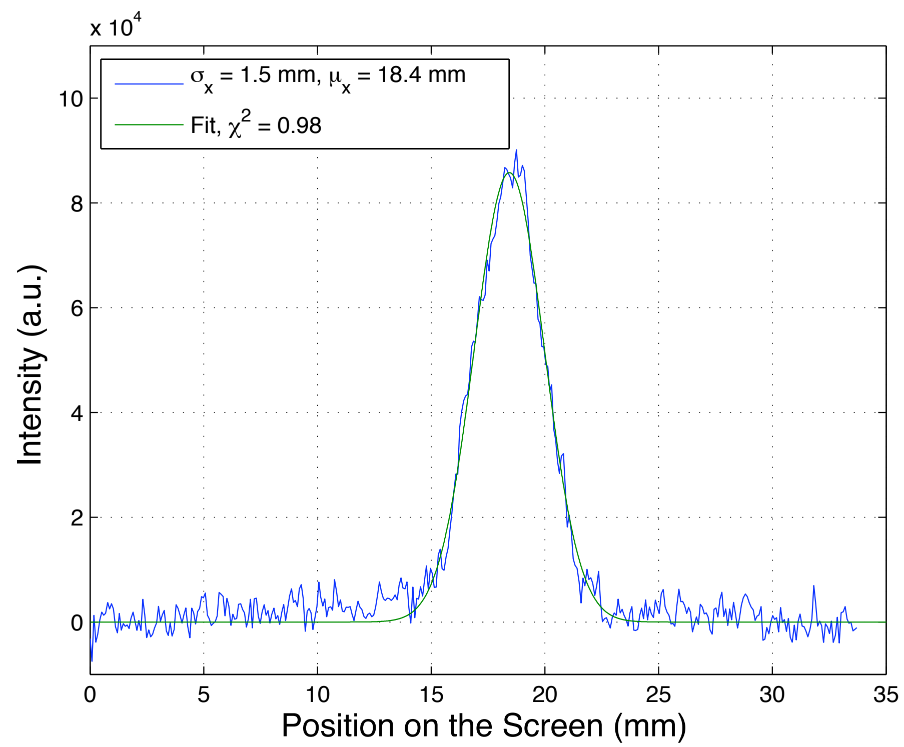

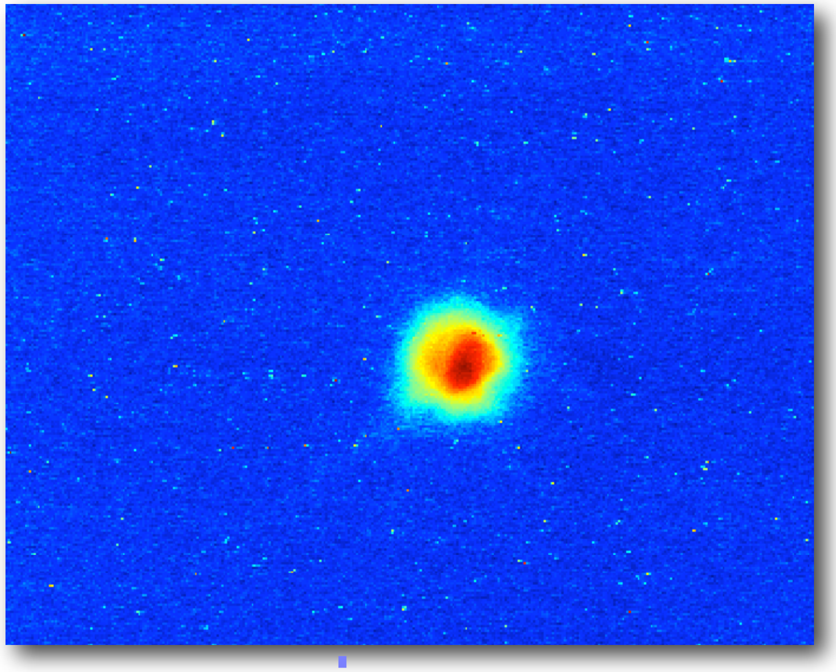

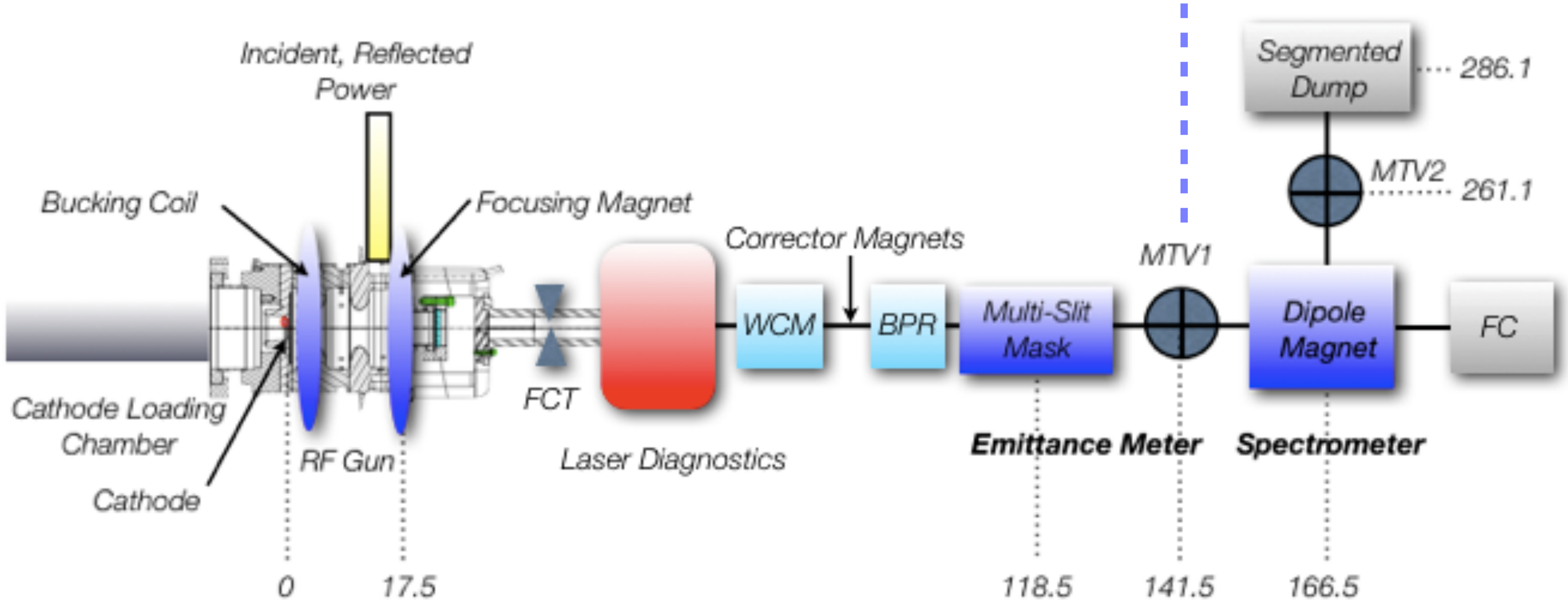

Transverse Phase Space

Beam size

Beam size

Single Shot Solenoid Scan

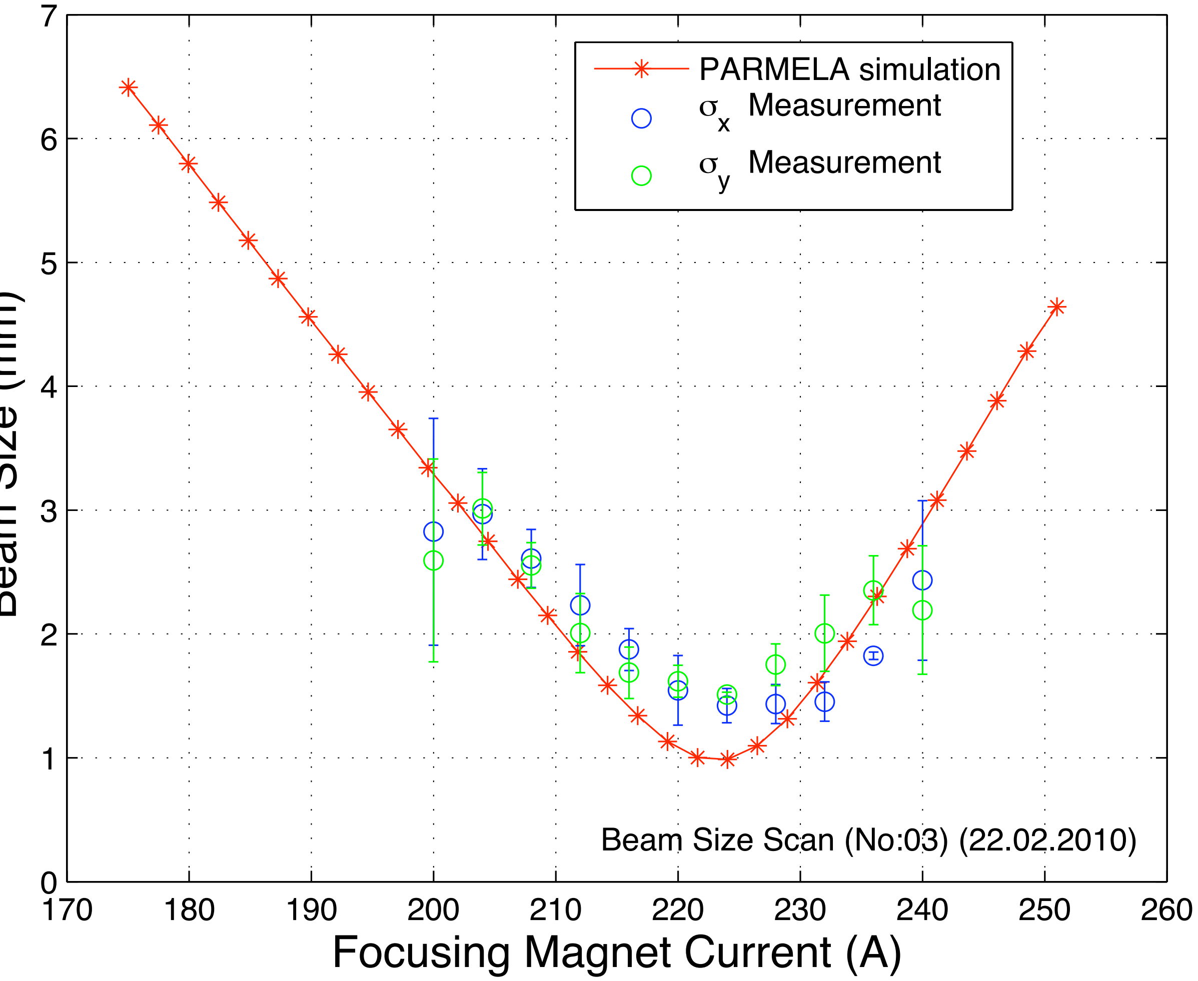

Beam size

Single Shot Solenoid Scan

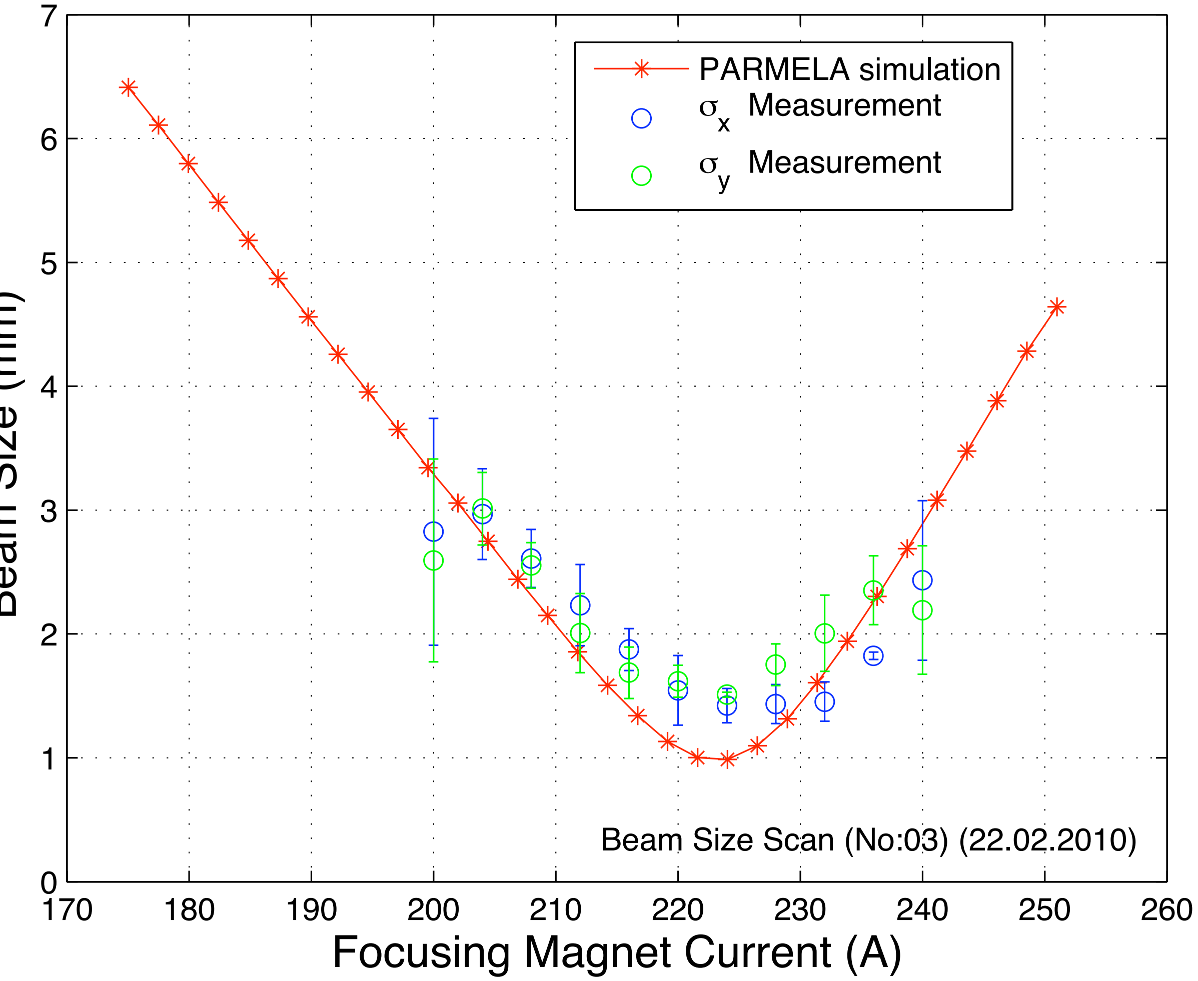

- Beam size is measured as a function of the focusing,

Beam size

Single Shot Solenoid Scan

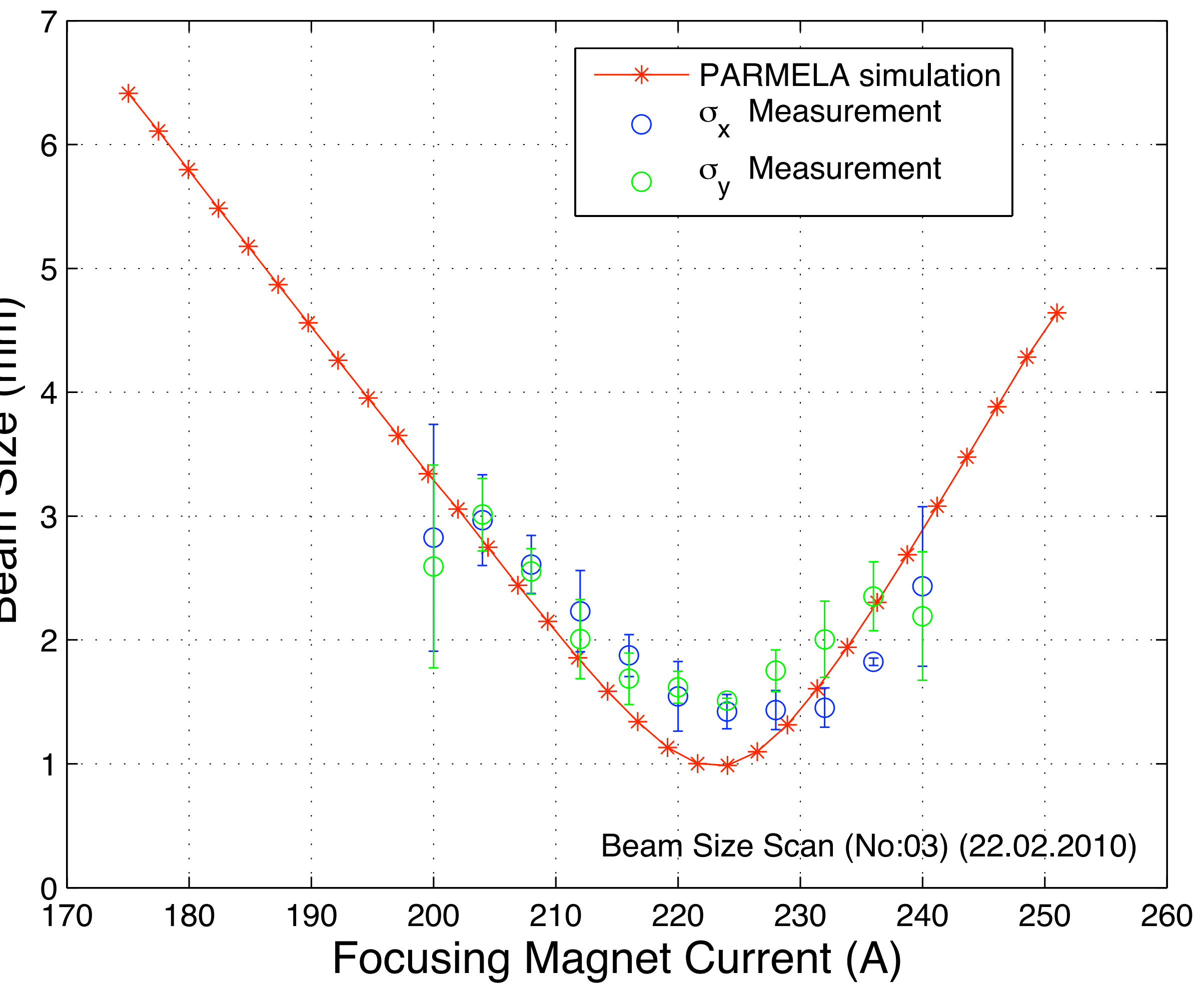

- Beam size is measured as a function of the focusing,
- A MatLab software has been developed for interfacing with the instrumentation for automatic data acquisition.

Beam size

Single Shot Solenoid Scan

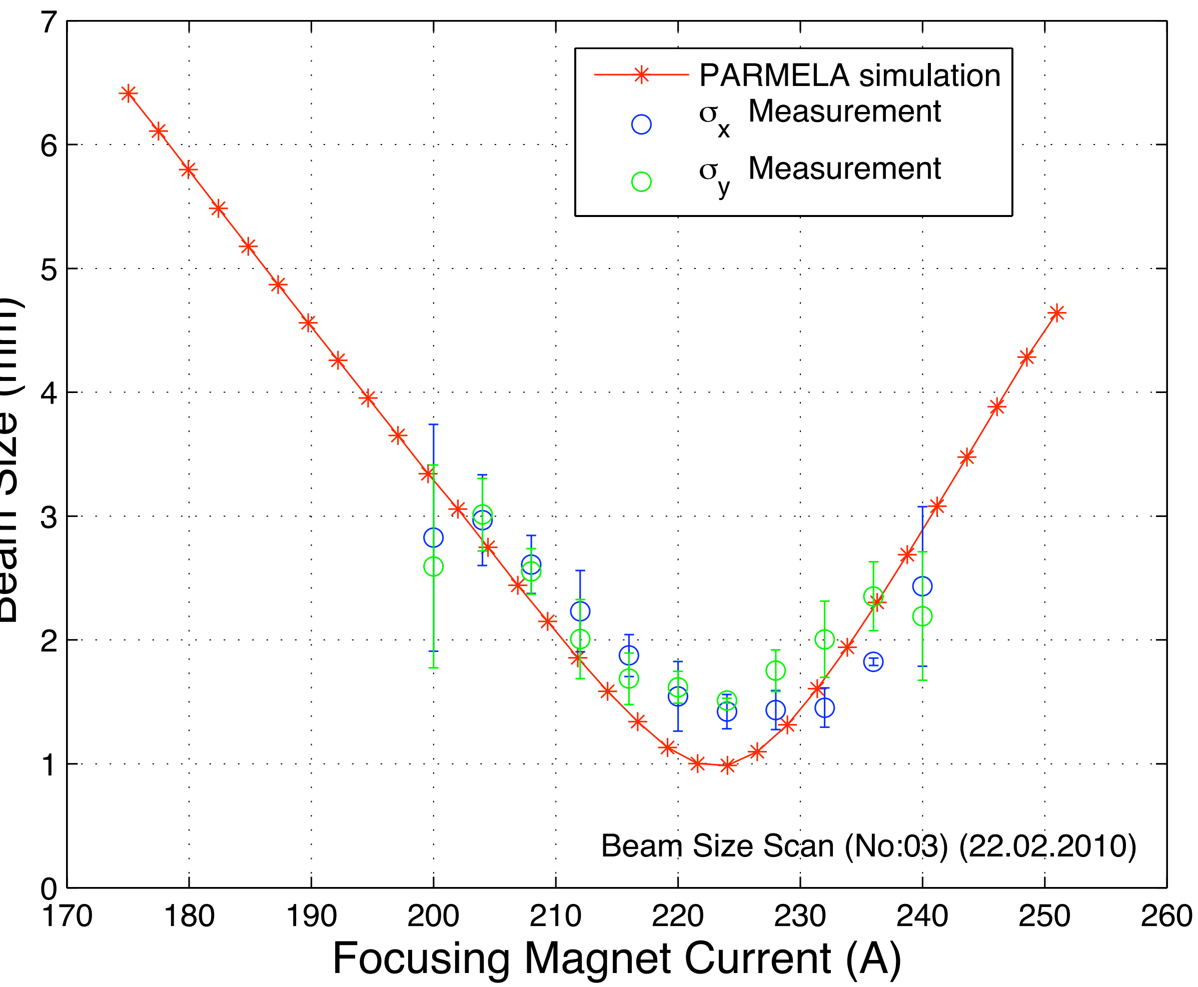

- Beam size is measured as a function of the focusing,
- A MatLab software has been developed for interfacing with the instrumentation for automatic data acquisition.
- A benchmark measurement

Beam size

Single Shot Solenoid Scan

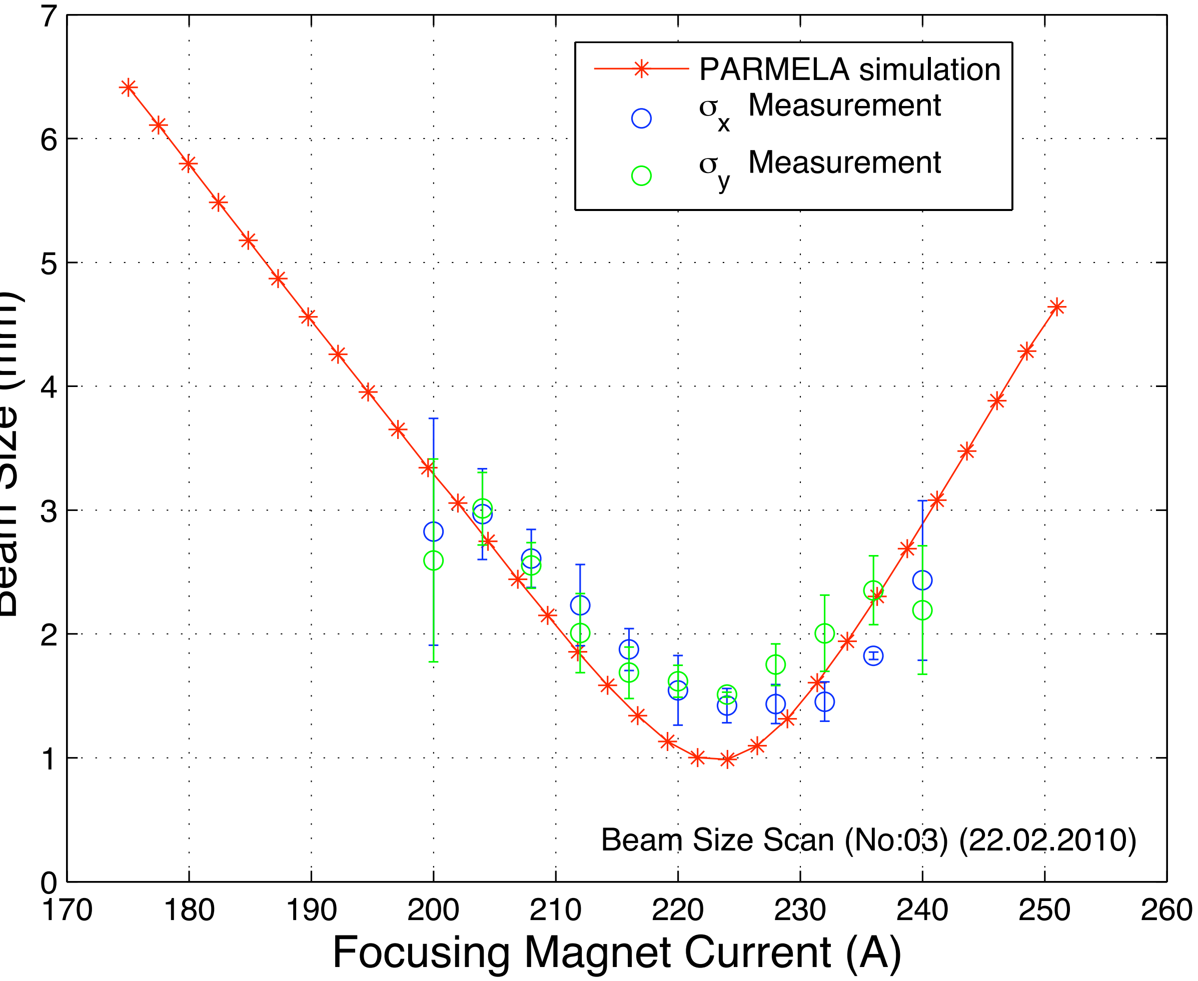

- Beam size is measured as a function of the focusing,
- A MatLab software has been developed for interfacing with the instrumentation for automatic data acquisition.
- A benchmark measurement
  - to diagnose the beam and the instrumentation,

Beam size

Single Shot Solenoid Scan

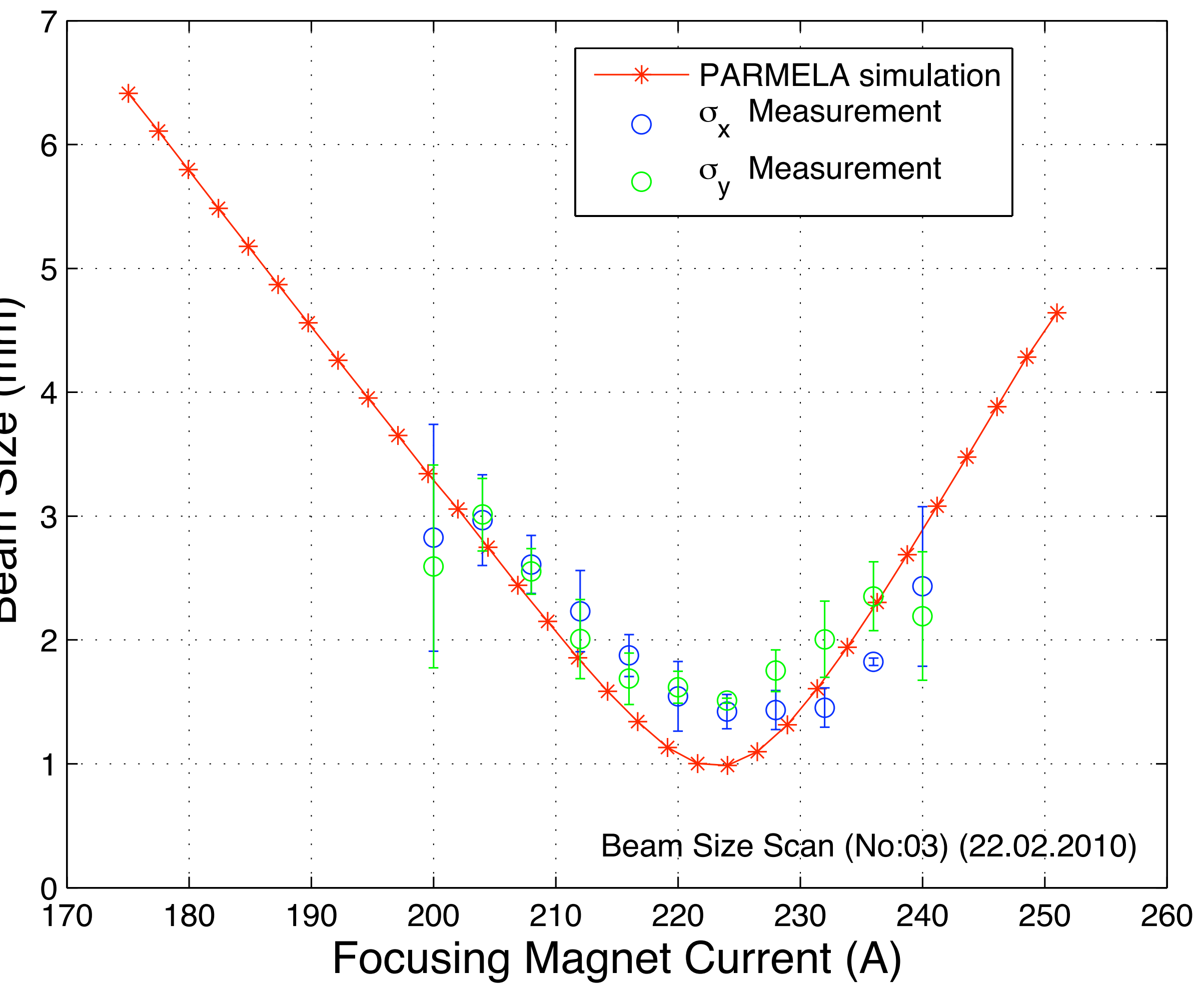

- Beam size is measured as a function of the focusing,
- A MatLab software has been developed for interfacing with the instrumentation for automatic data acquisition.
- A benchmark measurement
  - to diagnose the beam and the instrumentation,
  - to calibrate the input parameters for the simulations with respect to the actual system settings.

Beam size

Single Shot Solenoid Scan

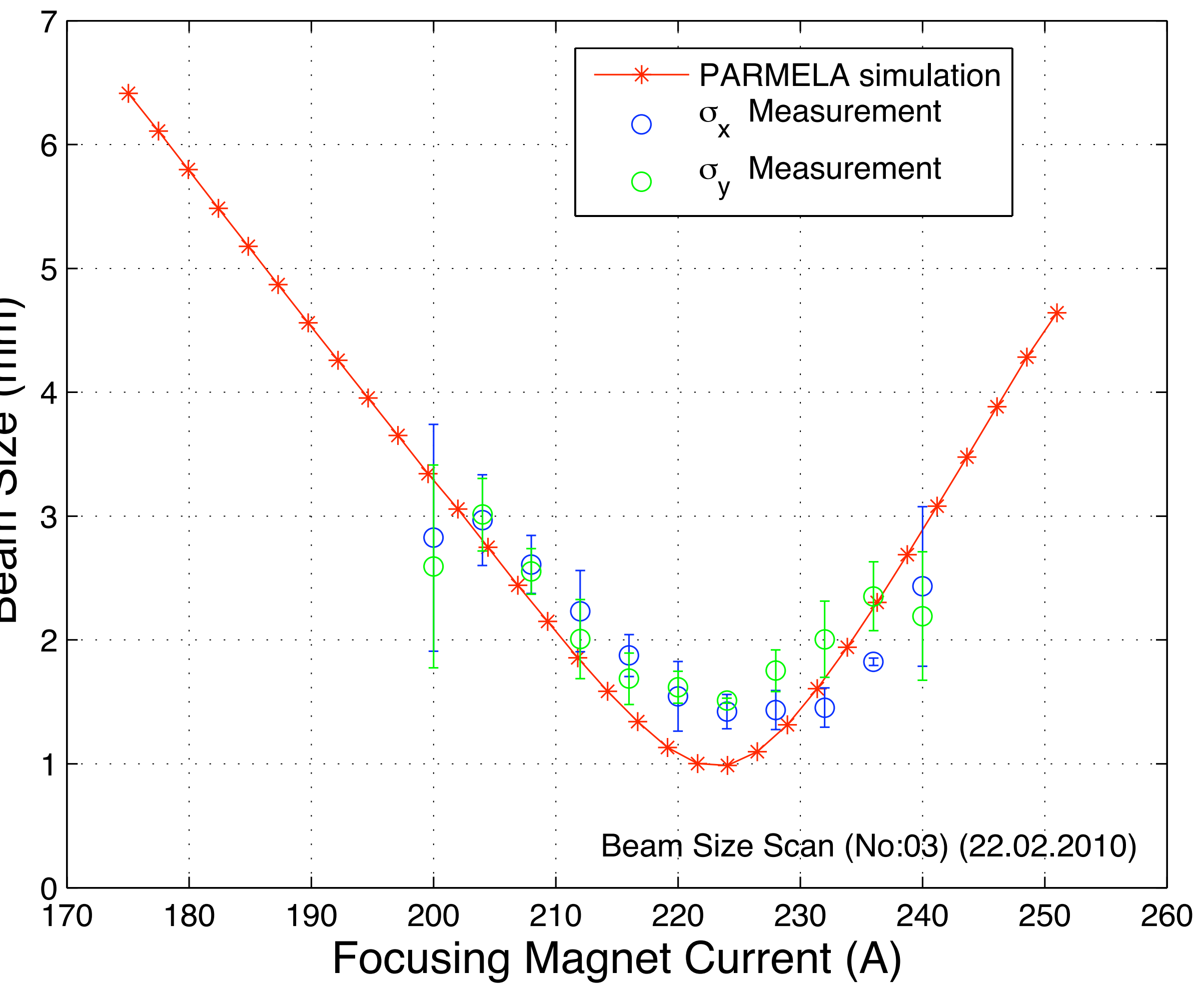

- Beam size is measured as a function of the focusing,
- A MatLab software has been developed for interfacing with the instrumentation for automatic data acquisition.
- A benchmark measurement
  - to diagnose the beam and the instrumentation,
  - to calibrate the input parameters for the simulations with respect to the actual system settings.
  - such as laser spot size, beam energy, focusing magnet current, RF phase, gradient, charge per bunch...

Beam size

Single Shot Solenoid Scan

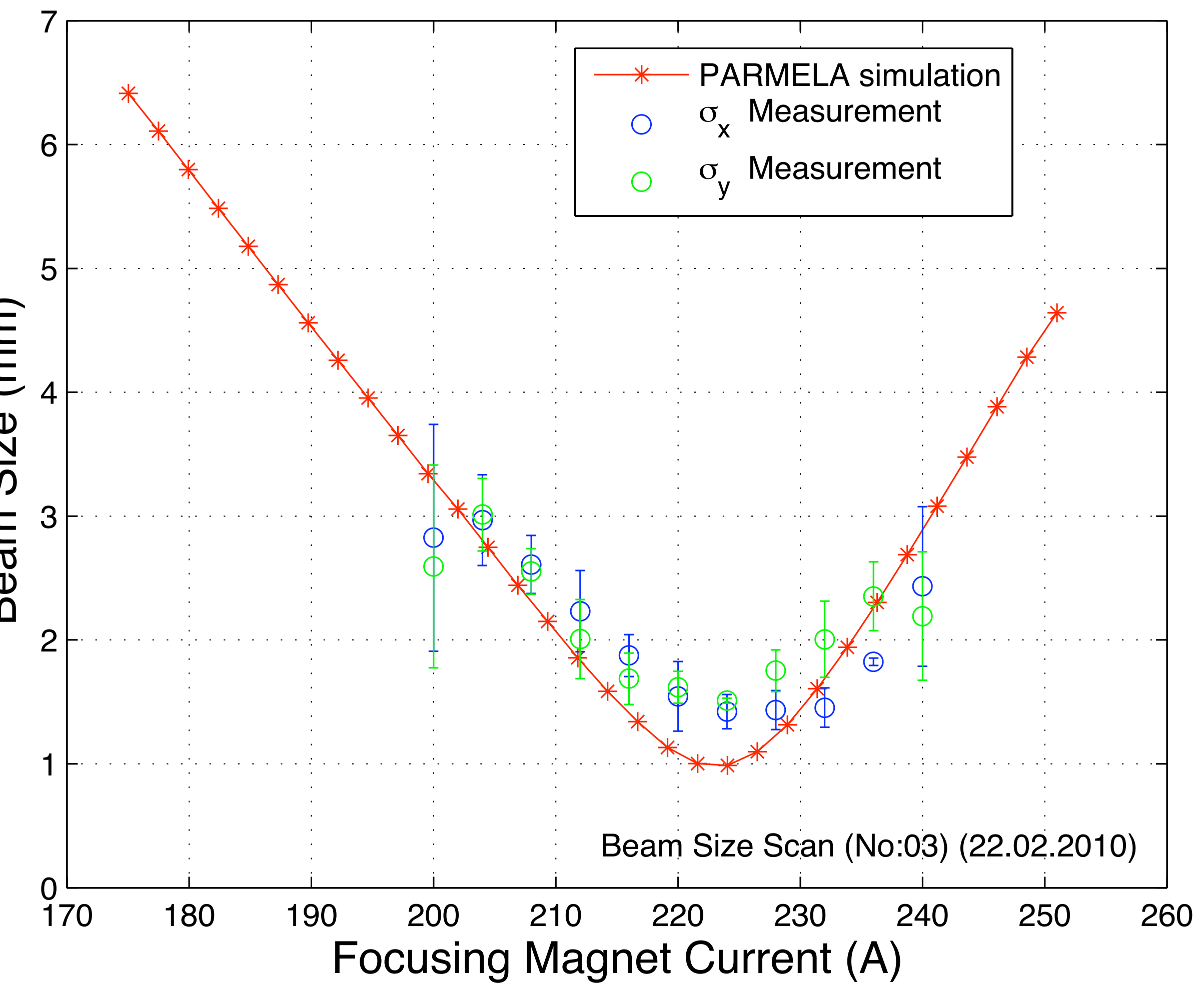

- Beam size is measured as a function of the focusing,
- A MatLab software has been developed for interfacing with the instrumentation for automatic data acquisition.
- A benchmark measurement
  - to diagnose the beam and the instrumentation,
  - to calibrate the input parameters for the simulations with respect to the actual system settings.
  - such as laser spot size, beam energy, focusing magnet current, RF phase, gradient, charge per bunch...
- The error bars indicate the shot-to-shot statistical deviations.

Beam size

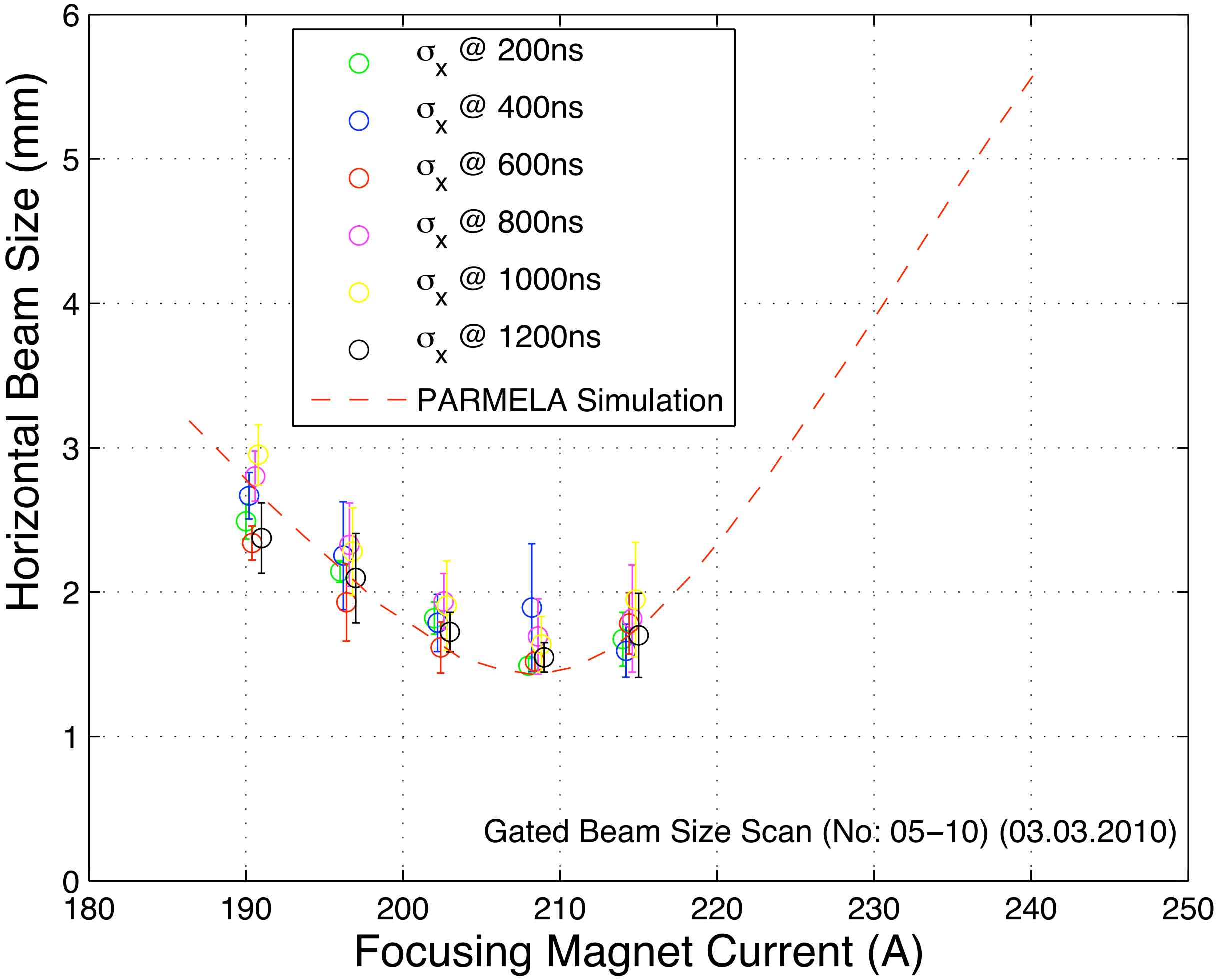

- Beam size is measured as a function of the focusing,
- A MatLab software has been developed for interfacing with the instrumentation for automatic data acquisition.
- A benchmark measurement
  - to diagnose the beam and the instrumentation,
  - to calibrate the input parameters for the simulations with respect to the actual system settings.
  - such as laser spot size, beam energy, focusing magnet current, RF phase, gradient, charge per bunch...
- The error bars indicate the shot-to-shot statistical deviations.

Beam size

Beam Size along the Pulse Train

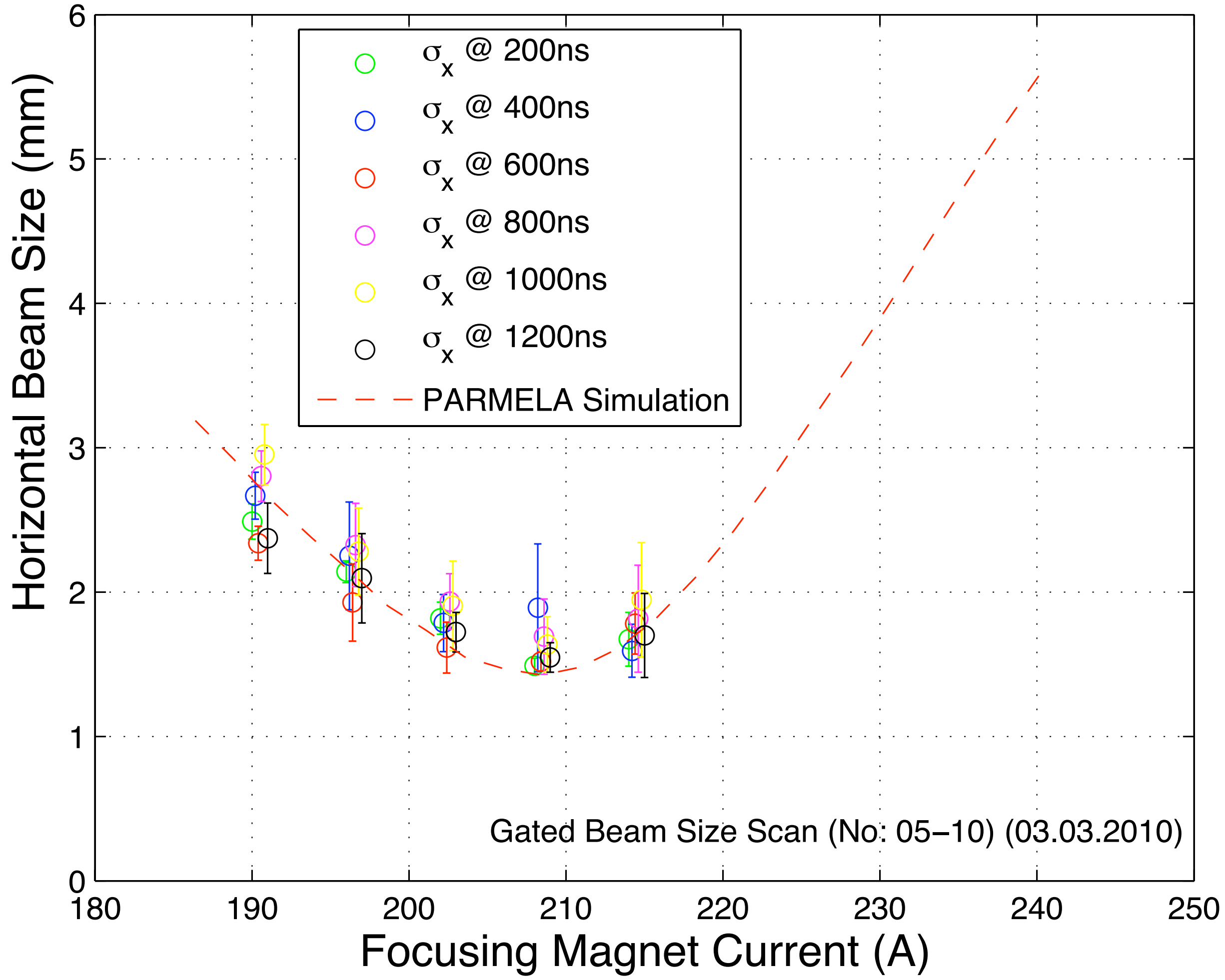

- Beam size is measured as a function of the focusing,
- A MatLab software has been developed for interfacing with the instrumentation for automatic data acquisition.
- A benchmark measurement
  - to diagnose the beam and the instrumentation,
  - to calibrate the input parameters for the simulations with respect to the actual system settings.
  - such as laser spot size, beam energy, focusing magnet current, RF phase, gradient, charge per bunch...
- The error bars indicate the shot-to-shot statistical deviations.
- Beam size can be measured as a time-resolved manner along the pulse train.

Beam size

Beam Size along the Pulse Train

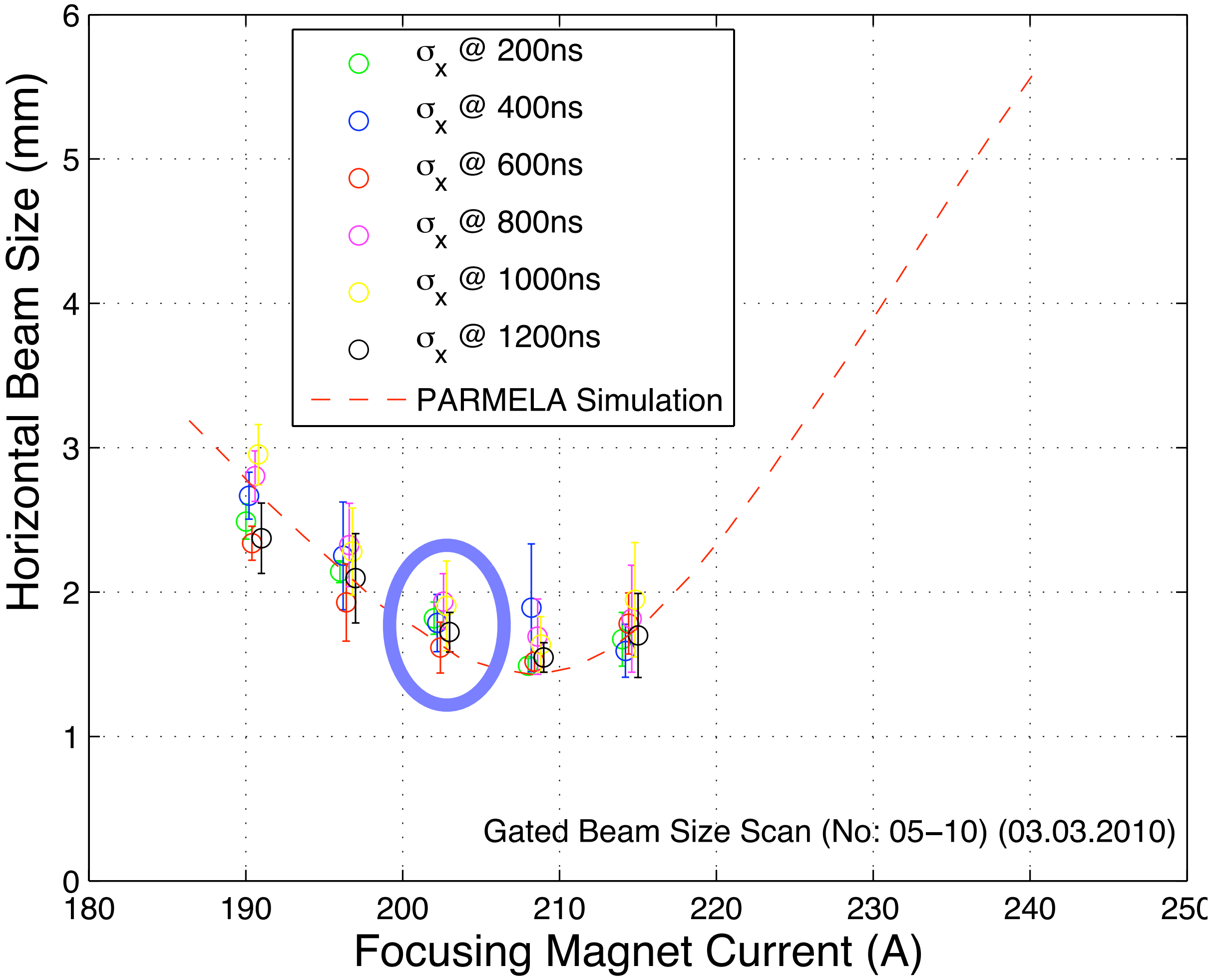

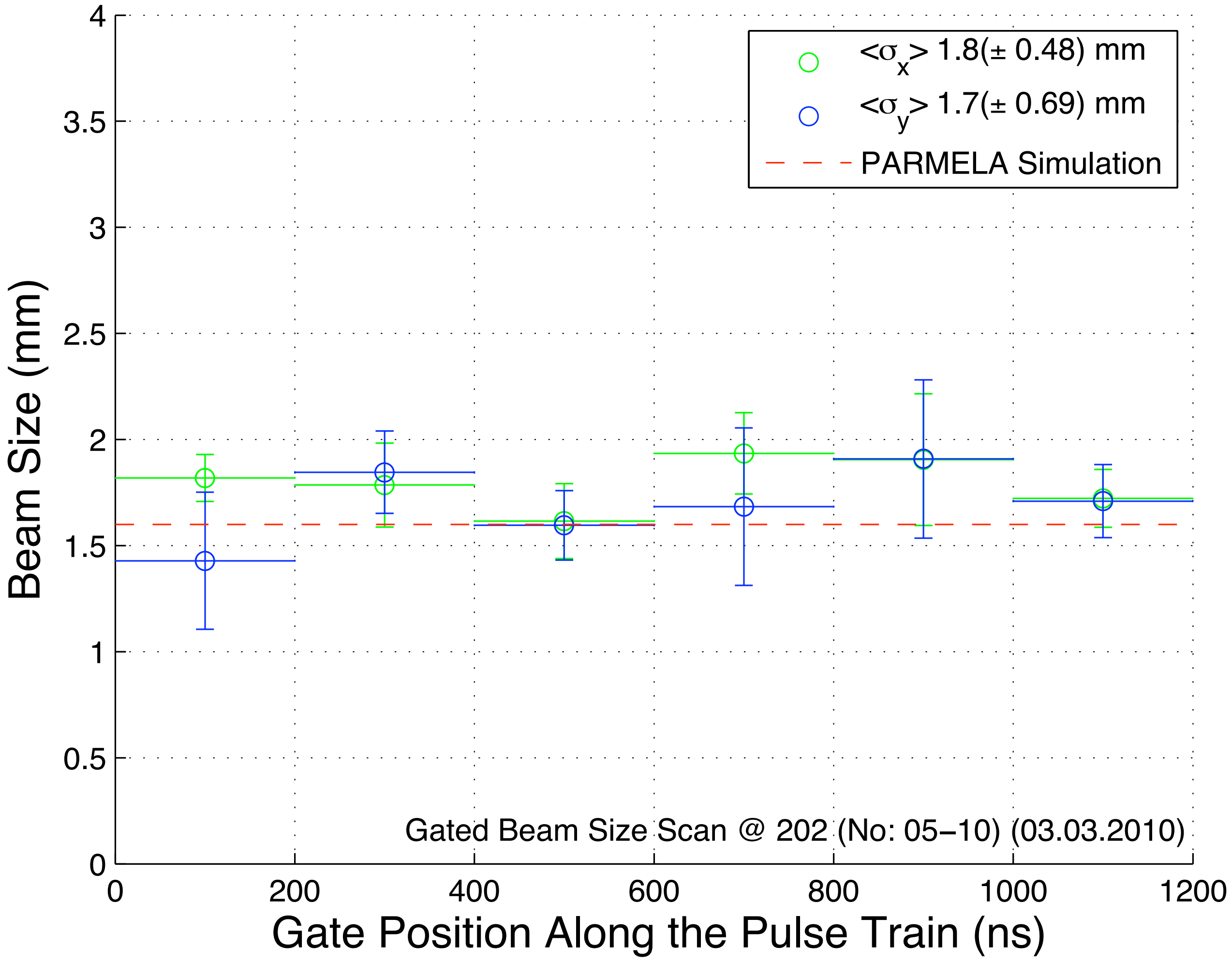

Beam size

Beam Size along the Pulse Train

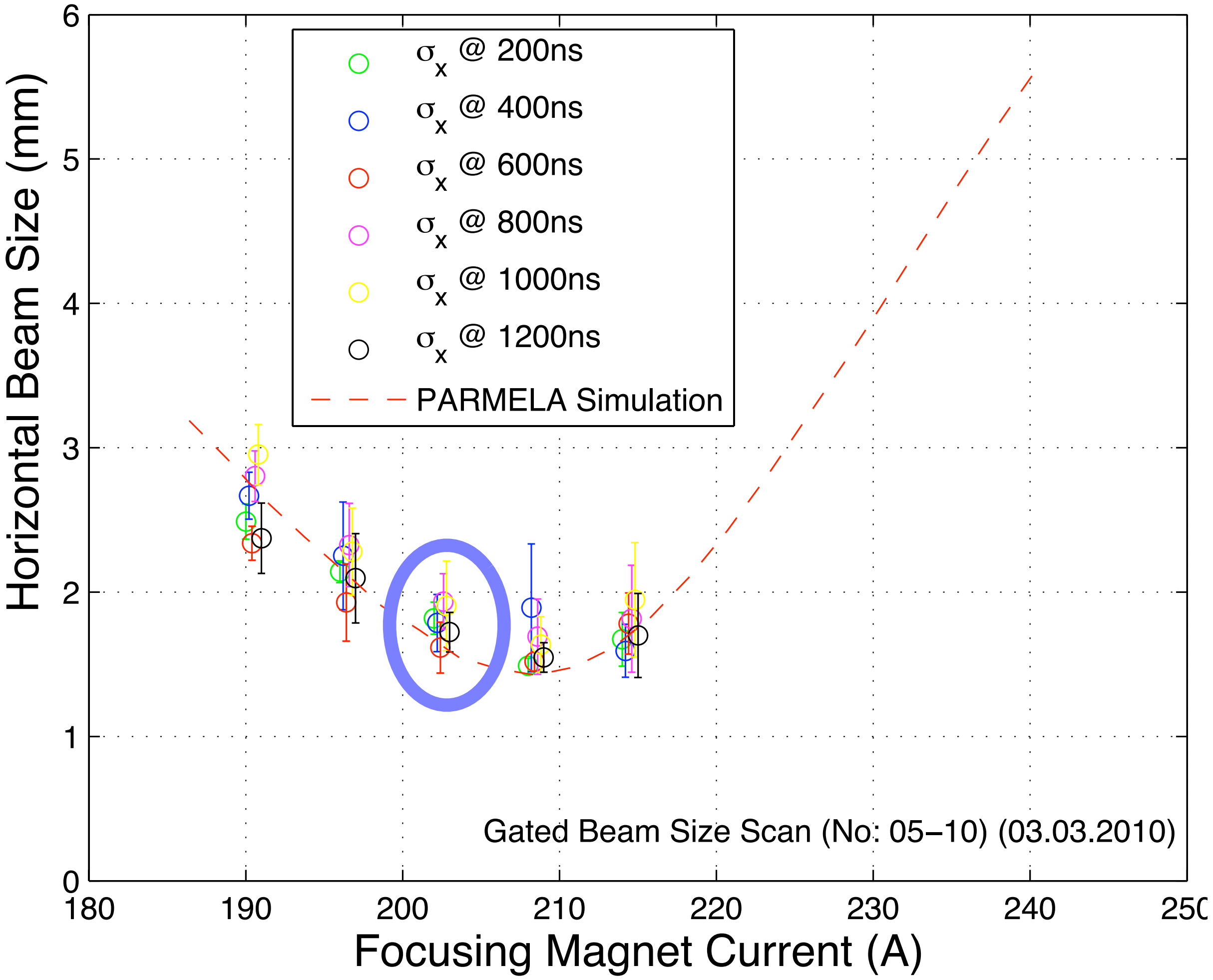

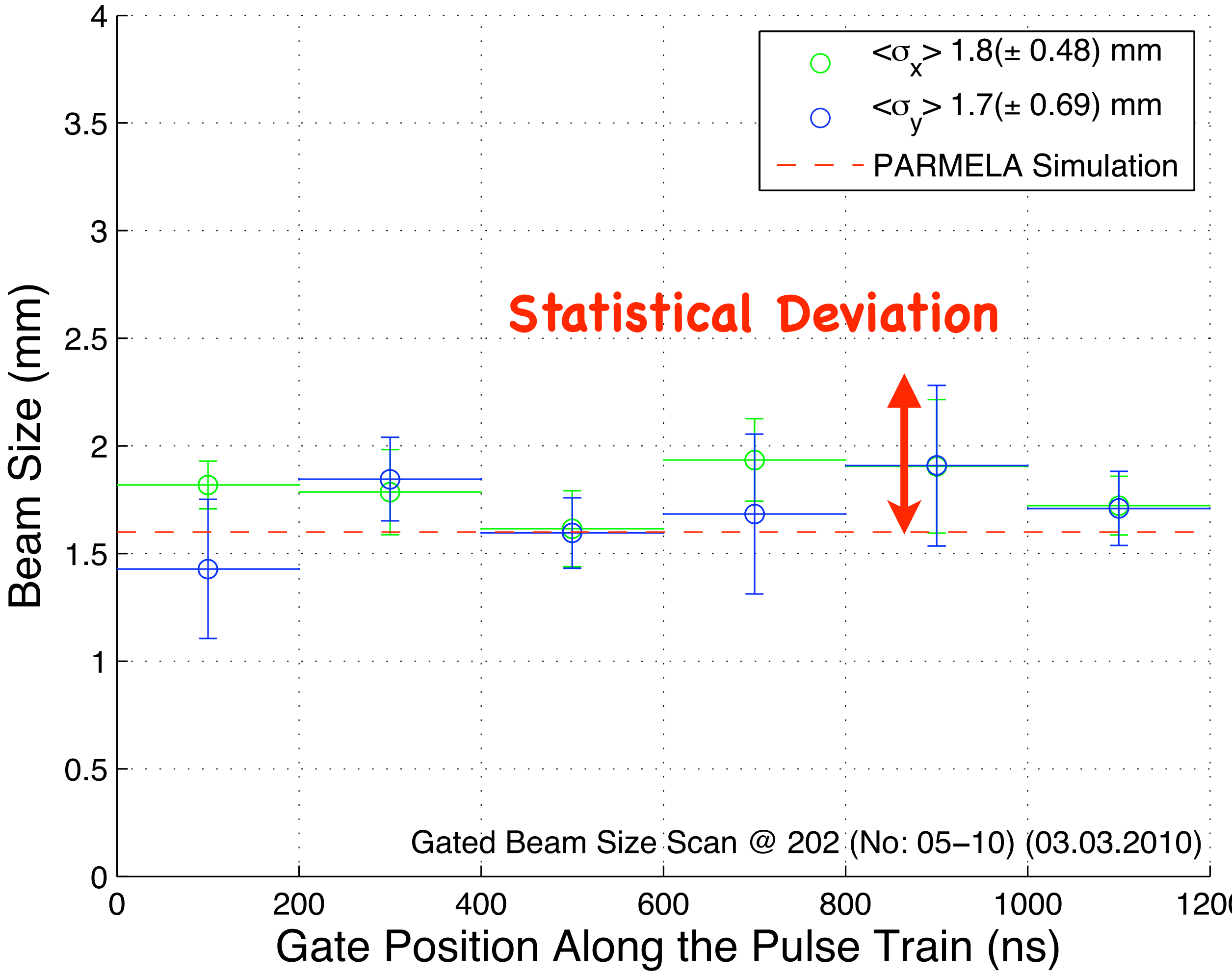

Beam size

Beam Size along the Pulse Train

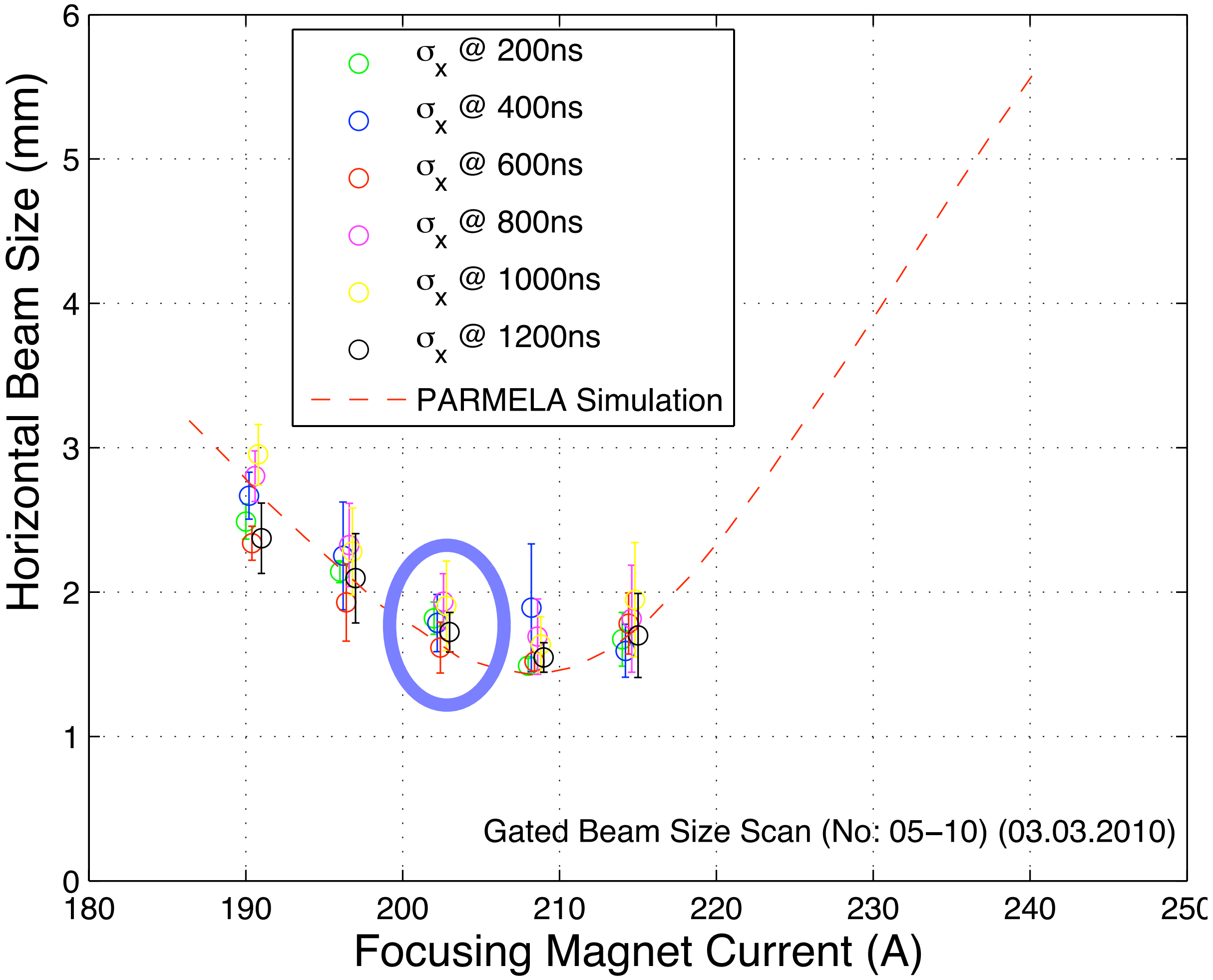

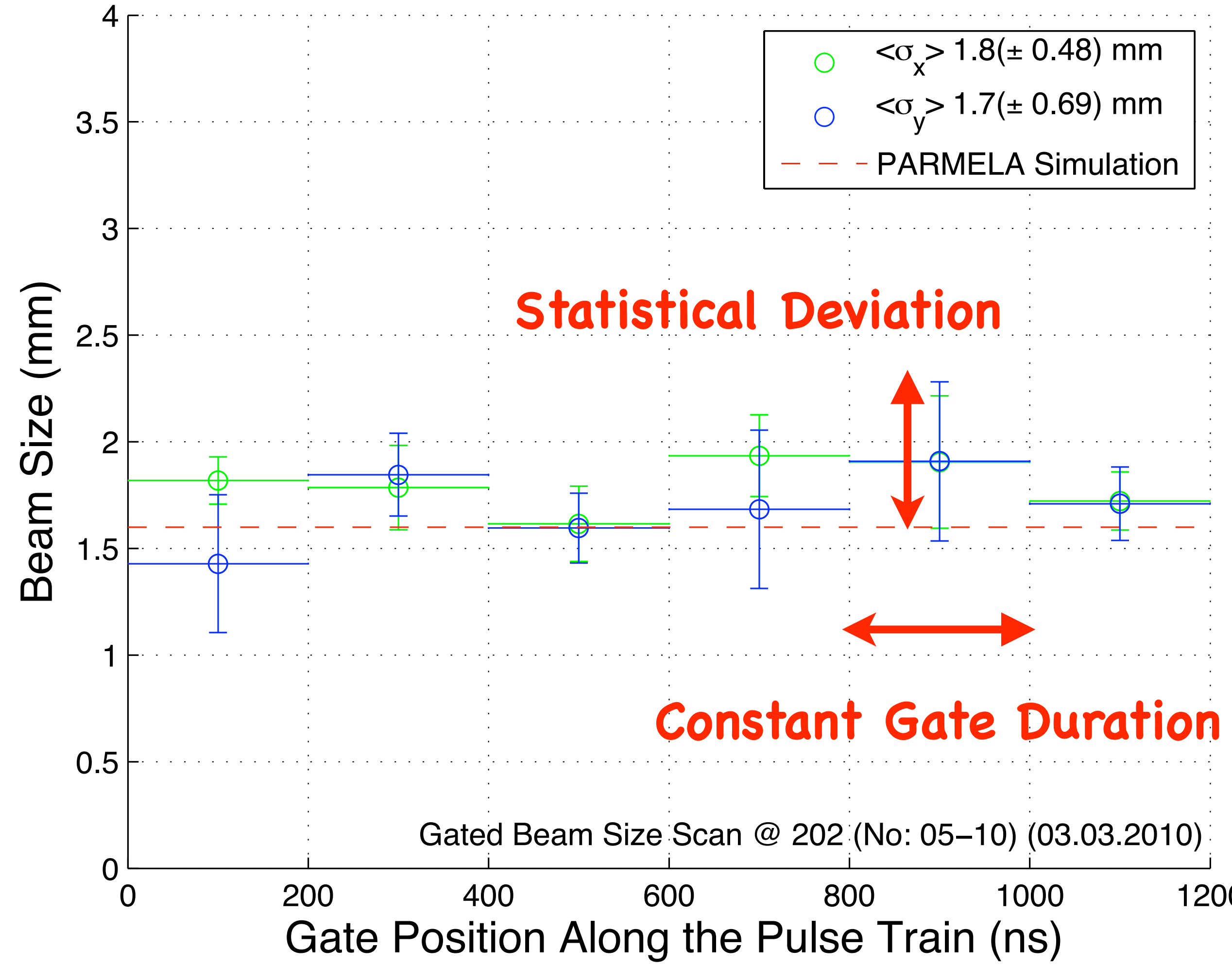

Emittance-Meter

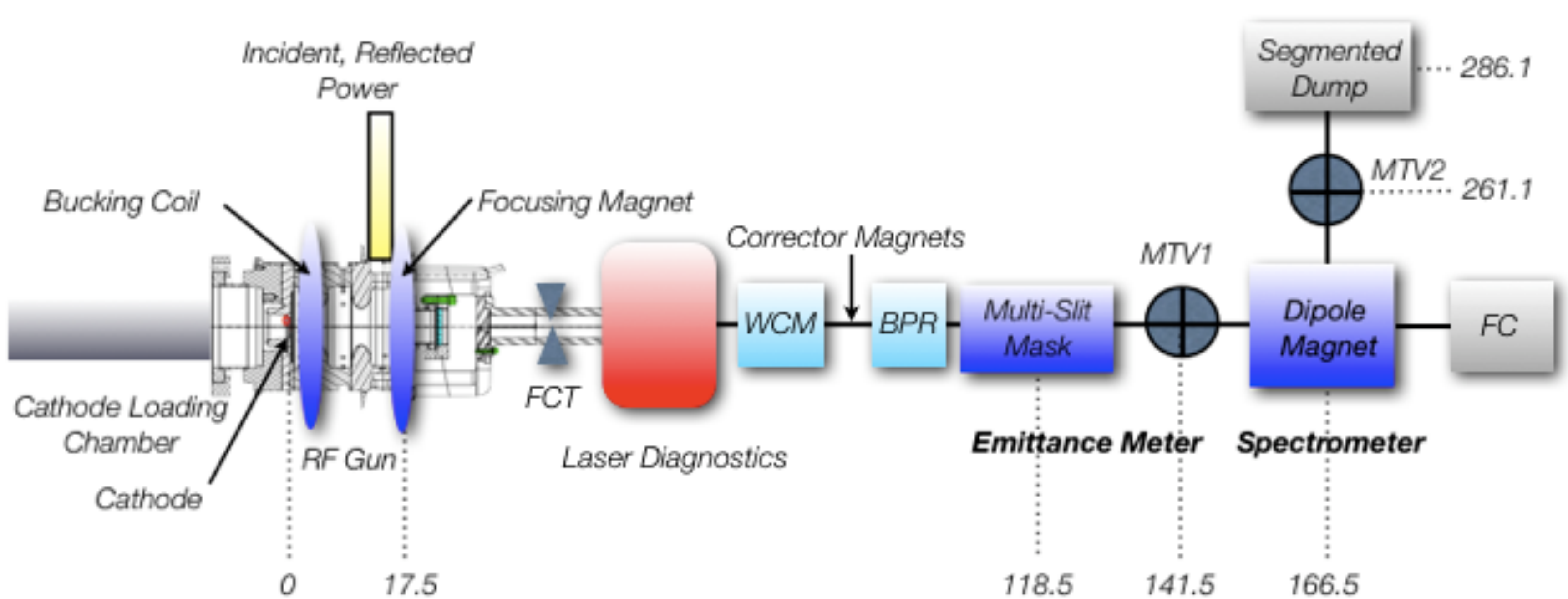

Emittance-Meter

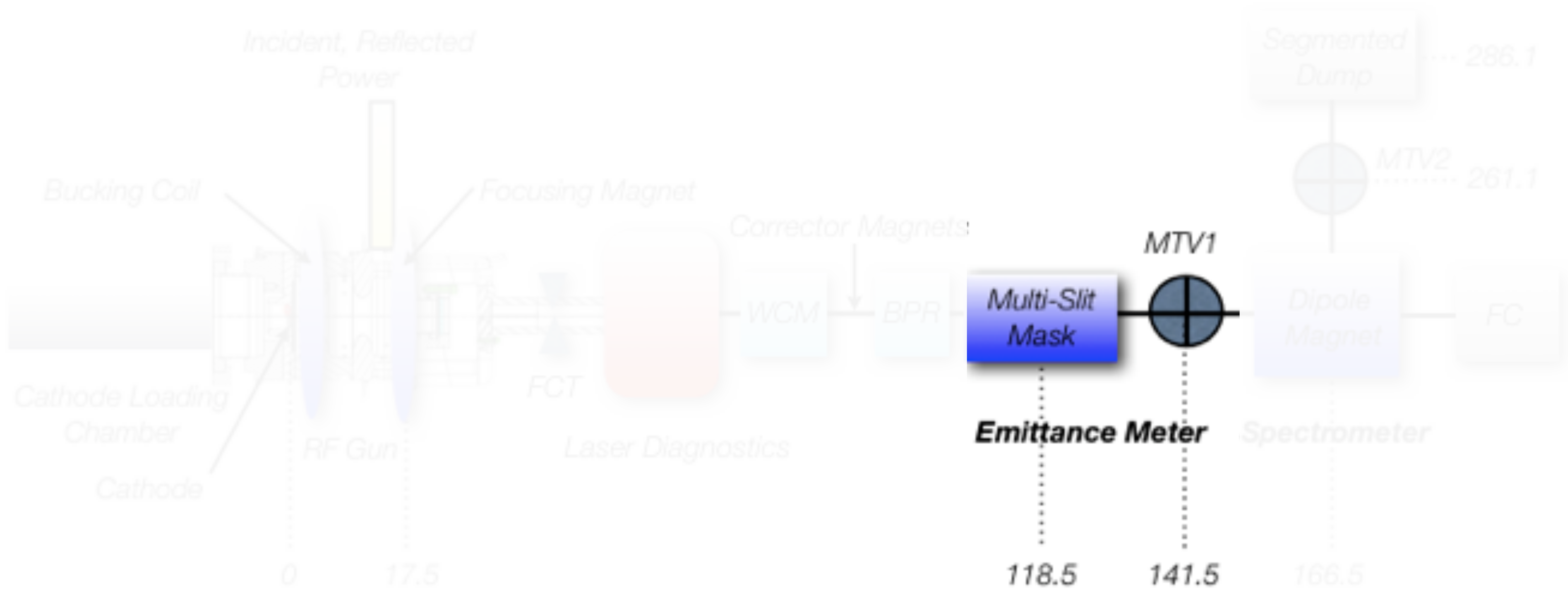

Emittance-Meter

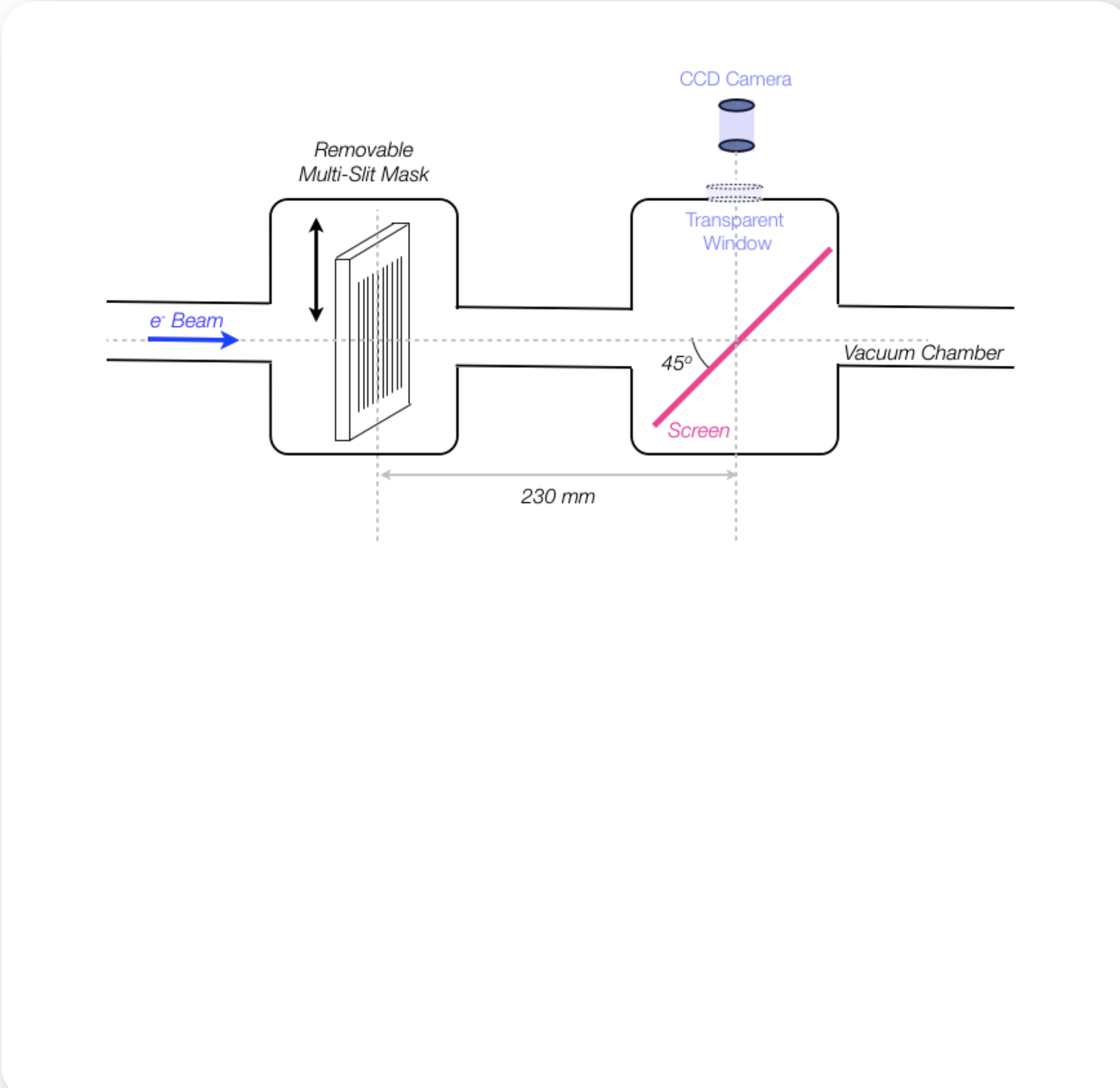

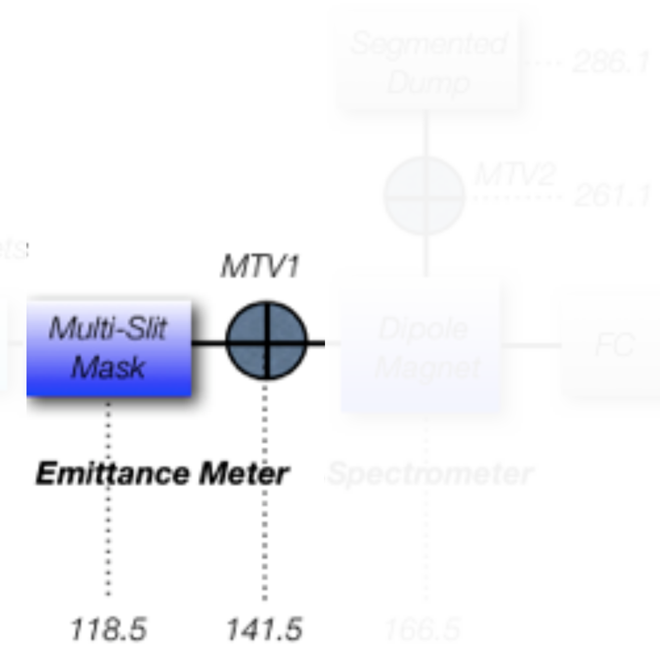

Emittance-Meter

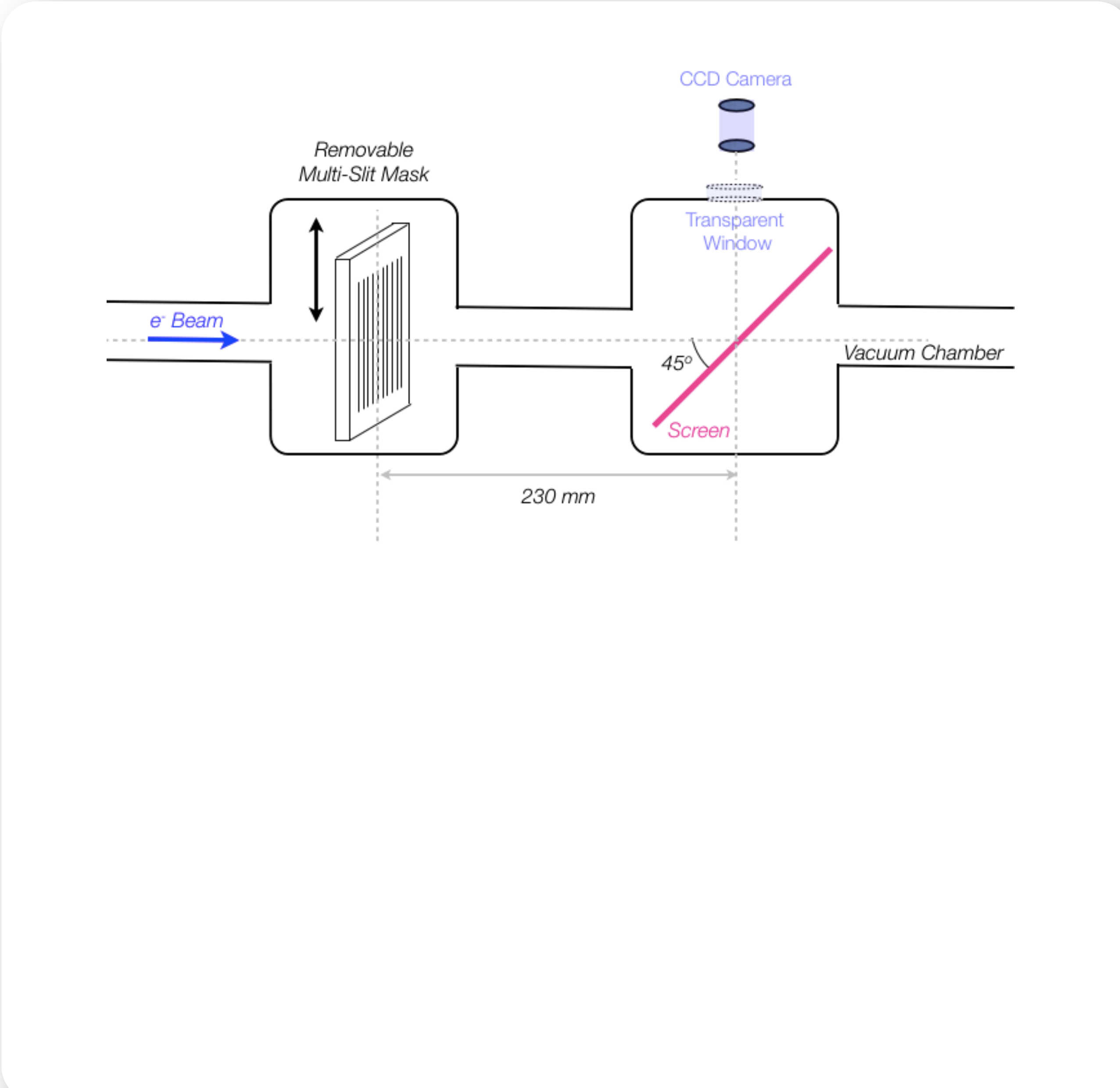

- Transverse emittance has been measured by using **multi-slit (MS) method**.

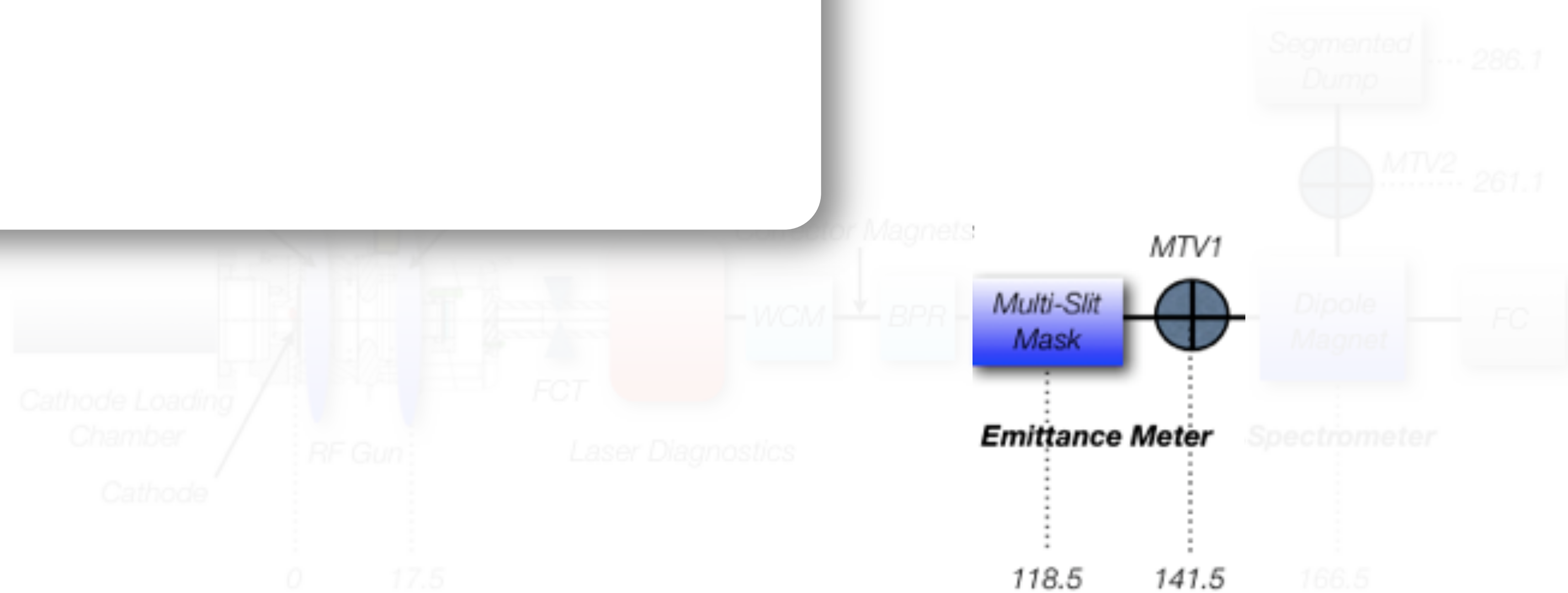

Emittance-Meter

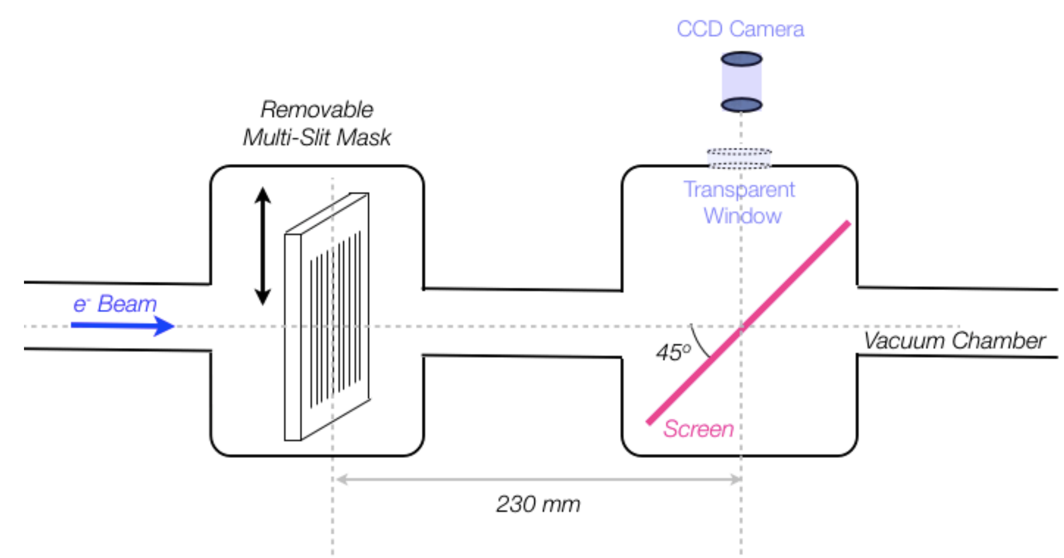

- Transverse emittance has been measured by using **multi-slit (MS) method**.
- The MS method is suitable for **the space charge dominated low-energy beams**.

Emittance-Meter

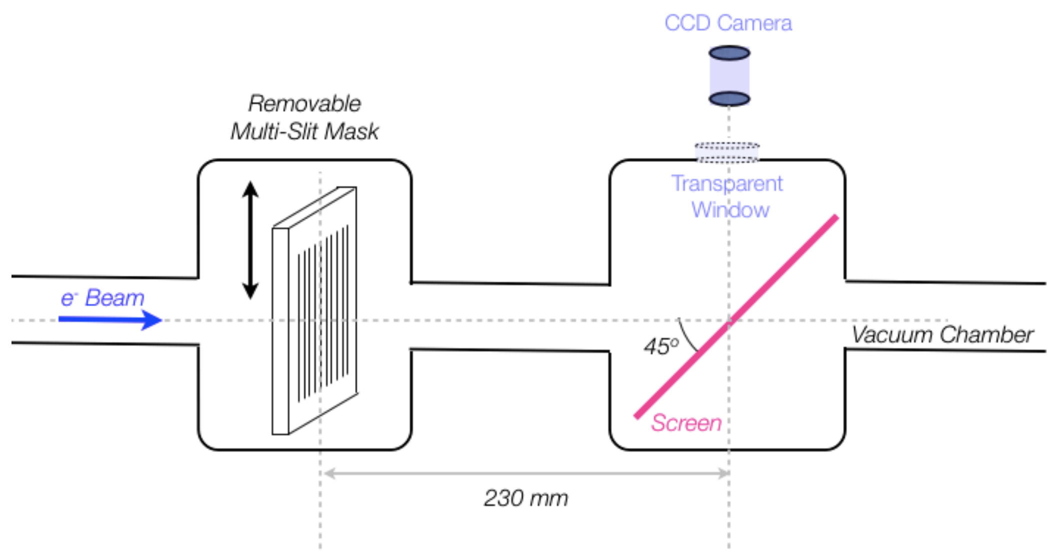

Emittance-Meter

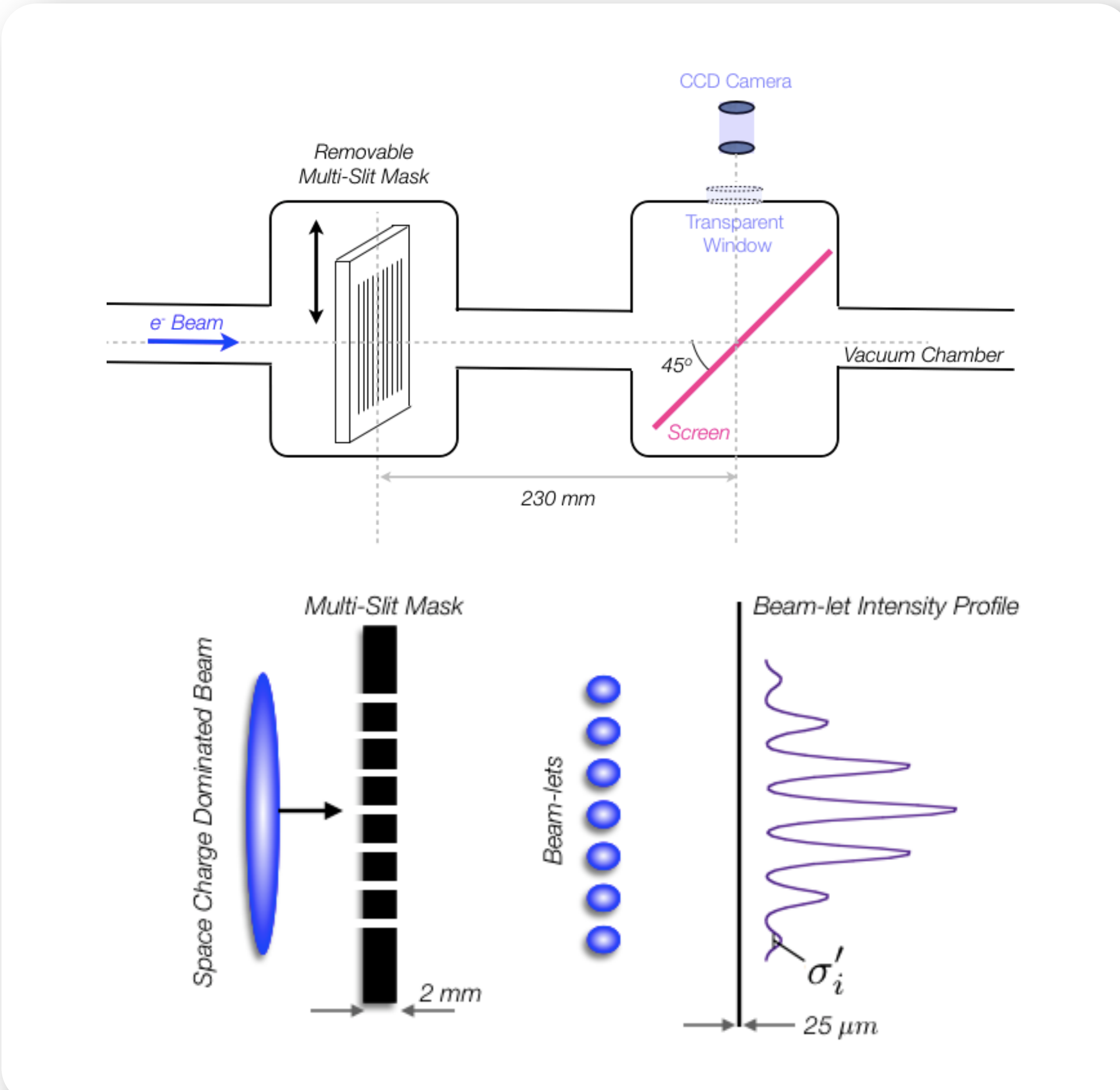

According to the MS method

Emittance-Meter

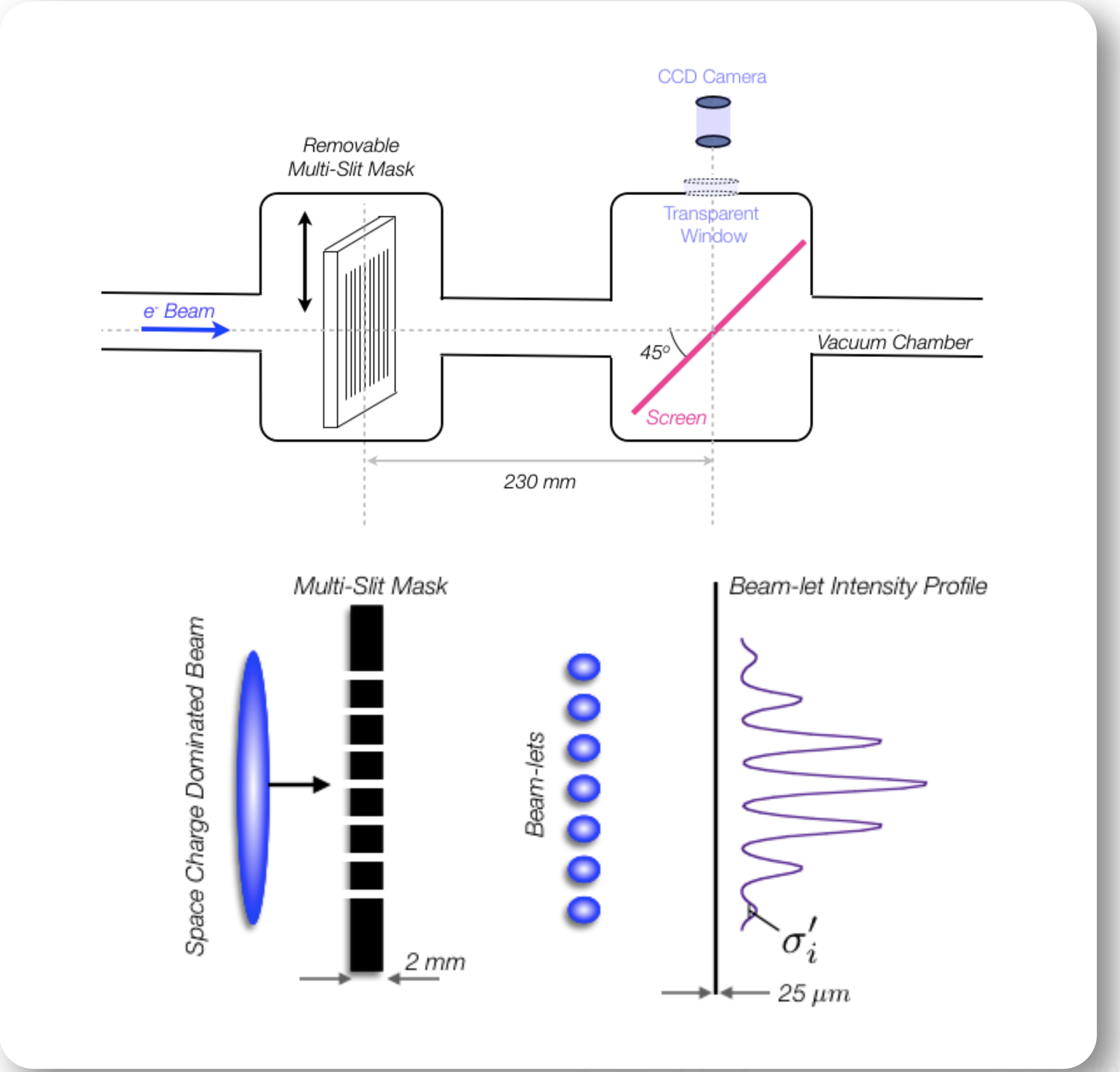

According to the MS method

- The MS mask is introduced in front of the beam,

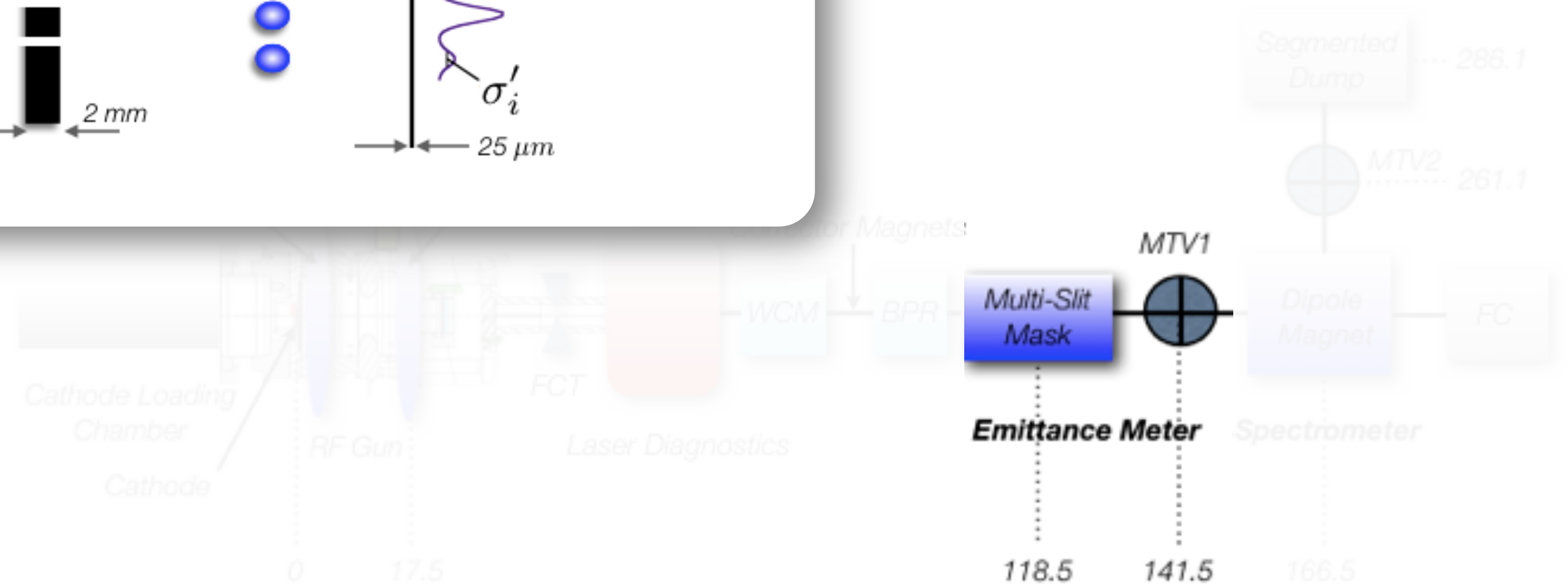

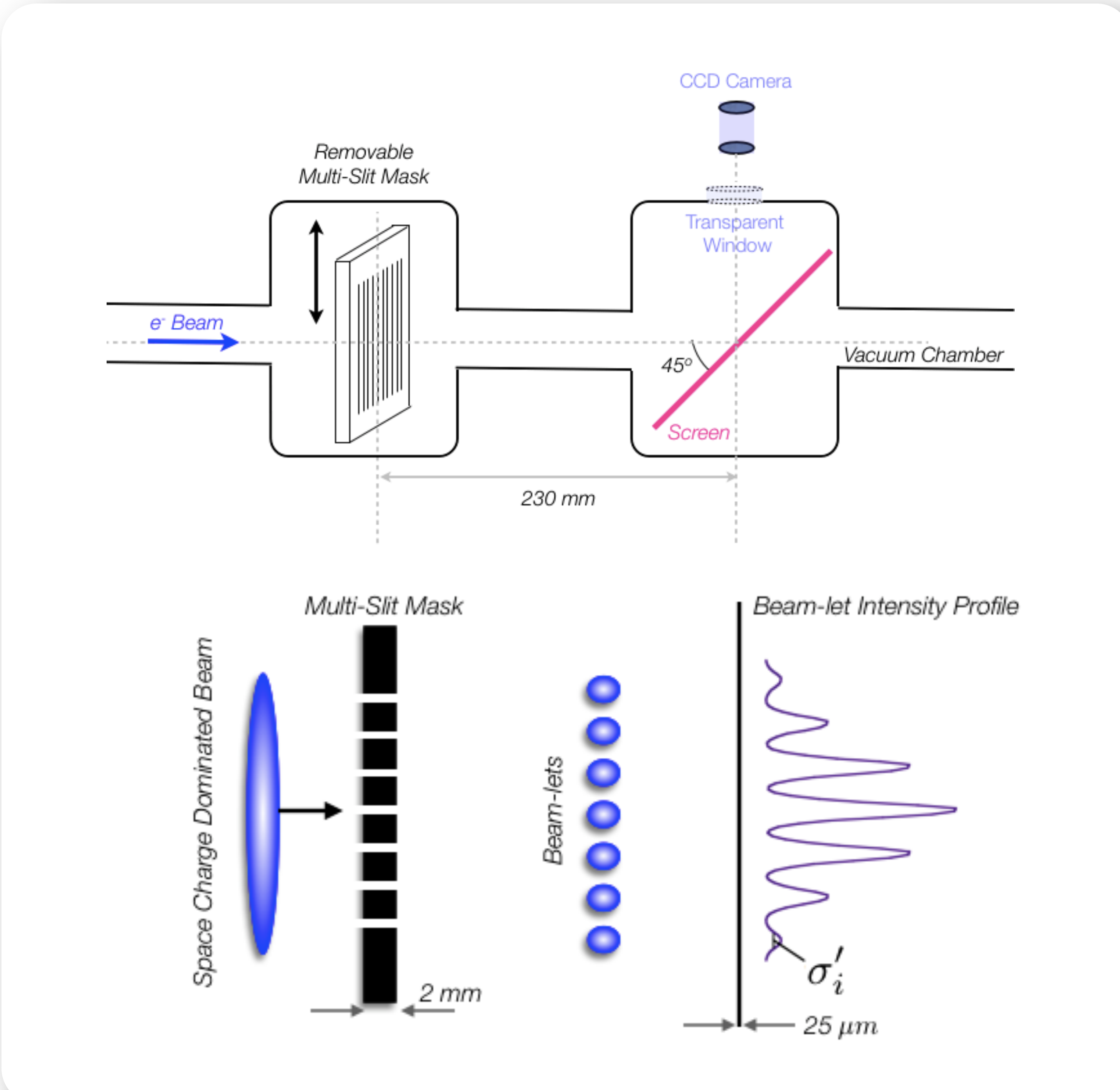

According to the MS method

- The MS mask is introduced in front of the beam,
- The beam is sliced into individual beamlets,

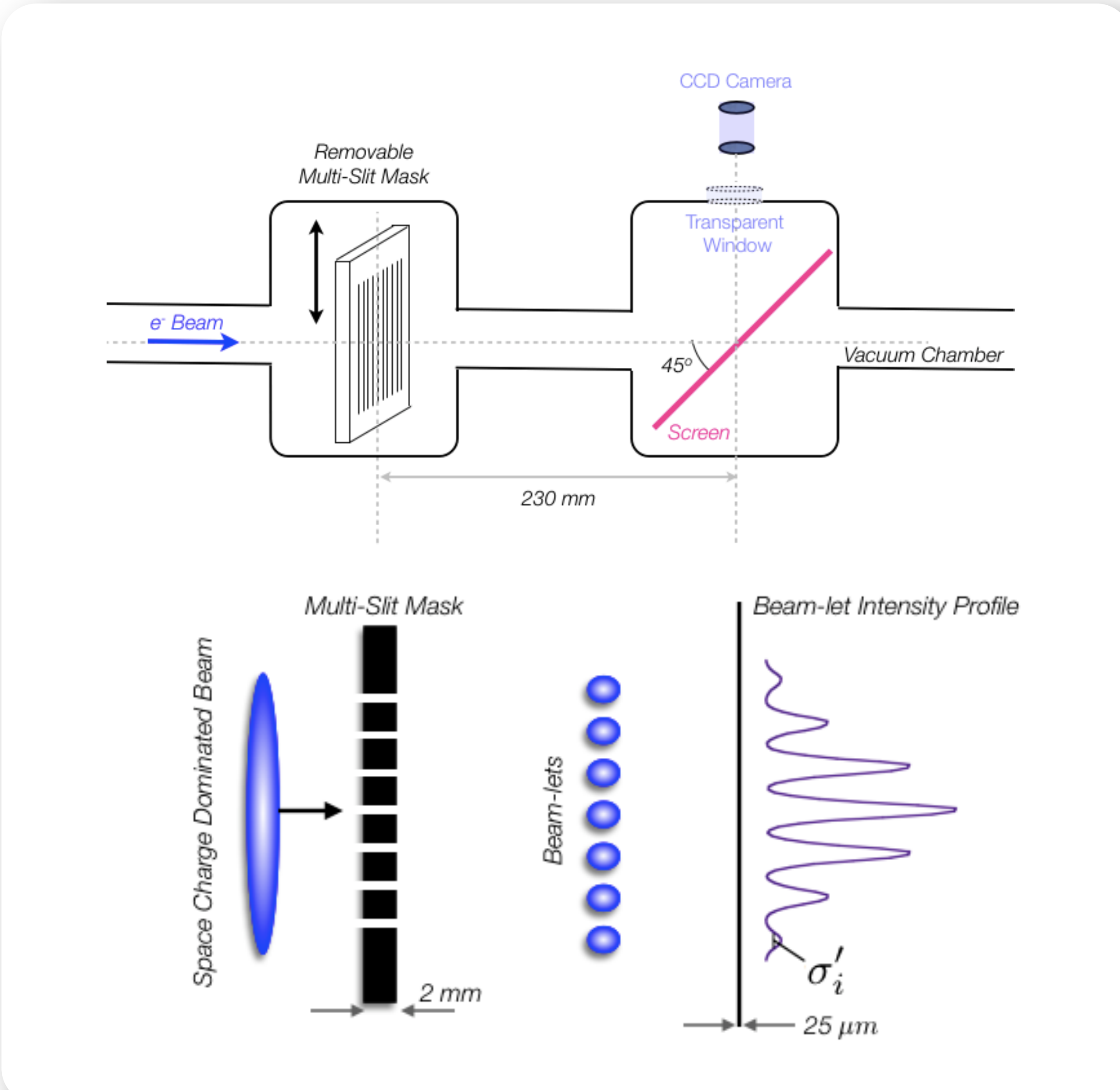

According to the MS method

- The MS mask is introduced in front of the beam,
- The beam is sliced into individual beamlets,
- The moments of the beamlets are determined from the beam profile,

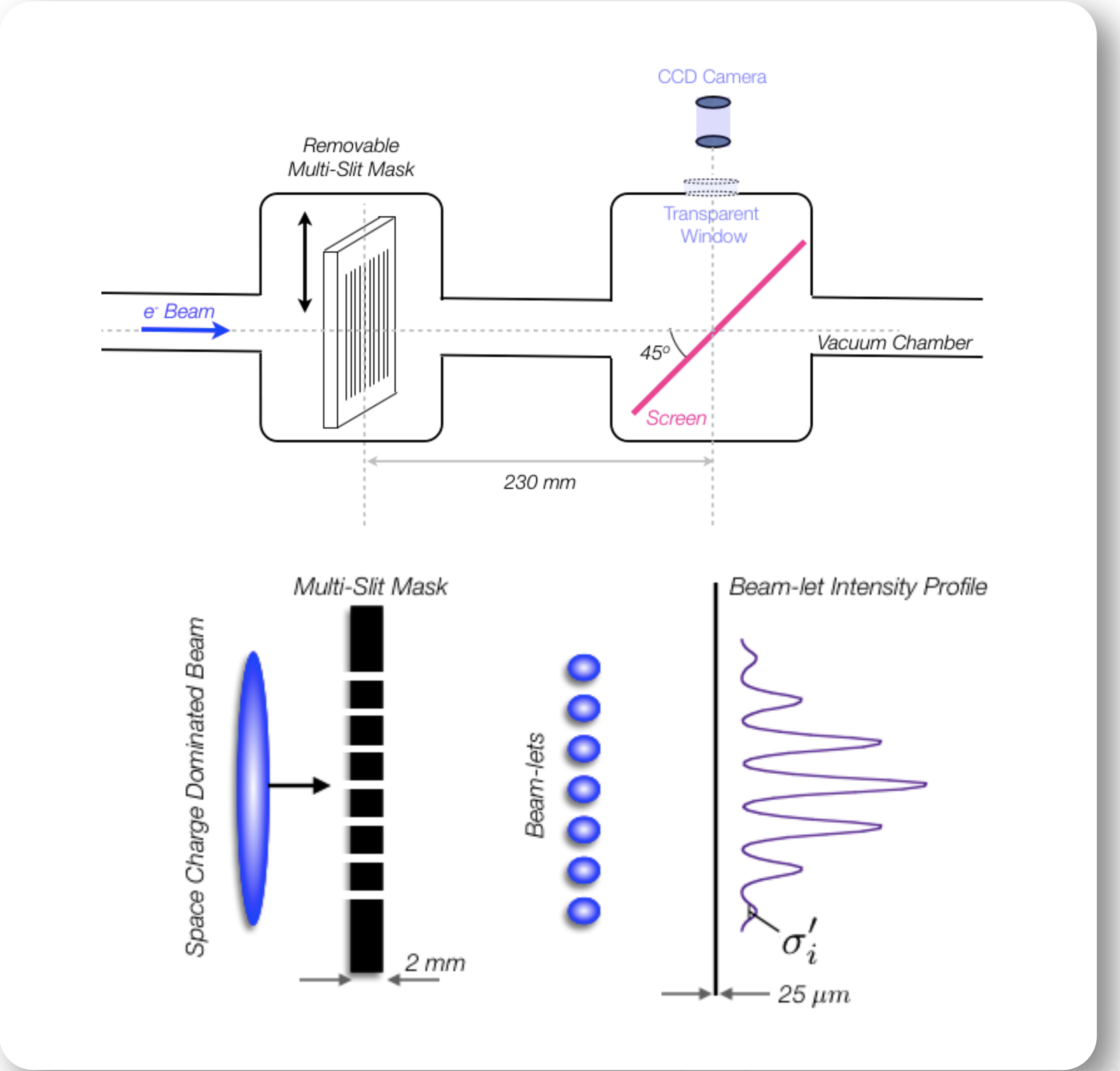

According to the MS method

- The MS mask is introduced in front of the beam,
- The beam is sliced into individual beamlets,
- The moments of the beamlets are determined from the beam profile,
- And the emittance of the former beam is calculated.

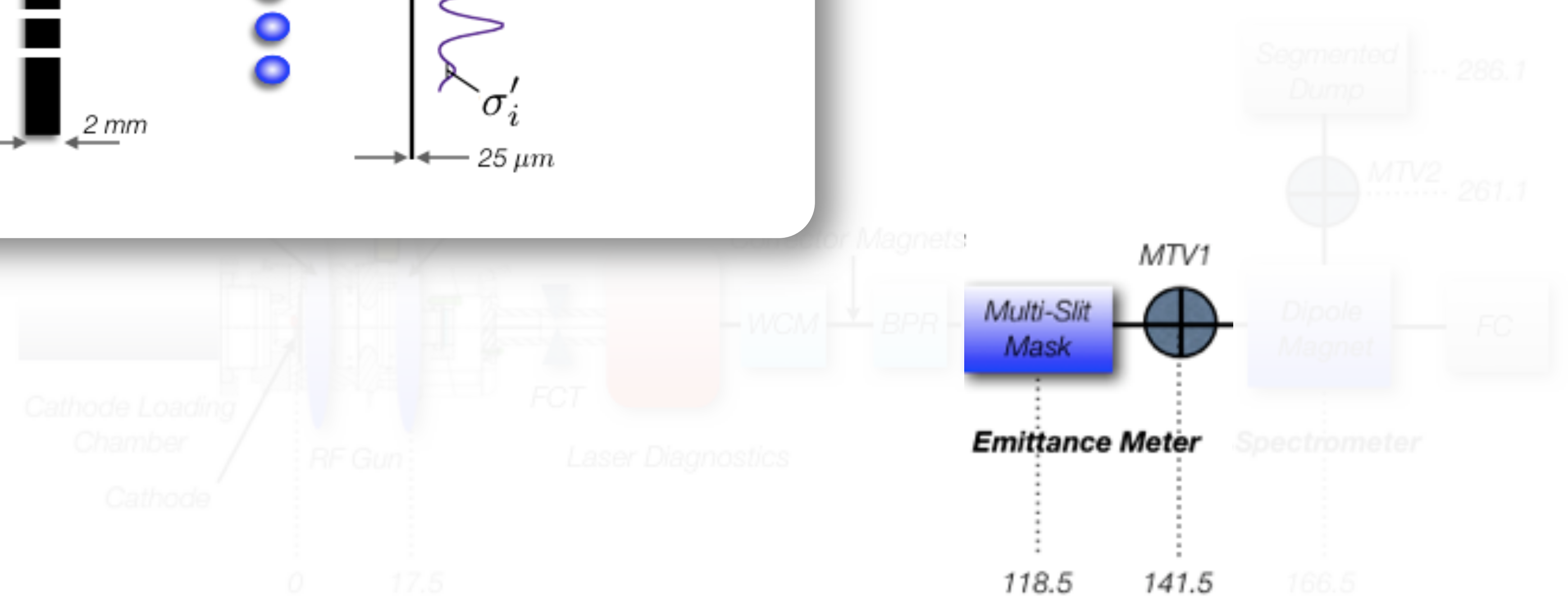

Emittance-Meter

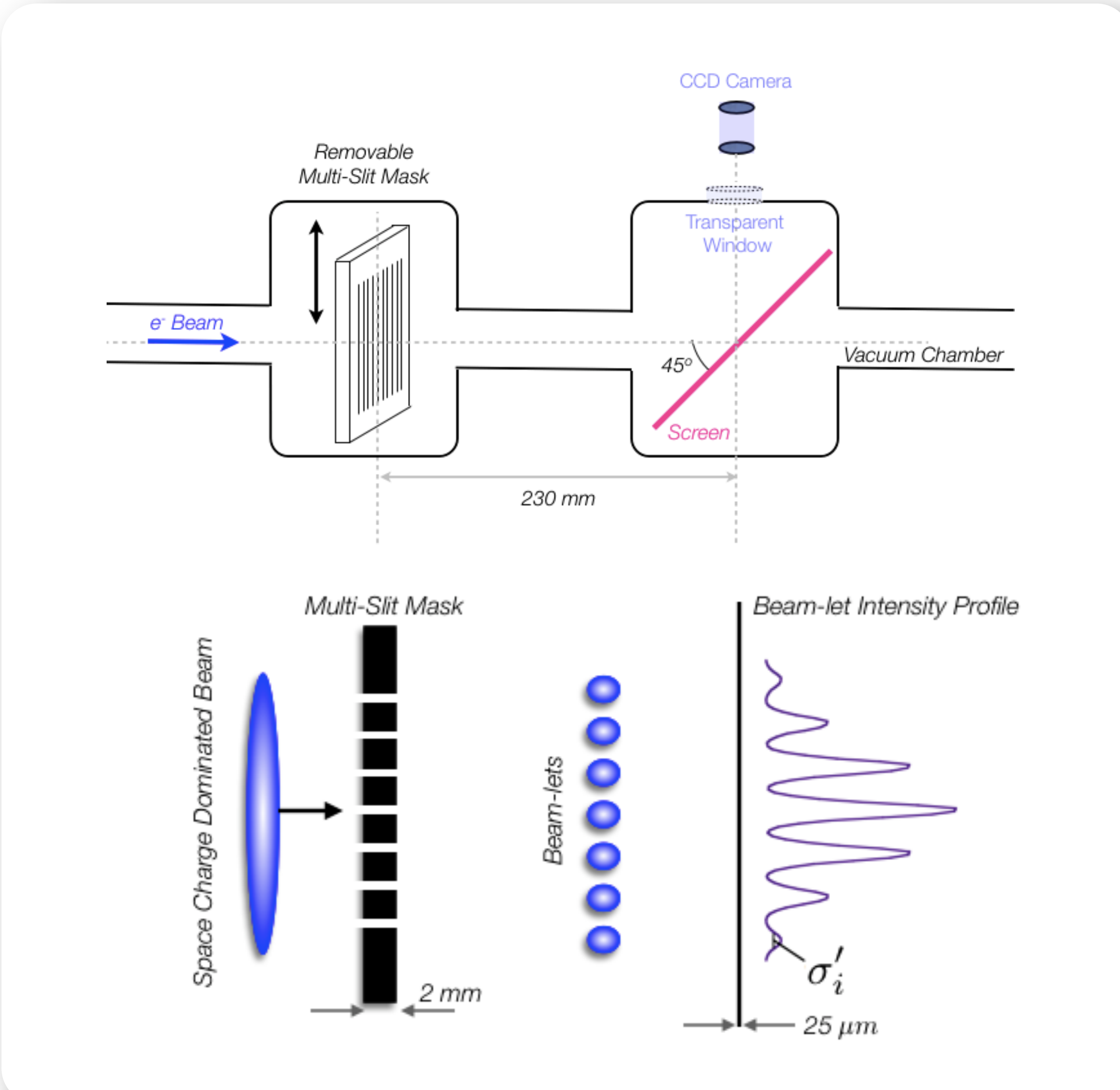

According to the MS method

- The MS mask is introduced in front of the beam,
- The beam is sliced into individual beamlets,
- The moments of the beamlets are determined from the beam profile,
- And the emittance of the former beam is calculated.
- Multi-slit method has been implemented for the first time at CERN during the PHIN commissioning studies.

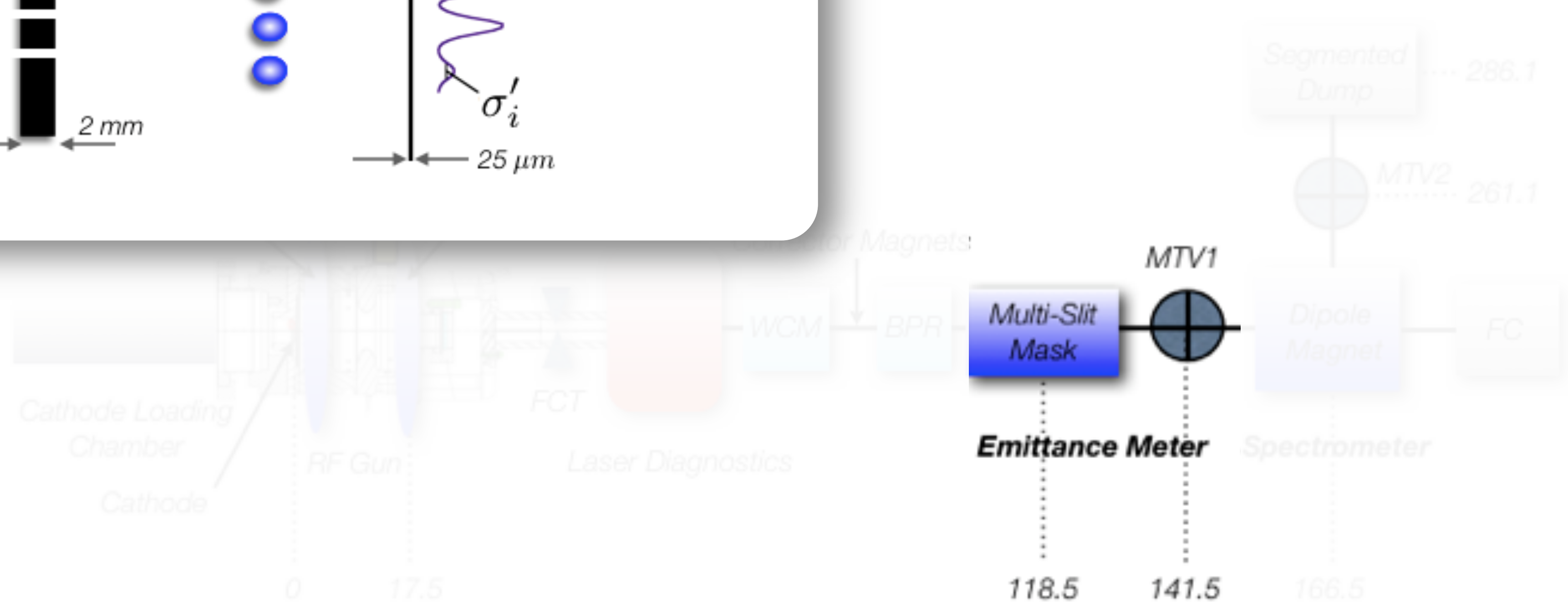

Emittance-Meter

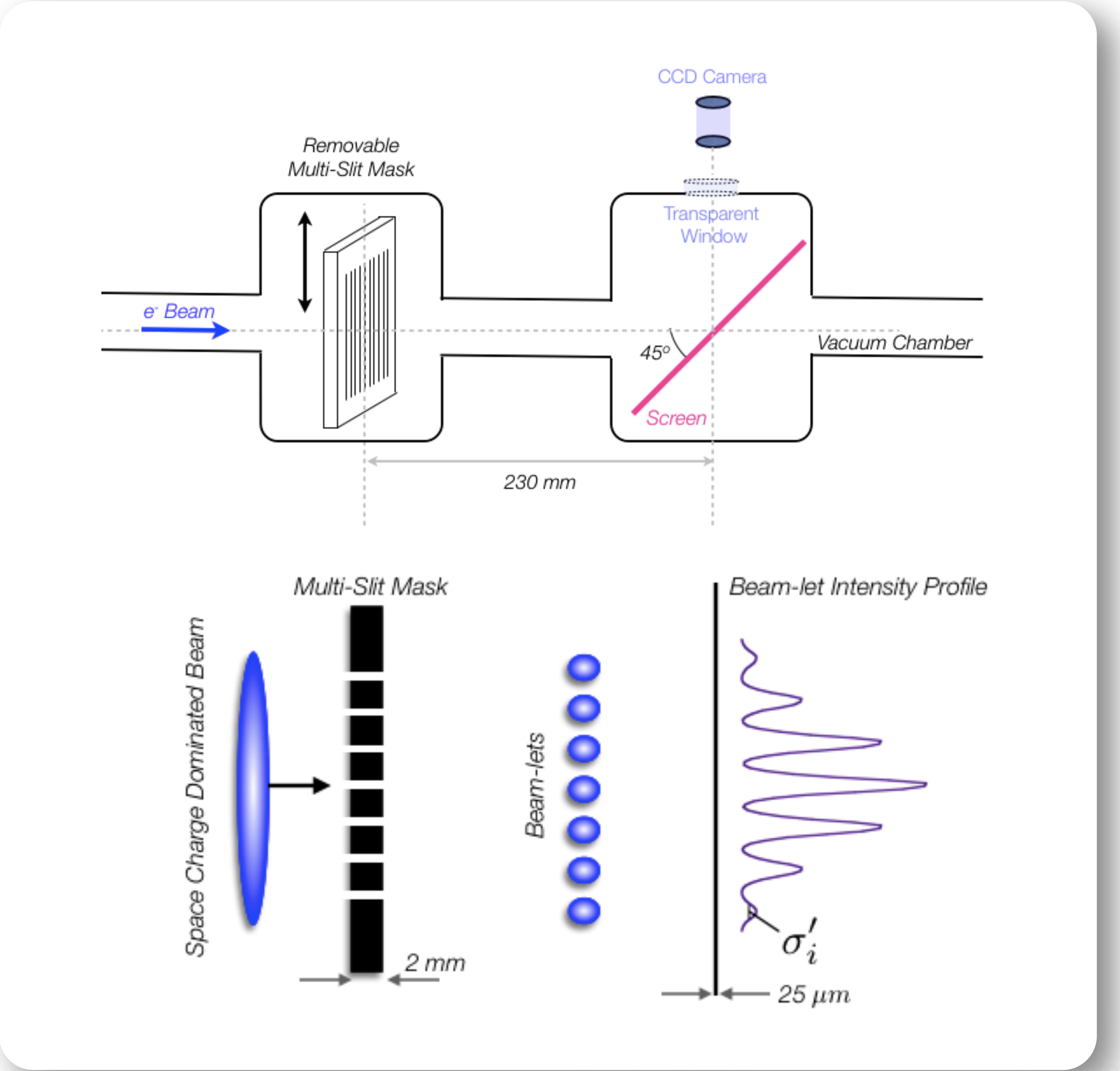

According to the MS method

- The MS mask is introduced in front of the beam,
- The beam is sliced into individual beamlets,
- The moments of the beamlets are determined from the beam profile,
- And the emittance of the former beam is calculated.
- Multi-slit method has been implemented for the first time at CERN during the PHIN commissioning studies.
- Development of an analysis method and producing several algorithms by considering different background (noise) patterns.

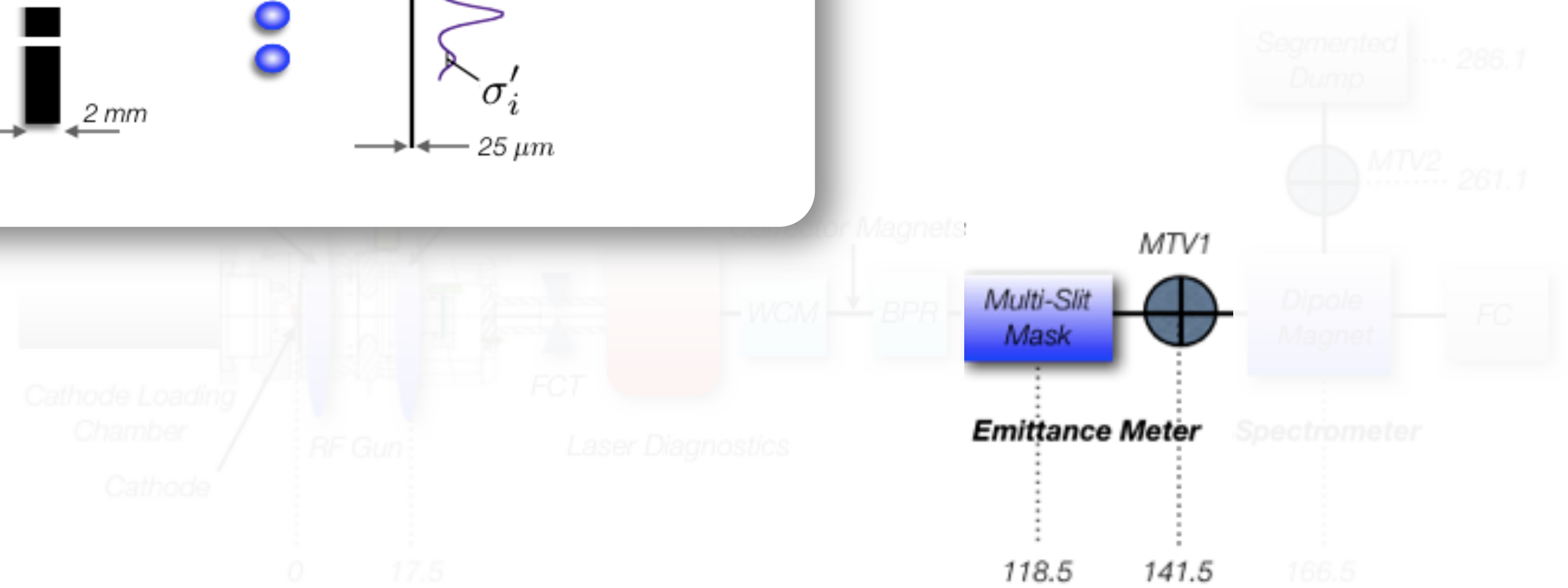

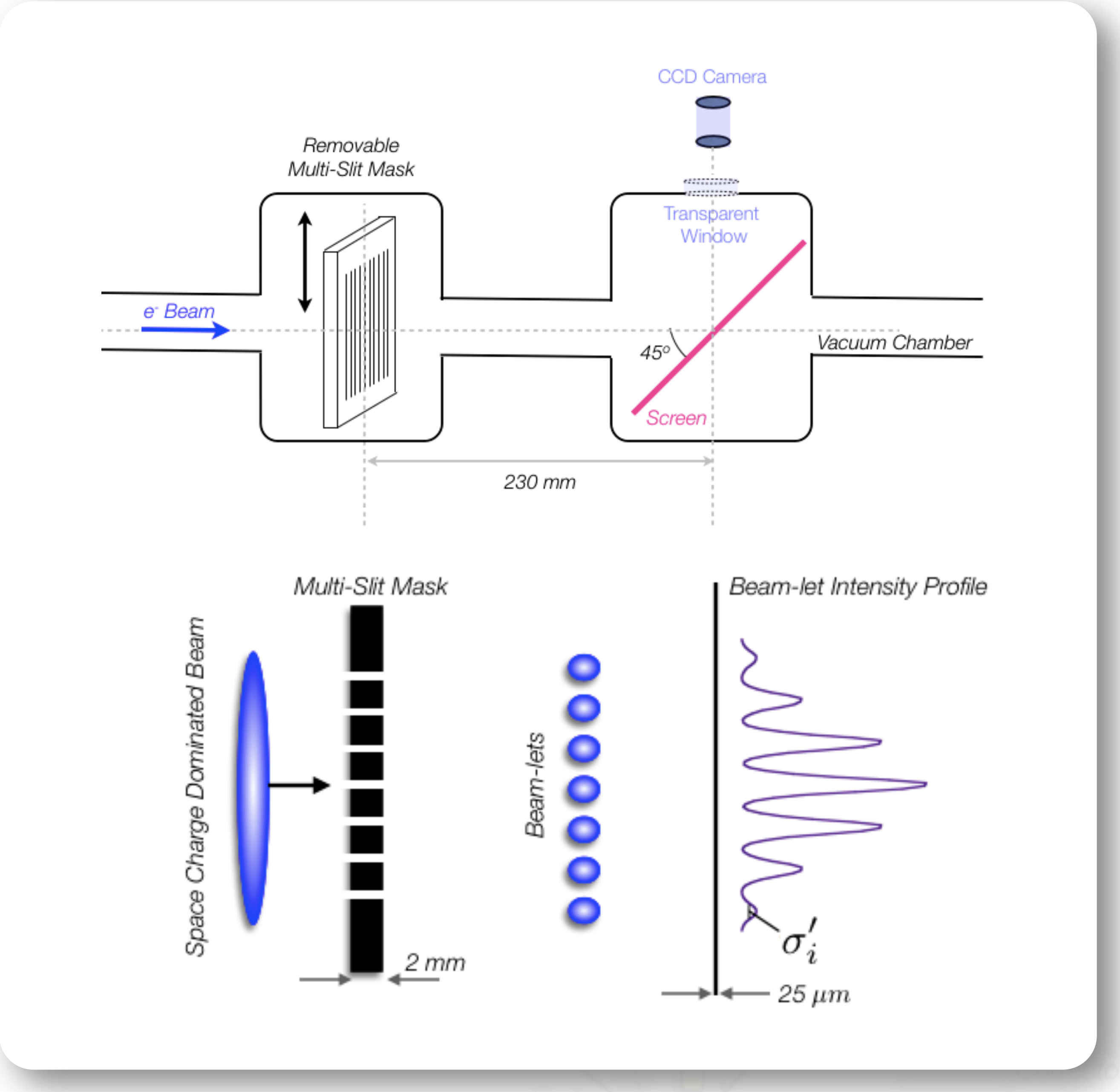

According to the MS method

- The MS mask is introduced in front of the beam,
- The beam is sliced into individual beamlets,
- The moments of the beamlets are determined from the beam profile,
- And the emittance of the former beam is calculated.
- Multi-slit method has been implemented for the first time at CERN during the PHIN commissioning studies.
- Development of an analysis method and producing several algorithms by considering different background (noise) patterns.
- **PHINEMA**: **PHIN** photo-injector **E**mittance **M**easurement and **A**nalysis software

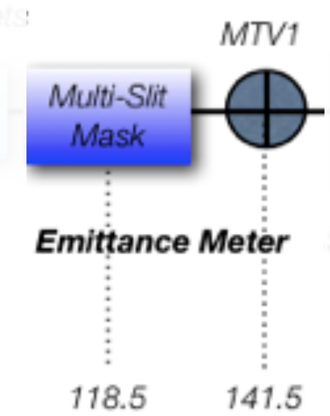

Emittance

Data Analysis

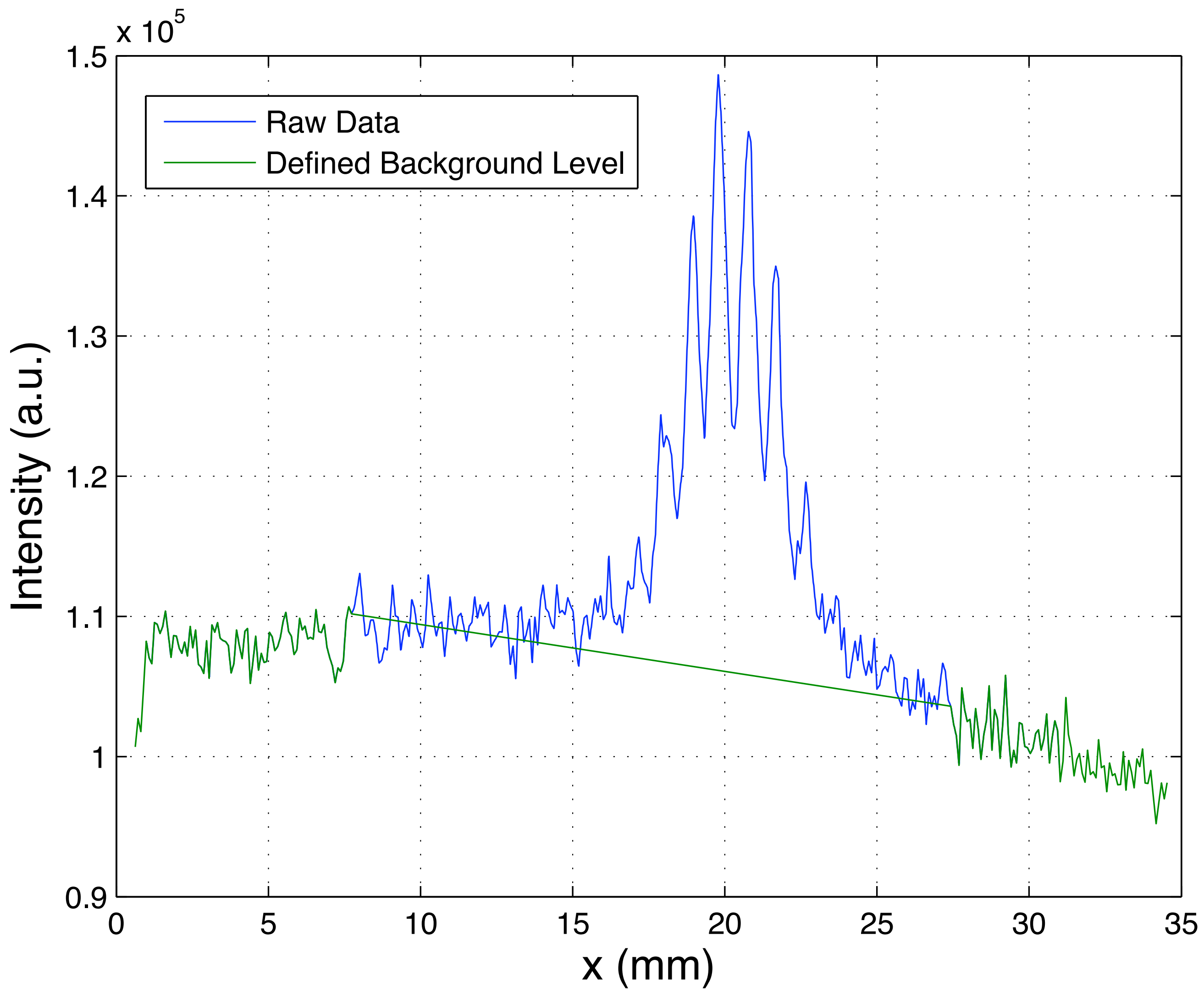

- A typical beam profile after the multi-slit mask,

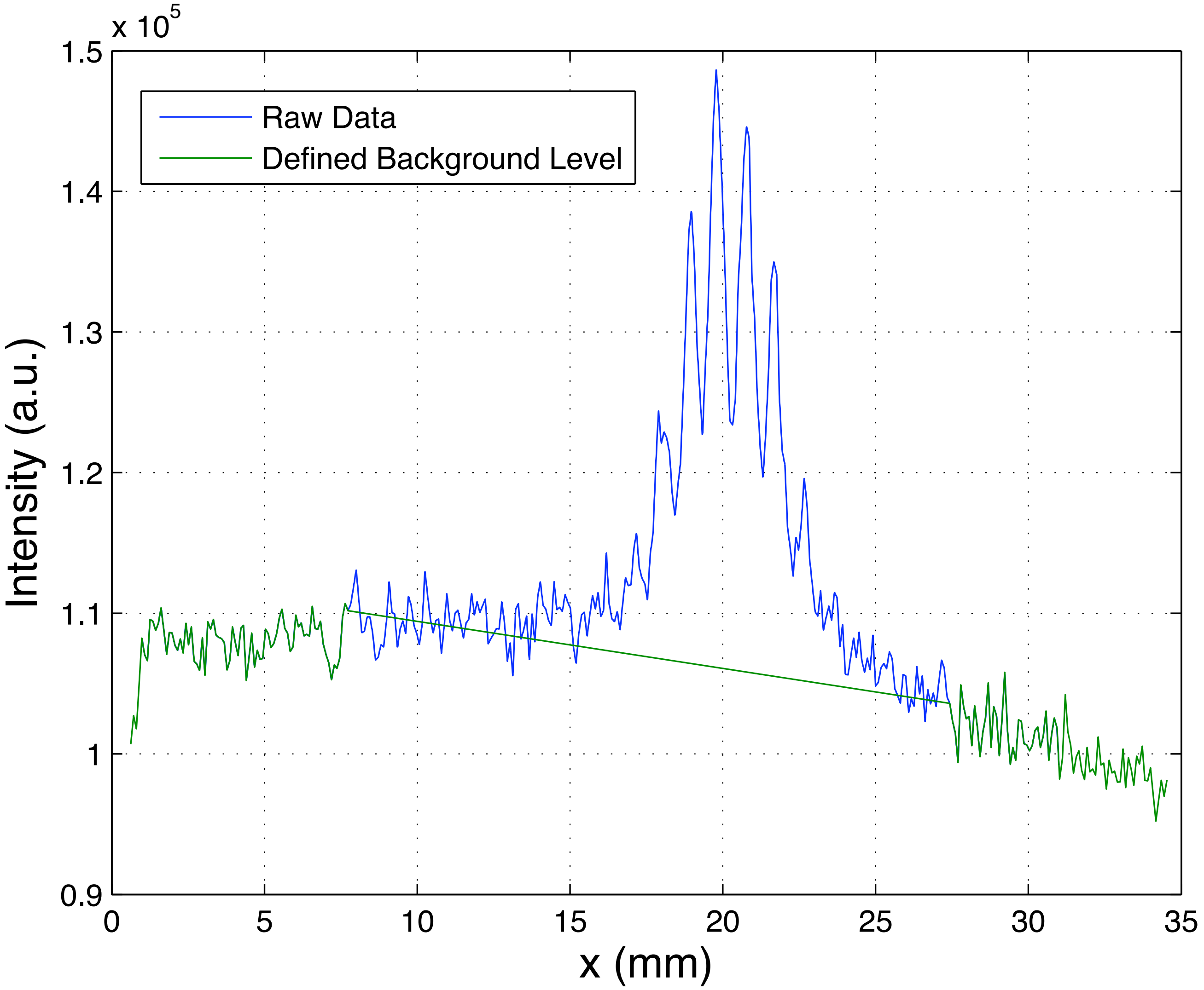

- A typical beam profile after the multi-slit mask,
- Data analysis procedure:
  - determination of the region of interest for the background,

Emittance

Data Analysis

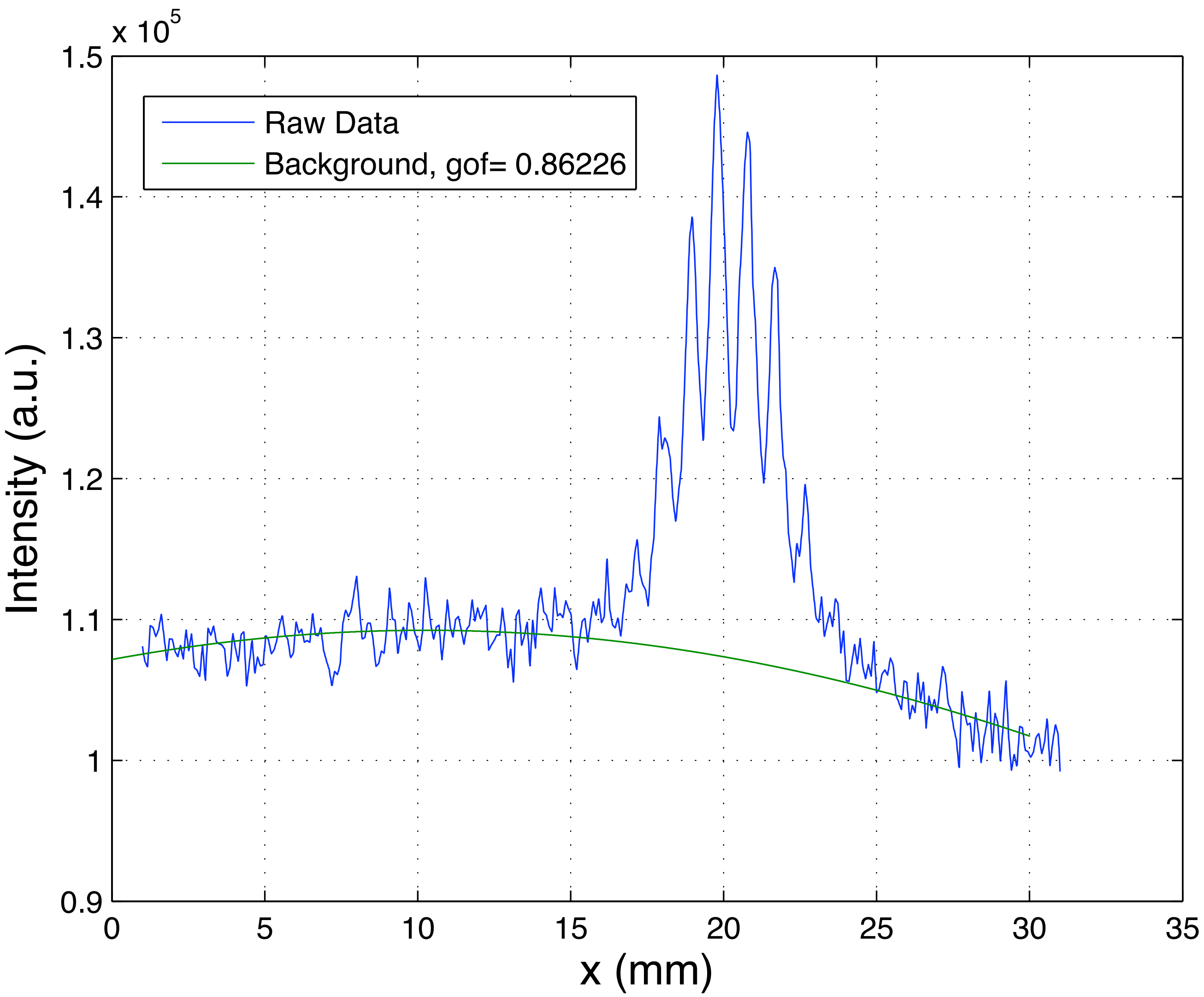

- A typical beam profile after the multi-slit mask,
- Data analysis procedure:
  - determination of the region of interest for the background,
  - fitting a model to the background,

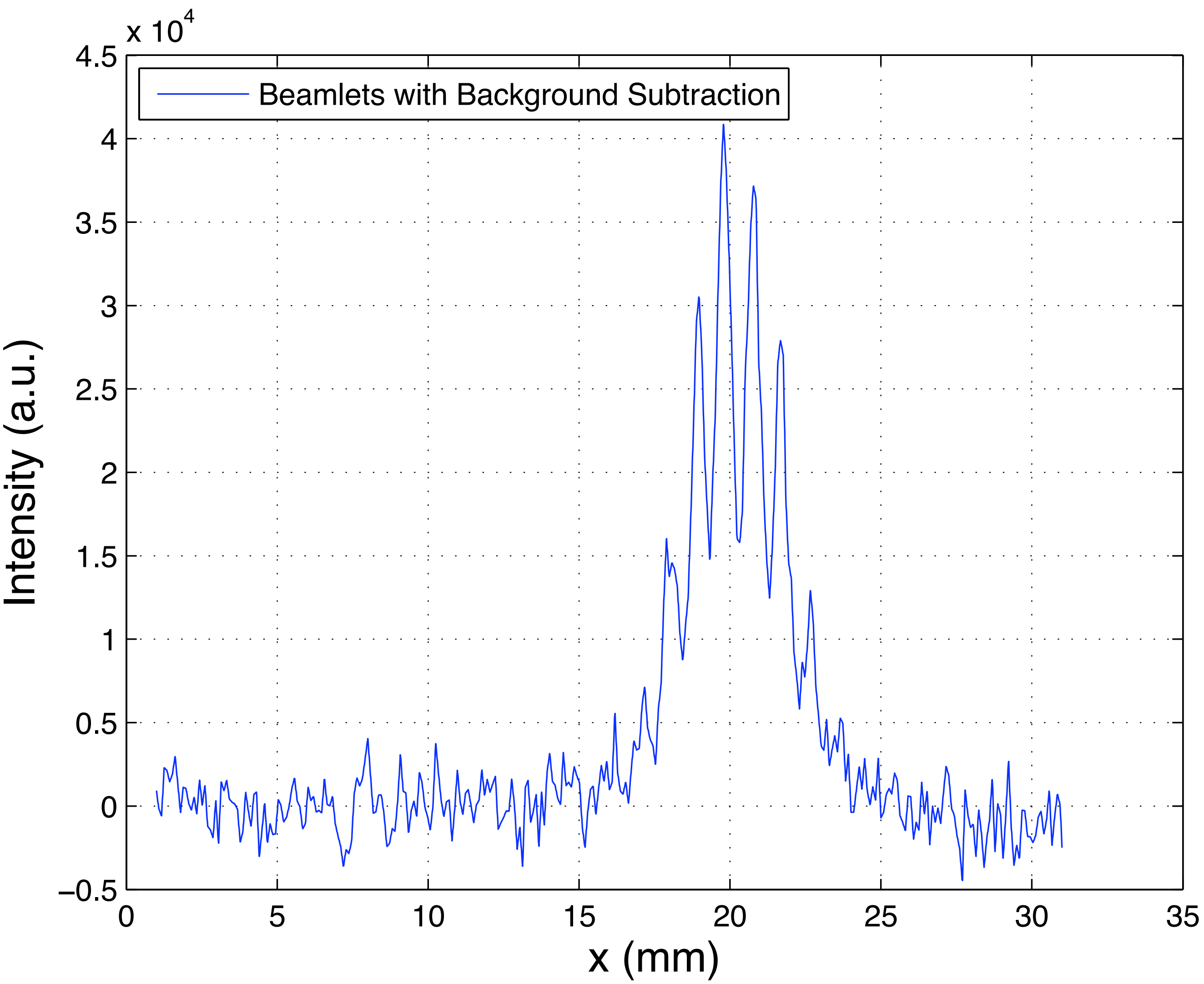

- A typical beam profile after the multi-slit mask,
- Data analysis procedure:
  - determination of the region of interest for the background,
  - fitting a model to the background,
  - subtraction of the proper background,

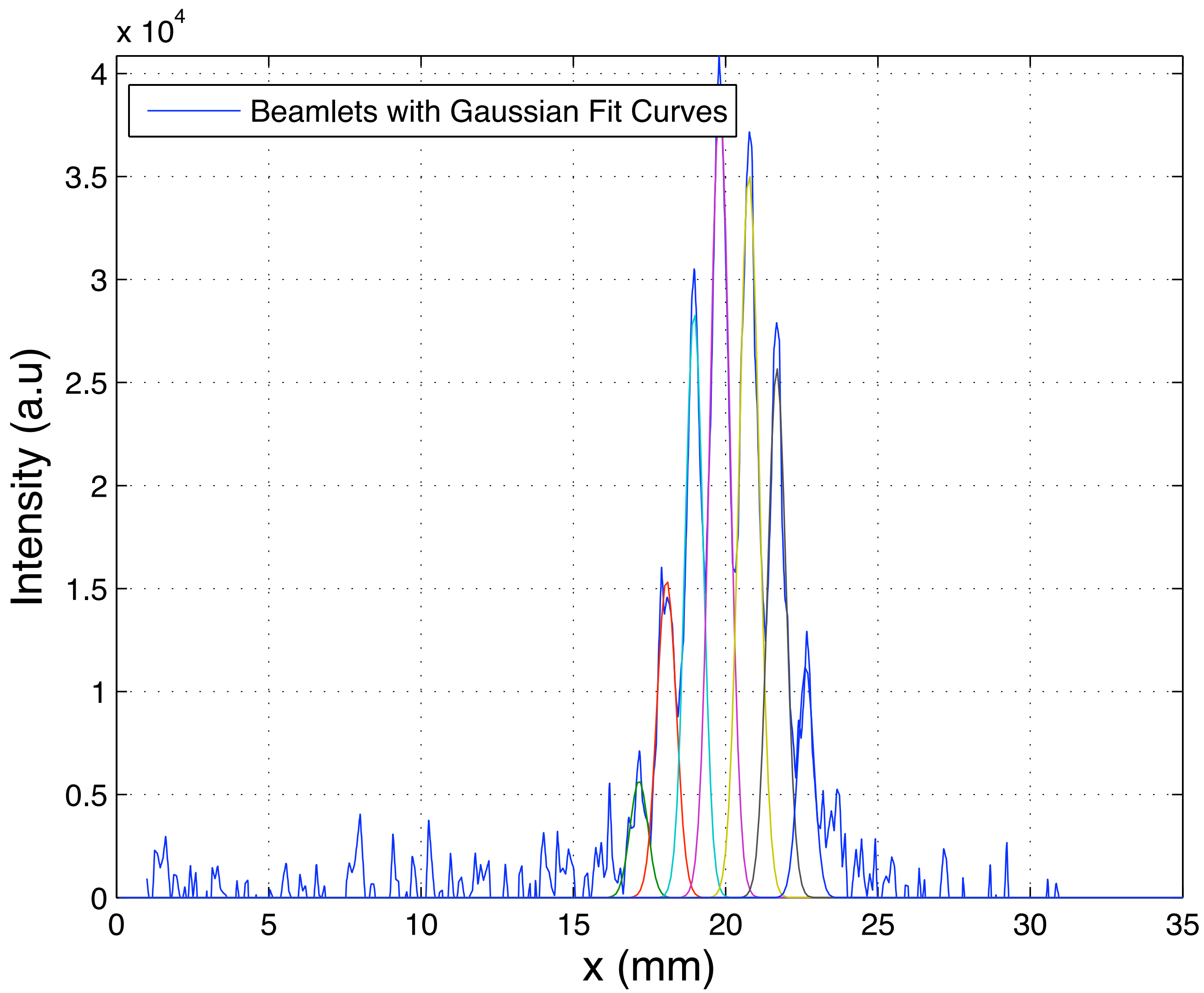

- A typical beam profile after the multi-slit mask,
- Data analysis procedure:
  - determination of the region of interest for the background,
  - fitting a model to the background,
  - subtraction of the proper background,
  - determination of the first and the second moments of the beamlets.

Emittance

Data Analysis

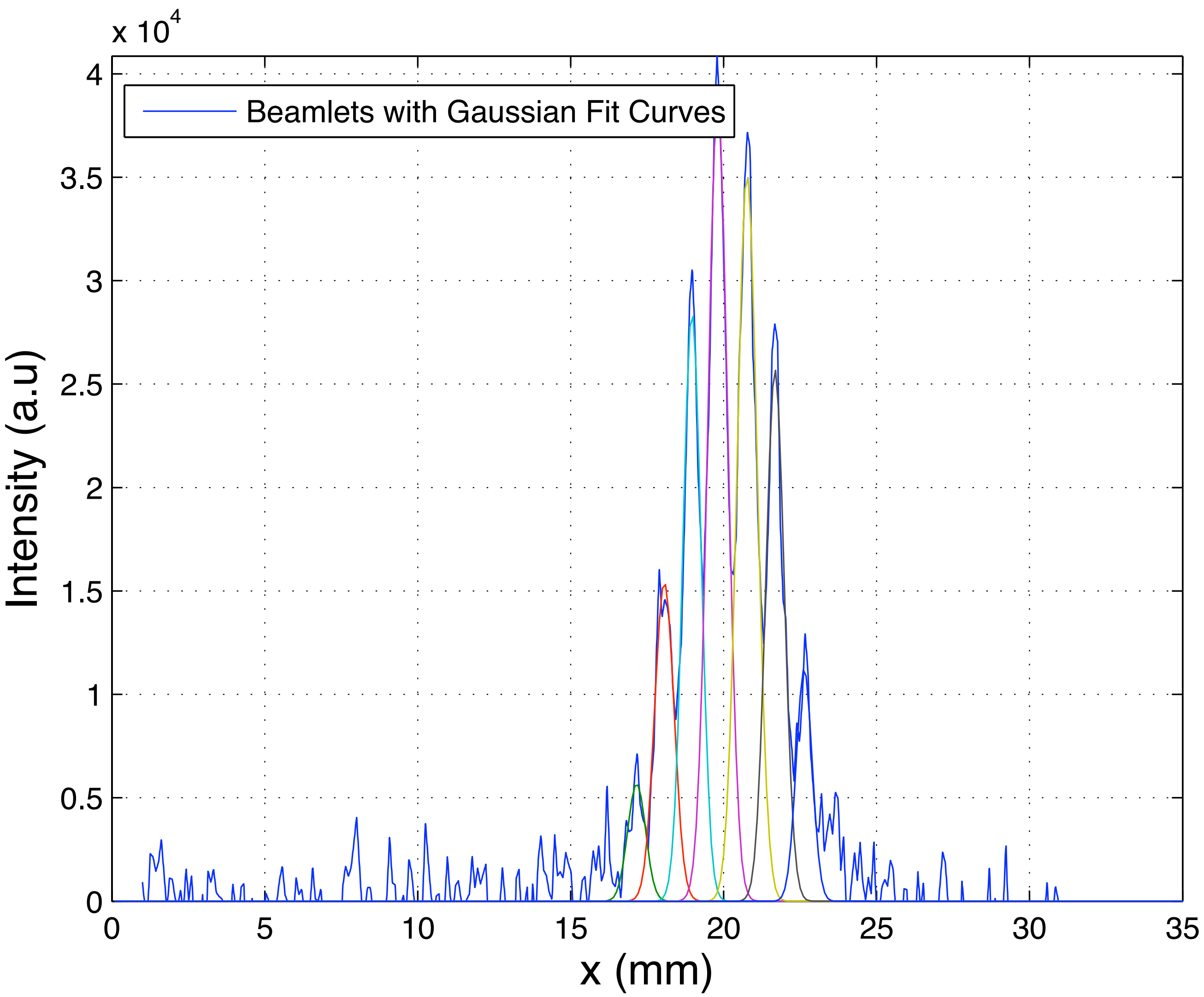

- A typical beam profile after the multi-slit mask,
- Data analysis procedure:
  - determination of the region of interest for the background,
  - fitting a model to the background,
  - subtraction of the proper background,
  - determination of the first and the second moments of the beamlets.
  - calculation of the geometric emittance

Emittance

Data Analysis

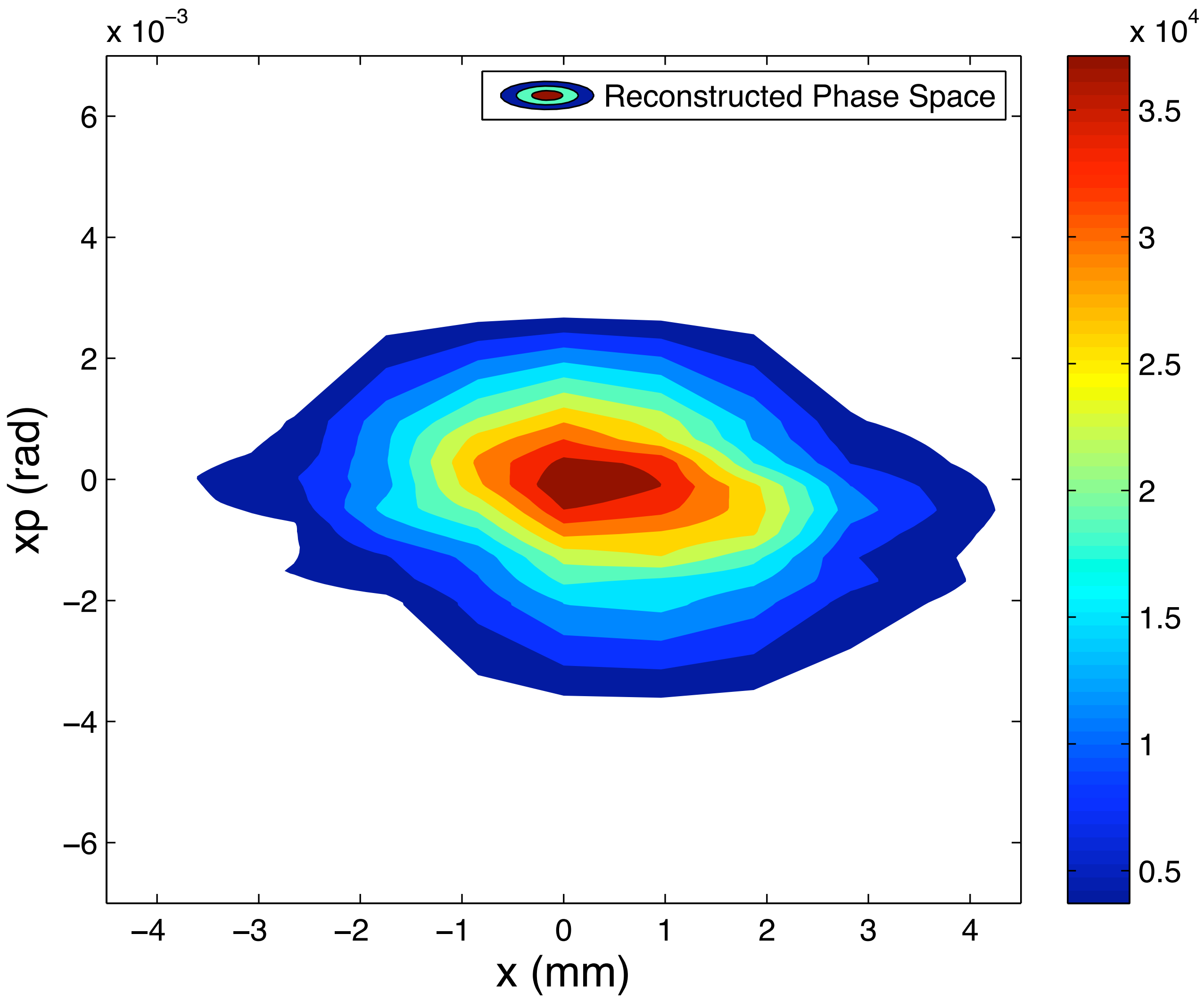

- A typical beam profile after the multi-slit mask,
- Data analysis procedure:
  - determination of the region of interest for the background,
  - fitting a model to the background,
  - subtraction of the proper background,
  - determination of the first and the second moments of the beamlets.
  - calculation of the geometric emittance
  - reconstruction of the phase space.

Emittance

Data Analysis

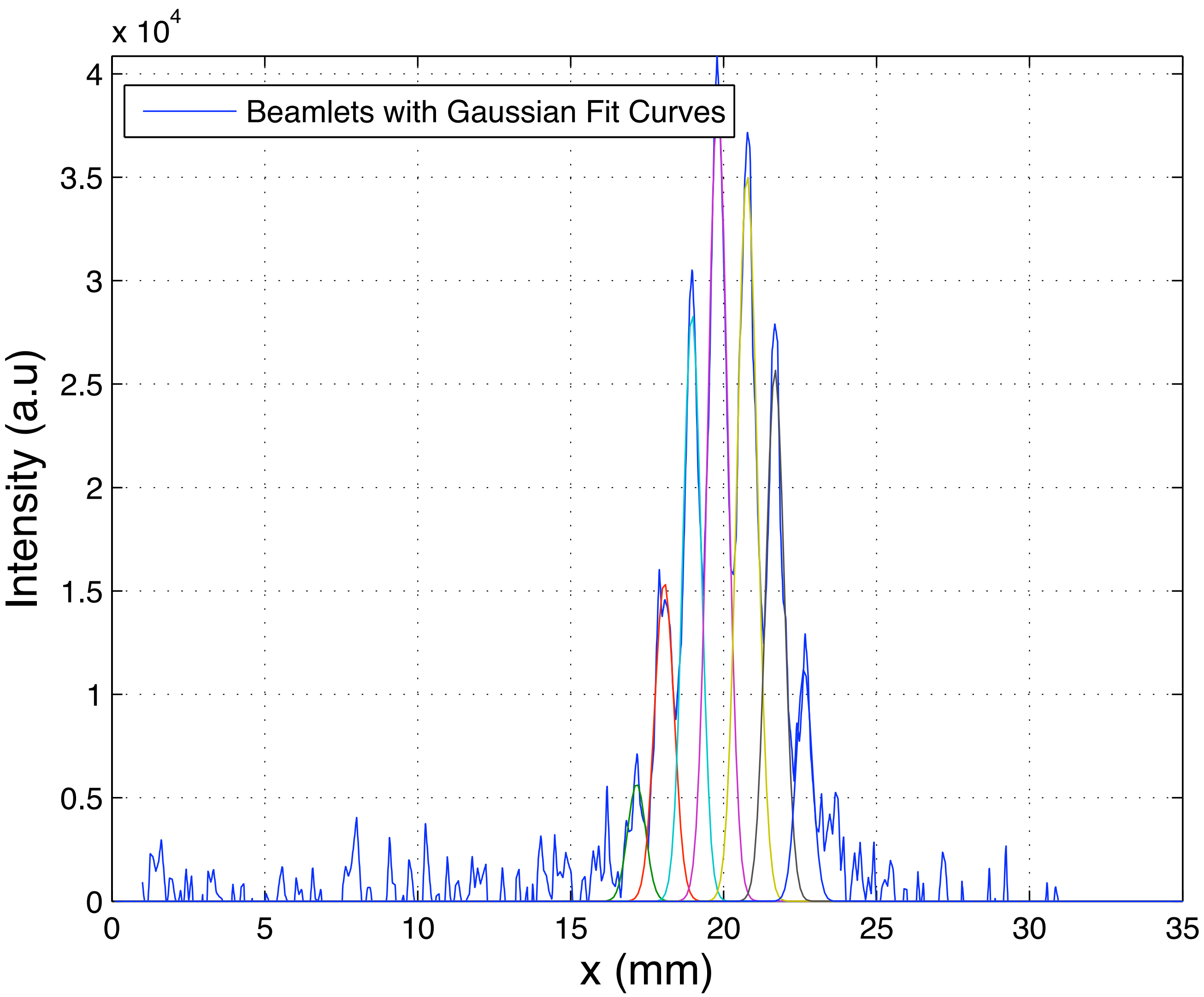

Emittance

Data Analysis

ρ_i , *intensity of individual beamlets.*

$x_{i,c}$, *mean positions of the beamlets.*

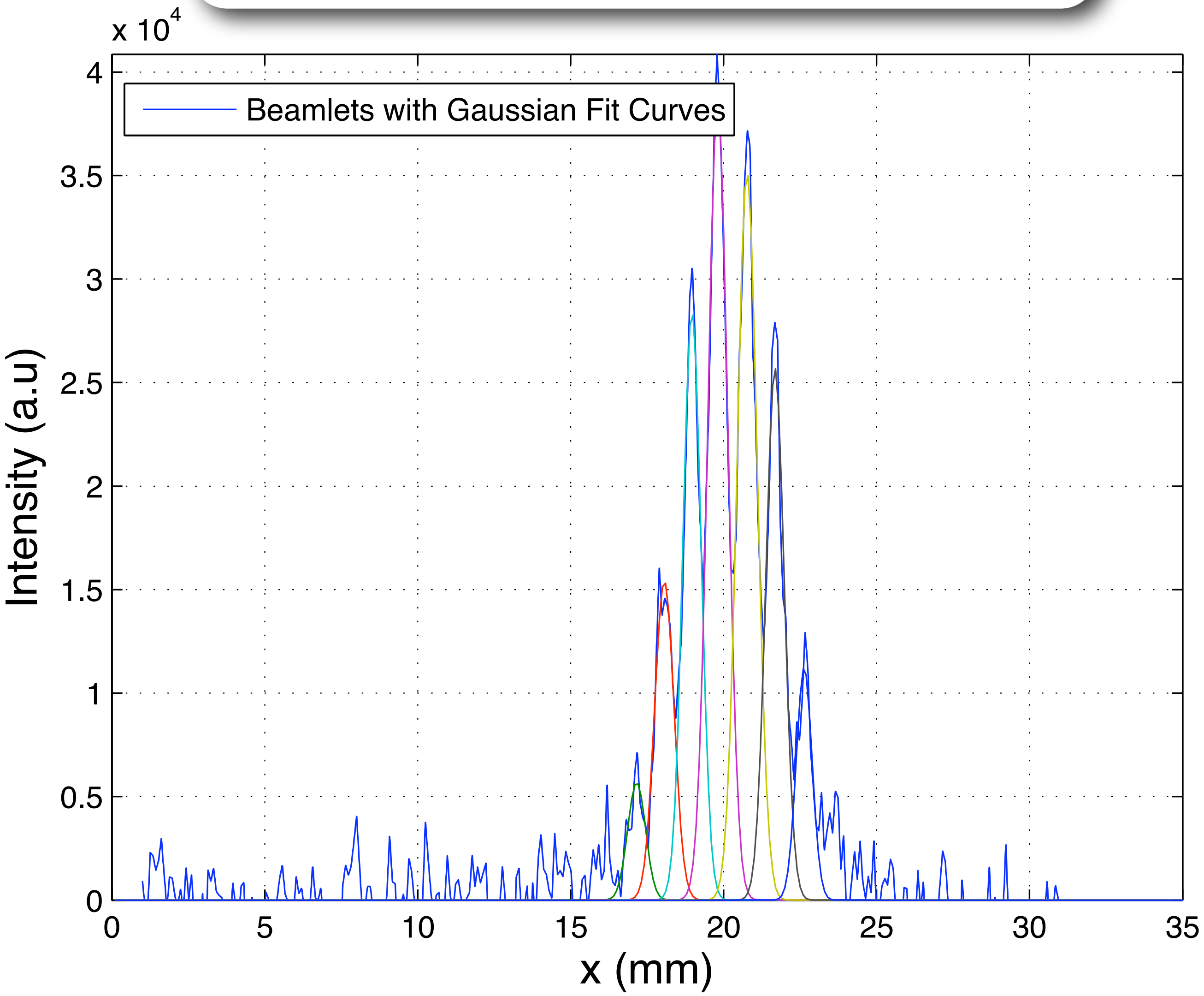

$x'_{i,c} = < x_i - iw > / L$, *divergences of the beamlets*

σ'_i , *spread on the divergences.*

Emittance

Data Analysis

ρ_i , intensity of individual beamlets.

$x_{i,c}$, mean positions of the beamlets.

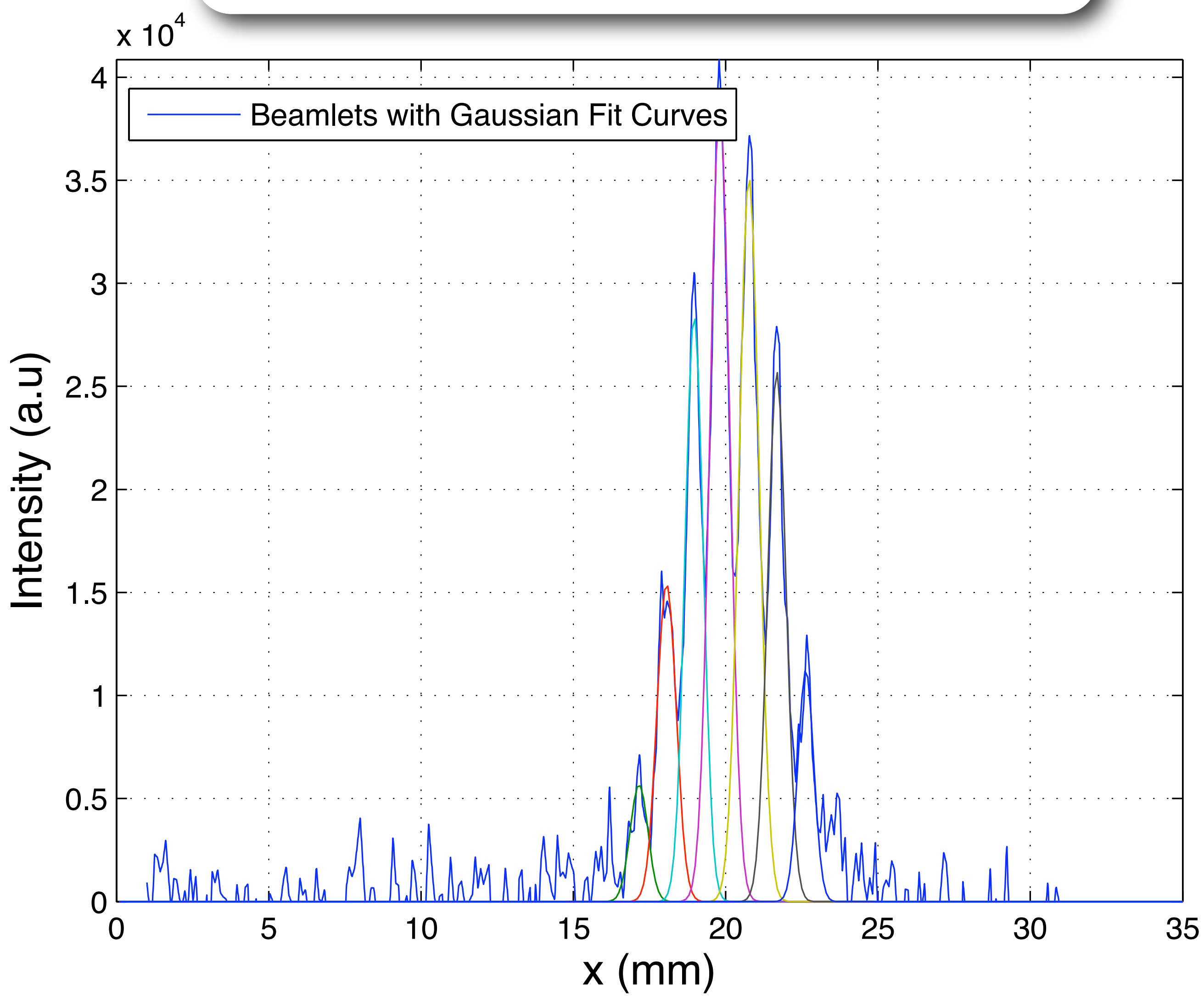

$x'_{i,c} = < x_i - iw > /L$, divergences of the beamlets

σ'_i , spread on the divergences.

Emittance Calculation

The definition of the transverse geometric emittance.

$$\epsilon_x \equiv \sqrt{< x^2 >< x'^2 > - < xx' >^2}$$

Emittance

Data Analysis

ρ_i , intensity of individual beamlets.

$x_{i,c}$, mean positions of the beamlets.

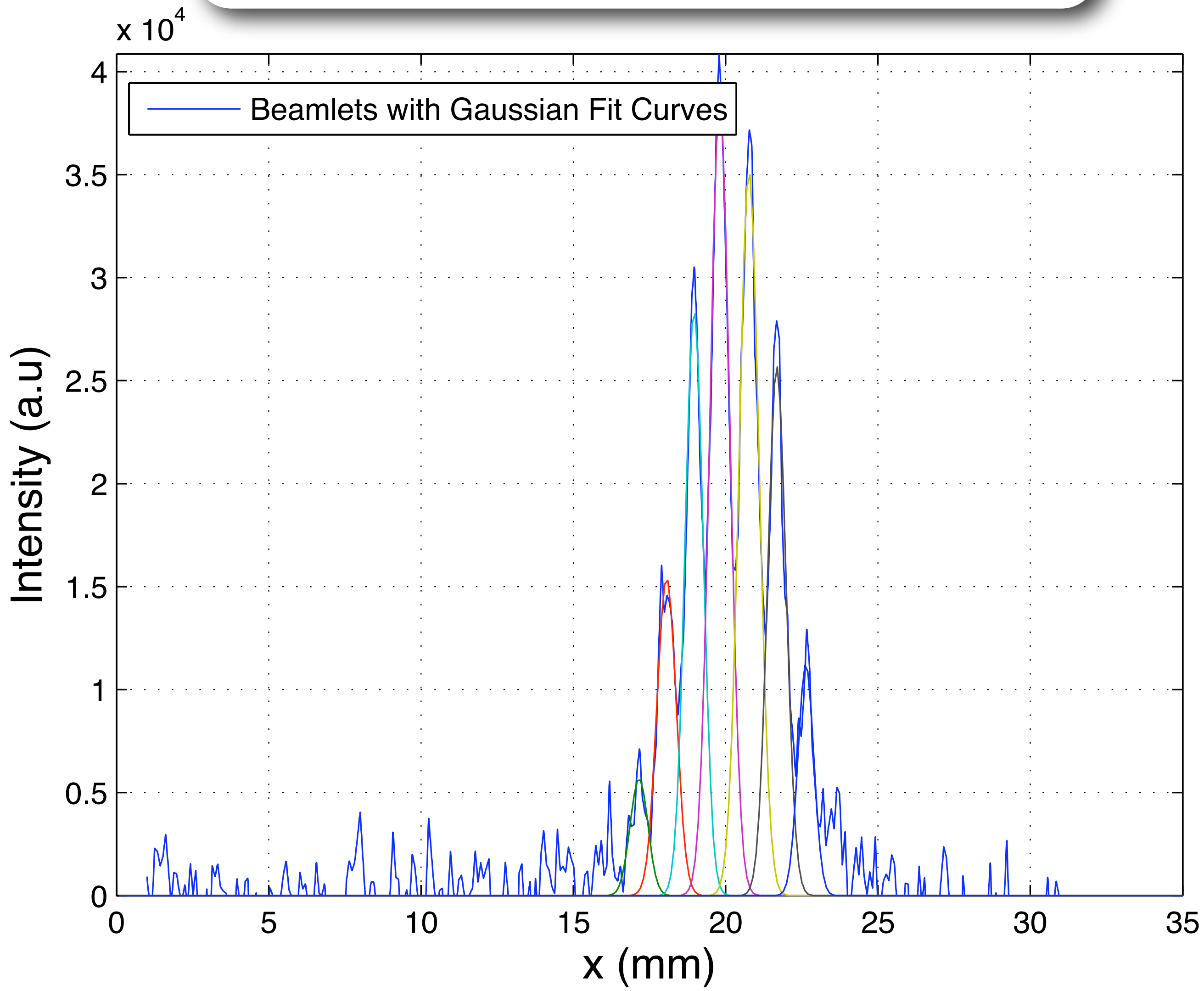

$x'_{i,c} =< x_i - iw > /L$, divergences of the beamlets

σ'_i , spread on the divergences.

Emittance Calculation

The definition of the transverse geometric emittance.

$$\epsilon_x \equiv \sqrt{< x^2 >< x'^2 > - < xx' >^2}$$

$$< x^2 >= \frac{\sum_{i=1}^{N} \rho_i x_{i,c}^2}{\sum_{i=1}^{N} \rho_i}$$

$$< x'^2 >= \frac{\sum_{i=1}^{N} \rho_i (x'^2_{i,c} - \sigma'^2_i)}{\sum_{i=1}^{N} \rho_i}$$

$$< xx' >= \frac{\sum_{i=1}^{N} \rho_i x_{i,c} x'_{i,c}}{\sum_{i=1}^{N} \rho_i}$$

Time-Resolved Emittance Measurement

Time-Resolved Emittance Measurement

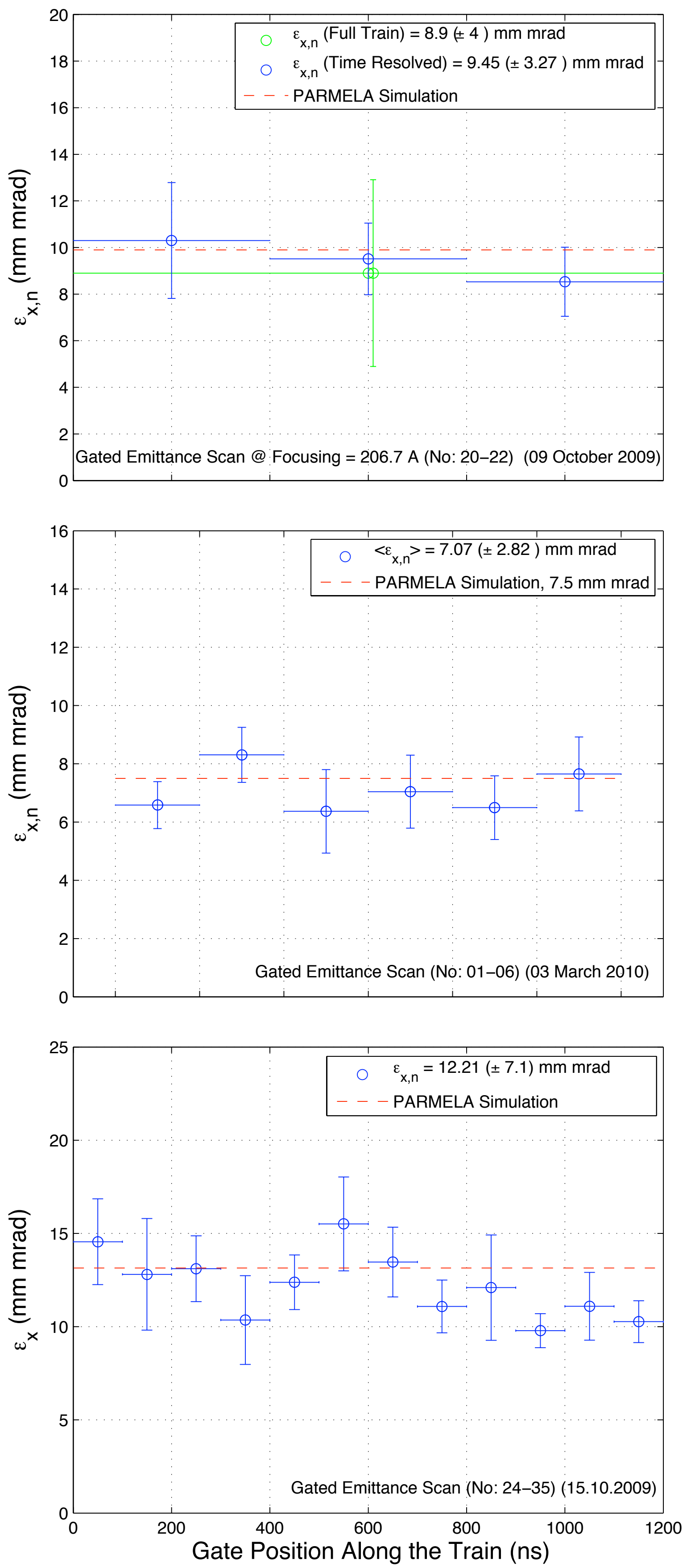

Time-Resolved Emittance Measurement

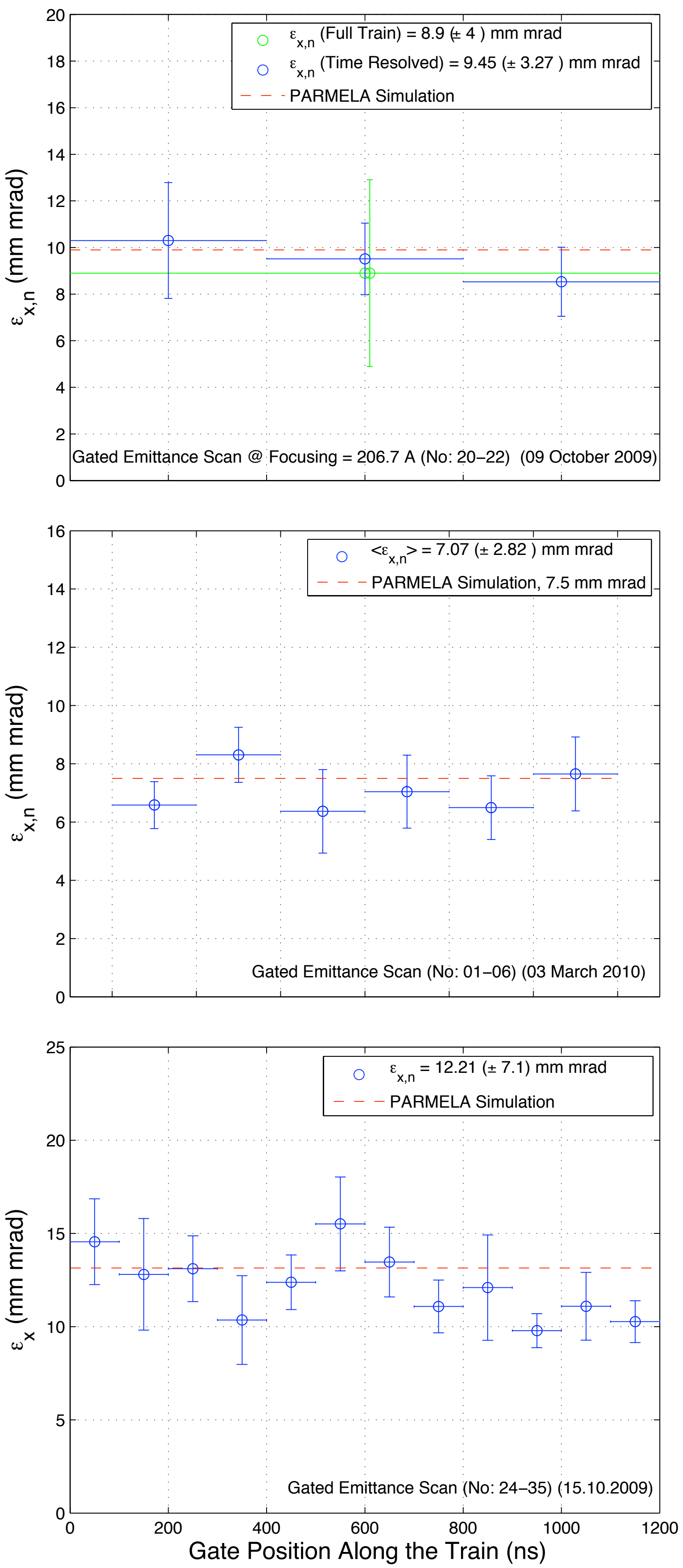

- Variation becomes visible with the increasing resolution along the pulse train.

Time-Resolved Emittance Measurement

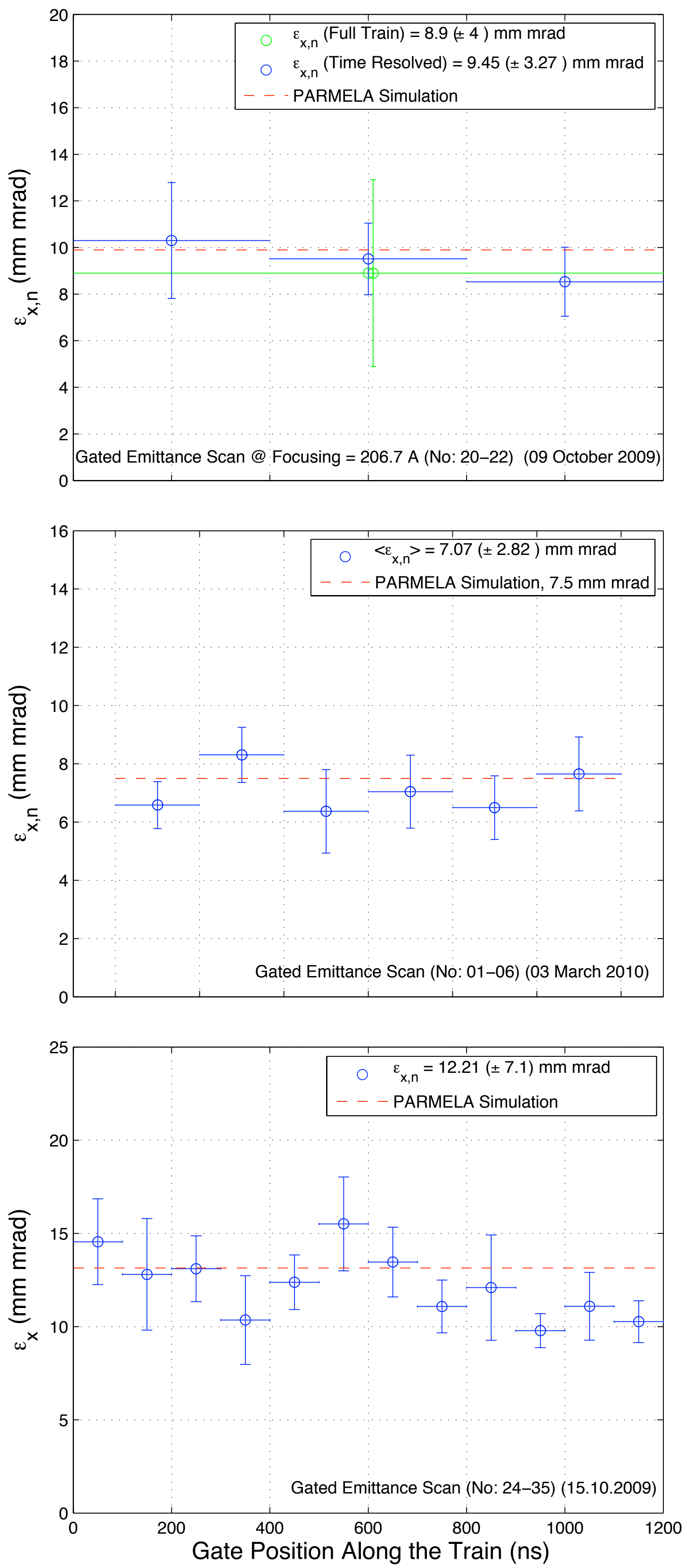

- Variation becomes visible with the increasing resolution along the pulse train.
- "Usual suspects": **Laser intensity fluctuations or RF pulse shape**?

Transverse Phase Space

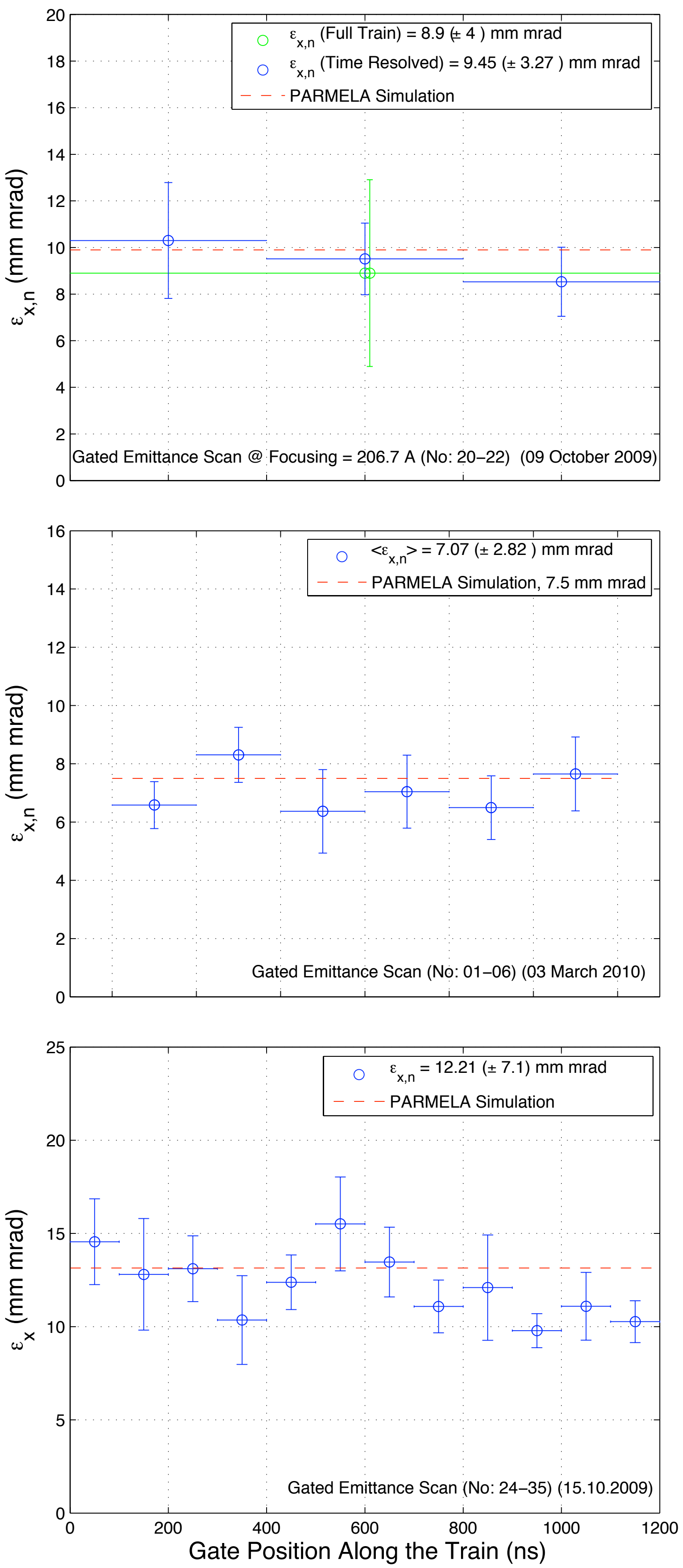

Time-Resolved Emittance Measurement

- Variation becomes visible with the increasing resolution along the pulse train.
- "Usual suspects": **Laser intensity fluctuations or RF pulse shape**?
- A correlation between RF pulse shape and the emittance variation along the pulse train has been determined.

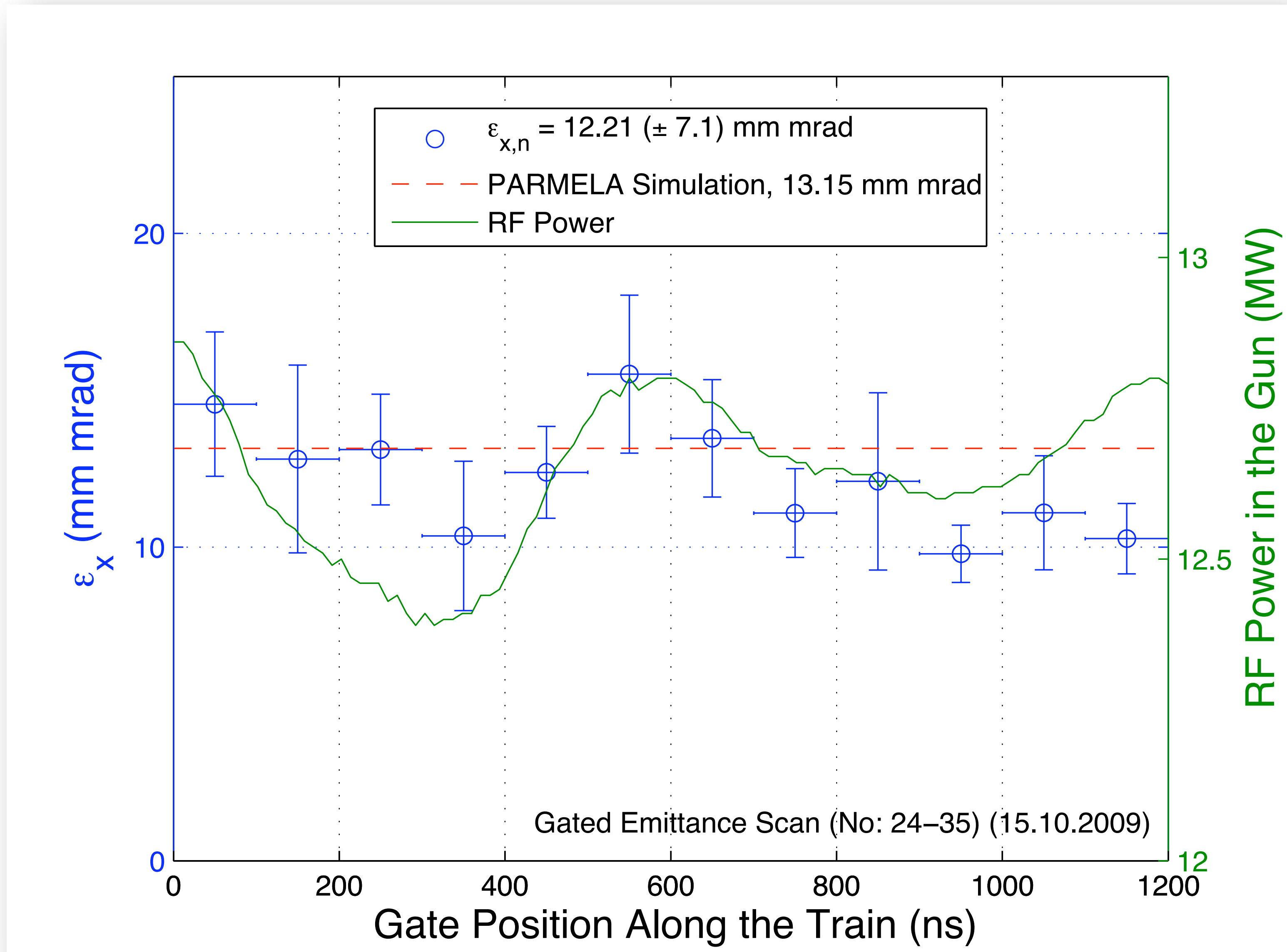

Longitudinal Phase Space

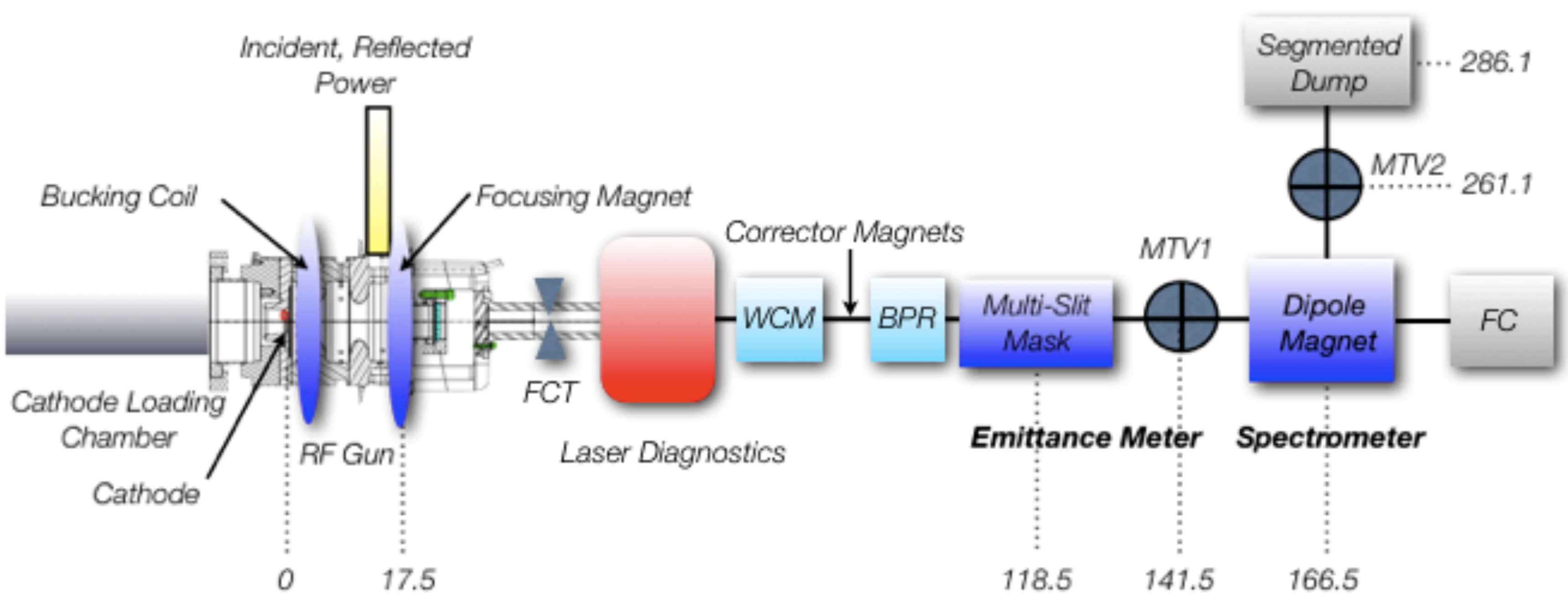

Longitudinal Phase Space

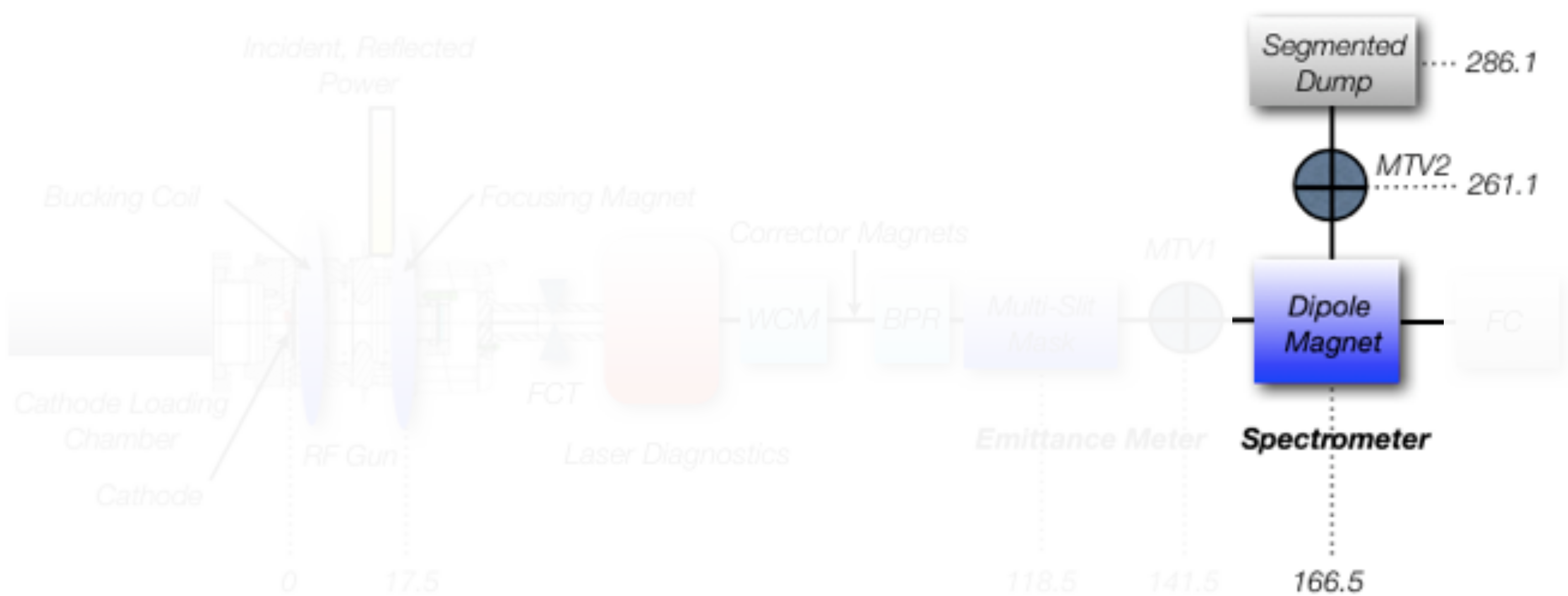

Spectrometer

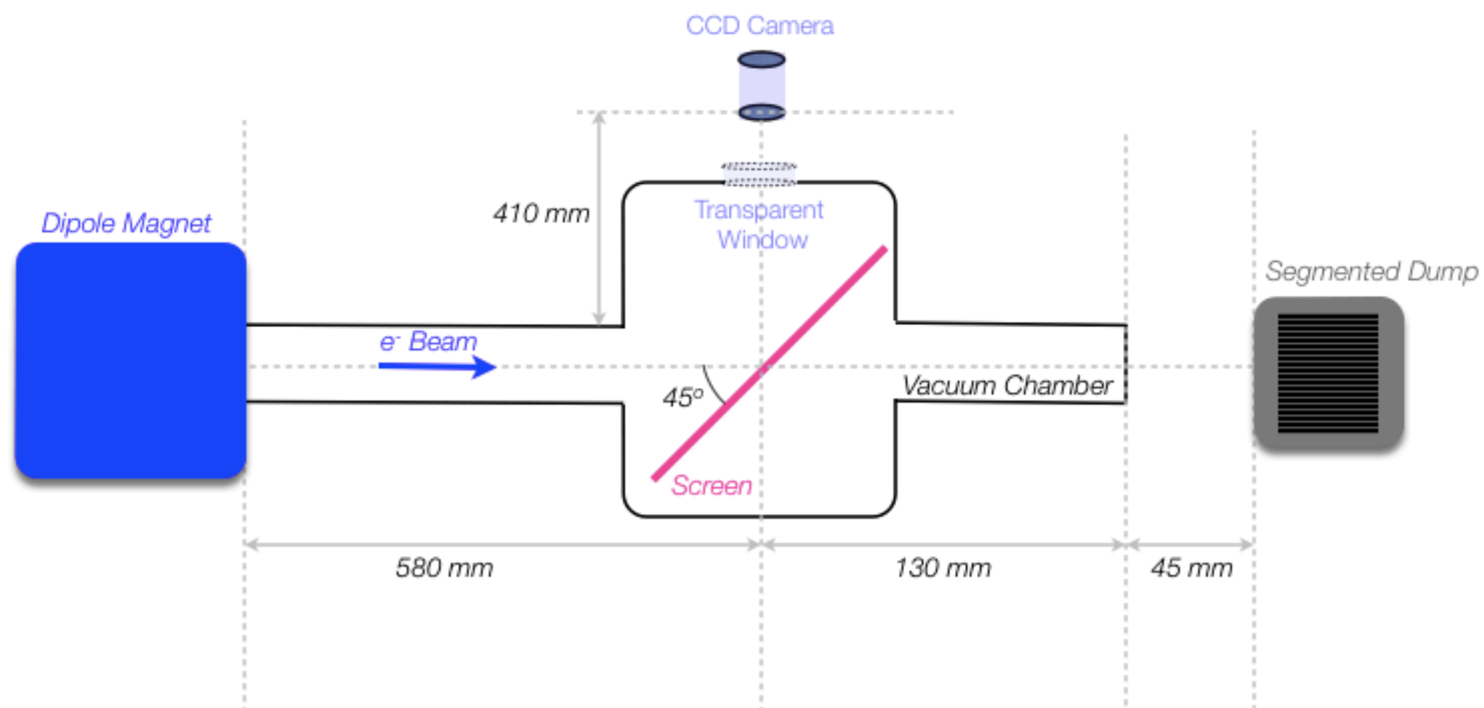

- A magnetic spectrometer has been used for the energy measurements.

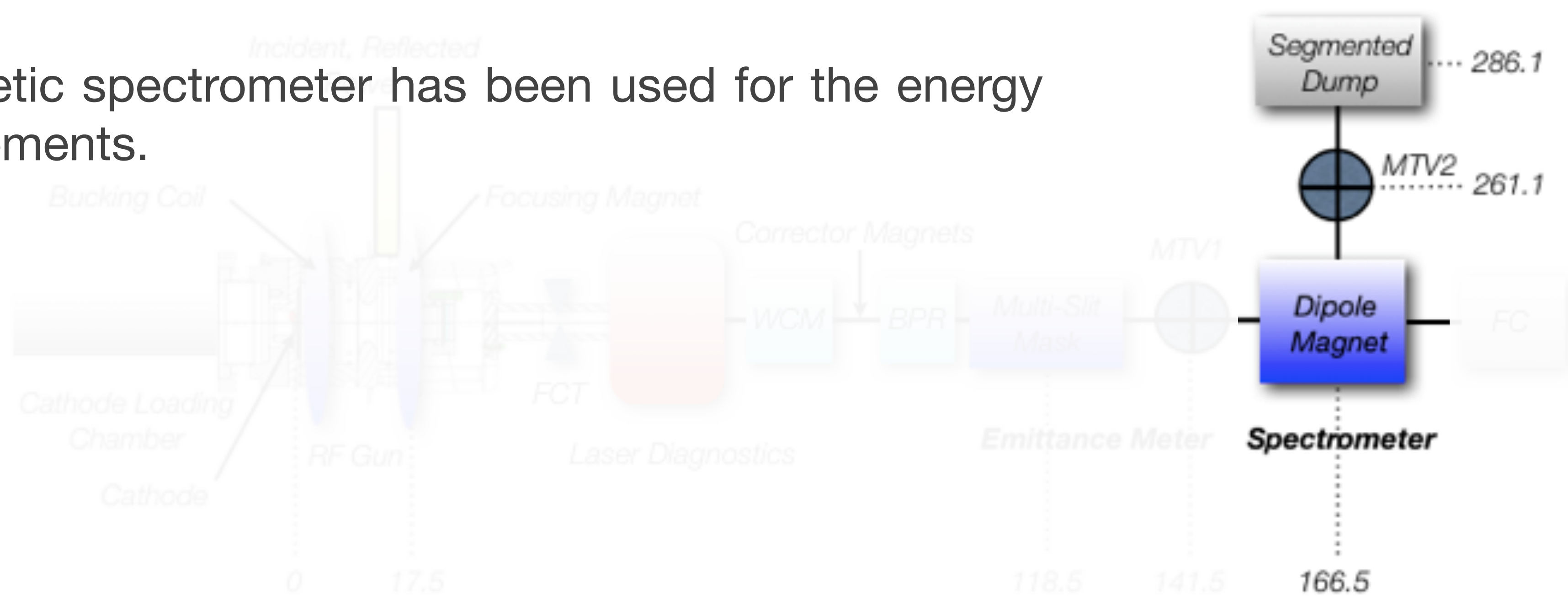

Spectrometer

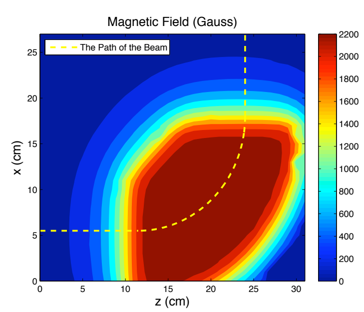

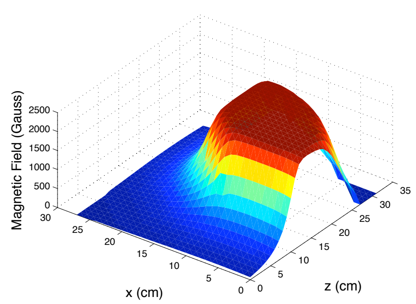

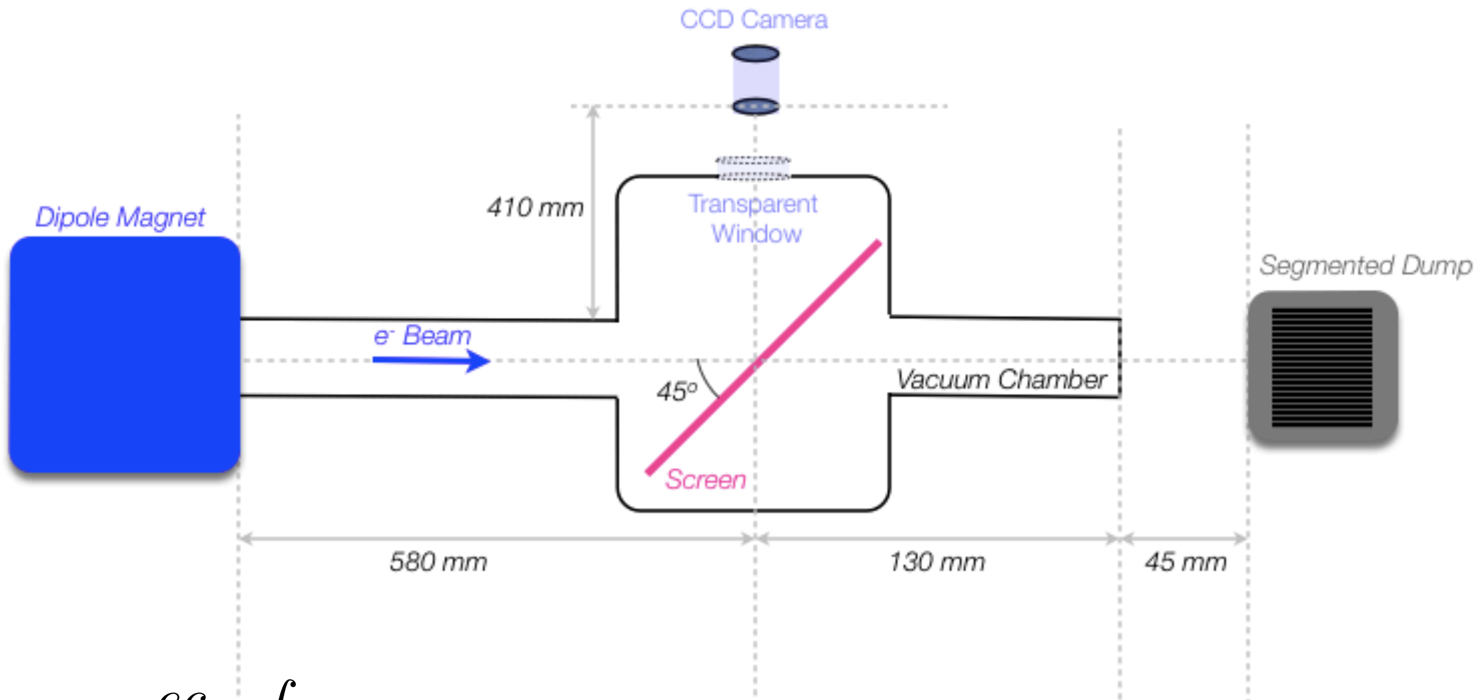

$$E = \frac{ec}{\alpha_{tot}} \int_{path} B_z ds$$

- A magnetic spectrometer has been used for the energy measurements.
- Principle: measurement of the beam momentum distribution after a dipole with a known magnetic field.

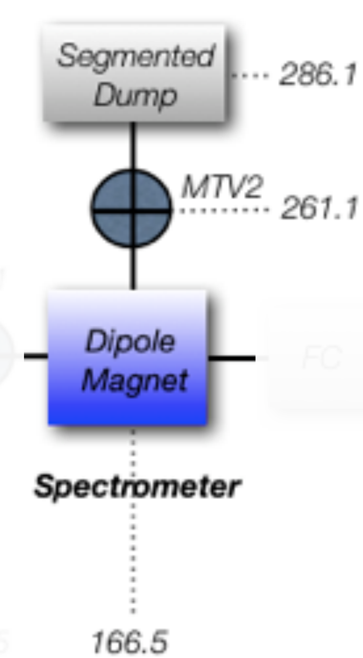

Spectrometer

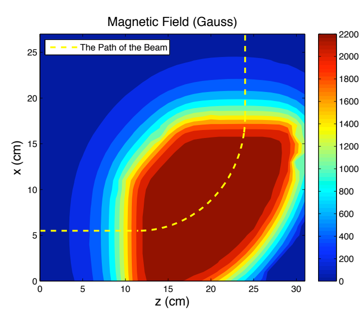

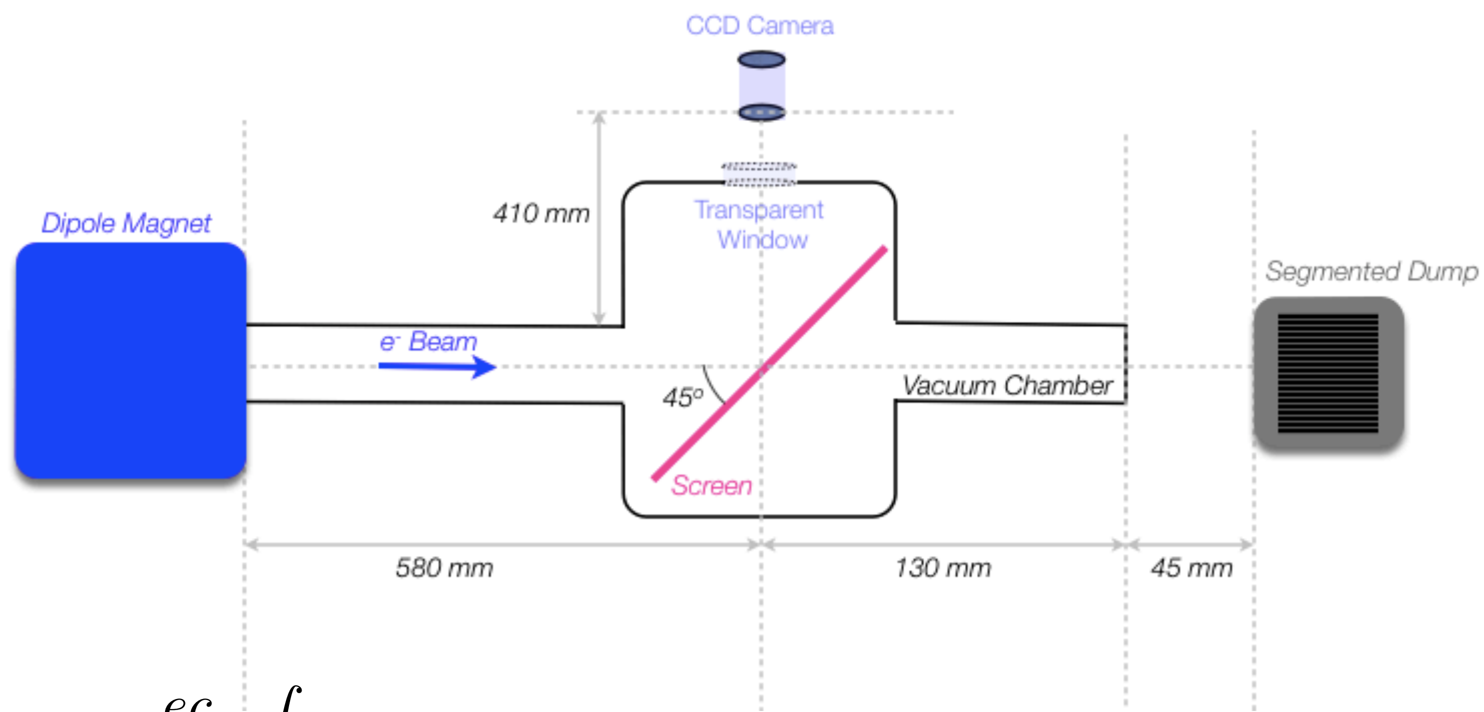

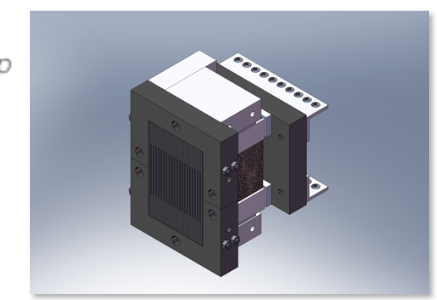

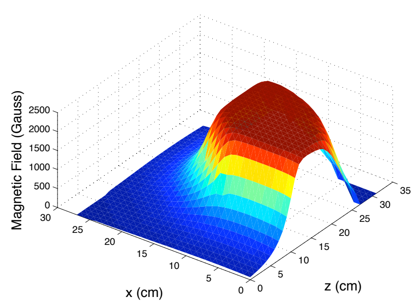

$$E = \frac{ec}{\alpha_{tot}} \int_{path} B_z ds$$

- A magnetic spectrometer has been used for the energy measurements.
- Principle: measurement of the beam momentum distribution after a dipole with a known magnetic field.
- Beam momentum distribution can be measured by an OTR profile monitor or a segmented dump.

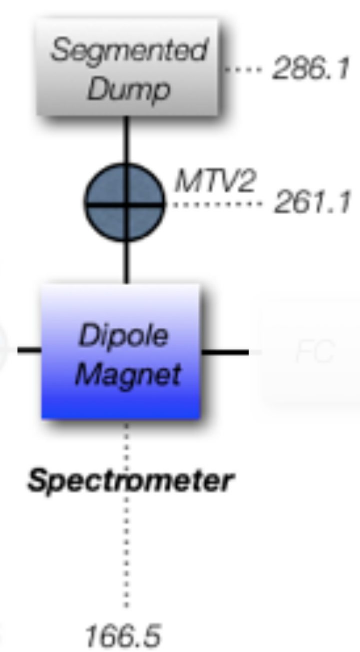

Energy Measurements with a Magnetic Spectrometer

OTR Monitoring

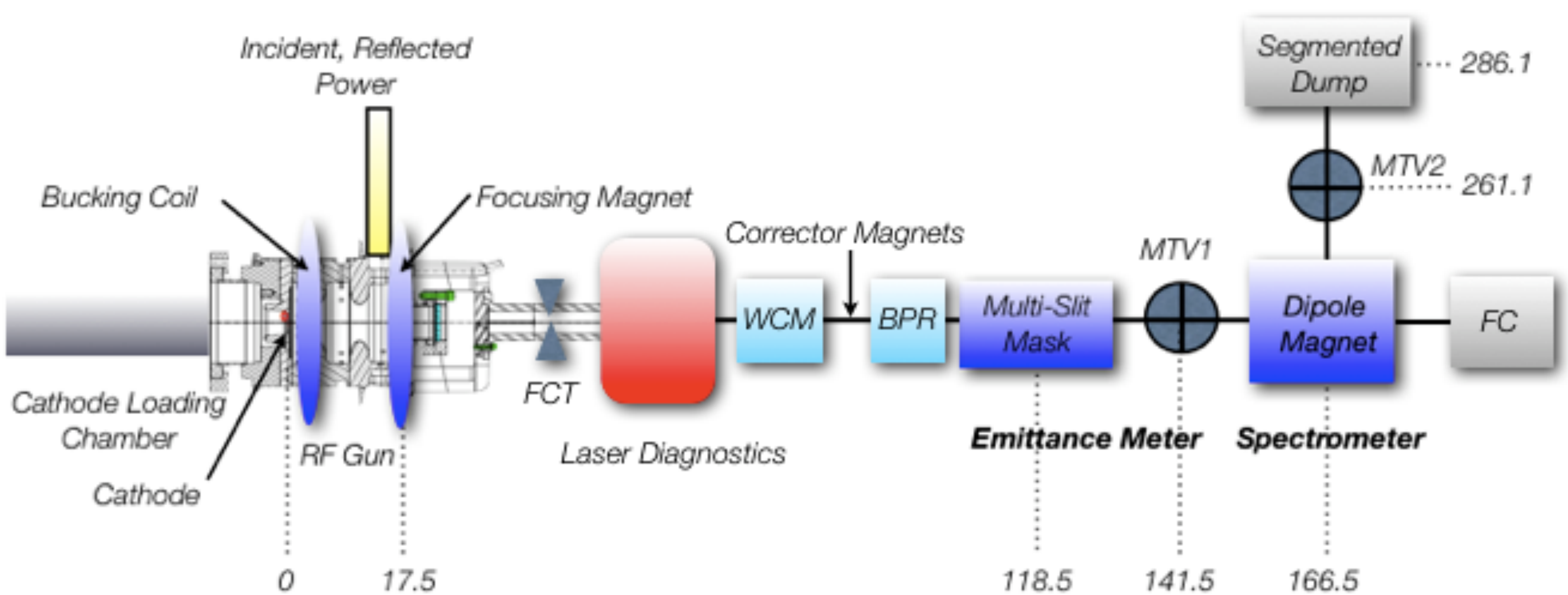

Energy Measurements with a Magnetic Spectrometer

OTR Monitoring

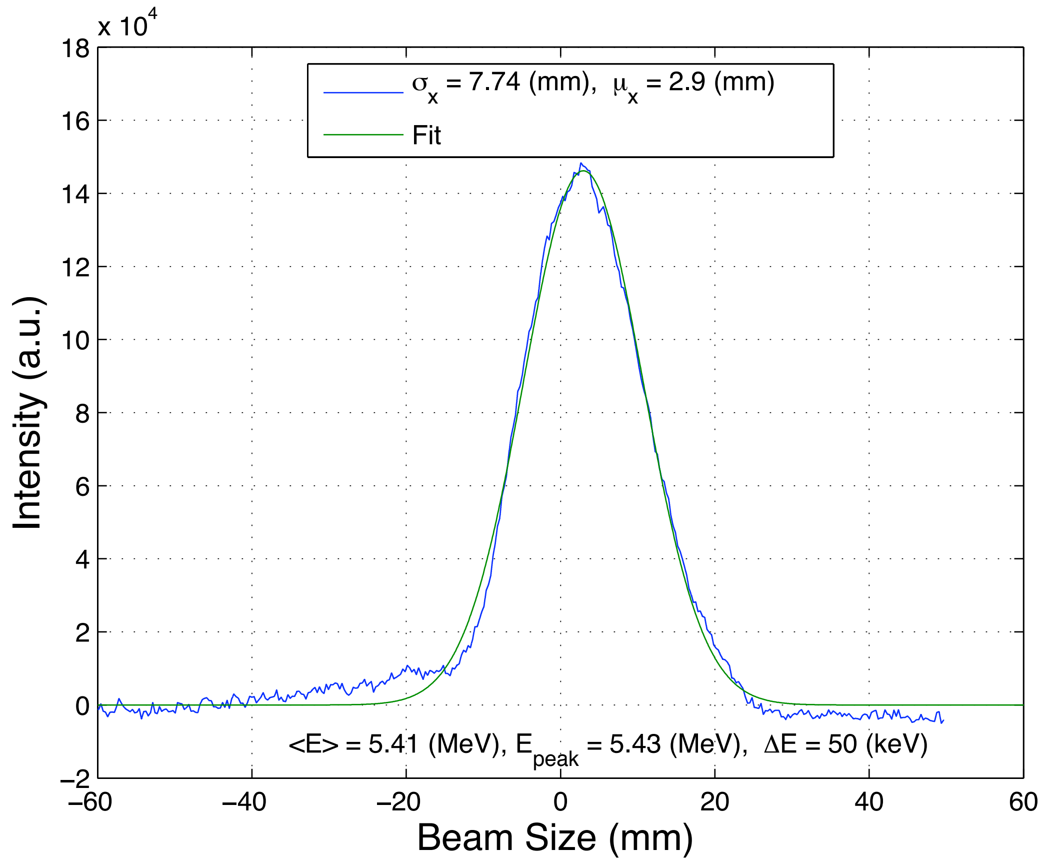

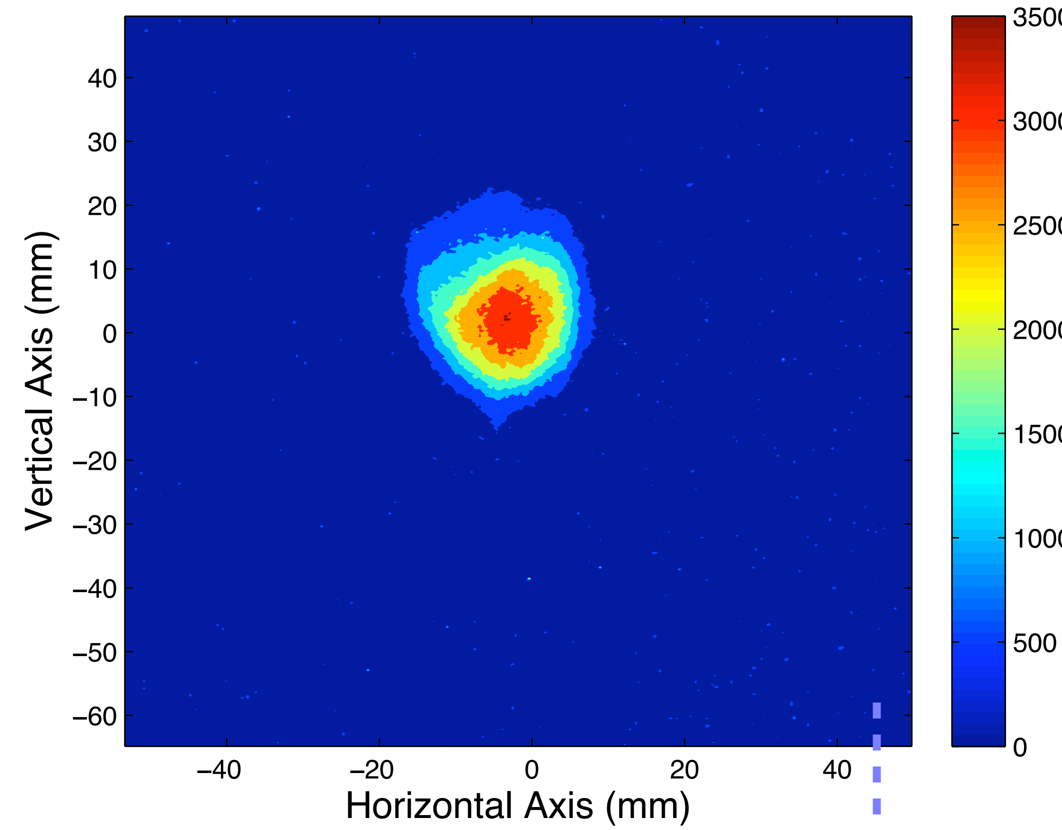

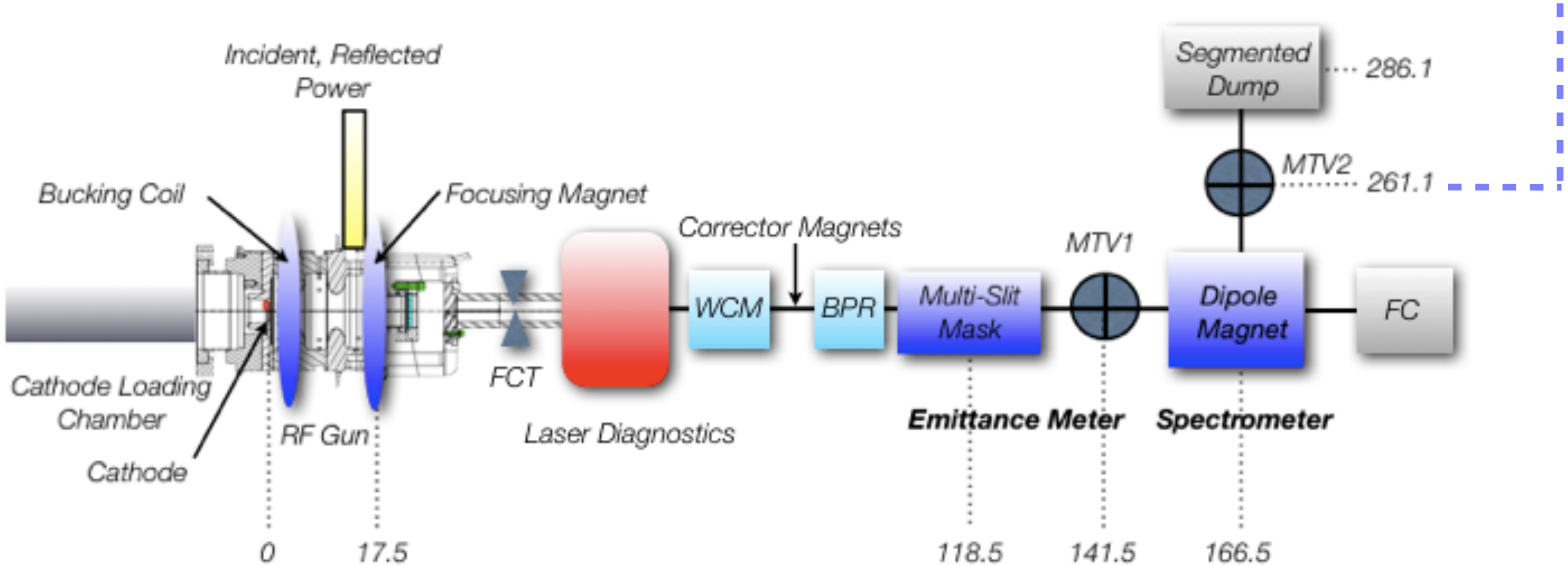

Energy Measurements with a Magnetic Spectrometer

OTR Monitoring

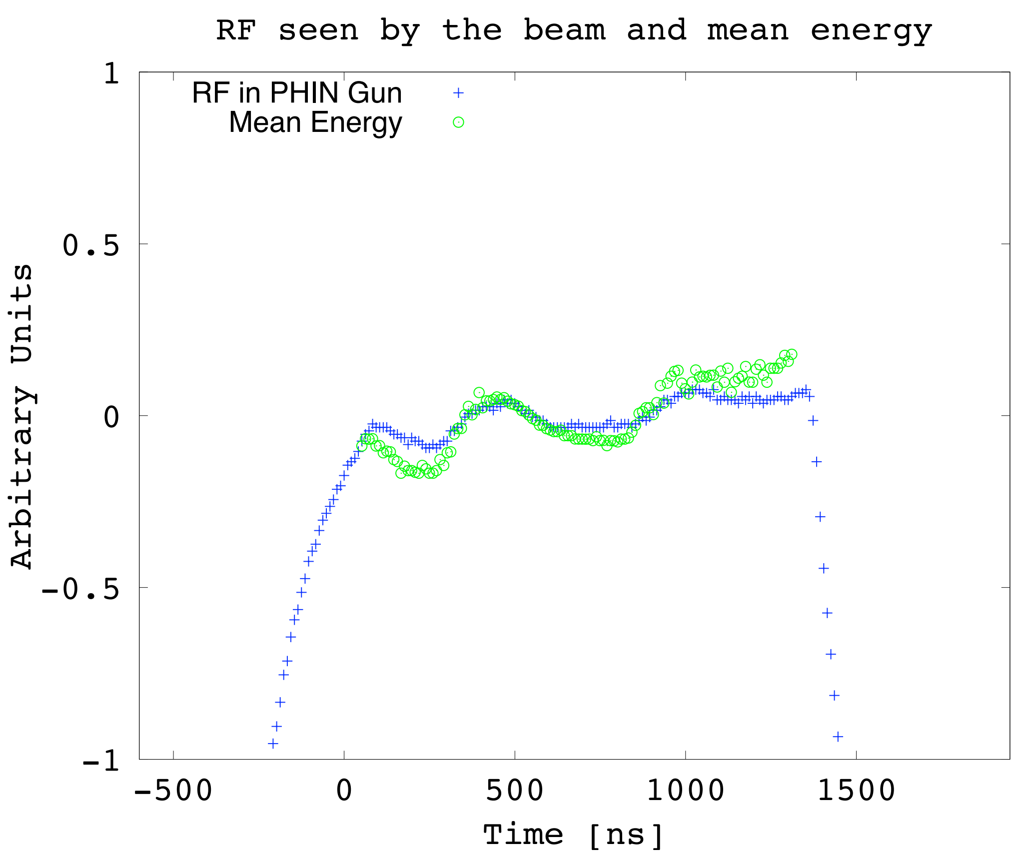

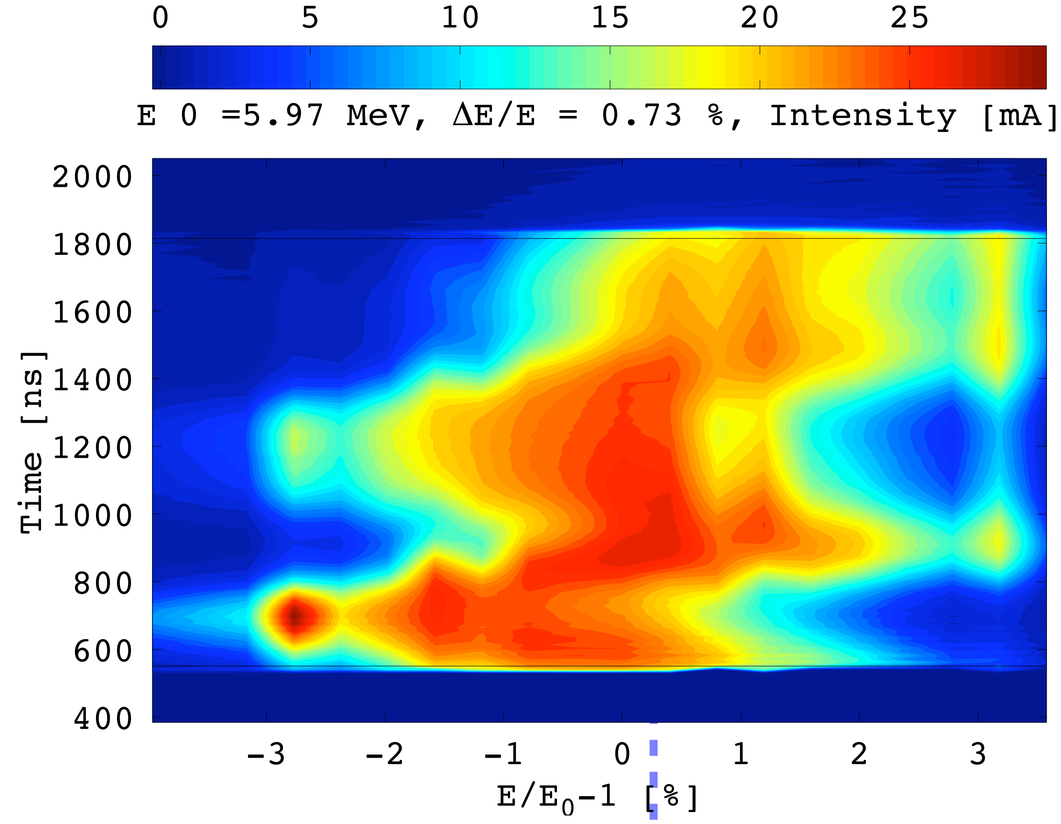

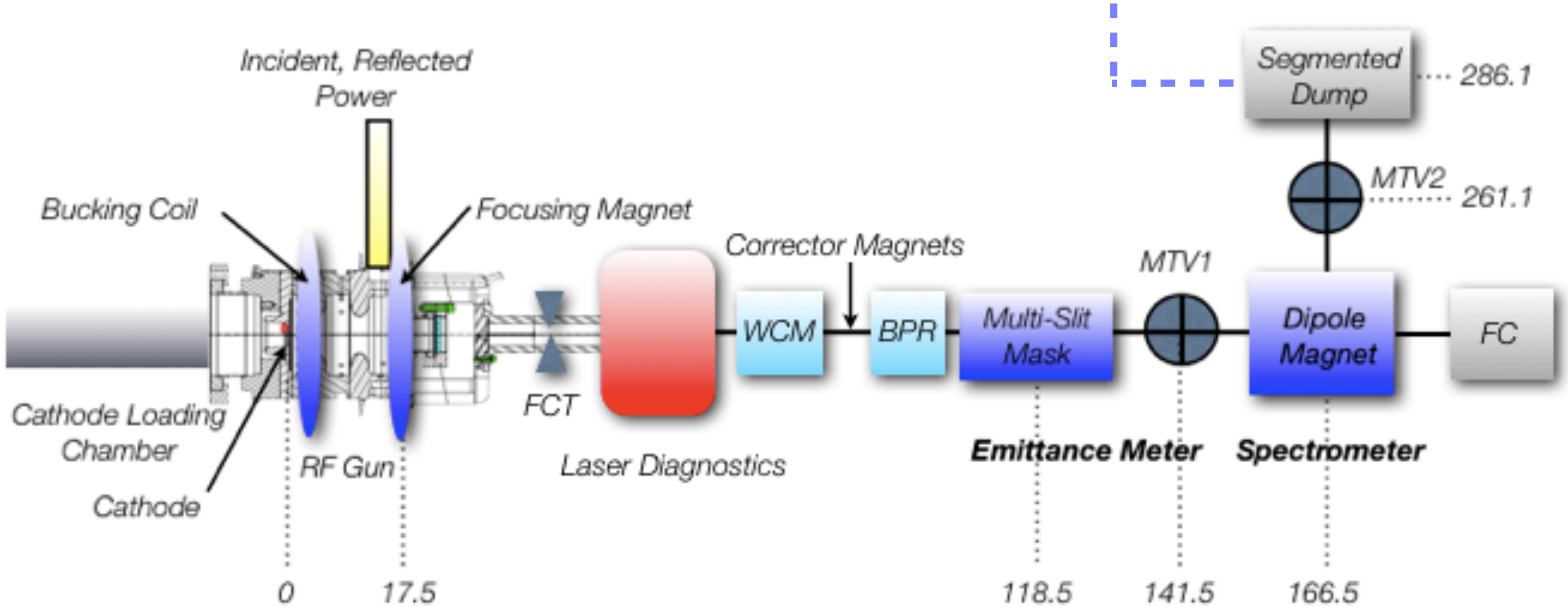

*Measurement has been done by Daniel Egger / EPFL.

Energy Measurements with a Magnetic Spectrometer

OTR Monitoring

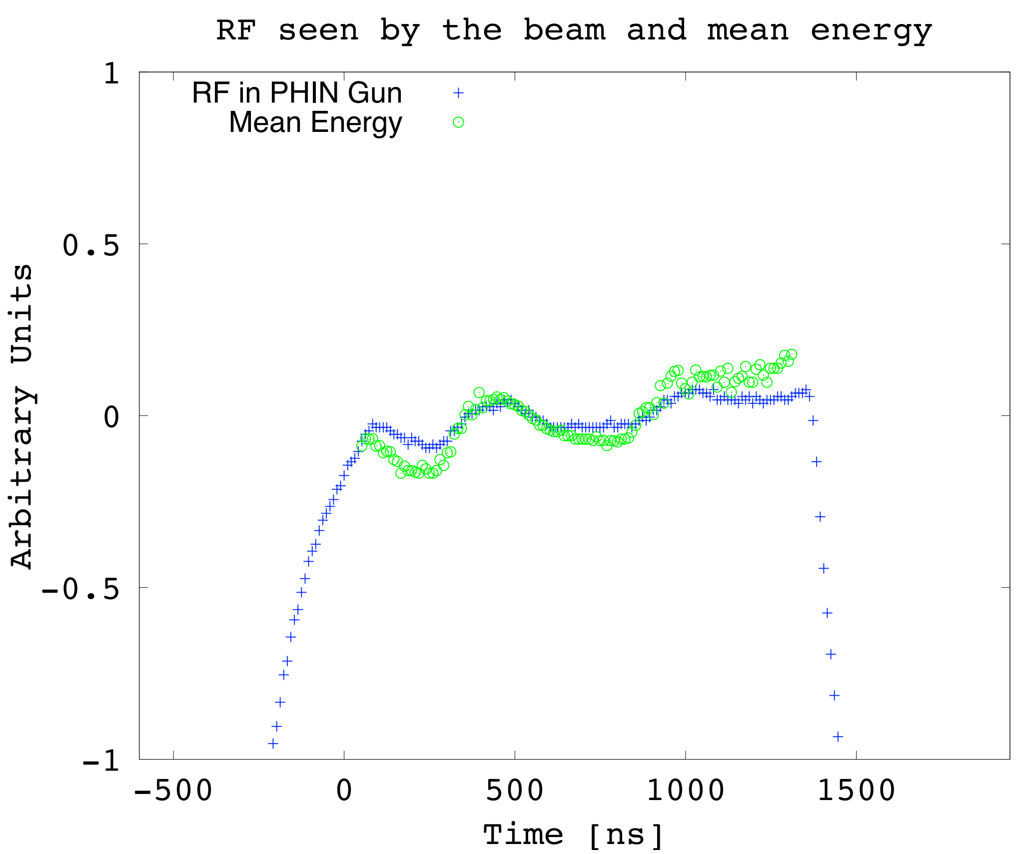

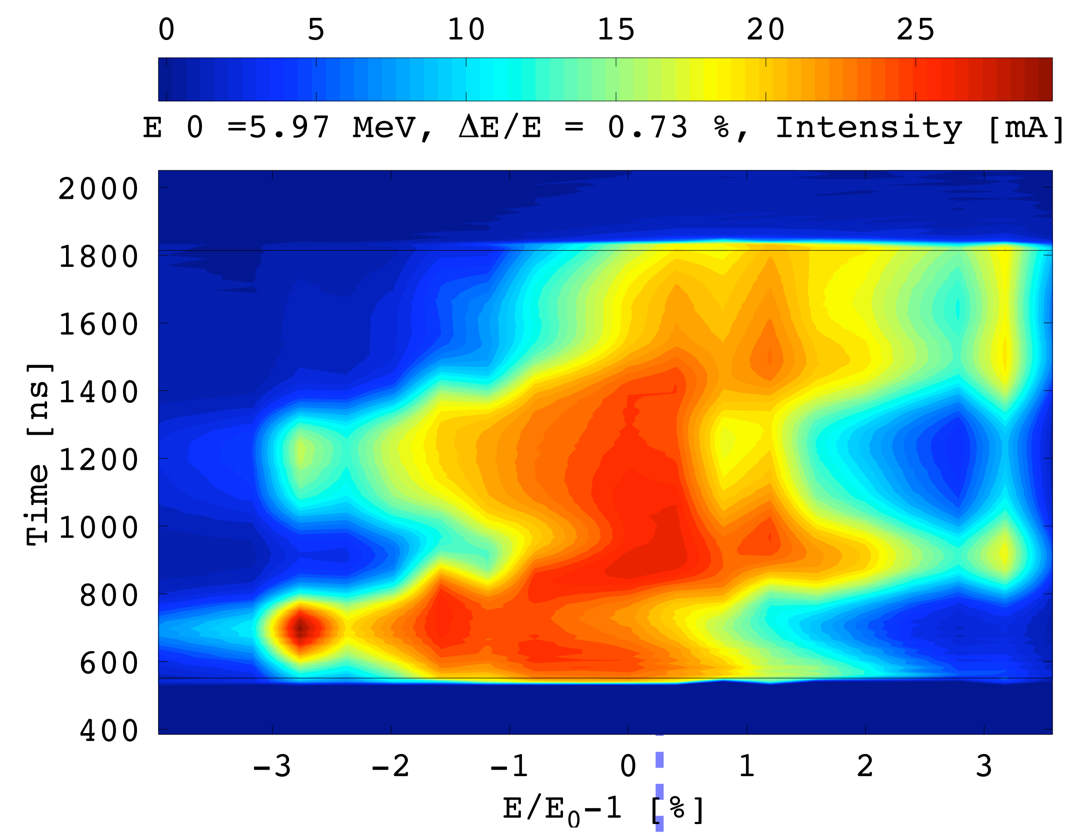

- Segmented dump measurements **also reveal the correlation between the beam and the RF pulse shape** which supports the time-resolved emittance and beam size measurements.

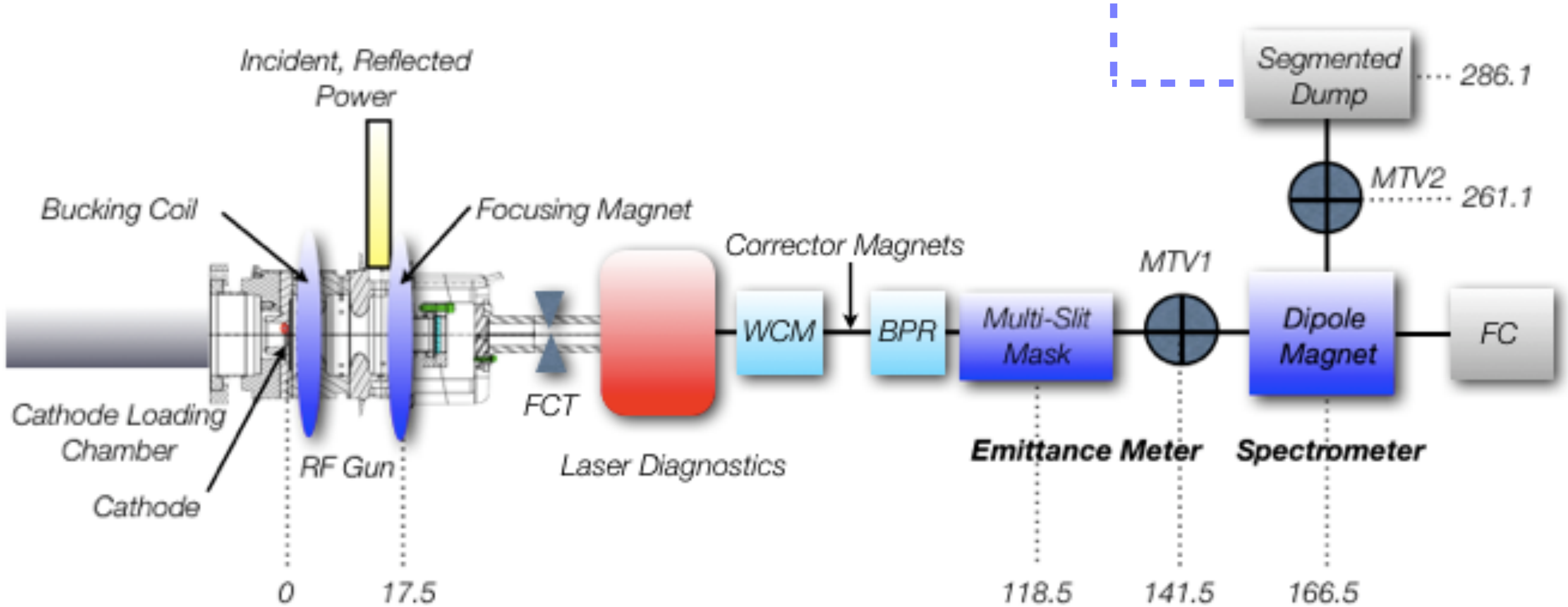

*Measurement has been done by Daniel Egger / EPFL.

Energy Measurements with a Magnetic Spectrometer

OTR Monitoring

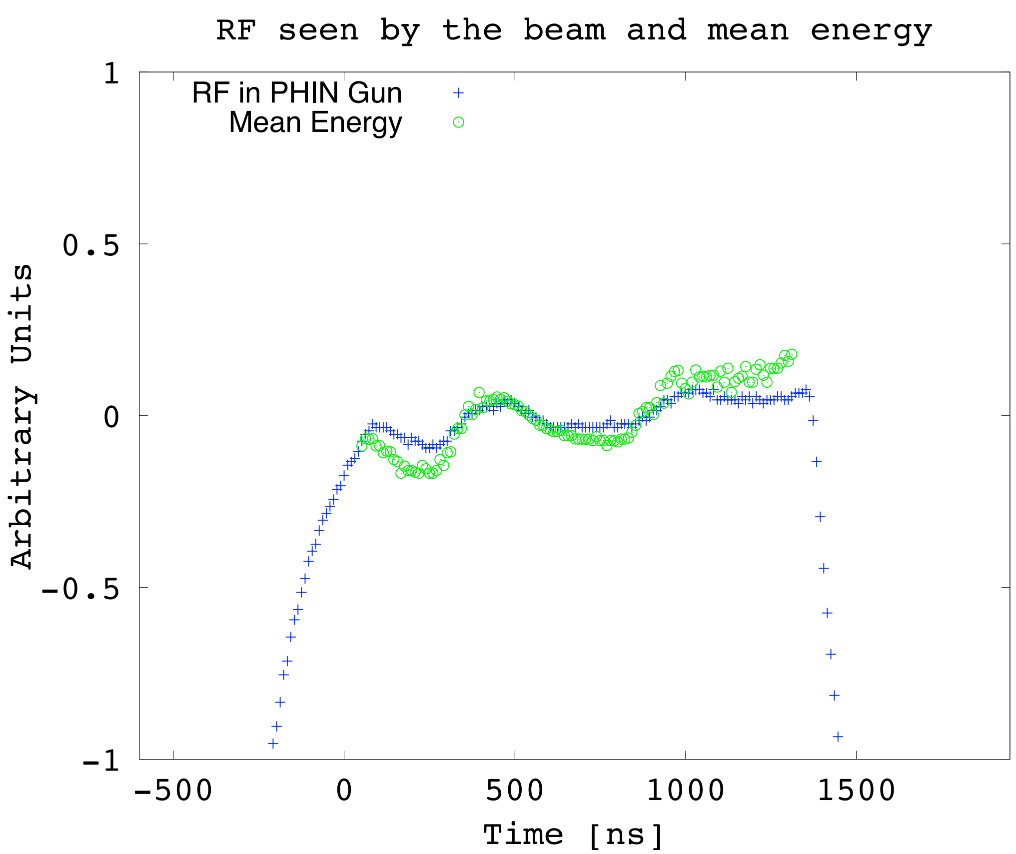

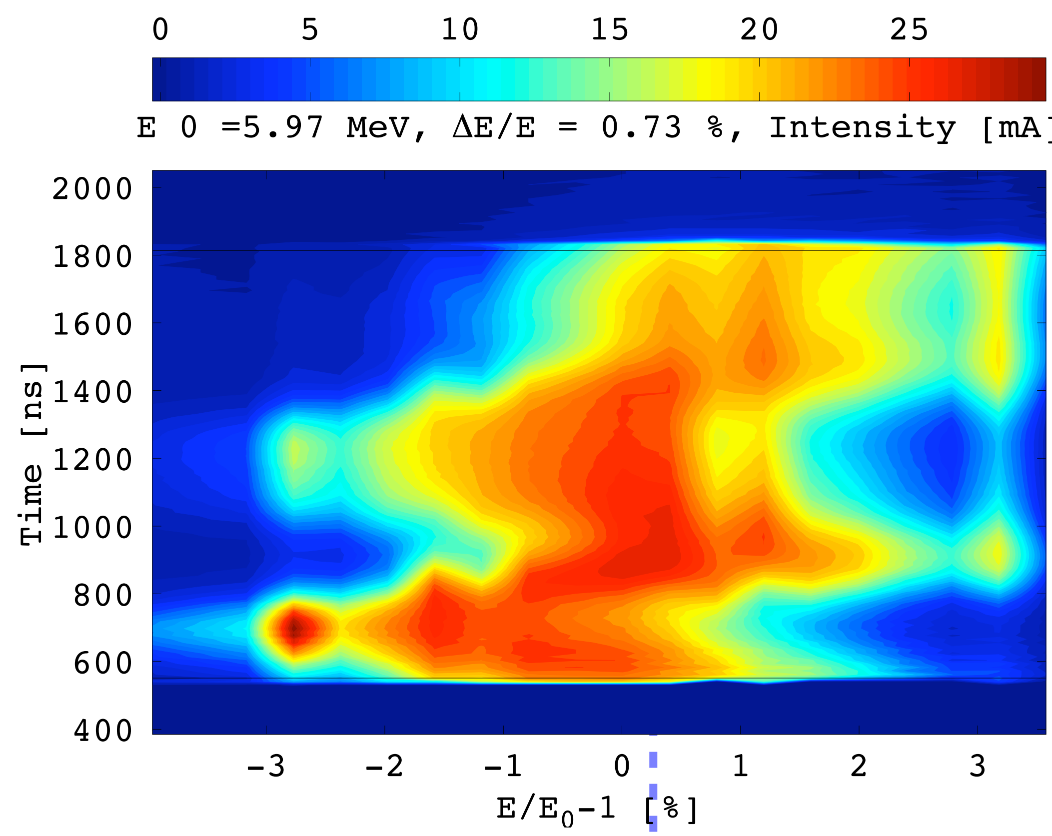

- Segmented dump measurements **also reveal the correlation between the beam and the RF pulse shape** which supports the time-resolved emittance and beam size measurements.
- The average energy spread along the pulse train has been characterized* as **0.7 (0.022)%**

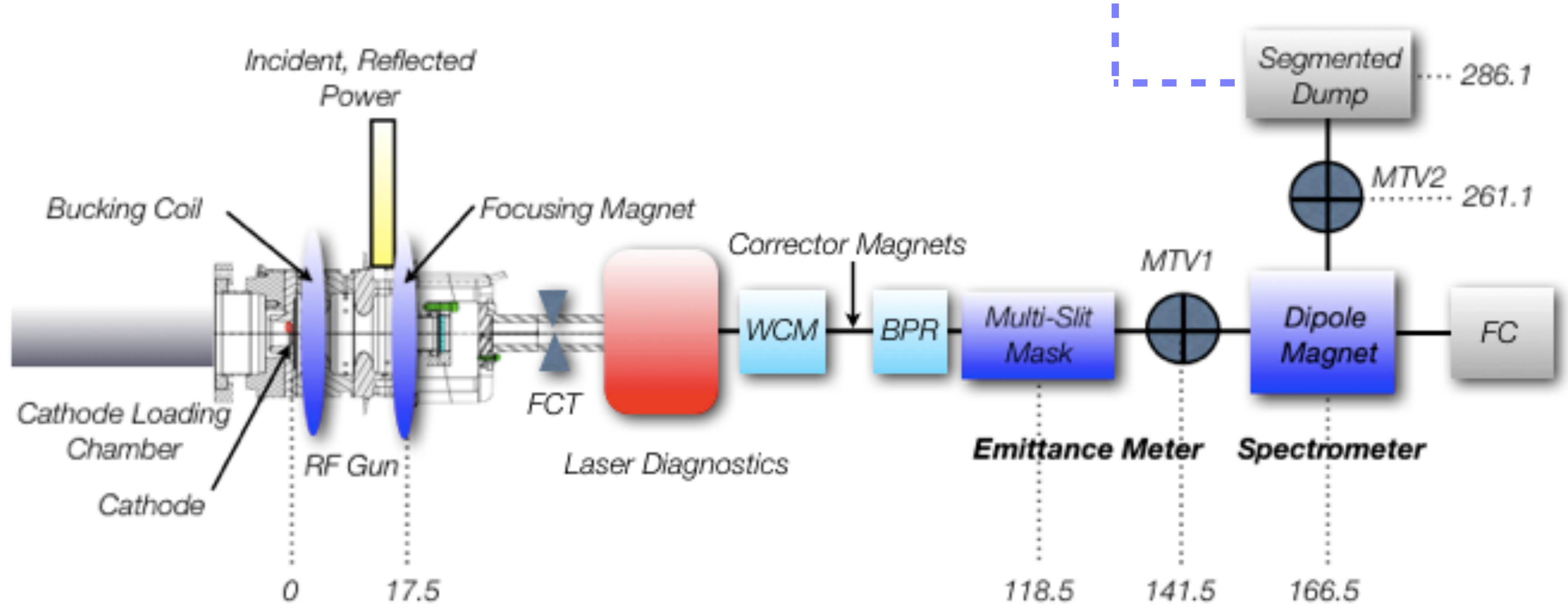

*Measurement has been done by Daniel Egger / EPFL.

Energy Measurements with a Magnetic Spectrometer

OTR Monitoring

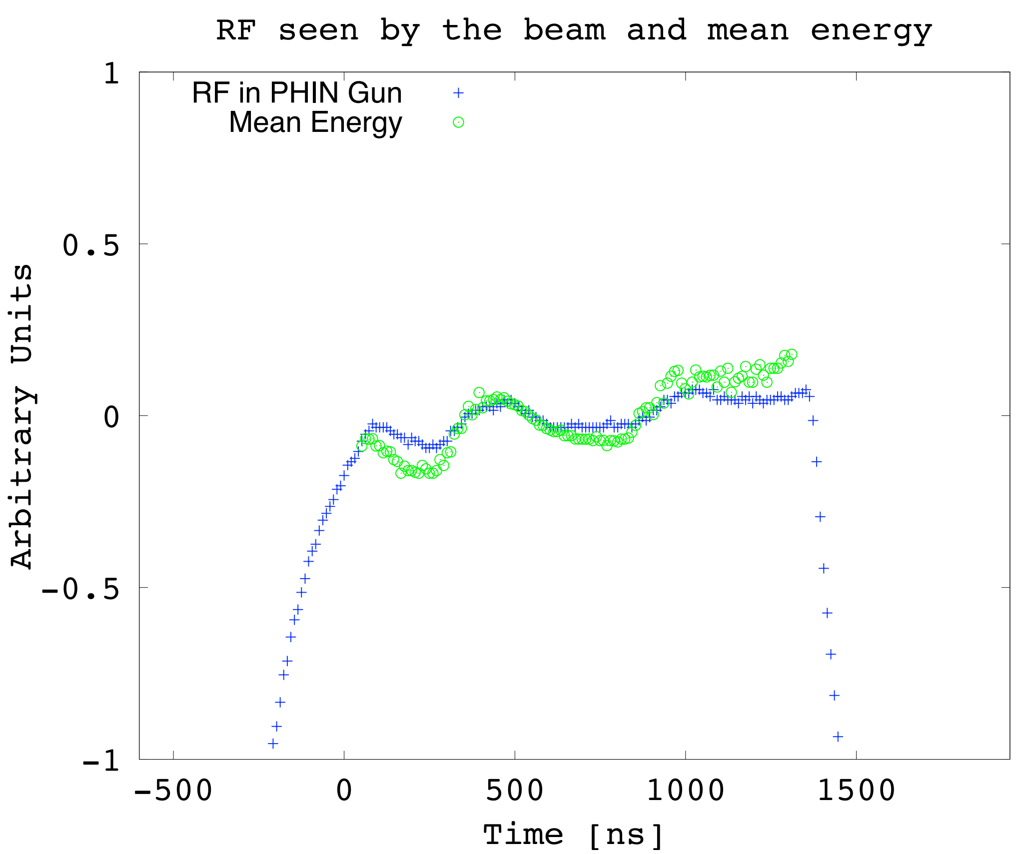

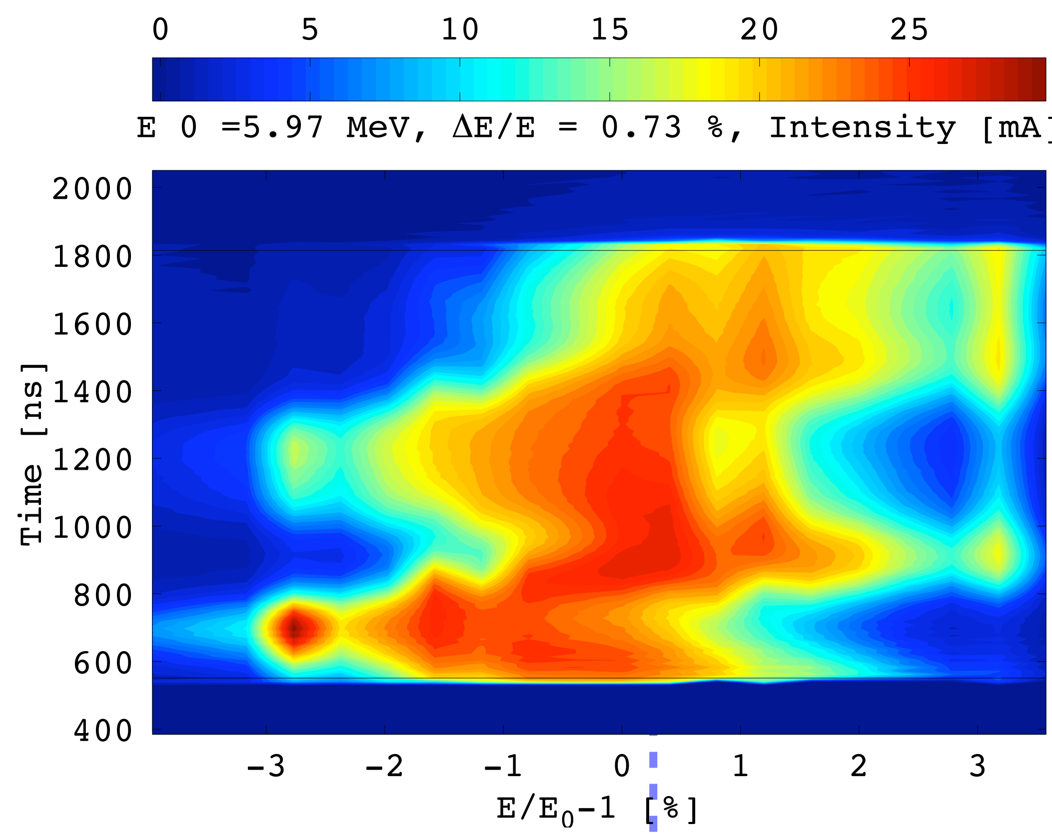

- Segmented dump measurements **also reveal the correlation between the beam and the RF pulse shape** which supports the time-resolved emittance and beam size measurements.
- The average energy spread along the pulse train has been characterized* as **0.7 (0.022)%**
- The result satisfies the PHIN specification for the energy spread.

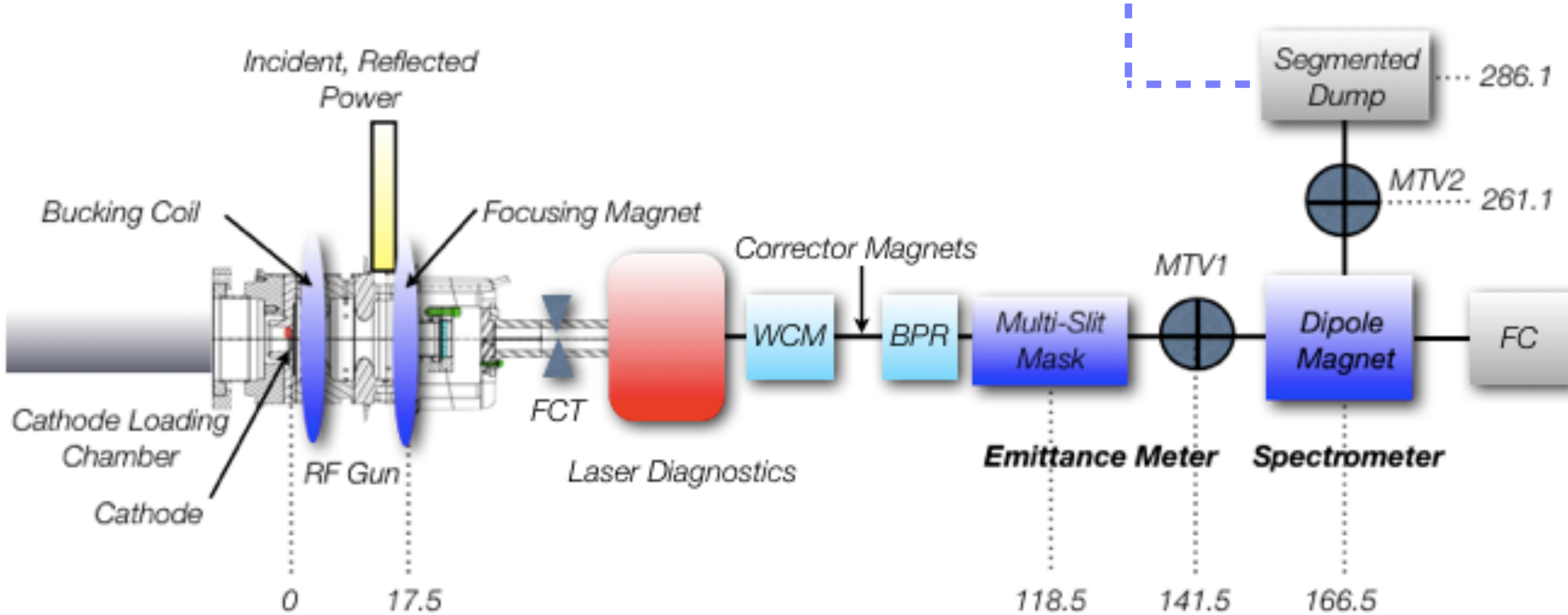

*Measurement has been done by Daniel Egger / EPFL.

- **Preface,** the original contribution in a deductive view of CLIC project
- **PHIN photoinjector,** objectives of the research
- **Beam instrumentation & characterization,** commissioning highlights of PHIN
- **Conclusions**

Parameter
RF
RF Gradient (MV/m)
RF Frequency (GHz)
Electron Beam
Charge per Bunch (nC)
Charge per Train (nC)
Train Length (ns)
Number of Bunches/Train
Current (A)
Normalized Emittance (mm mrad)
Energy (MeV)
Energy Spread (%)
Laser and Cathode
Charge Stability (%)
Cathode
Quantum Efficiency (%)
UV Laser Energy / Pulse (nJ)
Micropulse Repetition Rate (GHz)
Macropulse Repetition Rate (Hz)

Parameter	Specification
RF	
RF Gradient (MV/m)	85
RF Frequency (GHz)	2.99855
Electron Beam	
Charge per Bunch (nC)	2.33
Charge per Train (nC)	4446
Train Length (ns)	1273
Number of Bunches/Train	1908
Current (A)	3.5
Normalized Emittance (mm mrad)	<25
Energy (MeV)	5.5
Energy Spread (%)	≤1
Laser and Cathode	
Charge Stability (%)	<0.25
Cathode	Cs_2Te
Quantum Efficiency (%)	3
UV Laser Energy / Pulse (nJ)	370
Micropulse Repetition Rate (GHz)	1.5
Macropulse Repetition Rate (Hz)	1-5

Parameter	Specification	Achieved
RF		
RF Gradient (MV/m)	85	85
RF Frequency (GHz)	2.99855	2.99855
Electron Beam		
Charge per Bunch (nC)	2.33	4.4
Charge per Train (nC)	4446	5800
Train Length (ns)	1273	1300
Number of Bunches/Train	1908	1950
Current (A)	3.5	6.6
Normalized Emittance (mm mrad)	<25	14
Energy (MeV)	5.5	5.5
Energy Spread (%)	≤1	0.7
Laser and Cathode		
Charge Stability (%)	<0.25	0.8-2.4
Cathode	Cs_2Te	Cs_2Te
Quantum Efficiency (%)	3	18 (peak)
UV Laser Energy / Pulse (nJ)	370	400
Micropulse Repetition Rate (GHz)	1.5	1.5
Macropulse Repetition Rate (Hz)	1-5	1-5

Parameter	Specification	Achieved
RF		
RF Gradient (MV/m)	85	85
RF Frequency (GHz)	2.99855	2.99855
Electron Beam		
Charge per Bunch (nC)	2.33	4.4
Charge per Train (nC)	4446	5800
Train Length (ns)	1273	1300
Number of Bunches/Train	1908	1950
Current (A)	3.5	6.6
Normalized Emittance (mm mrad)	<25	14
Energy (MeV)	5.5	5.5
Energy Spread (%)	≤1	0.7
Laser and Cathode		
Charge Stability (%)	<0.25	0.8-2.4
Cathode	Cs_2Te	Cs_2Te
Quantum Efficiency (%)	3	18 (peak)
UV Laser Energy / Pulse (nJ)	370	400
Micropulse Repetition Rate (GHz)	1.5	1.5
Macropulse Repetition Rate (Hz)	1-5	1-5

- All the specifications have been **fulfilled** during the commissioning (except the charge stability)

Parameter	Specification	Achieved
RF		
RF Gradient (MV/m)	85	85
RF Frequency (GHz)	2.99855	2.99855
Electron Beam		
Charge per Bunch (nC)	2.33	4.4
Charge per Train (nC)	4446	5800
Train Length (ns)	1273	1300
Number of Bunches/Train	1908	1950
Current (A)	3.5	6.6
Normalized Emittance (mm mrad)	<25	14
Energy (MeV)	5.5	5.5
Energy Spread (%)	≤1	0.7
Laser and Cathode		
Charge Stability (%)	<0.25	0.8-2.4
Cathode	Cs_2Te	Cs_2Te
Quantum Efficiency (%)	3	18 (peak)
UV Laser Energy / Pulse (nJ)	370	400
Micropulse Repetition Rate (GHz)	1.5	1.5
Macropulse Repetition Rate (Hz)	1-5	1-5

- All the specifications have been **fulfilled** during the commissioning (except the charge stability)
- A **feedback stabilization** system is planned to be built for the laser intensity stability in order to improve the charge stability.

Parameter	Specification	Achieved
RF		
RF Gradient (MV/m)	85	85
RF Frequency (GHz)	2.99855	2.99855
Electron Beam		
Charge per Bunch (nC)	2.33	4.4
Charge per Train (nC)	4446	5800
Train Length (ns)	1273	1300
Number of Bunches/Train	1908	1950
Current (A)	3.5	6.6
Normalized Emittance (mm mrad)	<25	14
Energy (MeV)	5.5	5.5
Energy Spread (%)	≤1	0.7
Laser and Cathode		
Charge Stability (%)	<0.25	0.8-2.4
Cathode	Cs_2Te	Cs_2Te
Quantum Efficiency (%)	3	18 (peak)
UV Laser Energy / Pulse (nJ)	370	400
Micropulse Repetition Rate (GHz)	1.5	1.5
Macropulse Repetition Rate (Hz)	1-5	1-5

- All the specifications have been **fulfilled** during the commissioning (except the charge stability)
- A **feedback stabilization** system is planned to be built for the laser intensity stability in order to improve the charge stability.
- **Correlation** between the electron beam, the laser and the RF pulse shape has been understood via the measurements along the pulse train.

Parameter	Specification	Achieved
RF		
RF Gradient (MV/m)	85	85
RF Frequency (GHz)	2.99855	2.99855
Electron Beam		
Charge per Bunch (nC)	2.33	4.4
Charge per Train (nC)	4446	5800
Train Length (ns)	1273	1300
Number of Bunches/Train	1908	1950
Current (A)	3.5	6.6
Normalized Emittance (mm mrad)	<25	14
Energy (MeV)	5.5	5.5
Energy Spread (%)	≤1	0.7
Laser and Cathode		
Charge Stability (%)	<0.25	0.8-2.4
Cathode	Cs_2Te	Cs_2Te
Quantum Efficiency (%)	3	18 (peak)
UV Laser Energy / Pulse (nJ)	370	400
Micropulse Repetition Rate (GHz)	1.5	1.5
Macropulse Repetition Rate (Hz)	1-5	1-5

- All the specifications have been **fulfilled** during the commissioning (except the charge stability)
- A **feedback stabilization** system is planned to be built for the laser intensity stability in order to improve the charge stability.
- **Correlation** between the electron beam, the laser and the RF pulse shape has been understood via the measurements along the pulse train.
- All measurement results can be **reproduced successfully by the single bunch PARMELA simulations**.

- The aim of the research program is to **demonstrate the feasibility of a photoinjector** first as the CTF3 gun and further for the future CLIC drive beam source,

- The aim of the research program is to **demonstrate the feasibility of a photoinjector** first as the CTF3 gun and further for the future CLIC drive beam source,
- The stability of the beam properties have been characterized for **exceptionally long pulse train of 1.2 μs**,

- The aim of the research program is to **demonstrate the feasibility of a photoinjector** first as the CTF3 gun and further for the future CLIC drive beam source,
- The stability of the beam properties have been characterized for **exceptionally long pulse train of 1.2 μs**,
- It has been demonstrated that a photoinjector,

- The aim of the research program is to **demonstrate the feasibility of a photoinjector** first as the CTF3 gun and further for the future CLIC drive beam source,
- The stability of the beam properties have been characterized for **exceptionally long pulse train of 1.2 µs**,
- It has been demonstrated that a photoinjector,
  - is **feasible** to be a replacement for the CTF3 thermionic gun

- The aim of the research program is to **demonstrate the feasibility of a photoinjector** first as the CTF3 gun and further for the future CLIC drive beam source,
- The stability of the beam properties have been characterized for **exceptionally long pulse train of 1.2 μs**,
- It has been demonstrated that a photoinjector,
  - is **feasible** to be a replacement for the CTF3 thermionic gun
  - can **provide the specifications** required by CTF3

- The aim of the research program is to **demonstrate the feasibility of a photoinjector** first as the CTF3 gun and further for the future CLIC drive beam source,
- The stability of the beam properties have been characterized for **exceptionally long pulse train of 1.2 μs**,
- It has been demonstrated that a photoinjector,
  - is **feasible** to be a replacement for the CTF3 thermionic gun
  - can **provide the specifications** required by CTF3
  - generates **no parasitic charge** (satellites), therefore solves the current problem of CTF3 injector.

- The aim of the research program is to **demonstrate the feasibility of a photoinjector** first as the CTF3 gun and further for the future CLIC drive beam source,
- The stability of the beam properties have been characterized for **exceptionally long pulse train of 1.2 μs**,
- It has been demonstrated that a photoinjector,
  - is **feasible** to be a replacement for the CTF3 thermionic gun
  - can **provide the specifications** required by CTF3
  - generates **no parasitic charge** (satellites), therefore solves the current problem of CTF3 injector.

as a consequence:

- The aim of the research program is to **demonstrate the feasibility of a photoinjector** first as the CTF3 gun and further for the future CLIC drive beam source,
- The stability of the beam properties have been characterized for **exceptionally long pulse train of 1.2 μs**,
- It has been demonstrated that a photoinjector,
    - is **feasible** to be a replacement for the CTF3 thermionic gun
    - can **provide the specifications** required by CTF3
    - generates **no parasitic charge** (satellites), therefore solves the current problem of CTF3 injector.

as a consequence:

- The conceptual study of a 1 GHz **RF gun with the CLIC-DB specifications** has been initiated,
- The **preliminary beam dynamics simulations** have been performed
- The **results have been compared** with the ongoing CLIC-CDR baseline thermionic injector studies for CLIC DB,
- The photoinjector option has been emphasized as a **DB source candidate**.

- Systematic error analysis for the multi slit emittance measurement.

- Systematic error analysis for the multi slit emittance measurement.
- Correlation between the laser and the electron beam in terms of the beam position and the intensity.

- Systematic error analysis for the multi slit emittance measurement.
- Correlation between the laser and the electron beam in terms of the beam position and the intensity.
- An example approach on how to optimize the key parameters of a photoinjector.

- Systematic error analysis for the multi slit emittance measurement.
- Correlation between the laser and the electron beam in terms of the beam position and the intensity.
- An example approach on how to optimize the key parameters of a photoinjector.
- Beam loading compensation for the PHIN operation.

- Systematic error analysis for the multi slit emittance measurement.
- Correlation between the laser and the electron beam in terms of the beam position and the intensity.
- An example approach on how to optimize the key parameters of a photoinjector.
- Beam loading compensation for the PHIN operation.
- Background sources for the OTR monitoring systems and the possible cure.

- Systematic error analysis for the multi slit emittance measurement.
- Correlation between the laser and the electron beam in terms of the beam position and the intensity.
- An example approach on how to optimize the key parameters of a photoinjector.
- Beam loading compensation for the PHIN operation.
- Background sources for the OTR monitoring systems and the possible cure.
- A general remark on the beam emittance regardless of the type of the injector.

Thank you very much for your attention.

BACK-UP SLIDES

Emittance, Systematic Measurement Errors

Emittance, Systematic Measurement Errors

- Width of the slits,
- Distance between the screen and the mask,
- Shot-to-shot intensity stability of the beam,

Emittance, Systematic Measurement Errors

- Width of the slits,
- Distance between the screen and the mask,
- Shot-to-shot intensity stability of the beam,

Parameters	Value
Error on the mean position, σ_x (mm)	0.01
Error on the divergence, $\sigma_{x'}$ (mrad)	0.4
Error on the beamlet intensities, σ_ρ (a.u.)	0.04 x ρ_i

Emittance, Systematic Measurement Errors

- Width of the slits,
- Distance between the screen and the mask,
- Shot-to-shot intensity stability of the beam,

Parameters	Value
Error on the mean position, σ_x (mm)	0.01
Error on the divergence, $\sigma_{x'}$ (mrad)	0.4
Error on the beamlet intensities, σ_ρ (a.u.)	0.04 x ρ_i

$$\sigma_\epsilon^2 = \frac{(\rho_j x_j'^2)^2(4\rho_i^2 x_i^2 \sigma_{x_i}^2 + x_i^4 \sigma_{\rho_i}^2)}{4\epsilon^2(\sum_{i=1}^N \rho_i)^4}$$

$$+\frac{(\rho_j x_j^2)^2(4\rho_i^2 x_i'^2 \sigma_{x_i'}^2 + x_i'^4 \sigma_{\rho_i}^2)}{4\epsilon^2(\sum_{i=1}^N \rho_i)^4}$$

$$+\frac{(\rho_i^2 x_i'^2 \sigma_{x_i}^2 + \rho_i^2 x_i^2 \sigma_{x_i'}^2 + x_i^2 x_i'^2 \sigma_{\rho_i}^2)(\rho_i x_i x_i')^2}{\epsilon^2(\sum_{i=1}^N \rho_i)^4}$$

$$-\frac{2(\sum_{i=1}^N \rho_i x_i^2)(\sum_{j=1}^N \rho_j x_j'^2)(\sum_{i=1}^N \rho_i x_i x_i')^2(\sum_{i=1}^N \sigma_{\rho_i}^2)}{\epsilon^2(\sum_{i=1}^N \rho_i)^6}$$

$$+\frac{\epsilon^2(\sum_{i=1}^N \sigma_{\rho_i}^2)}{(\sum_{i=1}^N \rho_i)^6}$$

Emittance, Systematic Measurement Errors

- Width of the slits,
- Distance between the screen and the mask,
- Shot-to-shot intensity stability of the beam,

Parameters	Value
Error on the mean position, σ_x (mm)	0.01
Error on the divergence, $\sigma_{x'}$ (mrad)	0.4
Error on the beamlet intensities, σ_ρ (a.u.)	0.04 x ρ_i

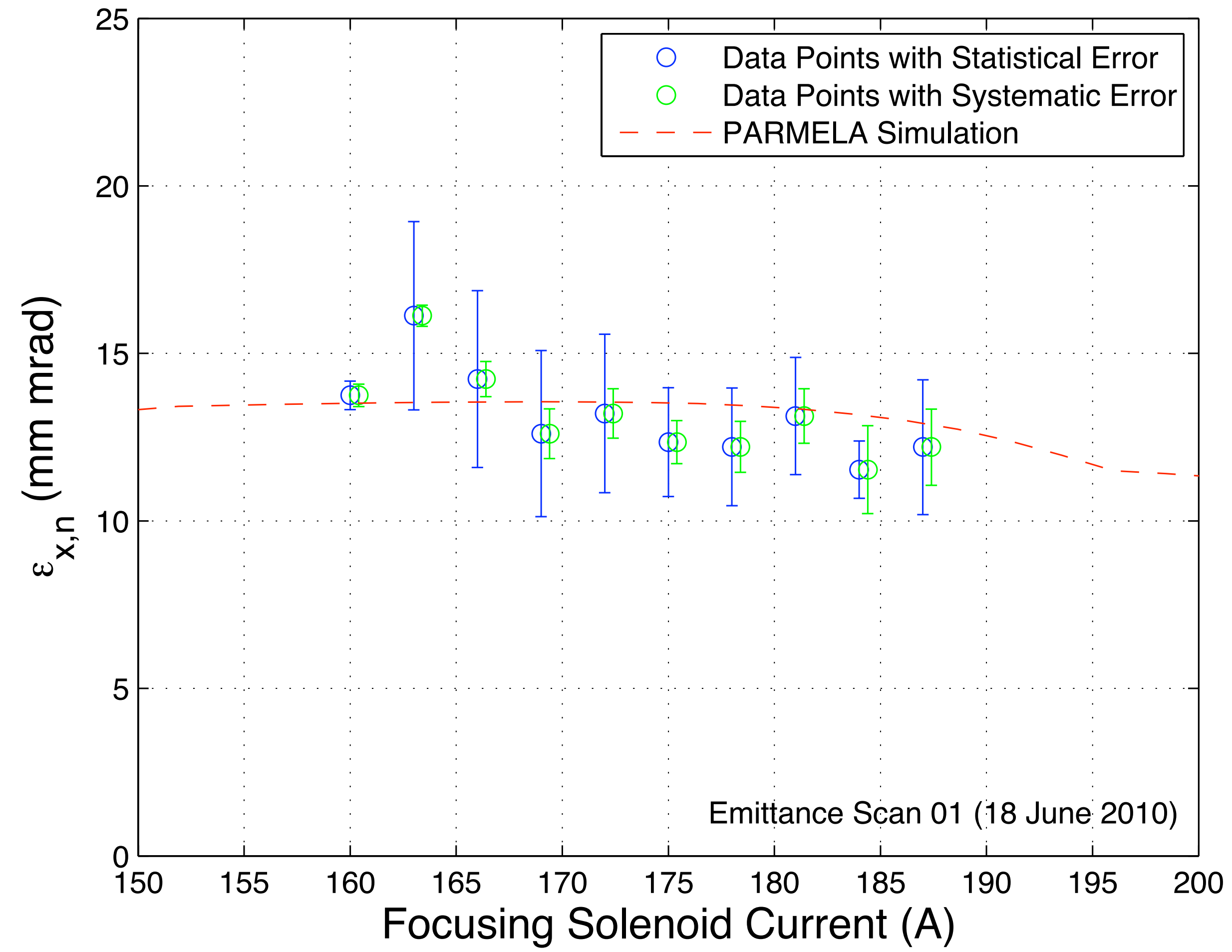

Emittance, Systematic Measurement Errors

- Width of the slits,
- Distance between the screen and the mask,
- Shot-to-shot intensity stability of the beam,

Parameters	Value
Error on the mean position, σ_x (mm)	0.01
Error on the divergence, $\sigma_{x'}$ (mrad)	0.4
Error on the beamlet intensities, σ_ρ (a.u.)	0.04 x ρ_i

- The statistical and the systematic errors are comparable for the PHIN beam emittance measurements.

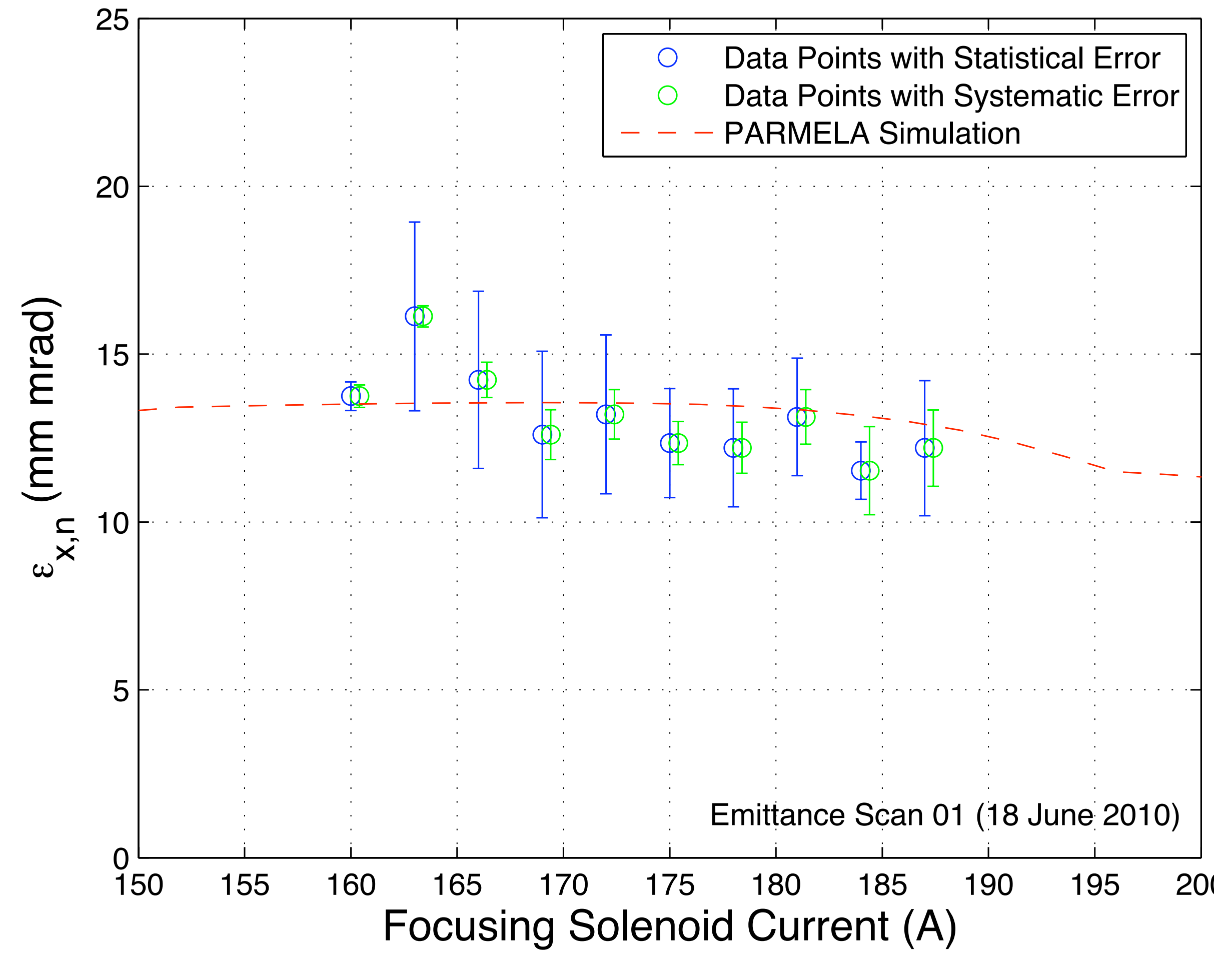

Emittance, Systematic Measurement Errors

- Width of the slits,
- Distance between the screen and the mask,
- Shot-to-shot intensity stability of the beam,

Parameters	Value
Error on the mean position, σ_x (mm)	0.01
Error on the divergence, $\sigma_{x'}$ (mrad)	0.4
Error on the beamlet intensities, σ_ρ (a.u.)	0.04 x ρ_i

- The statistical and the systematic errors are comparable for the PHIN beam emittance measurements.
- For the given particular example, the systematic error of the measurement is less than the statistical error.

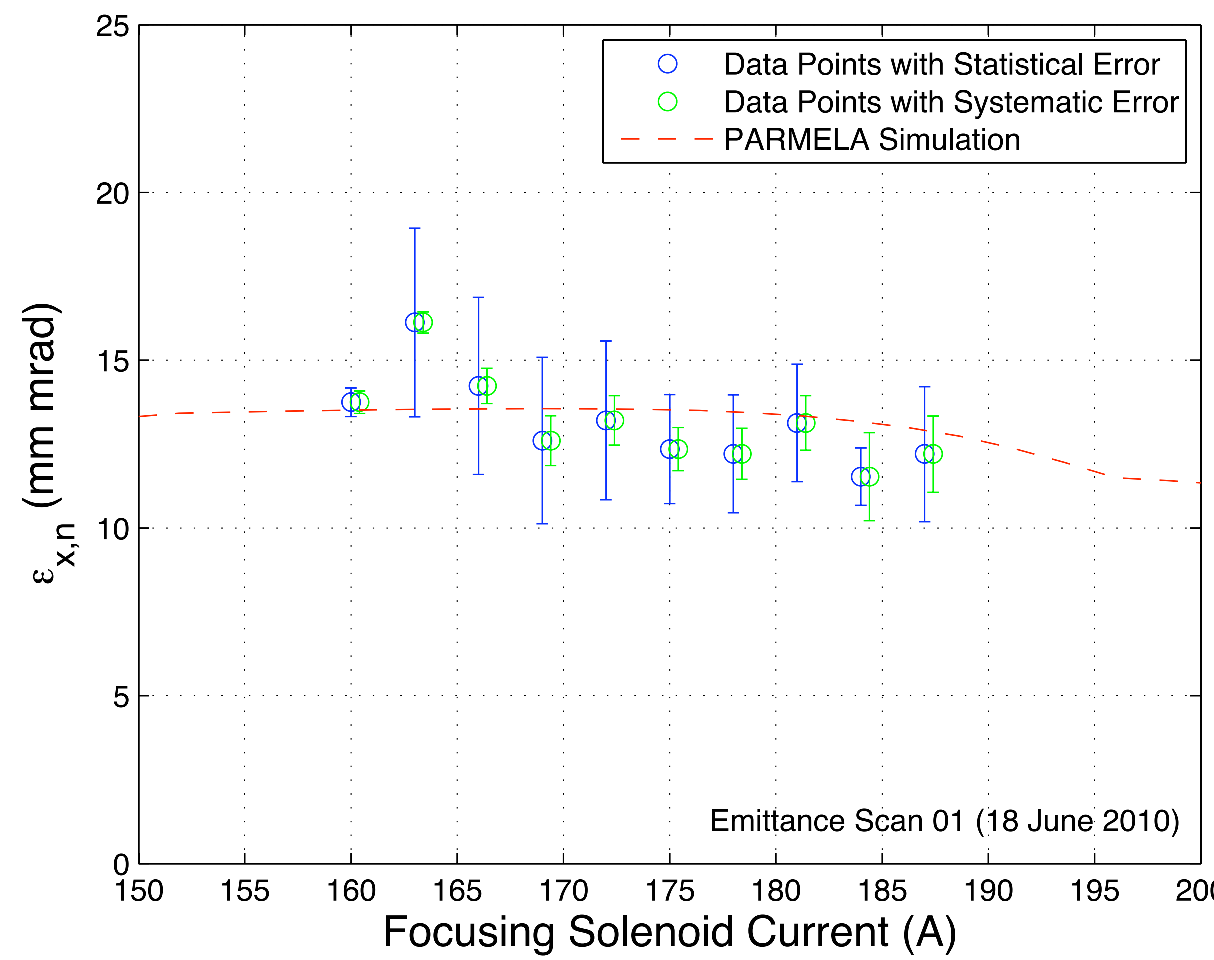

Emittance, Systematic Measurement Errors

- Width of the slits,
- Distance between the screen and the mask,
- Shot-to-shot intensity stability of the beam,

Parameters	Value
Error on the mean position, σ_x (mm)	0.01
Error on the divergence, $\sigma_{x'}$ (mrad)	0.4
Error on the beamlet intensities, σ_ρ (a.u.)	0.04 x ρ_i

- The statistical and the systematic errors are comparable for the PHIN beam emittance measurements.
- For the given particular example, the systematic error of the measurement is less than the statistical error.
- No limitations due to the measurement system

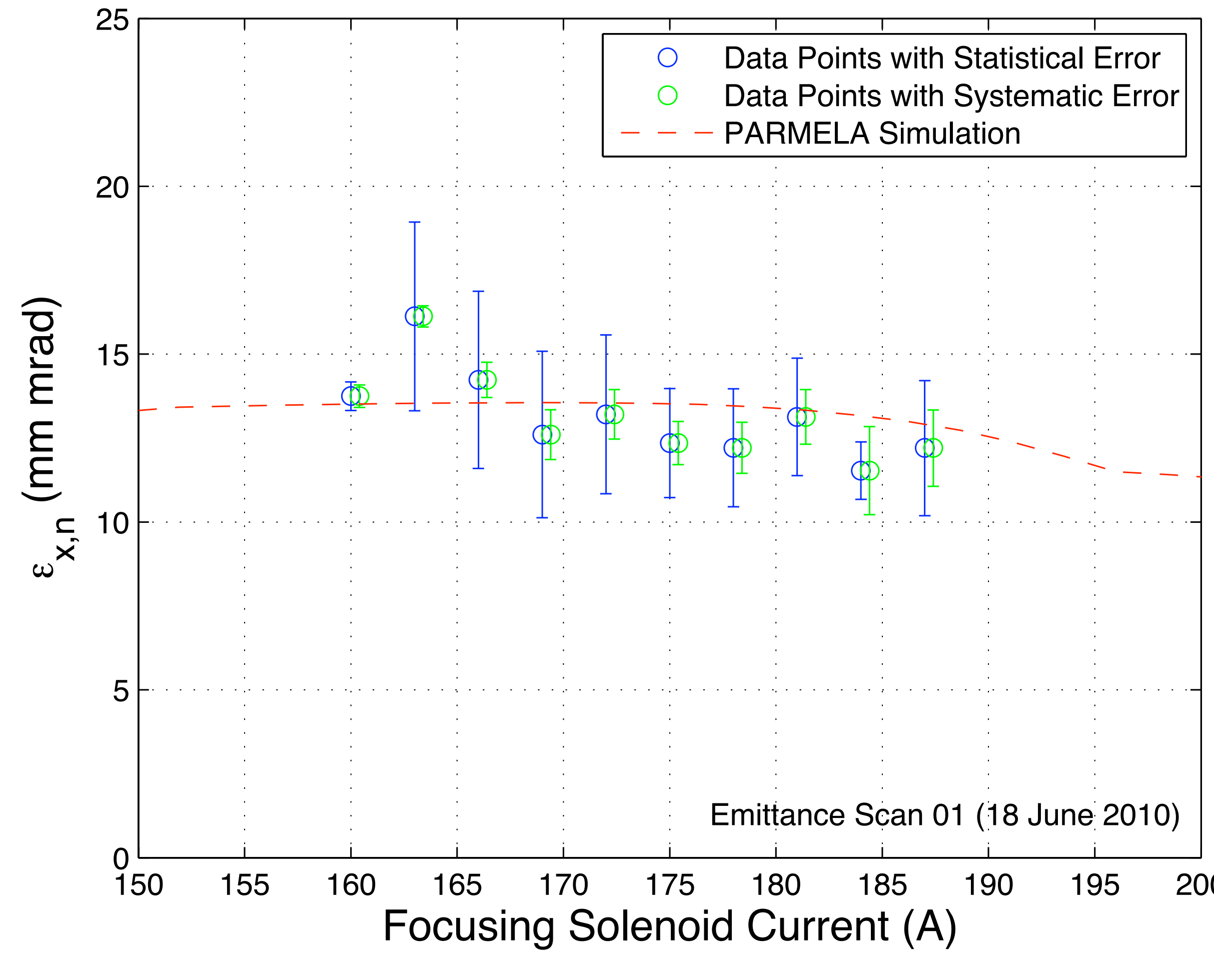

Emittance, Systematic Measurement Errors

- Width of the slits,
- Distance between the screen and the mask,
- Shot-to-shot intensity stability of the beam,

Parameters	**Value**
Error on the mean position, σ_x (mm)	0.01
Error on the divergence, $\sigma_{x'}$ (mrad)	0.4
Error on the beamlet intensities, σ_ρ (a.u.)	0.04 x ρ_i

- The statistical and the systematic errors are comparable for the PHIN beam emittance measurements.
- For the given particular example, the systematic error of the measurement is less than the statistical error.
- No limitations due to the measurement system
- Statistical errors reflect the shot-to-shot stability

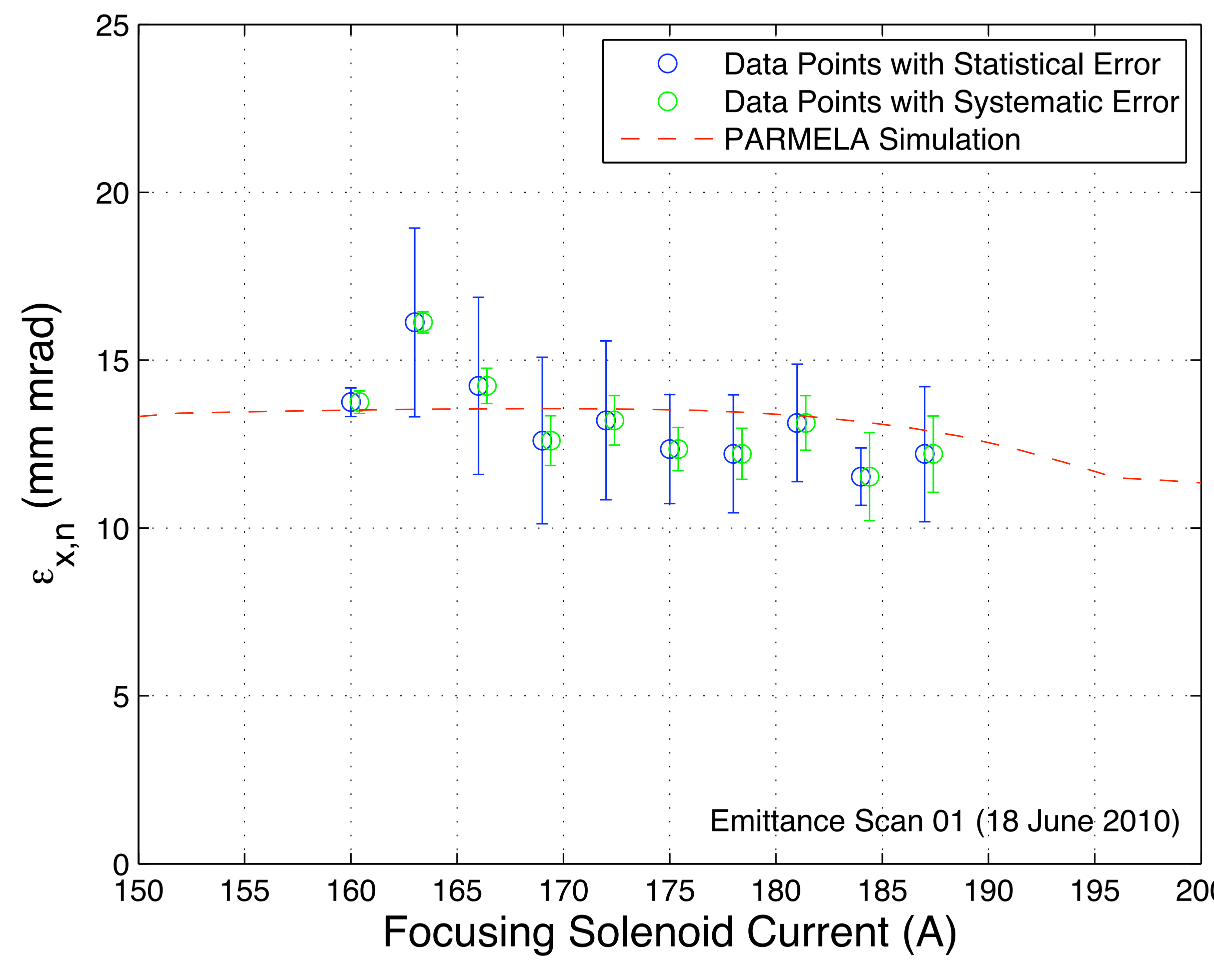

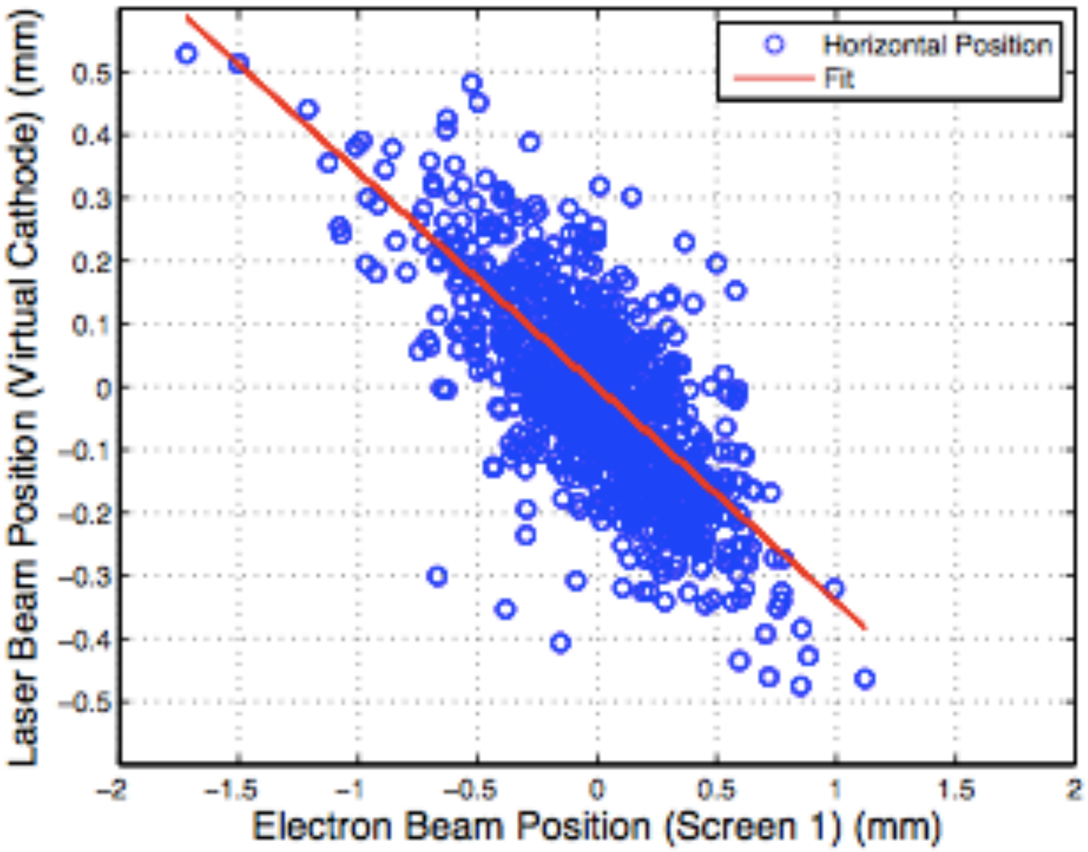
Horizontal Position
Fit
Laser Beam Position (Virtual Cathode) (mm)
Electron Beam Position (Screen 1) (mm)

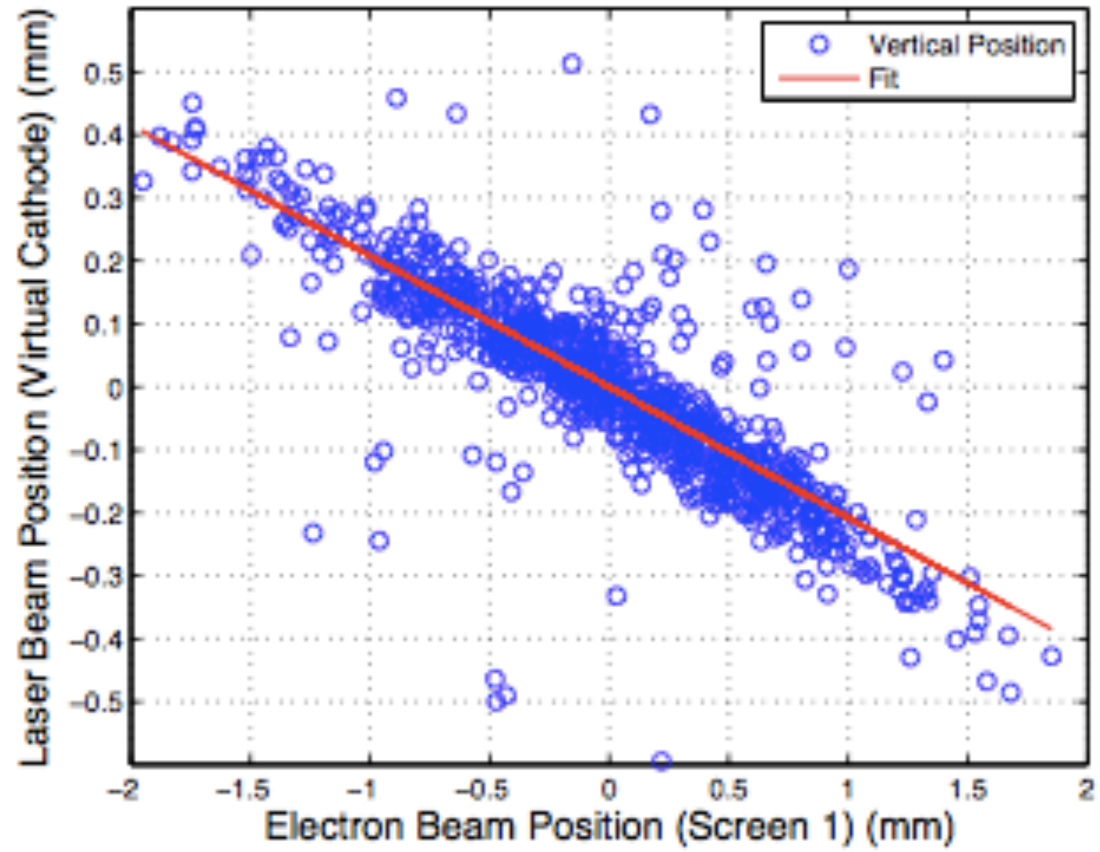
Vertical Position
Fit
Laser Beam Position (Virtual Cathode) (mm)
Electron Beam Position (Screen 1) (mm)

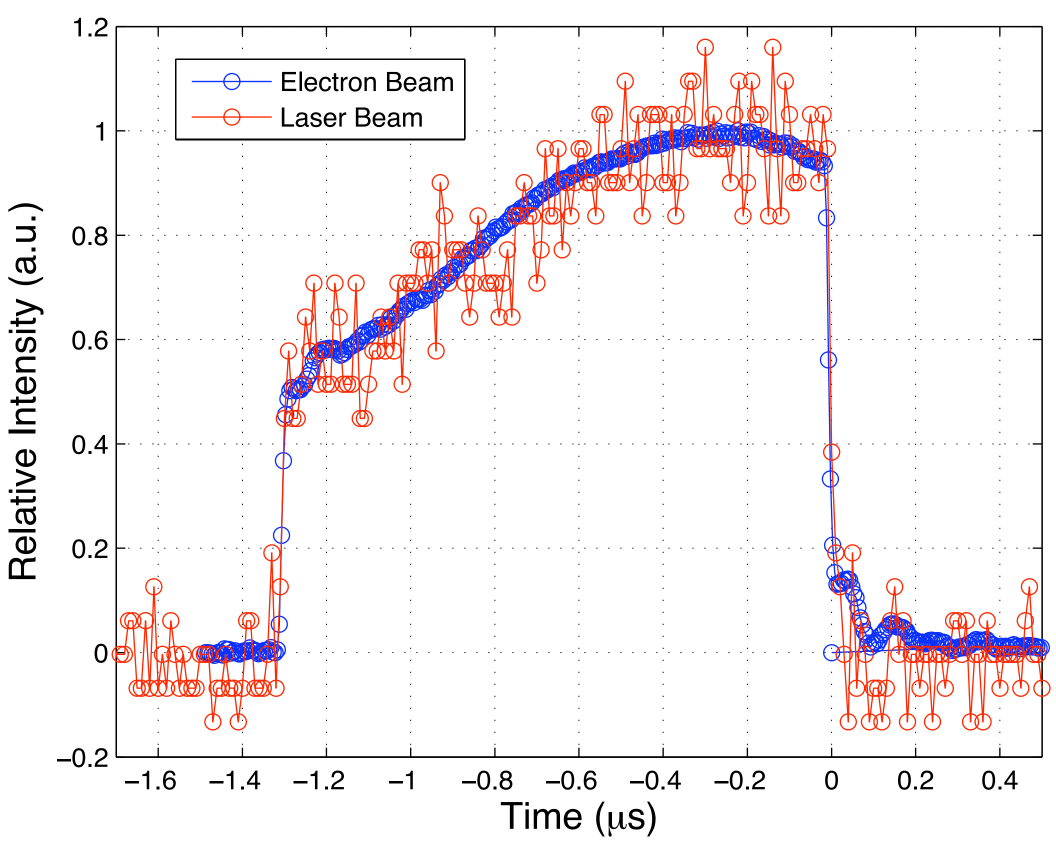
Electron Beam
Laser Beam
Relative Intensity (a.u.)
Time (μs)

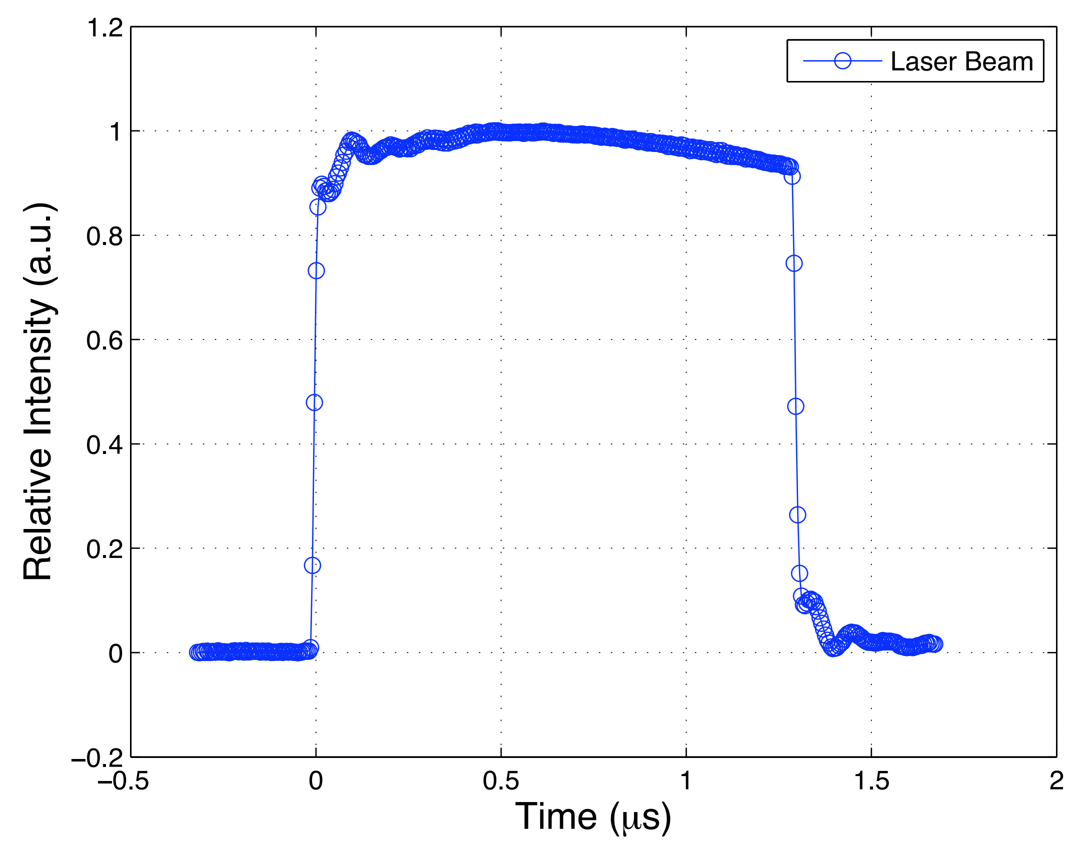
Laser Beam
Relative Intensity (a.u.)
Time (μs)

A practical model for the optimization studies, C. Travier's Model

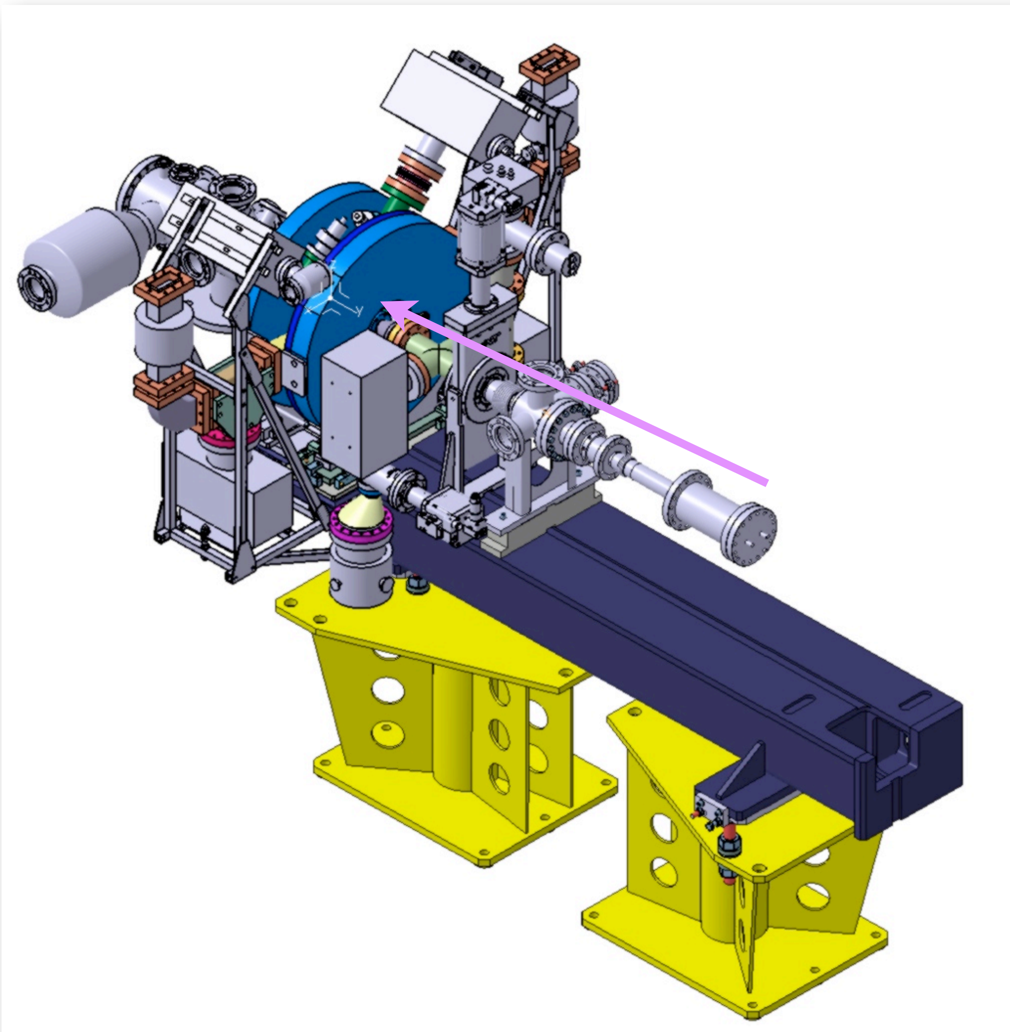

A practical model for the optimization studies, C. Travier's Model

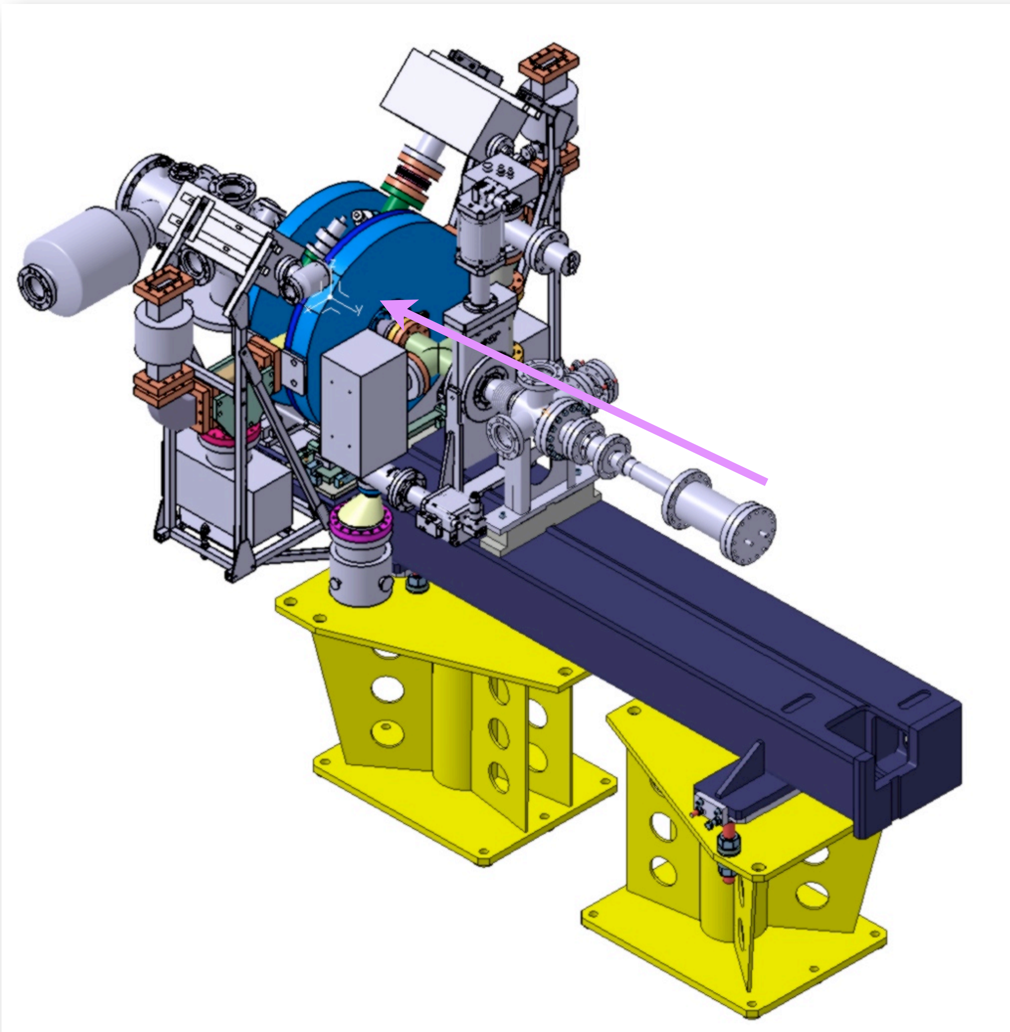

- **Production of the specified charge value, transmission,**

A practical model for the optimization studies, C. Travier's Model

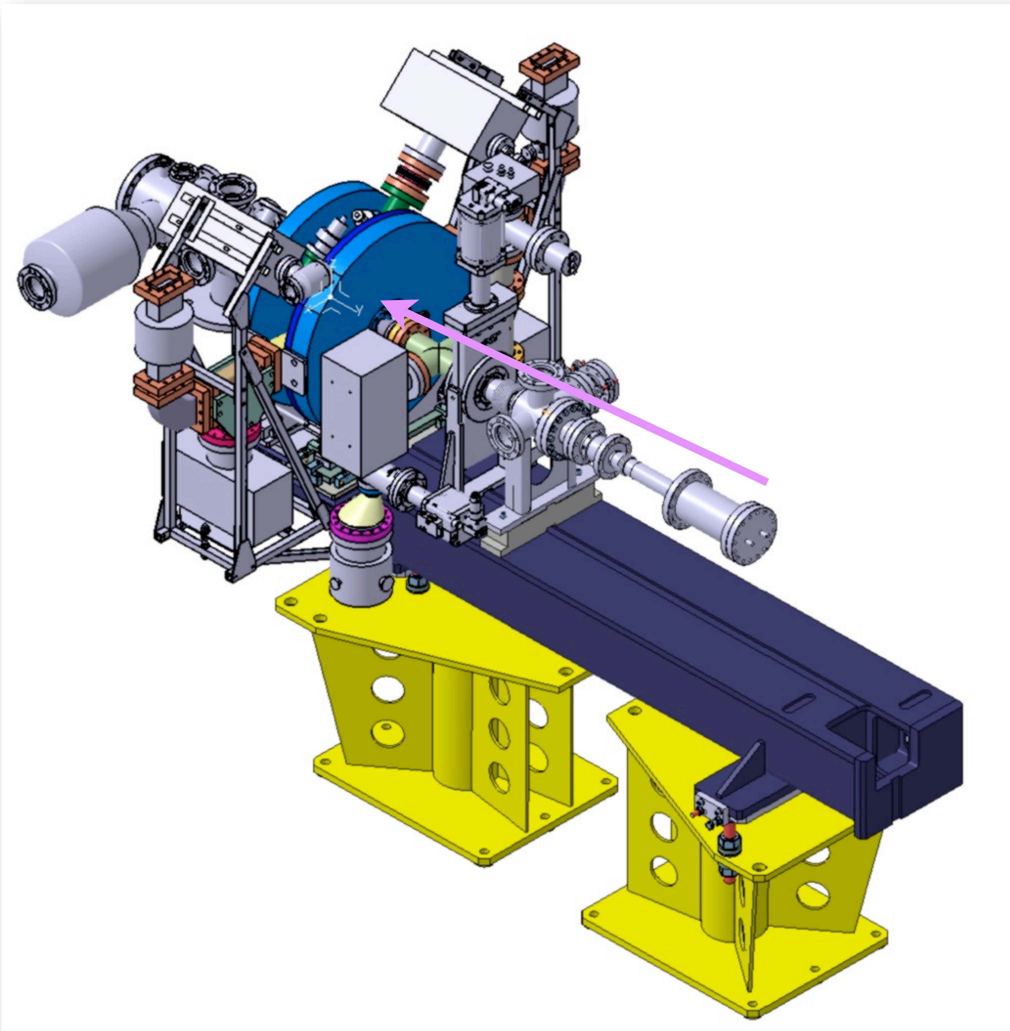

- **Production of the specified charge value, transmission,**
  - The nominal laser spot size,
  - Maximum achievable gradient,
  - The emission phase of the particles with respect to the RF field,

A practical model for the optimization studies, C. Travier's Model

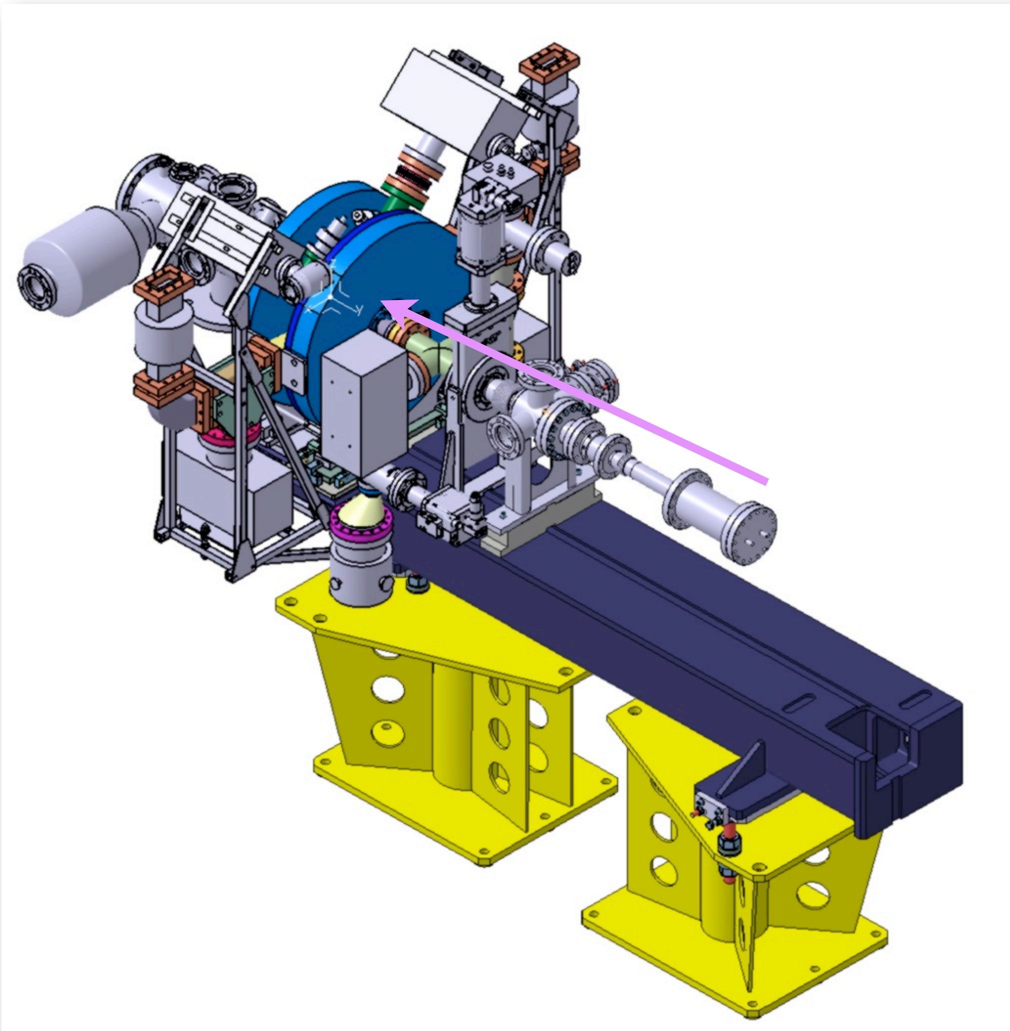

- **Production of the specified charge value, transmission,**
  - The nominal laser spot size,
  - Maximum achievable gradient,
  - The emission phase of the particles with respect to the RF field,
- **Compromise between minimum emittance and minimum energy spread,**

A practical model for the optimization studies, C. Travier's Model

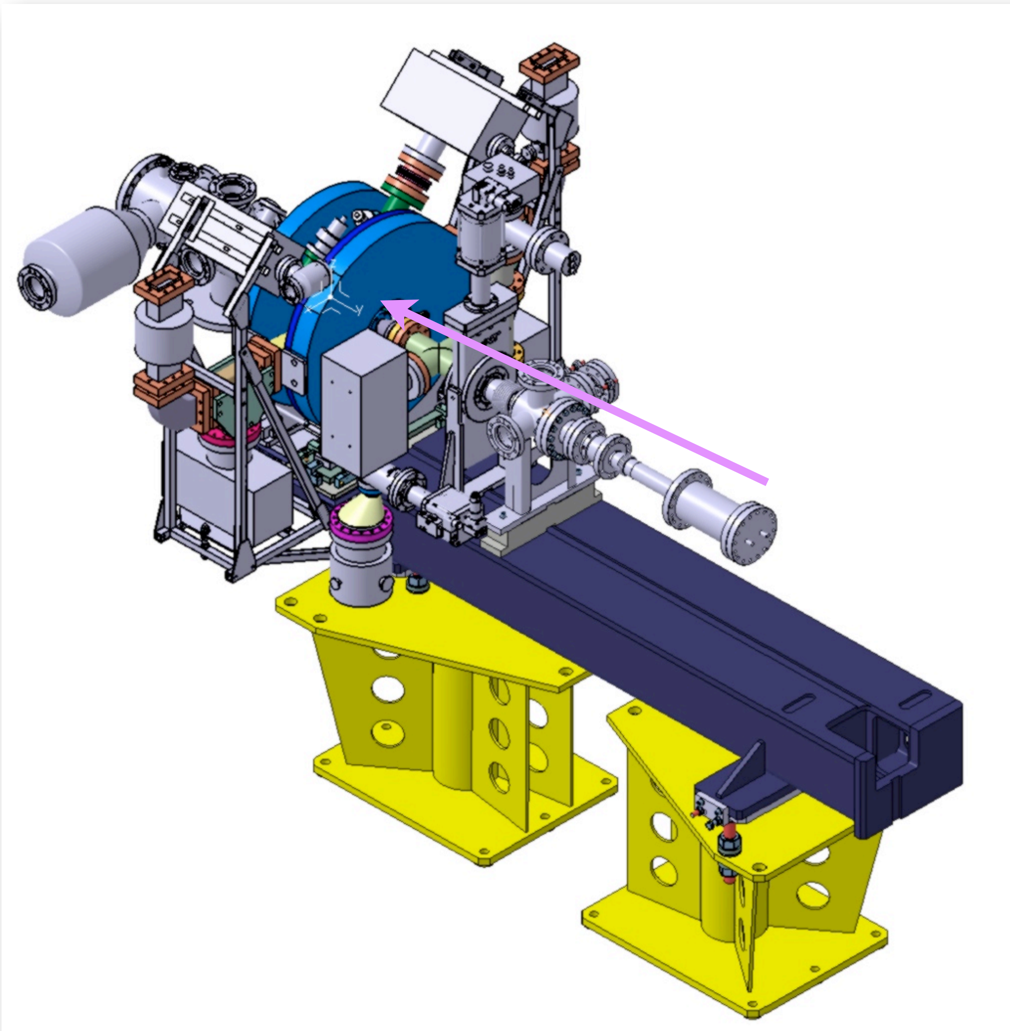

- **Production of the specified charge value, transmission,**
  - The nominal laser spot size,
  - Maximum achievable gradient,
  - The emission phase of the particles with respect to the RF field,
- **Compromise between minimum emittance and minimum energy spread,**
  - The proper beam focusing for the emittance compensation,

A practical model for the optimization studies, C. Travier's Model

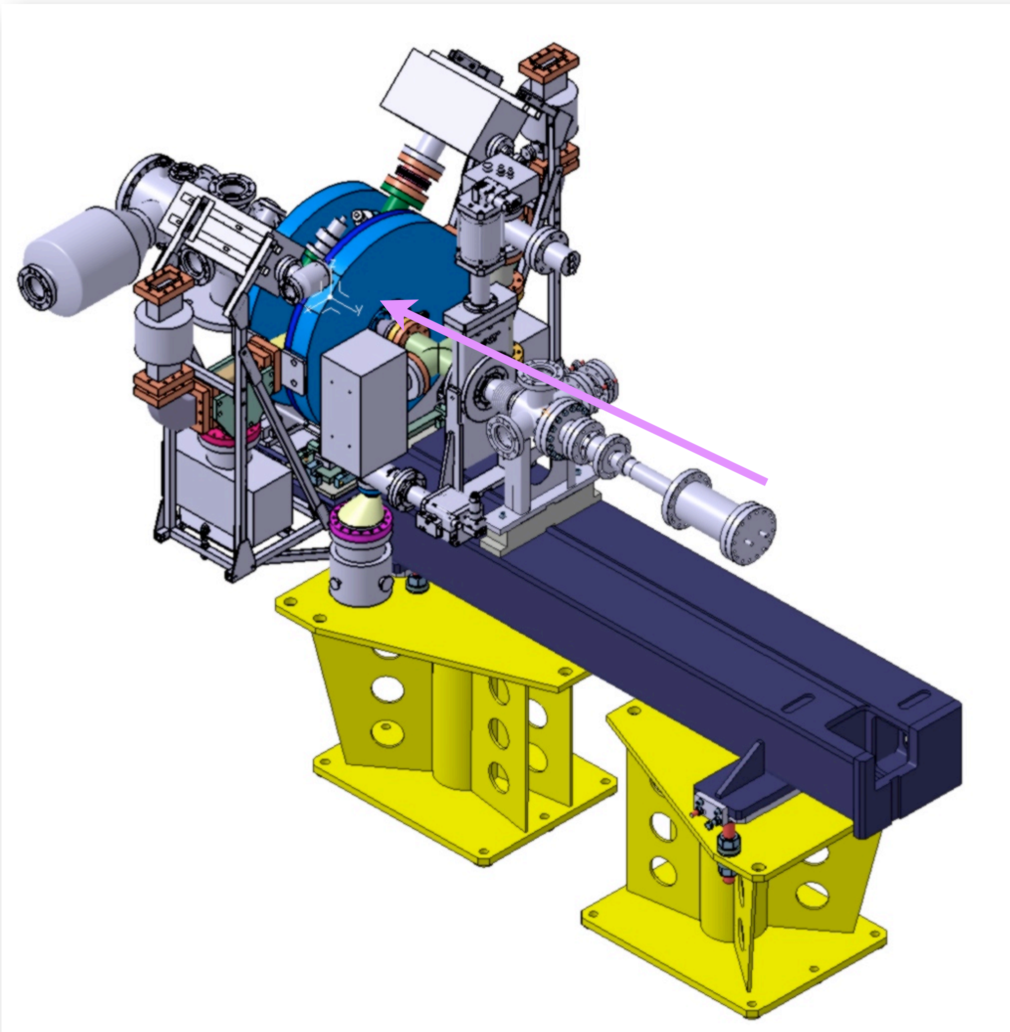

- **Production of the specified charge value, transmission,**
  - The nominal laser spot size,
  - Maximum achievable gradient,
  - The emission phase of the particles with respect to the RF field,
- **Compromise between minimum emittance and minimum energy spread,**
  - The proper beam focusing for the emittance compensation,
- **Eventually, determination of a working point for a particular set of specifications.**

Beam Loading Compensation

The beam loading compensation is studied and optimized for the PHIN photoinjector by adjusting the timing of the beam versus the RF pulse.

Beam Loading Compensation

The beam loading compensation is studied and optimized for the PHIN photoinjector by adjusting the timing of the beam versus the RF pulse.

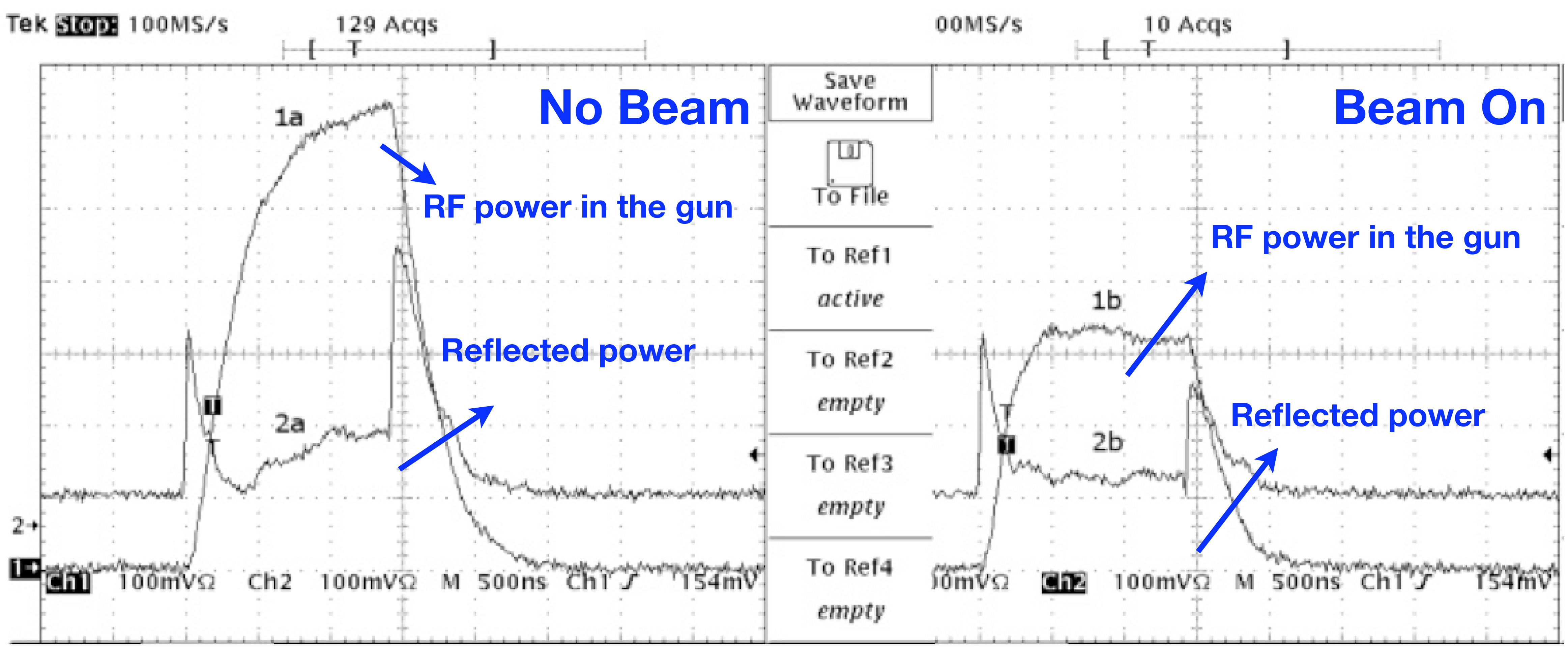

Beam Loading Compensation

The beam loading compensation is studied and optimized for the PHIN photoinjector by adjusting the timing of the beam versus the RF pulse.

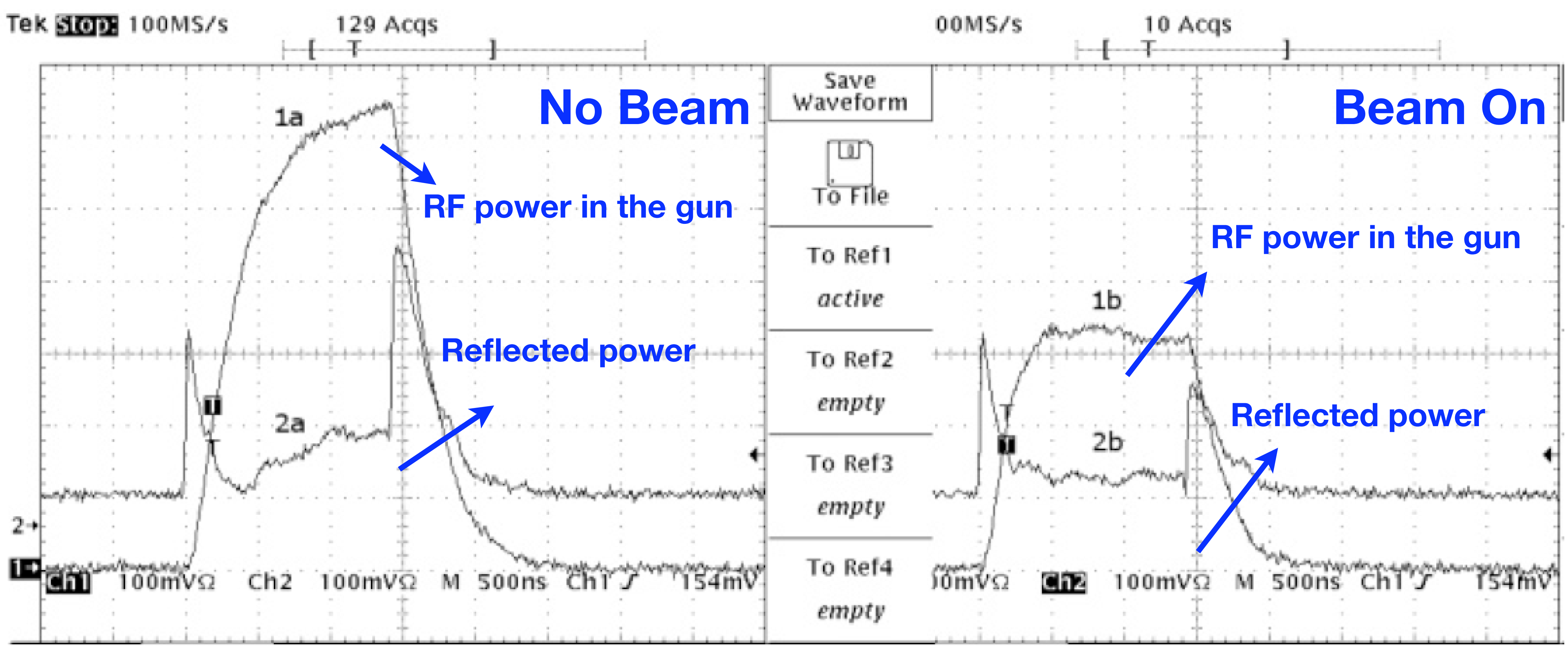

The PHIN commissioning measurements have been performed under the conditions where the beam loading is compensated.

Possible Sources

- the electrons that are not stopped by the slit-mask,
- the overlapping between the individual beamlets,
- x-rays
- external light pollution
- radiation due to the heating of the OTR screen

Possible Cure

First of all, consider the intensity of the beam, gain and spectral sensitivity of the camera, type of the observation screen, always respect the signal/noise ratio.

- thickness of the multi-slit mask,
- optimization of distance between the screen and the mask,
- shielding the camera properly,
- shielding or using a light-tight enclosure,
- offline treatment (usually the background has a Gaussian distribution in this case),

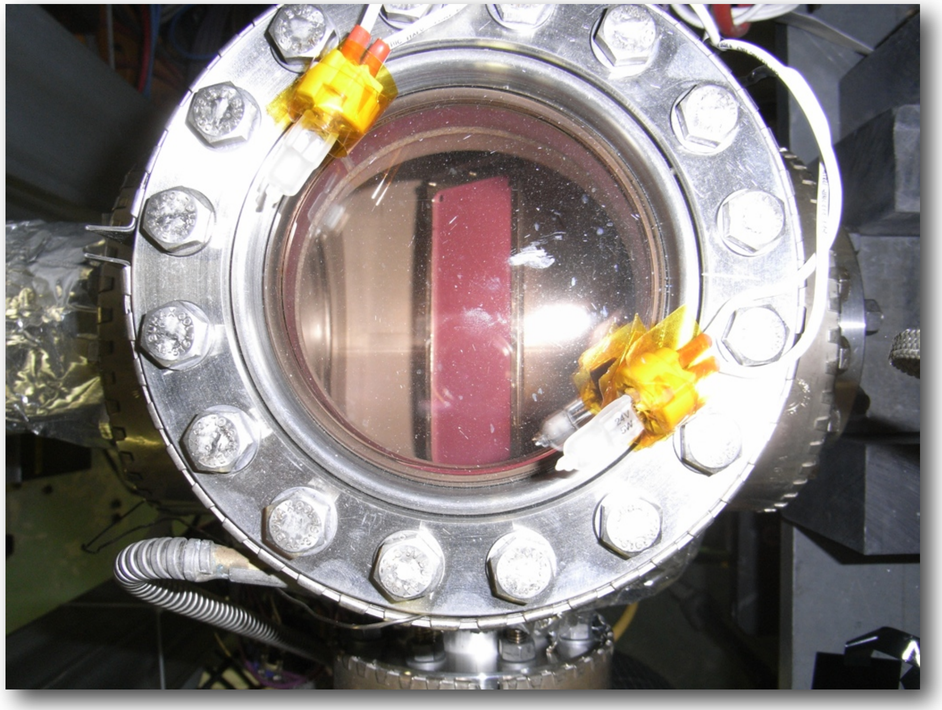

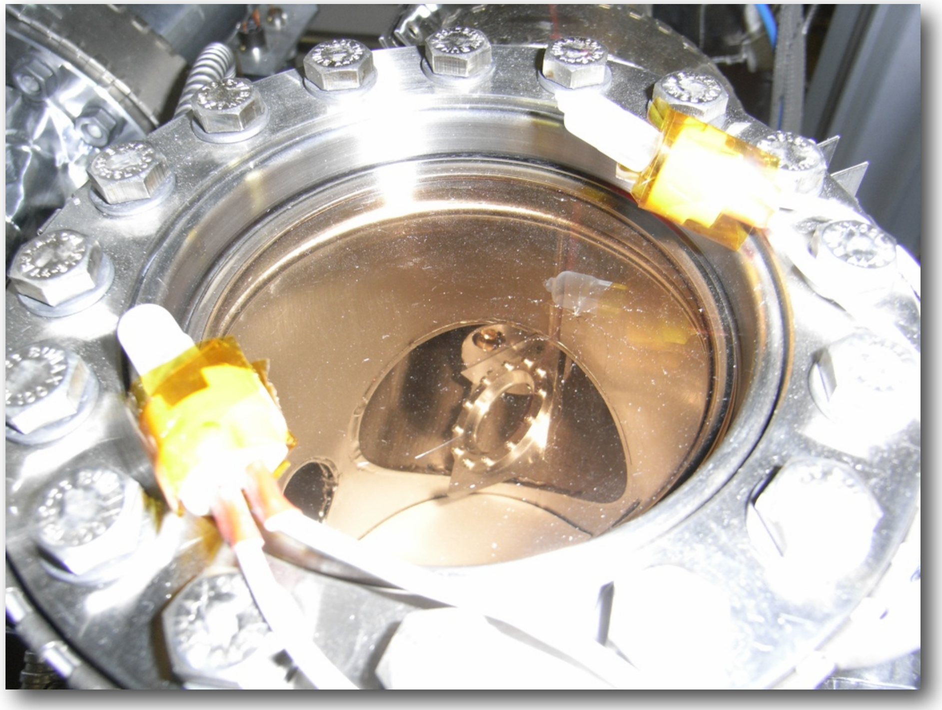

Transverse Normalized Beam Emittance along the Pulse Train

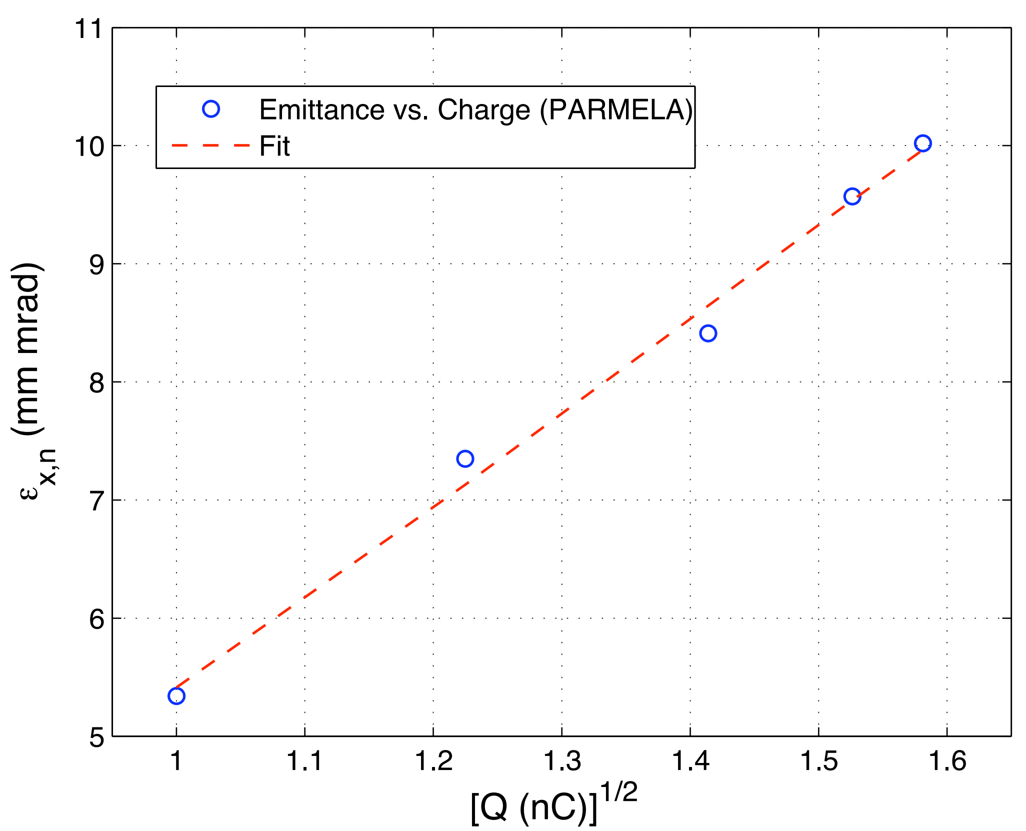

Transverse Normalized Beam Emittance along the Pulse Train

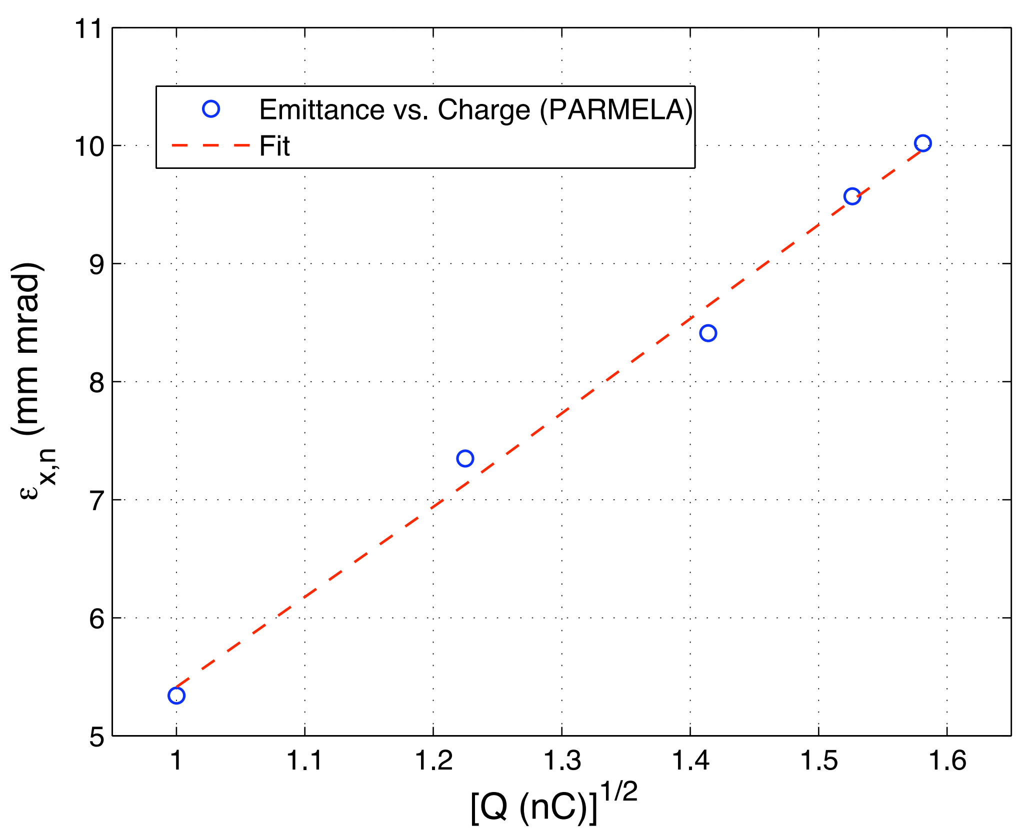

A general remark

Transverse Normalized Beam Emittance along the Pulse Train

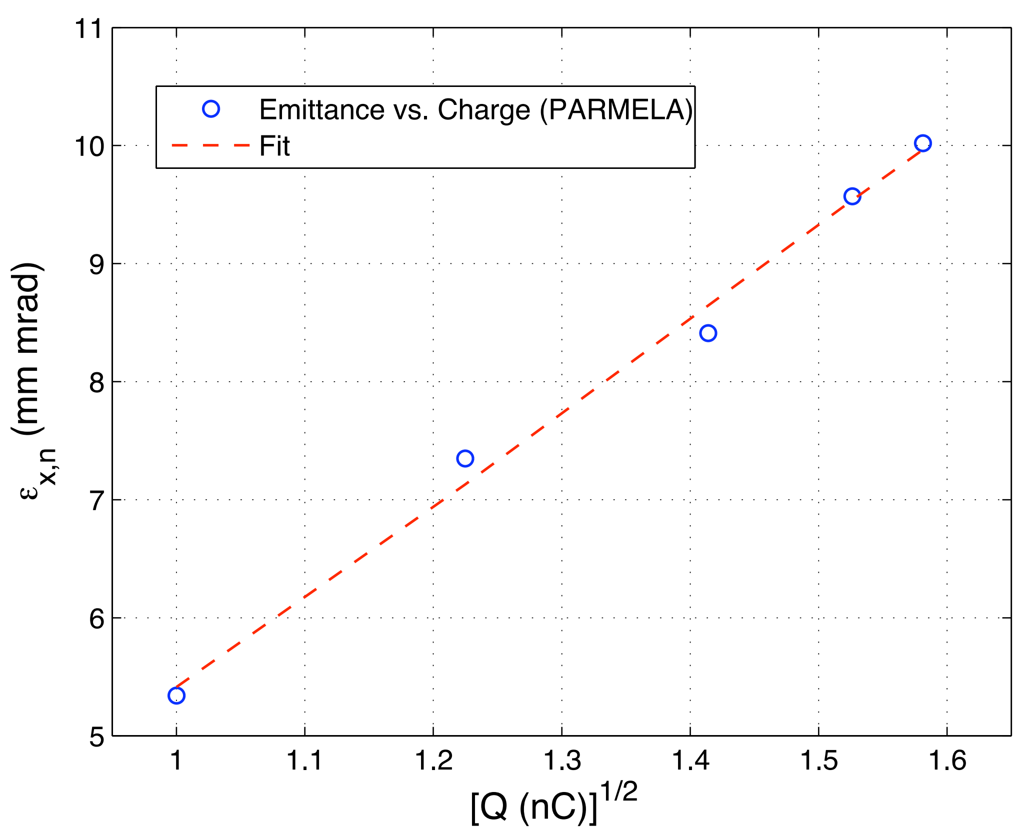

A general remark

As a conclusion from the ICFA Future Light Sources Conference
http://www-conf.slac.stanford.edu/icfa2010/

$$\epsilon_n[mm\,mrad] \approx 1\mu m\sqrt{Q[nC]}$$

Transverse Normalized Beam Emittance along the Pulse Train

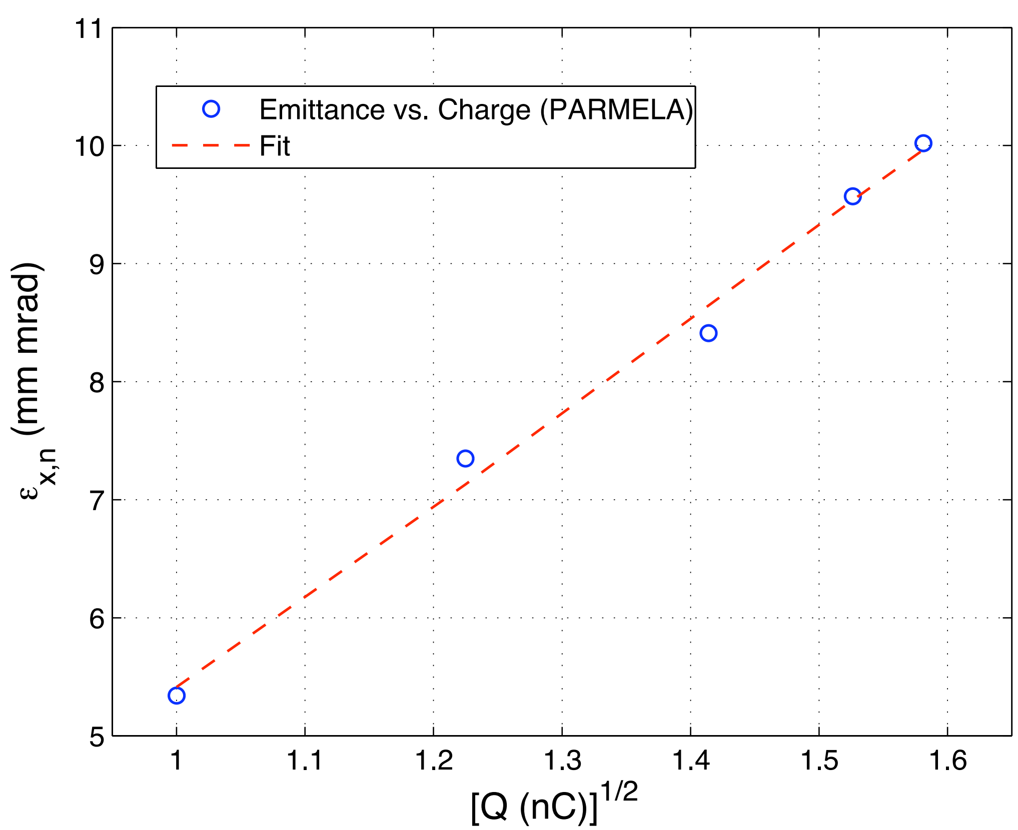

A general remark

As a conclusion from the ICFA Future Light Sources Conference http://www-conf.slac.stanford.edu/icfa2010/

$$\epsilon_n[mm\,mrad] \approx 1\mu m\sqrt{Q[nC]}$$

Numerical studies with PARMELA shows that:

- Provided that the working point is optimized for the proper emittance compensation, the above approximation holds,
- The proportionality constant is a function of the laser shape.
- Currently, laser shaping study in progress at PITZ.